21st Benelux Meeting on Systems and Control

March 19 – 21, 2002 Veldhoven, The Netherlands

Book of Abstracts

Bram de Jager and Hans Zwart (eds.) Book of Abstracts 21st Benelux Meeting on Systems and Control Technische Universiteit Eindhoven, Eindhoven, 2002 ISBN 90-386-2893-5

J.C. Golinval (University of Liege)

Table of Contents

Part 1: Contributed Lectures TA-1 Identification X.J.A. Bombois (TU Delft) G. Scorletti () B.D.O. Anderson, M. Gevers and P. Van den Hof () I. Goethals (KULeuven) B. De Moor & P. Van Dooren (KULeuven & UCL) J. Suykens & T. van Gestel (KULeuven & KULeuven) S.G. Douma (Delft University of Technology) P.M.J. Van den Hof (Delft University of Technology) S. de Waele (Delft University of Technology) P. M. T. Broersen () P. M. J. Van den Hof () Xinkai Chen (Kinki University) **TA-2 Control of Mechanical Systems** V. Duindam (University of Twente) S. Stramigioli (University of Twente) J.M.A. Scherpen (Delft University of Technology) Robust Attenuation of Robot-Tip Vibrations21 D. Kostic (Eindhoven University of Technology (TU/e)) B. de Jager (Eindhoven University of Technology (TU/e)) M. Steinbuch (Eindhoven University of Technology (TU/e)) D. Putra (Eindhoven University of Technology) H.A. van Essen (Eindhoven University of Technology) H. Nijmeijer (Eindhoven University of Technology) S. Postma (NIMR/ University of Twente) R.G.K.M. Aarts (University of Twente) O. Brüls (University of Liege)

TA-3 Control of Bio Processes
Optimization of an allergen production from CHO-K1 cell cultures
Simulation analysis of a one-dimensional model for the sedimentation tank in activated sludge wastewater treatment
Liesbeth B. Verdickt (BioTeC - Bioprocess Technology and Control) Jan F. Van Impe (BioTeC - Bioprocess Technology and Control)
Reconstruction of the dynamic oxygen uptake rate and carbon dioxide evolution rate during a pulse experiment: a white-box modeling approach
Distributed parameter modeling of a fixed-bed biofilter
Maximum likelihood estimation of pseudo-stoichiometric coefficient on the basis of incomplete data
TA-4 Modeling
Optimal parameter estimation as a means to measure atom positions from electron microscopy images
Nonlinear modelling of dynamic behaviour of looper in a hot finishing mill and control approach
Synchronization in a Population of Nearly Identical Oscillators
Bayesian inference for LS-SVMs on large datasets and its implementation
K. Pelckmans & B. De Moor & J. Vandewalle (K.U.Leuven) Port-Based Thermo-Fluid Models
TA-5 Discrete Event/Hybrid Systems
Semantics for Hybrid Systems
Systematic Modelling Approach for First Principle Dynamic Process Models

Petri Nets Model Based Fault Detection In Power Systems
Observer Design for a Class of Bimodal Piecewise Affine Systems
Maximal controlled invariant sets of switched linear systems
The van der behalf (Christophy)
TE-1 Nonlinear Systems
Kalman filters for nonlinear systems
Estimation of the convergence region for the local output regulation problem for nonlinear systems
Synthesis of rhythmic patterns in small networks of oscillators
On achievable non-linear behaviors
TE-2 H_{∞}/μ control
Generalized singular values and the rank approximation problem
An LMI approach to multiobjective robust dynamic output-feedback control for uncertain discrete-time systems
S. Kanev (University of Twente) M. Verhaegen (University of Twente)
Interior point method for reduced order controller synthesis of electro-mechanical servo-systems
Application of H_{∞} feedback control: Reference tracking on a half-axle test rig
v. De Cayper and W. Benandsenditer (Elvis International)
TE-3 Control of Chemical Systems
Auto-tuning of chemical processes using adaptive λ-tracking control
Model Reduction by Proper Orthogonal Decomposition
Oscillation Diagnosis in Control Loop - a Survey

M. Kinnaert (Université Libre de Bruxelles)
Modeling and predictive control of cement grinding circuits
Marcel Remy ()
TE-4 Optimization
Optimal Errors-in-Variables Smoothing
Real-Time Control using Interactive Sensing and Classification
Coverage control for distributed sensing networks
T. Karatas and F. Bullo (University of Illinois at Urbana-Champaign)
TE-5 Linear Systems
Global H ₂ -approximation in state-space: a case study
Performance and Convergence of Iterative Learning Control
A behavioral approach to decoding
Principal angles in system theory, information theory and signal processing
WA-1 Nonlinear Systems
Bang-bang control of underactuated mechanical systems
Point stabilization of the extended chain form with robustness to model uncertainties
Speed and drive torque actuation in active control of centrifugal compressors
Improved disturbance rejection in a DVD player using switching control

F.L.M. Cremers (Philips CFT) F.B.Sperling (Philips CFT)
Robust Trajectory Tracking Control with Discrete-Time Sliding-Mode Controller and Feedforward Controller 63 J. Wang (KULeuven) J. Swevers (KULeuven) H. Van Brussel (KULeuven)
WA-2 Control of Mechanical Systems
New Passivity Properties for Electro-Mechanical Systems
Controllers for hybrid isolation of structure borne sound in a demonstrator set-up
Decoupling of collocated actuator-sensor-pairs for active vibration control
Model based control of a passenger car using an active suspension
Control Design for Restraint Systems
WA-3 Identification
Estimation of an N-L-N Hammerstein-Wiener model
Identification of composite local linear state-space models using a projected gradient search
Identification of whole-body glutamine kinetics
Identification of the SIMONA research simulator motion system
Robot Identification for Accurate Dynamic Simulation
WA-4 Fault Handling/Adaptive Control
Disturbance detection on CD players using wavelets

One approach for the detection and estimation of a jump in discrete time LTI systems	75
Multiphase Adaptive Control based on Strong Robustness	76
Robust linear and nonlinear PID control based on identification	77
WA-5 Learning Control	
Optimal Finite time ILC design, with application to a waferstage	78
Application of learning feed-forward control to cam-follower systems	79
Evaluation of (unstable) non-causal systems for iterative learning	80
Reinforcement learning algorithms for continuous state-spaces	81
Allowed sloppy magnet placement due to learning control	82
WE-1 Stabilization	
Robust stabilization of linear time-delay systems	.83
Using Genetic Programming for finding Lyapunov functions	84
Tuning Rules for Passivity-Based Controllers D. Jeltsema (Delft University of Technology) J.M.A. Scherpen (Delft University of Technology)	85
Regular implementability, stabilization and pole placement of behaviors	86
WE-2 Aero Systems	
On the optimization of satellite orbit plane changes subject to time constraints and its applications	87
Cessna Citation II Aircraft Aerodynamic Model Parameter Identification	88

Sinar Juliana (TU Delft, Netherlands) Q.P. Chu (TU Delft, Netherlands) J.A. Mulder (TU Delft, Netherlands)
The range-dependence problem of clutter spectrum for non-sidelooking monostatic STAP radars
WE-3 Control of Bio Processes
Optimal input design for the estimation of kinetic parameters
Hybrid extended Luenberger - asymptotic observer for bioprocess state estimation
Sensitivity function based model reduction: a bacterial gene expression case study
Systematic model reduction for complex bioprocesses described by metabolic pathways
WE-4 Optimization
Optimal control with imprecise gain through dynamic programming
Linear Matrix Inequalities for Optimization of Rational Functions
The Newton method for invariant subspace computation
WE-5 Distributed Parameter Systems
Conjectures for exact observability for infinite-dimensional systems
Control of Variable Profiles in a Distributed Parameter System using Reduced Models
Spectral factorization of meromorphic functions of finite order for distributed parameter systems9 F. M. Callier (University of Namur (FUNDP)) J. J. Winkin (University of Namur (FUNDP))
The sub-optimal Hankel norm approximation problem for the Wiener class

ThA-1 Nonlinear Systems
Convergence criteria for nonlinear feedback controlled Euler - Lagrange systems
Symmetry results in partial synchronization
Energy functions and balancing for nonlinear discrete-time systems: an application example
Passivity as a tool for the analysis of limit cycles
ThA-2 Mechatronic Systems
An autonomous robot for harvesting of cucumbers in greenhouses
LPV system identification for electromechanical systems
Non-linear Control of Active Magnetic Bearings for Ultra High Precision Applications
Linear Parameter Varying Control of a Wafer Stage
ThA-4 Model Predictive Control
Potential benefits of ramp metering on motorways
Model predictive control for optimal coordination of ramp metering and variable speed control
MPC as a tool for optimal process operation of MSW combustion plants
Model predictive control algorithm with multiple linear models
ThA-5 Optimization
Optimal topology and geometry of controllable tensegrity systems

Milenko Masic (University of California at San Diego) Bob Skelton (University of California at San Diego)
A MILP approach to the optimization of emulsification
Soft-constrained feedback Nash Equilibria
Closed-loop stochastic economic optimization
Part 2: Plenary Lectures
Nonlinear Model Predictive Control: Theory and Applications
Adaptive λ-tracking: A simple self-tuning controller for practical control problems
Using Model-based Optimization to Improve Biotechnological Processes: Local Optimization Methods161 Dr Julio Banga (Process Engineering Group, IIM (CSIC); Spain)
Using Model-based Optimization to Improve Biotechnological Processes: Global Optimization Methods 175 Dr Julio Banga (Process Engineering Group, IIM (CSIC); Spain)
Minicourse: Financial Engineering and Control
Part 3: List of Participants
Alphabetical list

Part 1 Contributed Lectures

A new robust control design procedure based on a PE identification uncertainty set

Xavier Bombois

Dept. of Applied Physics

Delft University of Technology, The Netherlands

Email: X.J.A. Bombois@tnw.tudelft.nl

Gerard Scorletti LAP ISMRA, Caen, France

Brian Anderson Australian National University, Canberra, Australia

Michel Gevers CESAME, Universite Catholique de Louvain, Belgium

Paul Van den Hof Dept. of Applied Physics, Delft University of Technology, The Netherlands

1 Abstract

This paper is part of the wide-spread effort to connect timedomain prediction error (PE) identification and robustness theory. In the present paper, we propose a new and uniform robust control design procedure which is based on the model G_{mod} and the parametric uncertainty region \mathcal{D} delivered by PE identification and whose key step is a quality assessment procedure of the identified pair $\{G_{mod} \mathcal{D}\}$.

The new robust control design procedure. As just stated, the key step of our new robust control design procedure is a method to check whether the identified pair $\{G_{mod} \mathcal{D}\}$ is tuned for robust control design. This verification is based on the analysis of the behaviour of a set of controllers $\mathcal{C}(G_{mod})$ over all systems in the uncertainty region \mathcal{D} . This set $\mathcal{C}(G_{mod})$ is defined as the set of all controllers achieving a performance level Λ_{mod} with the identified model G_{mod} . This performance level Λ_{mod} (used for control design with the nominal model G_{mod}) is, as usually done in model-based control, chosen slightly better than the prescribed performance level Λ_0 . By definition, the controllers in $C(G_{mod})$ are therefore those that can result from a controller design step based on the model G_{mod} ; they are thus the only ones that are relevant in order to establish the quality of the pair $\{G_{mod} \mathcal{D}\}$. We then state that an identified pair $\{G_{mod} \ \mathcal{D}\}$ is tuned for "robust control design" if all controllers in the set $\mathcal{C}(G_{mod})$ which achieve the performance level Λ_{mod} with G_{mod} , achieve the prescribed performance Λ_0 with all systems in \mathcal{D} .

Determination of the robust controller C**.** In the case where the identified pair has been termed tuned for robust control design, all controllers in $\mathcal{C}(G_{mod})$ are appropriate robust controllers for the true system G_0 since they are guaranteed to achieve the prescribed performance level (i.e.

 Λ_0) with all systems in \mathcal{D} , and thus in particular with G_0 . The choice of a particular controller within that class can then be made on the basis of additional considerations such as lowest complexity.

New experiment design. Conversely, in the case where the quality of $\{G_{mod} \ \mathcal{D}\}$ is not judged satisfactory (the robustness test fails), we propose some guidelines (based on the results of the robustness test) in order to perform a new PE identification experiment providing a new pair "model-uncertainty region" that is likely to be better tuned for robust control design.

Imposing positive realness in subspace models by using regularization

Ivan Goethals, Tony Van Gestel,
Johan Suykens, Bart De Moor
K.U.Leuven ESAT - SCD - SISTA
Kasteelpark Arenberg 10, B-3001 Heverlee
{igoethal,vangeste,suykens,
demoor}@esat.kuleuven.ac.be

Paul Van Dooren UCL - CSAM Bâtiment Euler Avenue Georges Lemaitre 4, B1348 Louvain-la-Neuve vdooren@csam.ucl.ac.be

Abstract

The linear stochastic identification problem is concerned with systems and models of the form

$$\begin{array}{rcl}
x_{k+1} & = & Ax_k + w_k \\
y_k & = & Cx_k + v_k
\end{array} \tag{1}$$

with

$$E\left(\left[\begin{array}{c} w_p \\ v_p \end{array}\right] \left[\begin{array}{cc} w_q^t & v_q^t \end{array}\right]\right) = \left[\begin{array}{cc} Q & S \\ S^t & R \end{array}\right] \delta_{pq} \geq 0 \quad (2)$$

where $y_k \in \mathbb{R}$ symbolizes the output, $x_k \in \mathbb{R}^n$ the state, and $w_k \in \mathbb{R}^n$ and $v_k \in \mathbb{R}^l$ the state and output noise of the system at time step k. In the last decade, so-called subspace identification methods have been developed [1]. Typically in a first step, Kalman filter state sequences $\hat{X}_i \in \Re^{n \times j}$ and $\hat{X}_{i+1} \in \Re^{n \times j}$ of the system are estimated directly from input-output data using geometric operations. After the estimation of the state sequences the 'deterministic' model is easily obtained. For instance, matrices A and C can be calculated using simple least squares. Also available from the measurements and the Kalman states is the covariance sequence

$$\{\Lambda_0, \Lambda_1, \Lambda_2, \dots, \Lambda_i\} \tag{3}$$

with for every i

$$\Lambda_i = E\left[y_k y_{k-i}^t\right]. \tag{4}$$

From this covariance sequence, the noise covariance matrices Q, R and S are then calculated by writing the model in a so-called innovations form given as.

$$\begin{array}{rcl}
x_{k+1} & = & Ax_k + Ke_k \\
y_k & = & Cx_k + e_k.
\end{array}$$
(5)

This step, however, is only possible if the infinite sequence $\Lambda_i = E\left[y_k y_{k-i}^t\right]$ is a valid covariance sequence, with positive definite Toeplitz matrix. This is equivalent with the identified model being positive real.

Positive realness is an often overlooked but important property of the identified 'deterministic' system. It is a necessary condition to obtain the corresponding stochastic system. For instance, for a SISO system the spectral density will not be positive real for some points on the unit circle if the positive

realness property is not satisfied. Furthermore, the problem of positive realness arises in many cases, especially when the 'true' stochastic system has zeros or poles near the unit circle [2]. In such cases, stochastic subspace identification methods will fail to calculate correct error covariance matrices for state and output noise. The obtained model will also have no physical relevance and is therefore of limited use in practical applications.

In order to deal with the problem, we propose a regularization approach to impose positive realness on a formerly identified deterministic subspace model that is conceptually quite similar to the approach used in [3] to impose stability on subspace models. A numerically fast and reliable method is conceived using this approach. The performance is in general better or equal to that of already existing techniques. Furthermore the approach is found to be more reliable and robust.

Acknowledgements

Ivan Goethals is a research assistant with the FWO. Dr. Johan Suykens is an associate professor with the FWO. Our research is supported by: Research Council KUL: GOA-Mefisto 666, IDO, several PhD/postdoc & fellow grants; Flemish Government: FWO (several PhD/postdoc grants, projects G.0256.97, G.0115.01, G.0240.99, G.0197.02, G.0407.02, research communities ICCoS, ANMMM, AWI, IWT, GBOU-McKnow, Eureka-Impact, Eureka-FLiTE; Belgian Federal Government: DWTC (IUAP IV-02 (1996-2001) and IUAP V-10-29 (2002-2006), Development PODO-II; Direct contract research: Verhaert, Electrabel, Elia, Data4s, IP-COS;

- [1] P. Van Overschee, B. De Moor, "Subspace Identification for linear systems", Kluwer Academic Publishers, 1996
- [2] A. Dahlén, A. Lindquist, J. Marí, "Experimental evidence showing that stochastic subspace identification methods may fail", Systems & Control-Letters, 1998, volume 34, pages 303-312
- [3] T. Van Gestel, J. Suykens, P. Van Dooren, B. De Moor, "Identification of stable models in subspace identification by using regularization", IEEE Transactions on Automatic Control, 2001, 46(9), pages 1416–1420

The choice of uncertainty structure within identification for control

Sippe G. Douma Department of Applied Physics Delft University of Technology Lorentzweg 1, 2628 CJ Delft The Netherlands

Email: s.g.douma@tnw.tudelft.nl

Paul M.J. Van den Hof Department of Applied Physics Delft University of Technology Lorentzweg 1, 2628 CJ Delft The Netherlands

Email: p.m.j.vandenhof@tnw.tudelft.nl

1 Background and problem formulation

The necessity of providing control-relevant models has become well established in the field of system identification. Acknowledging the approximate nature of any model, research focussed on the tuning of the undermodelling error towards improved nominal control design. The developments in robust control then urged the employment of uncertainty bounds either for a robustness analysis of a nominal controller design or even directly for a robust controller design [1, 2]. This trend is resulting in the perception that system identification explicitly has to provide sets of models. The freedom in a system identification setup as experimental conditions, the objects to be identified (e.g. plant or Youla parameter) and the type of uncertainty structures should be exploited to provide model sets most suited for high performance controller design. A clear understanding of the interaction between an uncertainty set and associated achievable performance becomes most important.

Various uncertainty structures can be employed in describing a model set. Robust control provides robust stability and performance results for linear fractional transformation based structures as additive, (inverse) multiplicative and coprime uncertainty. The latter allows for more explicit results in terms of a Youla parameter uncertainty, the gap metric and the ν -gap metric [6]. From an identification point of view a parameter uncertainty structure follows naturally [1]. On the other hand, dealing with undermodelling effects leads to additive nonparametric bounds in the frequency domain [3, 4]. Here again the object to be identified (e.g. the plant directly, its coprime factors or a closed-loop transfer function) further determines the properties of the resulting model set. The problem addressed here is what arguments can be formulated justifying a particular choice of uncertainty structure when identifying for robust control.

2 Observations

Consider linear time-invariant single-input-single-output systems. A circular uncertainty region over a frequency grid can exactly and explicitly be described in all of the aforementioned uncertainty structures. All linear fractional transformations of the uncertainty $\Delta\left(\omega_{j}\right)$ with $\left|\Delta\left(\omega_{j}\right)\right| \leq \gamma_{j}$ can be transformed into one another unconservatively. Clearly, the nominal model and the uncertainty weighting function will change and might require a more complex description.

Ellipses or boxes do not retain their shape under these transformations. Moreover, probability density functions change under transformation [5].

Each uncertainty structure comes with a robust stability condition formulated in terms of a nominal stability, a frequency domain condition and a winding number condition (number of unstable poles and zeros) on the plants in the uncertainty set. When considering systems underlying the frequency domain uncertainty regions it is the last condition which poses the differentiation amongst uncertainty structures. In fact, during system identification an assumption on the stability of the identified object or an assumption of a continuous parameter perturbation is required in order to form the system sets.

While (worst-case) robust performance can be calculated, more explicit relationships between an uncertainty and the associated performance is required when tuning a system identification experiment. Results based on the Youla parameter uncertainty and the ν -gap in combination with a loop-shaping procedure prove useful in this context [2, 6].

- [1] Bombois, X., M. Gevers, G. Scorletti and B.D.O. Anderson (2001). Robustness analysis tools for an uncertainty set obtained by prediction error identification. *Automatica*, *37*, pp. 1629-1636.
- [2] de Callafon, R.A. and P.M.J. Van den Hof (1997). Suboptimal feedback control by a scheme of iterative identification and control design. *Math. Mod. of Syst.*, 3, 77-101.
- [3] De Vries, D.K. and P.M.J. Van den Hof (1995). Quantification of Uncertainty in Transfer Function Estimation: a Mixed Probabilistic-Worst-case Approach. *Automatica, Volume 31, no4*, 543-557.
- [4] Hakvoort, R.G. and P.M.J. Van den Hof (1997). Identification of probabilistic system uncertainty regions by explicit evaluation of bias and variance errors. *IEEE Trans. Autom. Control*, *AC-42*, 1516-1528.
- [5] Heath, W.P. (2001). Bias of indirect non-parametric transfer function estimates for plants in closed loop. *Automatica*, *37*, pp. 1529-1540.
- [6] Vinnicombe, G. (2001). Uncertainty and feedback: H_{∞} loop-shaping and the v-gap metric, Imperial College Press, London, UK.

Can data determine the best ARMA-model using the likelihood?

Stijn de Waele, P. M. T. Broersen and P. M. J. Van den Hof Department of Applied Physics Technische Universiteit Delft P.O. Box 5046, 2600 GA Delft The Netherlands

Email: S.deWaele@tn.tudelft.nl

1 Introduction

Combined Autoregressive Moving Average (ARMA) models can be used to characterize the statistical properties of signals. Examples of applications are radar target detection, speech coding and spectral analysis of climatologic data. In most theoretical results on ARMA parameter estimation it is assumed that the correct model order is know. In this paper we examine what happens if this assumption is rejected. Then, the model structure has to be determined from the data. This is typical for many practical situations, where accurate knowledge about the model order is lacking.

2 Error measure

An error measure is used to establish the quality of an estimated model. It compares the estimated signal properties (the pdf \hat{f}) to the true signal properties (pdf f). It cannot be calculated in practice because then only the realisation $x = \begin{pmatrix} x_1 & x_2 & \dots & x_N \end{pmatrix}$ of the stochastic signal is given, instead of the pdf f. The error of the model pdf with respect to the true pdf will be expressed using the Kullback-Leibler discrepancy KLD I. The Kullback-Leibler Index (KLI) is given by

$$i\left(\hat{f},f\right) = E_f\left\{-2\ln\hat{f}\left(X\right)\right\} \tag{1}$$

where $E_f\{\cdot\}$ indicates the expectation over the probability function f. The KLI is minimal for the true distribution. The KLD is given by

$$I\left(\hat{f},f\right) = i\left(\hat{f},f\right) - i\left(f,f\right). \tag{2}$$

The KLD is zero for the true pdf. An accurate approximation in the frequency domain is the spectral distortion SD of the estimated power spectrum \hat{h} with respect to the true power spectrum h:

$$\Delta\left(\hat{f},f\right) \approx SD\left(\hat{h},h\right) = \frac{N}{2\pi} \int_{-\pi}^{+\pi} \left(\ln \hat{h}\left(\omega\right) - \ln h\left(\omega\right)\right)^{2} d\omega.$$
(3)

3 The Likelihood

The likelihood L is defined as the probability density function of an estimated ARMA(p',q') model \hat{f} for the realisation x from which the model has been estimated:

$$L\left(x;\hat{\theta}\right) = \ln \hat{f}\left(x\right) = \ln f\left(x;\hat{\theta}\right). \tag{4}$$

An accurate approximation in the frequency domain is the spectral distortion of the model spectrum \hat{h} with respect to the raw periodogram h_{PER} .

$$L(x; \hat{\theta}) \approx SD(\hat{h}, h_{PER}).$$
 (5)

The frequency domain approximations for the KLD (3) and the likelihood (5) provide an illustration of the difference between the error measure and the fit criterion.

The likelihood is used as a criterion to fit an ARMA model to data in parameter estimation. The maximum likelihood is denote $L_{\rm max}$.

The likelihood is also used in statistical order selection. With order selection, a model order is selected from the data as the model order where an order selection criterion is minimal. A well-known order selection criterion is the Akaike Information Criterion AIC:

$$AIC = -2L_{\text{max}} + 2(p' + q')$$
 (6)

where L_{max} is the maximum likelihood.

4 Results

Simulation experiments show that the actual behavior of the likelihood and the KLD for model orders greater than the true model order deviates considerably from the asymptotic predictions. Given this result we can revert to the original question: Can data determine the best ARMA-model using the likelihood?

Order selection is a critical factor in answering this question. In the practical case where the optimal model order is not known exactly, overcomplete models are also considered for selection. For these models the likelihood tends to indicate that the model fits very well to the data. As a result these models are often selected with order selection. Unfortunately, the quality of overcomplete models is very poor. Therefore, the resulting model is less accurate than predicted by asymptotic theory. These result shows that the behavior of ARMA estimators changes considerably if the true model order is not known.

Identification for a class of movements under perspective observation

Xinkai Chen

Department of Intelligent Mechanics, Faculty of Biology Oriented Science & Technology, Kinki University, 930 Nishimitani, Uchita, Naga-gun, Wakayama 649-6493, Japan Tel: +81-736-77-3888, ext. 4303; Fax: +81-736-77-4754

E-mail: chen@mec.waka.kindai.ac.jp

Perspective observations arise naturally in the study of machine vision [1]. The observation via one or two cameras consists of the perspective projection of points in the 3-D scene onto the image plane. Thus, points in 3-D space are observed up to a homogeneous line. In the study of machine vision, observing the position of a moving object in the space by the image data with the aid of a CCD camera has been studied in the past years. A very typical method is the application of the extended Kalman filter (EKF) [2]. It is well known that the EKF may fail in some real applications, and the algorithm is very complicated. To overcome these difficulties, a very simple method is proposed by the authors in [4] recently.

Another important topic in the study of machine vision is the identification of the motion parameters by using the observed image data. This problem has received minor attention except the results in [3], where the EKF is applied to the identification problems for the time invariant motion parameters.

In this paper, we consider the position and the parameter estimation problem for a class of movements by using the perspective observation, where the parameters are all time-varying. The formulated problem can be converted into the observation of a dynamical system with nonlinearities. The algorithm proposed by the authors in [4] is extended to identify this class of nonlinear system. First, the parameters

relating to the rotation of the motion are identified, where the perspective observation obtained by only one camera is needed. Then the position of the moving object is identified, where the stereo vision is necessary. In the third step, the parameters relating to the straight movement are identified. The estimation errors of the position and the motion parameters are guaranteed to decrease exponentially until they become very small. Further, the ultimate estimation errors are controlled by the design parameters. The proposed algorithm is very simple and easy to be implemented. It is considered that the new observer can cope with a large class of practical perspective systems. Simulation results show that the new method is very effective.

- [1] N. Ayache, Artificial Vision for Mobile Robots, Stereo Vision and Multisensory Perception (MIT Press, Cambridge, MA, 1991).
- [2] L. Matthies, T. Kanade and R. Szeliski, "Kalman filter-based algorithm for estimating depth from image sequence," *International Journal of Computer Vision*, Vol. 3, pp. 209-236, 1989.
- [3] H. Kano, B.K. Ghosh and H. Kanai, "Single camera based motion and shape estimation using Extended Kalman Filtering," *Mathematical and Computer Modelling*, Vol. 34, pp. 511-525, 2001.
- [4] X. Chen and H. Kano, "A new state observer for perspective systems," *IEEE Trans. on Automatic Control*, accepted for publication (to appear in 2002).

Passive Compensation of Nonlinear Robot Dynamics

Vincent Duindam
University of Twente
Drebbel Institute
P.O. Box 217
7500 AE Enschede
The Netherlands
V.Duindam@utwente.nl

Stefano Stramigioli
University of Twente
Drebbel Institute
P.O. Box 217
7500 AE Enschede
The Netherlands
S.Stramigioli@utwente.nl

Jacquelien Scherpen
Delft University of Technology
Faculty of I.T.S.
P.O. Box 5031
2600 GA Delft
The Netherlands
J.M.A.Scherpen@its.tudelft.nl

1 Introduction

Many robot applications demand a robot to interact with an environment that is not exactly known beforehand. In these situations, the controller should be careful not to make the robot unstable, i.e. keep its kinetic energy bounded.

One way to accomplish this is to use a form of impedance control (introduced by Hogan [1]): the control torques are taken equal to the gradient of an (artificial) potential field with the minimum at the desired position. Thus, the controller mimics a spring connected between the robot and the desired position. The kinetic energy of the robot is determined by the potential field, and if this field has a global minimum, the kinetic energy is bounded.

However, if we 'release' the robot in the potential field, coriolis and centrifugal forces cause it to oscillate around the minimum in a seemingly chaotic way. We want to improve this behavior, such that the robot oscillates along a predefined curve instead of on the whole potential field. We *do* want to keep the nice passivity properties of the impedance controller, though, so we look for power-continuous (i.e. energy-conserving) extensions of the potential field.

2 Mathematical Framework

In order to have all results be coordinate-independent (and, as a pleasant side-effect, keep the equations short and readable), we use the mathematical framework of differential geometry [2] to describe the dynamics of the robot as well as the controller.

We use coordinates q and velocities \dot{q} to describe the current state (configuration and velocity) of the robot. We can then describe the dynamics of a robot as

$$\nabla_{\dot{a}}\dot{q} = g^{-1}\tau\tag{1}$$

where $\nabla_{\dot{q}}\dot{q}$ is the covariant directional derivative that describes the 'acceleration', g is the metric (inertia tensor), and τ are the control torques (one motor per joint). In this way, we can relate the necessary control torques in a one-to-one way to the desired accelerations.

We describe the desired curves using a vector field w in joint

space. The vector w(q) describes the direction of the desired curve at point q.

3 Control Law

We want to obtain a controller that makes the robot move along the curves defined by w (first constraint), while the change in kinetic energy is determined by the potential field (second constraint).

The first constraint results in a desired acceleration (A) in a direction perpendicular to the current velocity, i.e.

$$\left\langle \left(\nabla_{\dot{q}}\dot{q}\right)_{A},\dot{q}\right\rangle_{g}=0\tag{2}$$

with the inner product $\langle \cdot, \cdot \rangle_g$ defined by the metric. The second constraint results in a desired acceleration (B) in the same direction as the current velocity, i.e.

$$\left(\nabla_{\dot{q}}\dot{q}\right)_{R} = \alpha\dot{q} \tag{3}$$

with α a real number depending on the current state. The total controller is just the sum of these two parts. Additional terms can be added to be able to recover from disturbances or to add collinear damping.

The resulting controller can be easily explained by the control of a simple system like a point mass moving in the plane: we can change its direction by applying a force perpendicular to the current velocity (similar to Equation 2), and we can independently change its speed by applying a force in the same direction as the current velocity (similar to Equation 3).

In the presentation, we derive the actual control law and show some simulation results.

- [1] N. Hogan, "Impedance control: An approach to manipulation" *Journal of Dynamical Systems, Measurement and Control* 107(1), pp. 1–24, 1985.
- [2] M. Spivak, A Comprehensive Introduction to Differential Geometry, Berkeley: Publish or Perish, second edition, 1979.

Robust Attenuation of Robot-Tip Vibrations

Dragan Kostić, ¹ Bram de Jager, ² and Maarten Steinbuch ³ Department of Mechanical Engineering Eindhoven University of Technology (TU/e) P.O. Box 513, 5600 MB Eindhoven, The Netherlands

Email: ¹D.Kostic@tue.nl, ²A.G.de.Jager@wfw.wtb.tue.nl, and ³M.Steinbuch@tue.nl

Abstract

Flexible effects in robotic systems are under permanent study for the last two decades [1]-[5]. They became especially important after recognizing that the use of lightweight materials for robot construction may enable faster robot motions with the same actuators applied. Lightweight materials are used to improve efficiency in task execution and reduce power consumption. However, commonly these materials have low rigidity, that is, they bend during faster movements. The bending leads to vibrations at the robot tip that reduce the accuracy of trajectory tracking.

We propose a control concept that compensates for vibrations at the robot tip caused by structural flexibility. It is applicable to general spatial robot configurations. The number of translational and rotational directions along which reduction of vibrations is possible equals the number of degreesof-freedom. This method requires knowledge of the robot dynamics including flexibilities [5], and the use of additional sensors for detecting vibrations. We explain how to extract vibration information from sensor outputs. This information is used for identification of elastodynamics and for robust compensation of tip vibrations using feedback control. Elastodynamics enters the rigid-body dynamic model as a description of dynamic interaction between the end-effector and environment [5]. The combined model enables regulation of tip vibrations directly in the coordinate frame where the vibrations are measured. Accelerometers attached at the tip of the robot are used as vibration sensors.

This control concept is experimentally verified on a spatial RRR type of robot system [6]. The last link of the considered RRR robot is a slender beam. It is a dominant source of flexibility. Its elasticity causes profound vibrations at the tip. Angular oscillations do not arise. The rigid-body dynamics [7] of the RRR robot is derived in closed-form and identified with sufficient accuracy [8]. Elastodynamics is identified along each direction of tip movements using white noise excitations. To achieve attenuation of tip vibrations during commanded tip motions, we propose a robot control system having two complementary sub-systems: a nominal motion controller and a vibration compensator. The former one realizes joint motions in accordance with a prescribed tip trajectory. The latter one reduces oscillations at the tip. In our experiments we utilize a proportional-derivative feed-

back motion controller in addition to the feedforward component realized using the rigid-body dynamic model. For vibration compensation, an H_{∞} regulator [9] was used. Its practical usability and robust performance are experimentally verified.

The key contributions of the suggested control method are: (i) time-efficient identification of elastic effects that are appended to the model of rigid-body dynamics, (ii) use of the resulting non-linear dynamic model to simplify the problem of vibration compensation to an ordinary regulation problem, solvable using a well-developed linear theory, and (iii) robust compensation of tip vibrations.

- [1] W.J. Book, "Recursive Lagrangian Dynamics of Flexible Manipulator Arms," Int. J. Rob. Res., Vol. 3, No. 3, pp. 87-101, 1984.
- [2] D. Šurdilović, M. Vukobratović, "One Method for Efficient Dynamic Modeling of Flexible Manipulators," Mech. and Mach. Theory, Vol. 31, No. 3, pp. 297-315, 1996.
- [3] I. Kruise, "Modelling and Control of a Flexible Beam and Robot Arm," PhD Thesis, University of Twente, Enschede, The Netherlands, 1990.
- [4] A. de Luca, "Feedforward/Feedback Laws for the Control of Flexible Robots," Proc. IEEE Int. Conf. Rob. Autom., pp. 233-240, San Francisco, California, 2000.
- [5] F. Matsuno, Y. Sakawa, "A Simple Model of Flexible Manipulators with Six Axes and Vibration Control by Using Accelerometers," J. Rob. Sys., Vol. 7, No. 4, pp. 575-597, 1990.
- [6] B. van Beek, B. de Jager, "An Experimental Facility for Nonlinear Robot Control," Proc. IEEE Int. Conf. Control Appl., pp. 668-673, Hawai'i, 1999.
- [7] M. Vukobratović, V. Potkonjak, "Dynamics of Manipulation Robots: Theory and Application," Springer-Verlag, Berlin, 1982.
- [8] D. Kostić, R. Hensen, B. de Jager, M. Steinbuch, "Modeling and Identification of an RRR-robot," Proc. IEEE Conf. Dec. Control, pp. 1144-1149, Orlando, Florida, 2001.
- [9] J.C. Doyle, et. al, "State-Space Solutions to Standrad H_2 and H_∞ Control Problems," IEEE Trans. Autom. Control, Vol. 34, No. 8, pp. 831-847, 1989.

Coulomb Friction Induced Limit Cycles in PD controlled Flexible Joints

D. Putra H.A. van Essen H. Nijmeijer d.putra@tue.nl H.A.v.Essen@tue.nl H.Nijmeijer@tue.nl

Department of Mechanical Engineering, Eindhoven University of Technology P.O. Box 513 5600 MB Eindhoven The Netherlands

Abstract

Several authors proved that PD controlled positioning systems with single rigid joint and Coulomb friction cannot exhibit limit cycling [1]. This paper shows that if we take the joint flexibility into account the PD controlled positioning system can exhibit both stick-slip limit cycles and non-stick-slip limit cycles even though the PD controller parameters are tuned to locally stabilize the set point. The occurrence of limit cycles is caused by the interaction between Coulomb friction and flexibility in the closed loop system.

The shooting method and describing function method allow us to predict coexistence of a stable and an unstable limit cycles of the controlled system. The shooting method finds a limit cycle by solving a two-point boundary value problem iteratively. The stability analysis of limit cycles is done via fundamental solution matrix, which is obtained from a sensitivity analysis that is incorporated in the shooting method such that the stability of the computed limit cycle can be determined directly.

We combine the shooting method with a path following technique to trace branches of stable limit cycles and unstable limit cycles in order to get a bifurcation diagram of those limit cycles. The computed bifurcation diagram shows that the branch of stable limit cycles and the branch of unstable limit cycles collide and disappear at a certain gain value of the PD controller. This type of bifurcation of limit cycles is called fold bifurcation. The location of the fold bifurcation gives a guideline to tune the controller gain such that the controlled system does not exhibit limit cycling.

The flexible joint, which is depicted in Figure 1, is modeled by a spring with the stiffness K and a damper with the damping factor D that connect the link with the inertia J_l to the driving motor with the inertia J_m [2]. The frictional torque τ_{fm} , which consists of viscous and Coulomb frictions, counteracts the applied torque τ_m , which is produced by the PD controller.

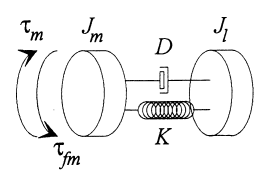


Figure 1 A model of flexible joints

Feedback signals to the PD controller are position and velocity of the link. We choose this controlled configuration because the objective is to control the position of the link without a necessity of an observer and to focus on the effect of interaction between friction and flexibility in the closed loop system. Moreover, Bonsignore et. al. [2] showed that output feedback controlled of such positioning systems exhibit limit cycling for some sets of pole placement. The Coulomb friction is given by

$$\tau_{C} = \begin{cases} F_{c} sign(\dot{x}_{m}) & \text{if } \dot{x}_{m} \neq 0 \\ \tau_{e} & \text{if } \dot{x}_{m} = 0 \text{ and } |\tau_{e}| < F_{c} \\ F_{c} sign(\tau_{e}) & \text{otherwise} \end{cases}$$

where F_c is the Coulomb friction level, \dot{x}_m is the motor velocity, and τ_e is the sum of the controller and potential spring torques, which are acting on the motor.

- [1] Armstrong-Helouvry, B., Dupont, P., and Canudas de Wit, C. "A Survey of Models, Analysis Tools, and Compensation Methods for the Control of Machines with Friction", *Automatica*, 30, p. 1083-1138, 1994.
- [2] Bonsignore, A., Ferretti, G., and Magnani, G., "Coulomb Friction Limit Cycles in Elastic Positioning Systems", *Journal of Dynamics Systems, Measurement, and Control, Transaction of the ASME,* 121, p. 298-301, June, 1999.

Weld Pool Control in Laser Welding

Sjoerd Postma
Netherlands Institute for Metals Research
P.O. Box 5008, 2600 GA, Delft
the Netherlands
s.postma@ctw.utwente.nl

Introduction

The objective of this work is the design of a feedback control system for the laser welding process, which is able to control the penetration depth of the weld. Firstly the possibilities to control the penetration depth of a weld when only partial penetration is demanded, for instance in the case of overlap configurations, will be discussed. Furthermore a controller which is able to guarantee full penetration will be introduced. Full penetration is an important quality in the production of Tailor Welded Blanks.

Experimental set-up

Optical signals emitted from the weld pool area are used as an indication of the status of the welding process, see figure 1. With four, co-axially placed, sensors it is possible to detect the transition from a fully to a partially penetrated weld in the thin mild steel sheets used. Also during partial penetration welding it is possible to relate the sensor signal strength with the penetration depth of the weld, see figure 2.

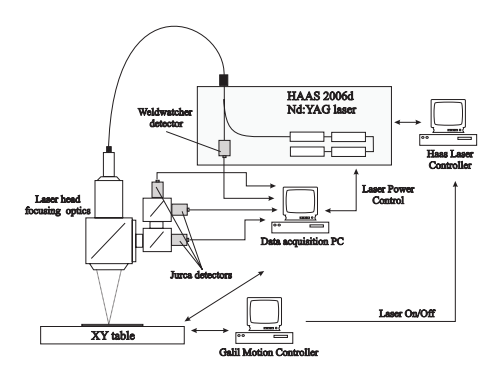


Figure 1: The experimental set-up.

System Identification

Detailed knowledge of the dynamic behaviour of the system is essential when designing a feedback control system. With the use of system identification dynamical models of the laser and the welding process (including sensor dynamics) have been obtained, in both a fully as well as in a partially penetrating parameter region.

Feedback control

Two feedback systems will be discussed. The first controller has been designed based on the identified dynamic model

Ronald G.K.M. Aarts
University of Twente, Faculty of Engineering
P.O. Box 217, 7500 AE, Enschede
the Netherlands
r.g.k.m.aarts@ctw.utwente.nl

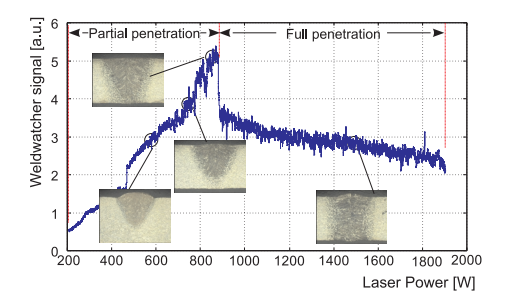


Figure 2: Weldwatcher sensor signal versus laser power at a speed of 100 mm/s. Typical weld cross-sections are included.

of the process. With this system the penetration depth in an overlap weld is controlled [1]. The objective here was to make a weld without penetrating the bottom plate. The system has been tested by varying the welding speed. In figure 3 an example of an experiment using this feedback is shown.

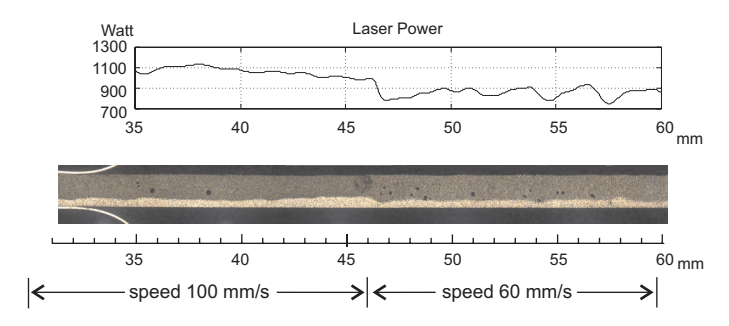


Figure 3: Longitudinal section of a controlled overlap welding experiment and the corresponding laser power.

A second kind of feedback was developed to maintain full penetration, based on a threshold condition indicating the difference between partial and full penetration. This controller is able to maintain full penetration near the edge between partial penetration, using the minimum laser power required for full penetration at a certain welding speed.

References

[1] S. Postma, R.G.K.M. Aarts, A.J.F.M. Hesemans, "Penetration feedback control in overlap laser welding of sheet metal", Proceeding of WESIC 2001, pp.495-503, June, 2001

Active Control of the Steel Strip in a Hot-Dip Galvanizing Line

O. Brüls

Université de Liège, Département d'Aérospatiale, Mécanique et Matériaux LTAS - Vibrations et Identification des Structures, Bât. B52/3, B-4000 Liège o.bruls@ulg.ac.be

J. C. Golinval

Université de Liège, Département d'Aérospatiale, Mécanique et Matériaux LTAS - Vibrations et Identification des Structures, Bât. B52/3, B-4000 Liège jc.golinval@ulg.ac.be

Abstract

This paper concerns the design of an active control system for a hot-dip galvanizing line. The control system aims at reducing the vibrations of the steel strip in order to improve the quality of the product.

The mechanical structure is quite flexible and many vibration modes need to be controlled. The actuators and the sensors are collocated and the control law is a direct velocity feedback [1], which doesn't require any model of the plant. This control law adds damping on all the vibration modes and it guarantees the stability of the system.

The position of the actuators is chosen to maximize the controllability and the observability [2]. The relevance of this strategy is discussed.

The natural frequencies of the mechanical system are evaluated using the Finite Element Method. In this particular example, it was found that the frequencies of the flexion vibration modes almost match the frequencies of the torsion modes. The corresponding pole/zero pattern leads to very small root loci where the damping increment is strongly limited.

A simulation of the closed loop system is required to evaluate the performance of the active control and to choose the feedback gain. The time-domain evolution of the mechanical structure is computed using the Finite Element Method and an implicit integration scheme, as described in [3]. Assuming that the control system is digital and neglecting the dynamics of the actuators, the control system is introduced into the mechanical simulation as a users' routine called at each sampling time of the digital controller. This quite general approach allows to deal with nonlinear effects either in the mechanical structure or in the control system, what opens new perspectives in integrated simulation of controlled flexible mechanisms.

The simulation shows that a single actuator is not able to control the whole steel strip. Even if the gain increases, the controlled point becomes quickly a fixed point, and the vibration of the rest of the structure is not significantly attenuated. At least three actuators are necessary to get the expected performance.

- [1] A. Preumont. *Vibration Control of Active Structures*. Kluwer Academic, 1997.
- [2] W. K. Gawronski. *Dynamics and Control of Structures*. Springer, 1998.
- [3] M. Géradin and A. Cardona. Flexible Multibody Dynamics: A Finite Element Approach. John Wiley & Son, 1997.

Optimization of an allergen production from CHO-K1 cell cultures

X. Hulhoven

Service d'Automatique et d'Analyse des Systèmes, Université Libre de Bruxelles, CP 165/55, 50, Av. F. D. Roosevelt, B-1050 Brussels, Belgium xhulhove@labauto.ulb.ac.be

Ph. Bogaerts

Service d'Automatique et d'Analyse des Systèmes, Université Libre de Bruxelles, CP 165/55, 50, Av. F. D. Roosevelt, B-1050 Brussels, Belgium Philippe.Bogaerts@ulb.ac.be

1 Abstract

The aim of this study is to optimize the production of an allergen (pro-Derp1) produced from CHO-K1 cell cultures. In order to achieve this optimization, a model of batch cell cultures in a two liter tank reactor is identified in a three step procedure. In a first step, all the identifiable reaction schemes are generated [1]. In the next step, the pseudostochiometric coefficients of each scheme are identified. Finally, the kinetic coefficients are identified from the best reaction scheme [2]. The identification procedure is made on the basis of a set of three experiments that can be distinguished according to their initial concentration in glucose, the dissolved oxygen setpoint and the stirrer speed setpoints. A fourth experiment is used in order to submit the model to a cross validation test. Since the validations tests lead to very satisfactory results, the model is used to determine the optimal experimental condition. In this algorithm, the optimization criterion is the final concentration in pro-Derp1 and the optimization variables are the initial concentration in glucose and glutamate and the dissolved oxygen and stirrer speed setpoint. In order to remain within a realistic domain of experimental conditions, the cost function minimization is submitted to constraints on each optimization variable.

- [1] Ph. Bogaerts and A. Vande Wouwer. "Systematic generation of identifiable macroscopic reaction scheme". 8^{th} Int. Conf. on Comp. application in biotechnology, june 24-27, 2001, pp. 13-18.
- [2] Ph. Bogaerts and R. Hanus. "Macroscopic modelling of bioprocesses with a view to engineering applications. In: Focus on biotechnolgy (Ph. Thonart and M. Ed. Hofman)", volume 5 (Engineering and Manufacturing for biotechnology). Kluwer Academic Publishers, (2000), pp. 77-110.

Simulation analysis of a one-dimensional model for the sedimentation tank in activated sludge wastewater treatment

Liesbeth VERDICKT Jan VAN IMPE*
BioTeC - Bioprocess Technology and Control
Katholieke Universiteit Leuven
Kasteelpark Arenberg 22 B-3001 Leuven (Belgium)
Email: jan.vanimpe@agr.kuleuven.ac.be
*Corresponding author

1 Abstract

One-dimensional models for describing the secondary settler in activated sludge wastewater treatment are important with respect to process control and optimization. The usual starting point for one-dimensional modelling of the dynamics of settlers is the solids flux theory of Kynch (1952) [3], which assumes that the settling process can be determined entirely by a continuity equation. The theory can be made operational in computer programs by splitting up the secondary settler into n horizontal layers of equal height, and by discretizing the continuity equation on these layers. A major problem of the flux theory is the fact that the continuity equation predicts a constant concentration profile to occur in the settler at steady state, which is in contradiction with experimental observations. models have been proposed that overcome this difficulty. Today, the model published by Takács et al. (1991) [5] is widely used [1, 4].

In this contribution, the model of Takács *et al.* is thoroughly studied at the simulation level. Simulations have been performed to analyze the dynamic behavior of the concentration profile and to examine the influence on the steady state concentration profile of (*i*) the loading characteristics (influent concentration and flow rate), and (*ii*) the number of layers considered in the settler.

Simulating the model of Takács *et al.* (1991) with different values of the feed concentration and the influent flow rate shows that at a low influent flux, the amount of solids transported to the effluent is negligible. A *moderate* increase of the influent solids flux induces a higher steady state concentration in the underflow, while the effluent concentration remains unaffected. However, a large influent flux increase overloads the settler, resulting in an non-negligible steady state effluent concentration (after breakthrough of the inlet layer).

Simulations for different values of n reveals a major shortcoming of this model, namely, the inconsistency of the predictions with respect to the number of layers. This results in an identification problem: the parameter values need adjustment each time the resolution of the model is changed. The model of Hamilton $et\ al.\ (1992)\ [2]$ is put

forward as an alternative, because of its ability to describe a non-constant concentration profile on which the number of layers only has a resolution effect.

2 Acknowledgments

Author Liesbeth Verdickt is a research assistant with the Fund for Scientific Research-Flanders (FWO). Work supported in part by Projects OT/99/24 and IDO/00/008 of the Research Council of the Katholieke Universiteit Leuven and the Belgian Program on Interuniversity Poles of Attraction, initiated by the Belgian State, Prime Minister's Office for Science, Technology and Culture. The scientific responsibility is assumed by its authors.

- [1] Grijspeerdt, K., Vanrolleghem, P. and Verstraete, W. (1995) Selection of one-dimensional sedimentation: models for on-line use. *Water Science and Technology*, **31(2)**, 193-204
- [2] Hamilton, J., Jain, R., Antoniou, P., Svoronos, S.A., Koopman, B. and Lyberatos, G. (1992) Modeling and pilot-scale experimental verification for predenitrification process. *Journal of Environmental Engineering-ASCE*, **118(1)**, 38-55.
- [3] Kynch, G.J. (1952) A theory of sedimentation. *Trans. Faraday Soc.*, **48**, 166-176.
- [4] Pons, M., Copp, J., Jeppsson, U. and Spanjers, H. (2001) Benchmarking the evaluation of control strategies in wastewater treatment: the four-year story of the COST benchmark. Proceedings of the 8th International Conference on Computer Applications in Biotechnology, Québec City (Canada).
- [5] Takács, I., Patry, G.G. and Nolasco, D. (1991) A dynamic model of the clarification-thickening process. *Water Research*, **25(10)**, 1263-1271.

Reconstruction of the dynamic oxygen uptake rate and carbon dioxide evolution rate during a pulse experiment: a white-box modeling approach

H.H.J. Bloemen¹, L. Wu¹, W.M. van Gulik¹, M.H.G. Verhaegen², and J.J. Heijnen¹

¹Kluyver Laboratory for Biotechnology Faculty of Applied Sciences Delft University of Technology Julianalaan 67, 2628 BC Delft The Netherlands {H.Bloemen / L.Wu / W.vanGulik / J.J.Heijnen}@tnw.tudelft.nl

Delft University of Technology P.O. Box 5031, 2600 GA Delft The Netherlands M.H.G.Verhaegen@its.tudelft.nl

²Control Laboratory

Faculty of Information Technology and Systems

1 Introduction

The purpose of metabolic modeling is, in the first place, to understand the in vivo kinetics of the metabolism of a (micro) organism, and in the second place, to possibly reprogram this metabolism. The models often describe the metabolism under the assumption that the amount of enzymes remains constant, e.g. [1]. Both to reveal the metabolism and to verify the metabolic models, pulse experiments are conducted to a steady state culture of the particular organism. In order to be able to neglect the biosynthesis of new enzymes, the data should be collected within a time window of a few minutes after the pulse. This motivates the development of rapid sampling techniques for analyzing the dynamics of the different intra and extra cellular metabolites in this time window, e.g. [2]. Besides, often measurements are available of the oxygen (O₂) and carbon dioxide (CO₂) concentrations in the offgas of a fermenter, measured by a gas analyzer, and of the dissolved oxygen (DO) concentration in the fermentation broth.

The latter measurements can be used to reconstruct the dynamics of the oxygen uptake rate (OUR) and carbon dioxide evolution rate (CER) after the pulse [3], and in turn can be used to analyze the metabolism and to verify the metabolic models. To reconstruct the OUR and CER first a model is required that describes the dynamic relation between the OUR and CER (the inputs of the model) and the measured quantities provided by the gas analyzer and the DO sensor (the outputs of the model). Using this offgas model, the OUR and CER can be reconstructed from the data (collected during the pulse experiment) by using estimation techniques.

2 Modeling

The OUR and CER cannot be directly manipulated or measured. However, in order to retrieve information about the off-gas subsystem of a fermenter, the O₂ and CO₂ concentrations of the gas feed can be varied in an identification experiment. In [3] a black-box modeling approach has been adopted. Alternatively, this research

considers a white-box modeling approach. The white-box modeling approach has several benefits:

- 1. for the identification of the model parameters the restriction that only the O_2 and CO_2 concentrations of the gas feed can be varied requires no approximation.
- 2. it is easy to incorporate the nonlinearity into the model that is due to a net gas production or consumption during the pulse experiment.

3 Estimation

Given an accurate model of the off-gas system, the OUR and CER can be reconstructed from measurements of the O_2 and CO_2 concentrations in the off-gas and the DO concentration. In this research the OUR and CER are modeled as integrated white noise. By augmenting the model of the off-gas system with these integrators, OUR and CER can be recovered by using Kalman filtering. It can be demonstrated that the influence of the nonlinearity of the model (due to a net gas production or consumption) on the estimate of the OUR, is significant. The measured responses of the outputs can be tracked accurately using Extended Kalman filtering for the nonlinear white-box model. In this way the dynamics of the OUR and CER, that are states of the augmented model, can be reconstructed accurately.

- [1] M. Rizzi, M. Baltes, U. Theobald, and M. Reuss, "In vivo analysis of metabolic dynamics in *Saccharomyces cerevisiae*: II. Mathematical model," Biotechnology and Bioengineering 55(4), pp. 592-608, 1997.
- [2] U. Theobald, W. Mailinger, M. Baltes, M. Rizzi, and M. Reuss, "In vivo analysis of metabolic dynamics in *Saccharomyces cerevisiae*: I. Experimental observations," Biotechnology and Bioengineering 55(2), pp. 305-316, 1997
- [3] L. Wu, H.C. Lange, W.M. van Gulik, and J.J. Heijnen, "Determination of *in vivo* oxygen uptake and carbon dioxide evolution rates from off-gas measurements under highly dynamic conditions," Submitted

Distributed parameter modeling of a fixed-bed biofilter

Alain Vande Wouwer, Christine Renotte and Marcel Remy Laboratoire d'Automatique, Faculté Polytechnique de Mons, 7000 Mons, Belgium (vdw@autom.fpms.ac.be)

Isabelle Queinnec Laboratoire d'Analyse et d'Architecture des Systèmes 31077 Toulouse, France (queinnec@laas.fr)

Philippe Bogaerts
Service d'Automatique et d'Analyse des Systèmes, Université Libre de Bruxelles,
1050 Brussels, Belgium
(pbogaert@labauto.ulb.ac.be)

Nitrogen removal is an important step in the treatment of municipal wastewater. Over the past several years, biofilter systems have received considerable attention; see for instance the conference proceedings and journals of the International Water Association (IWA) (e.g. [4]. The main advantages of these wastewater treatment systems are their ease of use, compactness, efficiency, and low energy consumption. New biofilters including dual-column systems have recently been proposed to achieve pretreatment, nitrogen and/or phosphorus removal [3, 5].

Based on experimental data collected from a pilot-scale fixed-bed biofilter, the objective of this work is to develop and validate a dynamic model, which allows the evolution of the several component concentration profiles to be reproduced. This model can be used for simulation purposes (e.g. for system analysis and design) or as a basis for the development of a software sensor (which can be used to estimate unmeasured variables on-line).

The modeling task involves the selection of appropriate reaction scheme and kinetics and the derivation of mass balance partial differential equations (PDEs). The unknown model parameters are estimated by minimizing an ad-hoc error criterion measuring the deviation between the experimental signals and the model prediction. Particular attention is paid to the assumptions on the measurement errors, and the corresponding formulation of an error criterion.

Actually, this work builds upon a previous modeling study reported in [1, 2], which was carried out using the same pilot plant. However, this study was based on the assumption that steady state operations were achieved after a few hours, which is not in agreement with experimental observations (in fact, the biofilter experiences very long transient phases due to the variations in the input flow rate and concentrations). As a consequence, the parameter estimation problem was not properly formulated, leading to severe model inaccuracies. Here, a new model structure is proposed, and a criterion taking into account the measurement errors is minimized to estimate the unknown model parameters and initial conditions.

- [1] Bourrel S. (1996). Estimation et Commande d'un Procédé à Paramètres Répartis Utilisé pour le Traitement Biologique de l'Eau à Potabiliser, Ph.D. Thesis, Université Paul Sabatier, Toulouse, France.
- [2] Bourrel S., Dochain D., Babary J.P. and I. Queinnec (2000). Modelling; Identification and Control of a Denitrifying biofilter, *Journal of process Control* 10, 73-91.
- [3] Falkentoft C.M., Harremoes P., Moesbeck H. and P. Wilderer (2000). Combined Denitrification and Phosphorus Removal in a Biofilter, *Water Science and Technology* 41, 493-501.
- [4] Oh J., Yoon S.M., and J.M. Park (2001). Denitrification in Submerged Biofilters of Concentrated-Nitrate Wastewater, *Water Science and Technology* 43, 217-223.
- [5] Pak D. and W. Chang (2000). Simultaneous Removal of Nitrogen and Phosphorus in a Two-Biofilter System, *Water Science and Technology* 41, 101-106.

Maximum likelihood estimation of pseudo-stoichiometric coefficient on the basis of incomplete data

J.-L. Delcoux, M. Kinnaert and Ph. Bogaerts
Service d'Automatique et d'Analyse des Systèmes, Université Libre de Bruxelles,
CP 165/55, 50, Av. F. D. Roosevelt, B-1050 Brussels, Belgium
jdelcoux@labauto.ulb.ac.be, kinnaert@labauto.ulb.ac.be, Philippe.Bogaerts@ulb.ac.be

1 Abstract

Mathematical modelling of bioprocesses can be based on mass balances at a macroscopic reaction scheme level. This paper deals with the use of incomplete data in the experimental identification of the pseudo-stoichiometric coefficient matrix. Data are made of measured component concentrations obtained at different times in different culture experiments. Incomplete data correspond to measurement times for which some component concentrations are not available.

A reaction scheme [1], involving N components, is of the form

$$\sum_{i \in R_k} (-\nu_{i,k}) \xi_i \stackrel{\varphi_k}{\to} \sum_{j \in P_k} \nu_{j,k} \xi_j \tag{1}$$

for k=1,...M where M is the number of reactions, ξ_i the i-th component, φ_k the reaction rate, $v_{i,k}$ and $v_{j,k}$ the pseudo-stoichiometric (yield) coefficients ($v_{i,k} < 0$ if ξ_i is consumed in reaction k and $v_{j,k} > 0$ if ξ_j is produced in reaction k), R_k the set of indices of the components which are reactants (or catalysts) in reaction k and k the set of indices of the components which are products (or catalysts or autocatalysts) in reaction k. The mass balance is written as

$$d\xi(t)/dt = K\varphi(\xi, t) - D(t)\xi(t) + u(t) \tag{2}$$

where $\xi \in \Re^N$ is the vector of concentrations, $K \in \Re^{N \times M}$ is the pseudo-stoichiometric coefficient matrix $(N \ge M)$, $\varphi \in \Re^M$ is the vector of reaction rates, $D \in \Re$ is the dilution rate and $u \in \Re^N$ is the vector of the net flow rates (incoming minus outgoing).

It is possible to identify K independently of the knowledge of φ . Let G be a matrix such that

$$G^T K = 0 (3)$$

By multiplying the mass balance by G^T a φ -independent differential equation is obtained. Its analytical solution is easily calculated and this allows one to identify K using a maximum likelihood method [3]. The identified K is the one that minimizes a cost function L where the experimental data ξ_{msk} appear. ξ_{msk} is the k-th measured point in the s-th culture experiment. Each ξ_{msk} appears in L combined with G in the product $G^T\xi_{msk}$. This product is generally impossible to calculate if each of the N components of ξ_{msk}

is not known. For that reason, the not completely known ξ_{msk} are usually rejected.

However these not completely known ξ_{msk} do contain information relative to the pseudo-stoichiometry. The present paper proposes a method to use this information anyway. Instead of an unique matrix G, different matrices G_{sk} are used. They are still solutions of eq. (3) but their rows corresponding to the missing components of ξ_{msk} are zero, which allows the calculation of the $G_{sk}^T\xi_{msk}$. The matrices G_{sk} are computed by performing a singular values decomposition of a suitable matrix deduced from K.

A four component case study has been presented by Bogaerts and Vande Wouwer [2]. They simulated the growth of a biomass X on two substrates S_1 and S_2 , with production of a product P. Details are given in [2]. The simulation results, corrupted by noise, were used as pseudo-experimental results in order to test their method of systematic generation of reaction schemes [2]. In the case M=2 reactions, six reaction schemes were obtained.

These pseudo-experimental results were modified by suppressing one of the 4 measurements in each of the pseudo-experimental points: in a quarter of the points, the data relative to X were suppressed, in a second quarter those relative to S_1 were suppressed, and so on. These modified results were used to perform systematic generation of reaction schemes. The six schemes obtained were remarkably similar to the ones obtained using the complete data.

- [1] Bastin G. and Dochain D. (1990) *On-line estimation* and adaptative control of bioreactors. Elsevier, Amsterdam
- [2] Ph. Bogaerts and A. Vande Wouwer. "Systematic generation of identifiable macroscopic reaction scheme". 8th Int. Conf. on Comp. application in biotechnology, june 24-27, 2001, pp. 13-18.
- [3] Ph. Bogaerts and R. Hanus. "Macroscopic modelling of bioprocesses with a view to engineering applications. In: Focus on biotechnolgy (Ph. Thonart and M. Ed. Hofman)", volume 5 (Engineering and Manufacturing for biotechnology). Kluwer Academic Publishers, (2000), pp. 77-110.

Optimal parameter estimation as a means to measure atom positions from electron microscopy images

Arjan den Dekker and Sandra Van Aert Signals, Systems and Control Group Department of Applied Physics Delft University of Technology P.O. Box 5046, 2600 GA Delft The Netherlands Email: a.j.dendekker@tn.tudelft.nl

1 Introduction

As scientists manage to control the structure of materials on an ever-finer scale, more and more materials are being developed with interesting properties, which are mainly related to their nanostructure. In parallel, one sees an evolution in solid-state theory where materials properties are increasingly better understood from first principles theoretical calculations. The merging of these fields will enable materials science to evolve into materials design [1], that is, from describing and understanding towards predicting of materials properties. If this evolution is to be continued, it is imperative that the characterization techniques keep pace. In order to correlate real properties with theoretical simulations, characterization methods in the future need to be able to determine atom positions in aperiodic structures with a precision of the order of 0.01 Å.

2 Method

In principle, high-resolution electron microscopy (HREM) is the most appropriate technique to provide the required precision, in spite of the fact that the resolution of modern electron microscopes does not exceed 1 Å. One is inclined to think that a precision of 0.01 Å requires a resolution of 0.01 Å, which is far beyond the present possibilities. However, precision and resolution are different things. It should be realized that it is precise measurement of the structure parameters of the specimen under study that one is interested in, and not the HREM images as such. Therefore, the electron microscope should be regarded as a measurement system and not as a pure imaging instrument. Extraction of structure information from (noisy) HREM images can then be formulated as a parameter estimation problem. For this purpose, a physical model is required describing the electron object interaction, the transfer in the microscope, as well as the image detection. This model contains unknown parameters characterizing the structure of the object, such as the positions of the atom columns. These parameters are estimated by fitting the model to the experimentally obtained images using a criterion of goodness of fit. This is usually a non-linear optimisation problem, since most structure parameters enter the model non-linearly.

3 Precision and experimental design: recent results

The attainable precision may be further increased if quantitative structure determination is accompanied by

statistical experimental design. Use of the concept of Fisher information allows one to derive an expression for the highest precision with which structure parameters can be estimated unbiasedly from a set of observations (i.e., image pixel values) assumed to obey a certain statistical distribution [2]. This expression can be used to evaluate the sensitivity of the precision to several adjustable experimental parameters. The optimum design of an HREM experiment is found in the sense of the experiment producing the highest attainable precision. Clearly, the availability of an expression for the attainable precision allows quantitative evaluation and comparison of microscopic settings and new instrumental developments. To illustrate this principle, suppose that the microscope is able to visualize an atom (or an atom column in projection) and that d is the width of the image of the atom, i.e., the 'resolution' in the sense of Lord Rayleigh. The thus defined resolution will depend on both object parameters, such as the weight of the column, and microscope parameters, such as defocus, and spherical aberration constant. Then it can be shown that the highest attainable precision (i.e., the lowest standard deviation) with which the position of the atom can be estimated is of the order of $d/N^{1/2}$, with N the total number of (detected) electron counts forming the image of the atom. It is now clear that if one wants to optimise the design of an HREM experiment in terms of precision, it is not only the resolution that matters but also the electron dose. For example, it turns out that although the incorporation of a monochromator in a transmission electron microscope (TEM) does improve the resolution, it usually doesn't pay off in terms of precision, since the improvement of resolution is accompanied by a loss of electrons and thus signal-to-noise ratio [3]. Another result is the finding that although the correction of the spherical aberration in a TEM improves the resolution, it does not generally result in a higher precision [4].

- [1] G.B. Olson, Science 288, 993-998 (2000).
- [2] A. van den Bos and A.J. den Dekker, In: P.W. Hawkes (ed.), Advances in Imaging and Electron Physics **117**, 241-360, Academic Press, 2001.
- [3] A.J. den Dekker, S. Van Aert, D. Van Dyck, A. van den Bos, and P. Geuens, Ultramicroscopy **89**, 275-290 (2001).
- [4] A.J. den Dekker, J. Sijbers, and D. Van Dyck, Journal of Microscopy **194**, 95-104 (1999).

Nonlinear modelling of dynamic behaviour of looper in a hot finishing mill and control approach

F. Renard, M. Remy Laboratoire d'Automatique, Faculté Polytechnique de Mons, Bd Dolez 31, B-7000 Mons, Belgium renard@fpms.ac.be B. Petit
IRSID (Usinor)
Voie Romaine - B.P. 30320
57283 Maizieres Les Metz, France bernard.petit@irsid.usinor.com

Abstract

The purpose of a hot finishing mill is to turn reheated steel slabs into strips which have the required thickness as constant as possible. Several passes of rolling are executed by tandem rolling with six or seven stands. Between each stand a motor driven looper is used to keep the strip tension at the reference. The looper fulfils an important role in tension control: it can absorb the excess amount of stored strip by adjusting the loop length of the strip between the stands. Tension and looper control is the key of successful operations in hot strip mill. Proper positioning of the looper is also important for stable operations, so the problem is simultaneous control of the looper position and the interstand tension.

In this lecture, a complete modelling of the process is presented. The modelling is applied to the Carlam hot strip mill of the steel maker Usinor (Charleroi, Belgium). Processing industrial data show the presence of strong nonlinearities (friction phenomenon, ...). Friction and especially static friction can severely limit the performance in terms of increasing tracking errors and the occurrence of limit cycle. In that way, a simple model of the friction characteristic is proposed and a method to identify the model parameters during fast industrial experiments has been developed on the basis of hysteresis cycle. The results show the importance of static friction levels.

Synchronization in a Population of Nearly Identical Oscillators

Jonathan Rogge
SYSTeMS
Universiteit Gent
B-9052 Zwijnaarde, Belgium
e-mail: jonathan.rogge@rug.ac.be

Dirk Aeyels
SYSTeMS
Universiteit Gent
B-9052 Zwijnaarde, Belgium
e-mail: dirk.aeyels@rug.ac.be

1 Constructing a model

Nowadays a lot of interest in Systems Theory is directed to problems in which separate systems are coupled to each other. We put some restrictions on the networks/populations that we want to investigate [1]. The term "cell" is used to indicate an indivisible subsystem of the network. We only consider networks where each cell interacts with all the other cells. The coupling is assumed to be uniform, i.e. between every pair of cells the interaction is of the same type and has the same strength. Each cell of the network is assumed to be a stable limit cycle oscillator. This means that each cell executes a periodic behaviour with a standard waveform to which it returns after small perturbations. The interaction between separate cells is assumed to be weak in order to ensure that each cell keeps moving on its limit cycle, without this cycle getting deformed. Therefore we assume that the state dynamics

$$\dot{x} = f_i(x), \qquad x \in \mathbb{R}^n, \quad f_i : \mathbb{R}^n \to \mathbb{R}^n$$

of each cell reduces to a "phase dynamics"

$$\dot{\theta} = \omega_i, \qquad \theta \in S^1, \quad \omega_i \in \mathbb{R},$$

with i indicating the index of the cell. When the limit cycle is parametrized properly in θ , ω_i is constant in time. This constant ω_i is called the natural frequency of the i-th cell. The only difference between the cells of the population is the difference in natural frequency.

The system equations of a population consisting of N cells are

$$\dot{\theta_i} = \omega_i + \frac{K}{N} \sum_{j=1}^N \sin(\theta_j - \theta_i), \quad i = 1, \dots, N.$$

The parameter K denotes the strength of the coupling and N is the number of cells. The interaction is implemented by a sine function. We study the model as such. Our model is therefore more detailed than the current approach in the literature [1], [2].

2 Partial and Full Synchronization

By changing the parameter K the behaviour of the system can change as well. For K=0, the state of each cell moves on its limit cycle with its own natural frequency. In the case

 $\omega_i \neq \omega_j$, $\forall i, j \in \{1, ..., N\}$, this behaviour is called incoherent. An *incoherent motion* is defined as follows: all phase differences $\theta_i - \theta_j$, $i \neq j$ are unbounded. If $K \neq 0$ the cells start to mutually influence each other. As long as this coupling strength is smaller than a threshold value K_P the cells act incoherently.

For K between the value K_P and some value K_T , one can discern a partially synchronizing of the population. A network of cells exhibits *partial synchronization* when between at least two cells of the network the phase difference has a lower and an upper bound. Those cells are said to entrain each other.

If the parameter K exceeds the threshold value K_T , the system starts to exhibit *full synchronization*, for all time t > T, for some T > 0. Full synchronization of the network means that the phase difference between every two cells of the network is constant in time.

If K increases further, the constant phase differences become smaller. If $K \to \infty$, the phase differences tend to zero and all the cells possess the same phase. For a network of three cells, one can calculate the value of K_T with the aid of bifurcation theory and in principle this can be done for any number of cells.

3 Relation to the literature

Our results can be compared to existing results in the literature. In [2], an analytical expression is obtained for a threshold value K_C between incoherence and partial synchronization. From our detailed model we realize that such a bifurcation indeed exists, but we do not have an analytical result. On the other hand, we can prove the existence of a bifurcation value K_T between partial and full synchronization. This seems to be an original result.

- [1] Y. Kuramoto. Cooperative dynamics of oscillator community. *Prog. Theoret. Phys. Suppl.*, 79:223–240, 1984.
- [2] S.H. Strogatz. From Kuramoto to Crawford: Exploring the onset of synchronization in populations of coupled oscillators. *Physica D*, 143:1–20, 2000.

Bayesian Inference for LS-SVMs on Large Datasets and its Implementation

Tony Van Gestel, Johan A.K. Suykens, Kristiaan Pelckmans, Bart De Moor & Joos Vandewalle ESAT SCD-SISTA, K.U.Leuven, Kasteelpark Arenberg 10, B-3001 Leuven, Belgium E-mail: {vangeste,suykens,kpelckma,demoor,vdwalle}@esat.kuleuven.ac.be

Abstract

In Support Vector Machines (SVMs) [7] and Least Squares Support Vector Machines (LS-SVMs) [3, 4] for nonlinear classification and function estimation the solutions are obtained from a convex quadratic programming problem and a linear Karush-Kuhn-Tucker system, respectively. As the Least Squares Support Vector Machines involve the use of a least squares cost function, the sparseness property of SVMs is lost. On the other hand the LS-SVMs have been related to regularization networks, Gaussian Processes and kernel Fisher Discriminant Analysis [1, 6, 8]. Sparseness in the LS-SVM can be obtained by sequentially pruning the support value spectrum, while robustness is obtained by using a weighted least squares cost function. Compared to multilayer perceptrons (MLPs), the SVMs have the advantage of solving a convex optimization problem, while the cost function for MLPs typically has multiple local minima. On the other hand the SVM formulations involve the use of a square kernel matrix with size equal to the number of data points. This makes a straightforward implementation of kernel methods computationally less attractive for large data sets. Therefor, large scale methods like conjugate gradient algorithms have been developed and implemented in LS-SVMlab in order to solve the optimization problem on the first level of inference.

A powerful tool to estimate the uncertainties on the prediction and classification of MLPs is the evidence framework [2]. Bayesian inference can also be used to select the regularization hyperparameters within the statistical framework and to perform model comparison. In Bayesian methods for LS-SVMs the kernel matrix also appears in expressions for Bayesian hyperparameter inference [5, 6]. The inverse kernel matrix is also needed when calculating error bars or class uncertainties on the output of the regressor or classifier, respectively.

Here we discuss large scale approximations for Bayesian inference for LS-SVMs. A practical implementation using the Nyström method is implemented in LS-SVMlab which allows to obtain approximate expressions at the different levels of inference within the evidence framework. Although being a sampling method, it can be shown that the approximation is exact when the sample feature space spans the feature space of the whole training data set. The Nyström method was implemented in the matlab LS-SVMlab tool-

box and applied on UCI data sets like, e.g., the the adult data set with 45222 data points. The use of the Nyström method allows to perform hyperparameter selection for LS-SVMs on the so-called second and third level of inference. This selection criterion yields comparable performances with hyperparameter selection from cross-validation. It also allows to infer the optimal kernel parameters of the kernel function, which can be related to the relevance of the different inputs. This inference is called Automatic Relevance Determination and is used for input selection in nonlinear kernel-based function estimation and classification.

Acknowledgments

This work was supported by grants and projects from the Flemish Gov.: (Research council KULeuven: Grants, GOA-Mefisto 666; FWO-Vlaanderen: Grants, res. proj. G.0240.99, G.0256.97, G.0407.02 and comm. (ICCoS and ANMMM); AWI: Bil. Int. Coll.; IWT: STWW Eureka SINOPSYS, IMPACT); from the Belgian Fed. Gov. (Interuniv. Attr. Poles: IUAP-IV/02, IV/24; Program Dur. Dev.); from the Eur. Comm.: (TMR Netw. (Alapedes, Niconet); Science: ERNSI). J.A.K. Suykens is a Postdoctoral Researcher with the Fund for Scientific Research-Flanders (FWO-Vlaanderen). The scientific responsibility is assumed by its authors.

- [1] Evgeniou, T., Pontil, M., & Poggio, T. "Regularization Networks and Support Vector Machines," *Advances in Computational Mathematics*, vol. 13, 1-50, 2001.
- [2] MacKay, D.J.C. "Probable Networks and Plausible Predictions A Review of Practical Bayesian Methods for Supervised Neural Networks," *Network: Computation in Neural Systems*, 6, 469-505, 1995.
- [3] Suykens, J.A.K. & Vandewalle, J. "Least squares support vector machine classifiers," *Neural Processing Letters*, *9*, 293-300, 1999.
- [4] Suykens, J.A.K., "Support Vector Machines: a nonlinear modelling and control perspective," *European Journal of Control*, Special Issue on fundamental issues in control, vol. 7, no. 2-3, Aug. 2001, pp. 311-327.
- [5] Van Gestel T., Suykens J.A.K., Baestaens D.-E., Lambrechts A., Lanckriet G., Vandaele B., De Moor B., Vandewalle J. "Predicting Financial Time Series using Least Squares Support Vector Machines within the Evidence Framework," *IEEE Transactions on Neural Networks*, vol. 12(4), pp. 809-821, 2001.
- [6] Van Gestel, T., Suykens J.A.K., Lanckriet, G., Lambrechts, A., De Moor, B. & Vandewalle, J. "Bayesian Framework for Least Squares Support Vector Machine Classifiers, Gaussian Processes and Kernel Fisher Discriminant Analysis," *Neural Computation*, in press.
- [7] Vapnik, V. Statistical learning theory, John Wiley, New-York, 1998.
- [8] Williams, C.K.I., & Seeger, M. "Using the Nyström Method to Speed Up Kernel Machines," In T. Leen, T. Dietterich, V. Tresp (Eds.), *Proc. NIPS'2000*, vol. 13, MIT press.

Port-Based Thermo-Fluid Models

Philippus J. Feenstra and Peter C. Breedveld
Drebbel Institute for Mechatronics & CE-lab, Faculty of Electrical Engineering
University of Twente,
P.O. Box 217, 7500 AE Enschede
The Netherlands
{p.j.feenstra, p.c.breedveld}@el.utwente.nl

1 Abstract

The port-based approach that can be represented by bond graphs or iconic diagrams optimally supports a multidomain-modeling context. This approach is for mechanical, hydraulic and electrical systems clearly described in the literature. However, thermal systems or in particular thermo-fluid systems can be described by various port-based approaches. Some of these approaches are discussed.

Two bond graph approaches are useful for modeling thermofluid systems in a simulation package (e.g. 20-sim). The pseudo bond approach (effort and flow are dynamically conjugated instead of power conjugated as in true powerbonds), by Karnopp et al [1] is easy to implement and therefore often used as its use of variables coincides with the common approach. However, it may lead to wrong results, e.g. in combination with transformers it becomes invalid. Breedveld's approach [2] provides insight and a more systematic way to model the convection process, unlike Karnopp's approach. (The term convection is used for energy transport by a moving fluid.) A drawback is that the engineer is not always acquainted with the conjugate power variables in this domain. Apart from the above-mentioned approaches, Brown's convection bond approach [3] is investigated; he proposes to use a convection bond in order to cancel the redundant information. The result of this new representation is a notation that differs significantly from conventional bond graphs and is not easily incorporated into most bond graph modeling environments. Finally, Shoureshi's approach [4] is examined for incompressible fluids, which does not correspond to thermodynamics and is simply incorrect. A major conclusion concerning the different approaches is that the three correct approaches can be transformed into each other, and give exactly the same results in the test case of an ideal gas with irreversible convection [5].

A second, but related topic is the causality assignment procedure of thermal elements. Causality assignment is necessary in order to get assignment statements in a form that is optimal for numerical simulation. The conventional causality assignment algorithms do not handle all assignments of thermal elements. A heat conduction- or RS-element has a particular causal constraint. A comparable situation occurs for a multiport C-element representing a single component

system. An algorithm is discussed for the causality assignment of a heat-conduction RS-element and for the three-port C

A model of a dual-sided air cylinder, see figure 1, will used as an example to illustrate the various approaches and representations.

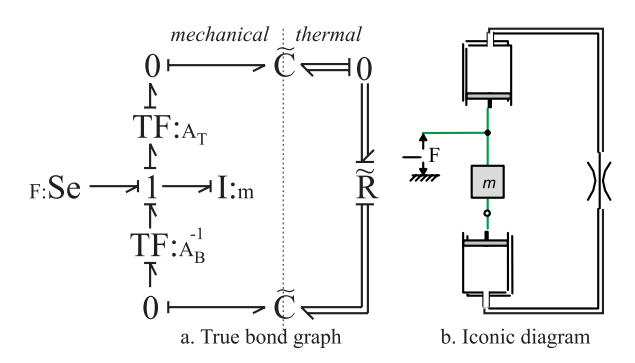


Figure 1: Dual sided air cylinder in two representations

- [1] Karnopp, D. et al (1990) Systems Dynamics: A Unified Approach, 2^{nd} edn, John Wiley and Sons, NY.
- [2] Breedveld, P.C. (1984) *Physical Systems Theory in Terms of Bond Graphs*, University of Twente, NL, distributed by the author.
- [3] Brown, F.T. (1991) *Convection bonds and bond graphs*, Journal of the Franklin Institute 328(5/6): 871-886.
- [4] Shoureshi, R et al (1984) Analytical and experimental investigation of flow-reversible heat exchangers using temperature-entropy bond graphs, Transactions of the ASME 106: 170-175.
- [5] Feenstra, P.J. (2000) A Library of Port-based Thermo-Fluid Submodels, M.Sc. Report 040R2000, Control Laboratory, University of Twente, NL.

Semantics for Hybrid Systems

P.J.L. Cuijpers, M.A. Reniers, W.P.M.H. Heemels TU/e P.J.L.Cuijpers@tue.nl

1 Abstract

The theory of hybrid systems studies the interaction between continuous and discrete behaviour. When discrete software is combined with mechanical and electrical components, or is interacting with, for example, chemical processes, an embedded system arises in which the interaction between the continuous behaviour of the components and processes and the discrete behaviour of the software is important. Although there are good methods for analizing continuous behaviour (control science / system theory) as well as for analizing discrete behaviour (computer science / automata and process theory), the interaction between those two fields is largely unexplored. There are only a few models that can handle (some) interaction, and often these models are still focussed on one of the two original fields.

In practice, often the discrete part of a system is described and analysed using methods from computer science, while the continuous part is handled by control science. The design is such that interaction is surpressed to a minimum. Because of this surpressed interaction, analysis is possible to some extend, but it limits the options during the design process. This is the main reason for the development of a theory on hybrid systems that allows for analysis of broader types of interaction.

In this presentation, we work on the mathematical modelling of hybrid systems, from a semantical point of view. We focus on two main existing semantical models for describing dynamics, namely the behavioural models, introduced by Polderman and Willems [1] and the (timed) transition system approach, known from computer science [3]. These two classical models are combined in three different ways, resulting in: hybrid automata [5], rich time behaviours [4] and a new model originating from the machines introduced by Sontag [2]. We compare the expressivity of these three models, and discuss their useability as models for hybrid systems.

- [1] J.W. Polderman and J.C. Willems Introduction to Mathematical Systems Theory, A Behavioural Approach Texts in Applied Mathematics, Volume 26 Springer-Verlag 1998
- [2] E.D. Sontag Mathematical Control Theory, Deterministic Finite Dimensional Systems Texts in Applied Mathematics, Volume 6 Springer-Verlag 1998

- [3] J.A. Bergstra and A. Ponse and S.A. Smolka Handbook of Process Algebra Elsevier 2001, Amsterdam
- [4] A.J. van der Schaft and J.M. Schumacher An Introduction to Hybrid Dynamical Systems Lecture Notes in Control and Information Sciences, Volume 251 Springer-Verlag 2000
- [5] N. Lynch and R. Segala and F. Vaandrager Hybrid I/O automata revisited In: Proceedings Fourth International Workshop on Hybrid Systems: Computation and Control (HSCC'01) Editors: M.D. Di Benedetto and A.L. Sangiovanni-Vincentelli Lecture Notes in Computer Science, Volume 2034, p. 403-417 Springer-Verlag 2001

Systematic Modelling Approach for First Principle Dynamic Process Models

M.R. Westerweele and H.A. Preisig
Systems and Control Group, Eindhoven University of Technology
P.O. Box 513, 5600 MB Eindhoven, The Netherlands
M.R. Westerweele@tue.nl

1 Introduction

We are concerned with the mathematical modelling of macroscopic physical-chemical-biological processes for the purpose of modelling chemical or biological plants. The ultimate goal of our research is to implement a structured modelling methodology in a computer program, called the Modeller, which aims at effectively assisting in the development of first principle based dynamic process models. The underlying methodology of such a computer program must, of course, be well structured and put on a firm scientific foundation, such that it can handle a wide range of problems. The output of the computer program is a first principles based mathematical model, which can serve as an input to existing modelling languages and/or simulation packages, such as gProms, ASCEND, Modelica, Matlab, Maple, Chi.

2 Modelling Methodology

The modelling methodology we use is based on the hierarchical decomposition of processes into networks of *elementary systems* and *physical connections* [4]. Elementary systems are regarded as thermodynamic simple systems and represent (lumped) capacities able to store extensive quantities (such as component mass, energy and momentum). The connections have no capacity and represent the transfer of extensive quantities between these systems.

3 Presentation

In this presentation we show that the dynamic part (i.e. the differential equations) of physical-chemical-biological processes can be represented in a concise, abstract canonical form, which can be totally isolated from the static part (i.e. the algebraic equations). This canonical form, which is the smallest representation possible, incorporates very visibly the structure of the process model as it was defined by the person who modelled the process[5]: The system decomposition (physical topology) and the species distribution (species topology) are very visible in the model definition. The transport and productions rates always appear linearly in the balance equations, when presented in this form. The nonlinearities of a process will therefore always emerge in the algebraic realations of the model. This formalization allows us to develop formal model reduction procedures, which are suitable for computer-based model reduction. Another important application of identifying structures in the modelling process, is to use the extra available information to perform efficient model manipulations in order to achieve, for example, superior numerical performance. Ideas to use model structure for DAE index reduction, for example, can be found in [1], [2] and [3].

Furthermore, it is shown that the separation of the dynamics and statics of the process model makes it possible to do far reaching analysis (such as completeness checks, consistency, causal order) at the level of the individual systems and connections (during the modelling session). This is different from what is being done by current modelling languages (such as Modelica, ABBACUS II, ASCEND): they all gather all information from a modelling-session, then throw it all on one big stack and then the symbolic analysis is done.

- [1] W. Marquardt. Numerical methods for the simulation of differential-algebraic process models. In R. Berber, editor, *Methods of model based control*, volume 293 of *NATO-ASI Ser. E, Applied Sciences*, pages 42–79. Kluwer Academic Publ., Dordrecht, 1995.
- [2] Håvard I. Moe. *Dynamic process simulation: studies on modeling and index reduction*. PhD thesis, University of Trondheim, 1995.
- [3] M. Akhssay M.R. Westerweele and H.A. Preisig. Modelling of systems with equilibrium reactions. pages 697–700. Vienna University of Technology, Austria, February 2000.
- [4] Heinz A. Preisig. Computer aided modeling: species topology. In *Preprints IFAC Symp. ADCHEM'94*, pages 143–148, Kyoto, Japan, May 1994.
- [5] M.R. Westerweele and H.A. Preisig, Minimal representation of first principle process models. ESCAPE, S47-S52. Elsevier Science Ltd. Scanticon Comwell Kolding. May 2001

Petri Nets Model Based Fault Detection In Power Systems

George Jiroveanu Systems Research Group, Ghent University jirog@systems.rug.ac.be

Rene Boel Systems Research Group, Ghent University Rene.Boel@rug.ac.be

Abstract

When a fault occurs in a certain transmission or distribution network, circuit breakers must automatically open switches to ensure that power is no longer fed to the faulty line or to the smallest possibile zone including the fault.

The circuit breakers (CBs) are controlled at the local level by relays. When a relay detects a fault in its covering zone it automatically triggers the appropriate circuit breaker to clear the fault. Relays are also responsabile for sending signals about their observation and about their action to the dispatching center (via separate comunication links).

The monitoring system in the dispatching center can receive several tens of messages per second making the interpretation difficult, especially in the case of multiple faults or incorrect operation of protective devices (PDs) [1, 2].

Automatic interpretation of alarms (messages from different substation about CBs and PDs activity) may have either of the following objectives:

- to determine the causes of a dysfunction, to provide explanation to the operator or to predict future behavior of the system (e.g. to assess the degree of emergency of a situation)
- to react automatically like a back-up protection in case of circuit breaker failure or missoperation of any protective device. Expert systems have been proposed for this back-up fault detection and protection [4].

In the last years the model based approach to fault detection has become more and more important thanks to the advances in available tools. We design fault diagnosis algorithms based on mathematical model, describing the power systems as a timed discrete event systems. Although the power system itself is a continous time system, its protection scheme may be viewed as a discrete event system.

Petri Nets are basicaly developed for describing and analysing information flow, and they are excellent tools for modeling asynchronous concurrent systems such as computer systems and manufacturing systems, as well as power protection systems [3, 5, 6].

We have developed a timed Petri Net model of the PDs in a substation. Some of the events in this model are observable, while others (e.g. short-circuits) are unobservable. Using timed Petri Nets models for different substations (capturing the interactions between PDs and CBs) and a model of the information they exchange, we derive a hierachical fault diagnoser. The first level contains local diagnosers that analyse the behavior of the PDs and CBs using only information from the substation in which they are placed. They send a "condensed report" to the high level diagnoser. Based on the information from different substations, the high level dispatching center may decide the proper action for the faulted area.

This fault diagnoser allows fast location of any modelled fault even when some of the sensors and actuators are unreliable. The method can be used for on-line aplications in both transmission and distribution networks to assist dispatching center operators during emergencies. It can e.g. be used to determine the circuit breakers to be triggerd so as to disconnect the smallest possible zone needed to prevent unsafe operations of the power system.

- [1] C.Fukui and J.Kawakami. An expert system for fault section estimation using information from protective relays and circuit breaker. *IEEE Trans. on Power Delivery*, 1(4):83–90, 1986.
- [2] M.O. Cordier, P. Laborie, and et. al. Monitoring and alarm interpretation in industrial environments. *AI Communications Journal*, 11(3/4):139–173, 1998.
- [3] C. Hadjicostis and G. Verghese. Power systems monitoring based on relay and circuit breaker. *IEE Proc.-Gener. Transm. Distrib.*, 147(5):299–303, 2000.
- [4] J.C.Tan, P.A. Crossley, D. Kirschen, and J. Goody. An expert system for the back-up protection of a transmission network. *IEEE Trans. On Power Delivery*, 15(2):508–513, 2000.
- [5] L. Jenkins and H.P. Khincha. Deterministic and stochastic Petri net models of protection schemes. *IEEE Trans. On Power Delivery*, 7(1):84–90, 1992.
- [6] K.L.Lo, H.S.Ng, D.M. Grant, and J.Trecat. Extended Petri net models for fault diagnosis for substation automation. *IEE Proc.-Gener. Transm. Distrib*, 146(3):229–234, 1999.

Observer Design for a Class of Bimodal Piecewise Affine Systems

Aleksandar Juloski
Faculty of Electrical Engineering
Eindhoven University of Technology
Eindhoven
The Netherlands
a.juloski@tue.nl

Maurice Heemels
Faculty of Electrical Engineering
Eindhoven University of Technology
Eindhoven
The Netherlands
m.heemels@tue.nl

1 Introduction

Piecewise affine systems received considerable amount of attention recently, because they frequently arise, for example, as an approximation for more complex nonlinear systems, or as a simple class of hybrid systems.

Stability analysis for piecewise affine systems has been cast as a set of linear matrix inequalities in [1]. Stabilizing state feedback design, essentially based on the results in [1], was presented, for example, in [3].

In [2] stabilizing output feedback design was presented. Proposed output feedback controller consists of an observer and a state feedback controller. However, observer and controller design are not separated steps, and can not be separated.

In this work we consider a simple class of piecewise affine systems and propose an observer design procedure. The proposed observer does not require information about the currently active linear dynamics. Related, but far less general, approach was presented in [4].

2 Problem statement

We consider the following class of bimodal piecewise affine systems:

$$\dot{x} = \begin{cases} A_1 x + B u, & H^T x \le 0 \\ A_2 x + B u, & H^T x > 0 \end{cases}$$
 (1)

$$y = Cx, (2)$$

where $x \in \mathbf{R}^n$, $y \in \mathbf{R}^p$, $u \in \mathbf{R}^m$, $A_1, A_2 \in \mathbf{R}^{n \times n}$, $B \in \mathbf{R}^{n \times m}$, $C \in \mathbf{R}^{p \times n}$ and $H \in \mathbf{R}^{n \times 1}$.

Proposed observer for the system (1),(2) has the following structure:

$$\dot{\hat{x}} = \begin{cases} A_1 \hat{x} + Bu + L_1(y - \hat{y}), & H^T \hat{x} \leq 0 \\ A_2 \hat{x} + Bu + L_2(y - \hat{y}), & H^T \hat{x} > 0 \end{cases}$$
(3)

$$\hat{\mathbf{y}} = C\hat{\mathbf{x}},\tag{4}$$

where $\hat{x} \in \mathbf{R}^n$, $\hat{y} \in \mathbf{R}^p$, $L_1, L_2 \in \mathbf{R}^{n \times p}$.

Design problem for the observer structure (3), (4) is to determine observer gains L_1 , L_2 , such that $\|\hat{x}(t) - x(t)\| \to 0$ as $t \to \infty$, for every $\hat{x}(0)$, x(0).

3 Design procedure

Sufficient conditions for global asymptotic stability of the state observation error, based on Lyapunov arguments, are obtained, and presented in the form of linear matrix inequalities.

Following the same line of reasoning basic observer structure (3), (4) can be extended, to include output prediction error $y - \hat{y}$ in the observer switching surface, to improve convergence of the estimate.

An illustrative example is presented.

4 Conclusions

The observer is proposed that has a simple structure, and can be easily implemented in practice. Also, design procedure is numerically efficient.

Future work will focus on generalizations of presented observer design procedure to include more general class of piecewise affine systems, and hybrid systems. Also, another important research issue is the design of a control strategy on the basis of the observed state.

- [1] Johansson M., Rantzer A., Computation of Piecewise Quadratic Lyapunov Functions for Hybrid Systems, IEEE Transactions on Automatic Control, vol 43, no 4, pp. 555-559
- [2] Rodrigues L., How J., Output Feedback Controller Synthesis for Piecewise-Affine Systems with Multiple Equilibria, Proceedings of the 40th IEEE Conference on Decision and Control, Orlando, Florida USA, December 2001
- [3] Hassibi A., Boyd S., Quadratic Stabilization and Control of Piecewise-Linear Systems, Proc. 1998 American Control Conference, pp. 3659-64
- [4] de Goeij G.W., Observer Design for a Beam System with One-Sided Spring, M.Sc. Thesis, Vakgroep Fundamentele Werktuigkunde, TUE, November 1999

Maximal Controlled Invariant Sets of Switched Linear Systems

A.A. Julius
Faculty of Mathematical Sciences
University of Twente
Email: A.A.Julius@math.utwente.nl

A.J. van der Schaft Faculty of Mathematical Sciences University of Twente Email: A.J.vanderSchaft@math.utwente.nl

1 Abstract

In this paper, controlled invariant sets of switched linear systems are studied. In particular, the problem of finding the maximal controlled invariant set (MCIS) contained in a linear space is addressed.

Control of dynamic systems by switchings have been studied intensively. Typical results include stability properties [1], sliding mode analysis [2][3] and reachability and controllability issues [4].

The study of controlled invariance in this paper is motivated by controller design paradigm based on viability theory. See, for example, [5] and [6].

The dynamics of the systems considered in this paper can be described by a family of state-space representations with shared state-space

$$\dot{x}(t) = A_i x(t) + B_i u(t),$$

 $i \in \{1, 2, \dots, m\}.$

The system admits two inputs, namely the continuous input u(t) and the discrete input Δ_k that induces the switchings between the dynamics in the family.

There are two main cases studied in this paper. The first case deals with the situation where infinitely often switchings are not allowed. The second case deals with the situation where they are allowed.

If infinitely often switchings are not allowed, consider the following iteration.

$$V_0 = \mathcal{V},\tag{1a}$$

$$V_{i+1} = V_i \cap \left(\bigcup_{j=1}^{n_i} \bigcup_{k=1}^m \mathcal{V}_{ij} \cap A_k^{-1} \left(\mathcal{V}_{ij} + \operatorname{Im} B_k \right) \right). \tag{1b}$$

Here V_{ij} is a linear space and $V = \bigcup_j V_{ij}$. The following theorem can be proved about this iteration.

Theorem 1 Let the iteration (1) converge to V, i.e. there is a p > 0 such that

$$i \ge p \iff V_{i+1} = V_i = V.$$

Then V is the maximal controlled invariant set contained in V.

It is also proved that the iteration follows some tree structure and that this tree terminates, hence guaranteeing convergence of the iteration after just a finite number of steps. The limit set of the iteration turns out to be the union of the maximal controlled invariant subspaces of each individual mode.

If infinitely often switchings are allowed, then the following iteration is used instead

$$V_0 = \mathcal{V},\tag{2a}$$

$$V_{i+1} = \{ x \in V_i \mid vel(x) \cap T_{V_i}(x) \neq \emptyset \}.$$
 (2b)

The symbol vel(x) denotes the polyhedral set of possible velocity vectors and $T_V(x)$ denotes the tangent cone of V at x respectively. As in the other case, it is proved that if the iteration converges, it will be to the MCIS.

Another result is that (2) is a generalization of (1), and by imposing certain conditions, both (1) and (2) boil down to the well known algorithm for the construction of maximal controlled invariant subspace of linear systems [7].

- [1] DeCarlo, R.A., Branicky, M.S., Pettersson, S., & Lennartson, B., Perscpectives and Results on the Stability and Stabilizability of Hybrid Systems., *Proc. of the IEEE*, 88(7):1069-1082, 2000.
- [2] Bernhardsson, B., Johansson, K.H. & Malmborg, J., Some Properties of Switched Systems, *in the IFAC World Congress, Beijing*, 1999.
- [3] Johansson, K.H., Rantzer, A. & Astrom, K.J., Fast Switches in Relay Feedback Systems, *Automatica*, 35:539-552, 1999.
- [4] Ge, S.S., Sun, Z. & Lee, T.H., Reachability and Controllability of Switched Linear Discrete-Time Systems, *IEEE Trans. Aut. Control*, 46:1437-1441, 2001.
- [5] van der Schaft, A.J. & Schumacher, J.M., *An Introduction to Hybrid Dynamical Systems*, Springer-Verlag, London, 2000.
- [6] Ramadge, P.J. & Wonham, W.M., Supervisory Control of a Class of Discrete Event Processes, *SIAM J Contr. Opt.*, 25:206-230, 1987.
- [7] Wonham, W.M., *Linear Multivariable Control: a Geometric Approach*, Springer Verlag, New York, 1985.

Kalman Filters for Nonlinear Systems

T. Lefebvre, H. Bruyninckx, J. De Schutter
Katholieke Universiteit Leuven
Department of Mechanical Engineering
Division of Production Engineering, Machine Design and Automation (PMA)
Celestijnenlaan 300B, B-3001 Heverlee, Belgium
Email: Tine.Lefebvre@mech.kuleuven.ac.be

1 Abstract

Kalman Filters (KFs) are often used as minimum mean square error (MMSE) state estimators. Although these estimators are known to give optimal estimates only when the system's process and measurement functions are linear, they are quite often used for systems with nonlinear functions. Different KF estimators linearize these functions in different ways. In order to *choose* an estimator for a certain problem, it is important to have a good insight in the performance of each of the estimators on this kind of problems.

The performance of the estimators is expressed in terms of the consistency of the state estimates (the state vector and its covariance matrix) and their information content. An estimate is *consistent* if the covariance matrix is large enough to reflect the uncertainty on the estimate. In order to obtain consistent estimates, one could artificially increase the covariance matrix. However, increasing the covariance matrix too much corresponds to loosing information about the real accuracy of the estimate. Therefore, the quality of an estimate is not only determined by its consistency, but also by its *information content*. The larger the covariance matrix of an estimate is, the smaller is its information content.

The first part of the presentation analyzes the performance of some well-known KFs-i.e., the Extended Kalman Filter (EKF), the Iterated Extended Kalman Filter (IEKF) and the Linear Regression Kalman Filter (LRKF)—when they deal with nonlinear process and measurement updates. The EKF linearizes the process and measurement functions around the previous state estimate. The linearization errors are not taken into account, except if the user provides some approximation of these errors, e.g. obtained by extensive off-line tuning. The IEKF linearizes the process function in the same way as the EKF. The measurement function is linearized around the next state estimate (obtained by iteration). Again, the linearization errors are not taken into account, except if the user approximates these. The LRKF is a unified description of a class of KFs, including the Unscented Kalman Filter (UKF, [1, 2]). The LRKF (i) linearizes the process and measurement functions by a statistical linear regression of the functions through some sampling points in the uncertainty region around the state estimate; and (ii) defines the uncertainty due to linearization errors as the covariance matrix of the deviations between the function values of the

nonlinear and the linearized function in the sampling points.

Besides some well known issues, such as the consistency of the LRKF state estimates and the inconsistency of the EKF state estimates, some less known, but important results are clarified: (i) a good performance of an estimator in the process or measurement update, does not guarantee a good performance in the other update; therefore, it can be interesting to use different estimators for both; (ii) the LRKF measurement update often returns consistent, but non-informative estimates; and (iii) the IEKF measurement update yields consistent and informative state estimates when the state—or at least the part of it that causes the nonlinearity in the measurement function—is instantaneously fully observable.

The second part of the presentation proposes a "Cascading Kalman Filter", consisting of multiple stages of KFs. The core idea of this new estimator is to estimate different state variables than the desired ones, but which depend *linearly* on the measurements. There can be more "new" state variables than the original problem has. In this case, (nonlinear) constraints between the "new" state variables exist; but, are not introduced in the (linear) KF. Whenever necessary, the desired state can be estimated from its initial state estimate (prior) and the last "new" state estimate. This last step is performed by an IEKF which gives good results if the measurements up to that time step fully observe the desired state estimate. The Cascading Kalman Filter can easily be implemented for static state estimates. Although they can not be extended in general to dynamical systems, some examples of dynamical state estimation are also given.

- [1] S. Julier, J. Uhlmann and H.F. Durrant-Whyte, "A New Method for the Nonlinear Transformation of Means and Covariances in Filters and Estimators", IEEE Trans. on Automatic Con trol, vol. 45, no. 3, pp. 477–482, 2000.
- T. [2] Lefebvre, H. Bruyninckx and "Comment on "A New J. De Schutter, Method Nonlinear for Transformation of Means Covariances Filters and Estimators"", http://www.mech.kuleuven.ac.be/~tlefebvr/publicaties/01P081.ps, Submitted to IEEE Trans. on Automatic Control", 2001.

Estimation of the convergence region for the local output regulation problem for nonlinear systems

Alexei Pavlov

Eindhoven University of Technology, Faculty of Mechanical Engineering, Den Dolech 2, P.O. Box 513, 5600 MB Eindhoven, The Netherlands. e-mail: A.Pavlov@tue.nl

1 Introduction

The presentation is devoted to the problem of asymptotic regulation of the output of a dynamic system, which is subject to disturbances generated by an external system. Many problems in control theory can be considered as particular cases of the output regulation problem: tracking of a class of reference signals, rejecting a class of disturbances, stabilization, partial stabilization or controlled synchronization. For linear systems, the problem is completely solved resulting in the well-known "internal model principle". For nonlinear systems, the problem is much more complicated and the complete solution is found only in the case of the local problem setting. In particular, necessary and sufficient conditions for the solvability of the local output regulation problem were obtained and a procedure for designing a controller, which solves the problem, was found [1]. A controller resulting from this procedure solves the output regulation problem only for small initial conditions of the closedloop system. From an engineering point of view, such solution is not satisfactory, since the region of admissible initial conditions is not specified. Thus, once a controller solving the local output regulation problem is found, there is a need to determine this region.

In this presentation, we first review the conditions for the solvability of the local output regulation problem, as well as the procedure of constructing a controller solving the problem and, second, explain a method for estimating the set of initial conditions, for which the controller solves the problem.

2 Local output regulation problem

In the context of the output regulation problem, we consider systems modelled by equations of the form

$$\dot{x} = f(x, u, w)$$
 (1)
 $y = h_m(x, w), e = h_r(x, w),$

with state $x \in X \subset \mathbb{R}^n$, input $u \in U \subset \mathbb{R}^m$, measured output $y \in \mathbb{R}^l$, regulated output $e \in \mathbb{R}^p$ and exogenous disturbance input $w \in W \subset R^r$ generated by the exosystem

$$\dot{w} = s(w). \tag{2}$$

The local output regulation problem can be formulated as follows: *find an output feedback controller of the form*

$$\dot{\xi} = \eta(\xi, y), \quad u = \theta(\xi, y), \tag{3}$$

such that for the closed-loop system (1)-(3) for small initial conditions $(x(0), \xi(0), w(0))$ the regulated output converges to zero: $e(t) \to 0$ as $t \to \infty$. Once a controller solving the local output regulation problem is found, we have to estimate the region of initial conditions $(x(0), \xi(0), w(0))$, for which the regulated output e converges to zero.

3 Estimation of the convergence region

For the region of admissible w(0) we present an estimate in the form of a ball $B: |w| \le r$, for some r > 0. The number r is chosen such that solutions of the system (2) starting in B are defined and small for all $t \in \mathbb{R}$. The region of admissible $(x(0), \xi(0))$ is estimated by an ellipsoid E of the form $(x^T, \xi^T)P(x^T, \xi^T)^T \leq R$ for some R > 0 and some positive definite matrix P. The ellipsoid is chosen such that for any w(t), a solution of (2) passing through the ball B, the closed-loop system (1), (3) has a unique solution $\bar{x}(t)$, such that it lies in E for all $t \in \mathbb{R}$ and all other solutions of (1), (3), starting in E, converge to $\bar{x}(t)$. Such property of the closed-loop system is called *convergence* [2]. The conditions for convergence allow to find the matrix P and the numbers R > 0, r > 0, which determine the ball Band the ellipsoid E. The conditions for the solvability of the local output regulation problem and the form of the controller solving the problem imply that the regulated output $e = h_r(x, w)$ is equal to zero on $(\bar{x}(t), w(t))$. Thus, the regulated output e tends to zero on any solution of (1)-(3) starting in $(x(0), \xi(0), w(0)) \in E \times B$.

4 Conclusions

We have proposed a method for estimating the region of convergence for a controller solving the local output regulation problem.

References

- [1] C.I. Byrnes, F. Delli Priscoli, A. Isidori. *Output regulation of uncertain nonlinear systems*. Birkhauser: Boston, 1997.
- [2] B.P. Demidovich. *Lectures on stability theory*. Nauka: Moscow, 1967 (in Russian).

Acknowledgments: this research is supported by the Netherlands Organization for Scientific Research (NWO).

Synthesis of rhythmic patterns in small networks of oscillators

F. Defays

Université de Liège, Institut Montefiore Bât. B28, Sart-Tilman 4000 Liège, Belgium fabien.defays@ulg.ac.be

R. Sepulchre

Université de Liège, Institut Montefiore Bât. B28, Sart-Tilman 4000 Liège, Belgium r.sepulchre@ulg.ac.be

Abstract

Central pattern generators play an important role in the control of animal locomotion. They consist of an intraspinal network of neurons able to generate and to sustain a cyclic activity. Although animals have neural networks composed of a huge number of neurons, Golubitsky $et\ al\ [1,\ 2]$ studied the smallest network able to reproduce basic rhythmics of gaits. They have proved that eight "cells" correctly connected are able to reproduce standard gaits phase relations of a quadruped.

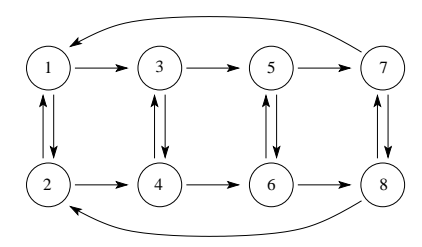


Figure 1: Central Pattern Generator : network model developed by Golubitsky et al [1, 2]

In the network displayed in Fig 1, each "cell" is a nonlinear oscillator. We choose for this oscillator the simplest model of "neural" oscillator [3] consisting in the feedback interconnection of an inhibitory state with an excitatory state:

$$\left\{ \begin{array}{l} \tau \cdot \dot{x_E} = -x_E + \mathrm{sat}(x_E - x_I + input) \\ \tau \cdot \dot{x_I} = -x_I + \mathrm{sat}(x_E) \end{array} \right.$$

For networks made of such oscillators, we address the synthesis problem of selecting the interconnection structure such as to impose a specific rhythmic pattern in the network, i.e. phase differences between each oscillator. Moreover, we constrain the interconnection structure to satisfy Dale's principle, i.e. that excitatory (resp. inhibitory) states, may have only excitatory (resp. inhibitory) actions on other states. Our synthesis method uses averaging theory for the analysis of two interconnected oscillators, following [4]. This analysis is extended to the complete network using symmetry considerations.

To conclude we designed a central pattern generator able to reproduce rhythmics patterns of gaits, with cell models matching the basics biological features of animal neurons.

- [1] M. Golubitsky, I. Stewart, P-L. Buono, J.J. Collins, "Symmetry in locomotor central pattern generators and animal gaits", Nature 401 (1999), pp 693-695
- [2] M. Golubitsky, I. Stewart, P-L. Buono, J.J. Collins, "A modular network for legged locomotion", Physica D 115 (1998), pp 56-72
- [3] H.R. Wilson, "Spikes, Decisions and Actions dynamical foundations of neuroscience", Oxford University Press, 1999
- [4] F.C. Hoppensteadt, E.M. Izhikevich, "Synaptic organizations and dynamical properties of weakly connected neural oscillators", Biological Cybernetics 75 (1996), pp 117-127
- [5] F. Defays, "Mécanismes neuronaux de la locomotion animale", Engineering diploma thesis, University of Liège, 2001

¹Standard gaits are composed of walk, trot and pace

On achievable non-linear behaviors

Arjan van der Schaft
Faculty of Mathematical Sciences
University of Twente
P.O.Box 217, 7500AE Enschede
The Netherlands
a.j.vanderschaft@math.utwente.nl

1 Abstract

The behavioral approach to systems and control theory has led to an elegant characterization of the set of all behaviors which are achievable by interconnecting (on a set of *shared variables*) a given linear time-invariant system (the *plant*) with another arbitrary linear time-invariant system (the *controller*). This characterization (in some circles known as *Willems' lemma*) takes the form of a double inclusion

$$\mathfrak{N}\subset\mathfrak{K}\subset\mathfrak{P}$$

with \mathfrak{R} denoting an achievable behavior, and \mathfrak{N} and \mathfrak{P} denoting, respectively, the *hidden* and the *manifest* plant behavior, see e.g. [1, 2, 3].

Purpose of this presentation is to give an alternative, and supposedly simpler, proof of this lemma, and to show how this alternative proof directly leads to a *nonlinear* generalization of Willems' lemma. Also some implications to the control of port-Hamiltonian (nonlinear) systems will be indicated.

- [1] J.C. Willems, H.L. Trentelman, Synthesis of dissipative systems using quadratic differential forms, to appear.
- [2] H.L. Trentelman, A truly behavioral approach to the H_{∞} control problem. In J.W. Polderman and H.L. Trentelman, editors, The Mathematics of Systems and Control: from Intelligent Control to Behavioral Systems, pp. 177-190, 1999.
- [3] J. W. Polderman, I. Mareels, A behavioral approach to adaptive control, In J.W. Polderman and H.L. Trentelman, editors, The Mathematics of Systems and Control: from Intelligent Control to Behavioral Systems, pp. 119-130, 1999.

Generalized singular values and the rank approximation problem

Hardy B. Siahaan
Department of Electrical Engineering
Eindhoven University of Technology
P.O. Box 513, 5600 MB Eindhoven
The Netherlands
h.siahaan@tue.nl

1 Summary

Singular values and singular value decompositions are among the most important tools in linear algebra that have played a key role in systems analysis, control system design, model reduction, data compression, perturbation theory, signal analysis and many applications in numerical linear algebra [1]. The purpose of this presentation is to propose a definition of a set of singular values associated with a linear operator defined on arbitrary normed linear spaces. This generalizes the usual notion of singular values and singular value decompositions to operators defined on spaces equipped with the p-norm, where p is arbitrary. Basic properties of these generalized singular values are derived and we consider their relevance in the problem of optimal rank approximation and a problem of optimal system identification. We give sufficient conditions for the existence of optimal rank approximants in the p-induced norm and provide a characterization of autoregressive models which are optimal in the sense that they minimize a misfit criterion which reflects the p-norm of a residual signal.

2 Definitions

Let \mathcal{X} and \mathcal{Y} be two finite dimensional vector spaces of dimension n and m and let $M: \mathcal{X} \to \mathcal{Y}$ be linear. For any p, let

$$||x||_p := \begin{cases} \left(\sum_{i=1}^n |x_i|^p\right)^{1/p} & \text{if } p < \infty \\ \max_{i=1,\dots,n} |x_i| & \text{if } p = \infty \end{cases}$$

and define the induced p-norm of M as

$$||M|| := \sup_{0 \neq x \in \mathcal{X}} \frac{||Mx||_p}{||x||_p}.$$

The induced p-norm singular values of M are the numbers

$$\sigma_k^{(p)} := \inf_{d \in \mathcal{X}, \atop d \in \mathcal{X}_{n-k+1}} \sup_{0 \neq x \in \mathcal{L}} \frac{\|Mx\|_p}{\|x\|_p}$$

where k runs from 1 till n. It is easily seen that these numbers are ordered according to $\sigma_1^{(p)} \geq \ldots \geq \sigma_n^{(p)} \geq 0$ and that (for any p) the first r singular values are non-zero if and only if M has rank r.

Siep Weiland
Department of Electrical Engineering
Eindhoven University of Technology
P.O. Box 513, 5600 MB Eindhoven
The Netherlands

s.weiland@tue.nl

3 Problem formulations

The above singular values turn out the key tool in the solution of the following problems.

3.1 Rank deficiency

A reliable numerical implementation to determine rank *M* usually calculates the *numerical rank* defined as

$$\operatorname{rank}(M,\varepsilon) := \min_{\|M-M'\| \le \varepsilon} \operatorname{rank}(M')$$

where $\varepsilon > 0$ is an accuracy level and p defines the norm of interest.

3.2 Rank approximation

The problem of approximating M by a linear map M': $\mathcal{X} \to \mathcal{Y}$ of rank at most k ($k < \operatorname{rank} M$), such that the p-induced norm

$$||M-M'||$$

is minimal. We refer to this problem as the *optimal rank* approximation problem.

3.3 System identification

Given data $\tilde{w}(t)$, t = 1, ..., N, we consider the problem of finding autoregressive models of the form

$$\sum_{i=0}^{n} r_i w(t+i) = 0, \qquad t \in \mathbb{Z}_+$$
 (1)

where the unknown parameter vector $r = (r_0, ..., r_n)$ minimizes the identification criterion

$$\mu(r, \tilde{w}) := \frac{\|e\|_p}{\|r\|_p}$$

where e is the residual of (1). Note the relevance of this problem for different values of p. In particular, for $p = \infty$ this problem minimizes the amplitude of the residual signal e.

We will show the relevance of generalized singular values for each of these problems.

References

[1] G.H. Golub and C.F. van Loan, "Matrix computations", The John Hopkins University Press, 1989.

An LMI Approach to Multiobjective Robust Dynamic Output-Feedback Control for Uncertain Discrete-Time Systems

Stoyan Kanev
Faculty of Applied Physics, SCE group
University of Twente,
P.O. Box 217, 7500 AE ENSCHEDE
The Netherlands
S.K.Kanev@TN.UTwente.NL

Michel Verhaegen
Faculty of Applied Physics, SCE group
University of Twente,
P.O. Box 217, 7500 AE ENSCHEDE
The Netherlands
M.Verhaegen@TN.UTwente.NL

1 Abstract

This note discusses an LMI framework to the design of robust multiobjective dynamic output-feedback controllers for discrete-time systems with structured uncertainty. The control objectives considered are guaranteed \mathcal{H}_2 norm, guaranteed \mathcal{H}_∞ norm and regional pole-placement. The uncertainty that can be dealt with by the proposed approach is allowed to have a quite general structure – it is just assumed to be such that the state-space matrices of the uncertain system belong to a given convex set.

2 Introduction

Much attention has been focused on controller and filter design based on LMIs in the last decade due to the recent development of computationally fast and numerically reliable algorithms for solving convex optimization problems subject to LMI constraints. Due to the well-known separation theory, in the case when no uncertainty is present these filters can directly be coupled with their dual state-feedback controllers to yield optimal output-feedback controllers. For uncertain systems, trying to solve the coupled problem of output-feedback controller design for system with structured uncertainty one immediately faces a nonlinear, non-convex problem.

3 Outline of the approach

In [1] a novel approach to the design of guaranteed-cost robust \mathcal{H}_2 and \mathcal{H}_∞ dynamic output-feedback controllers was proposed. It is well-known that both objectives define a nonlinear, non-convex problem. To circumvent this difficulty, a two-stage design approach is proposed. First, a multiobjective robust state-feedback is designed, represented by the state-feedback gain matrix F, and second, the matrix F is fixed constant in the design of the other matrices of the dynamic output-feedback controller. Although the second step remains non-convex, it is shown that by restricting the Lyapunov function for the closed-loop system to have a certain block-diagonal structure, this problem can be recast into an LMI feasibility problem. The conservatism that is sacrificed by imposing this structural constraint on the Lyapunov function is, however, well justified by the ability of the approach

to explicitly deal with structured uncertainties in the system.

The approach discussed here makes use of the results obtained in [1], and focuses on the design of *multiobjective* dynamic output-feedback controllers for discrete-time systems with structured uncertainties. A sufficient condition, based on LMIs, to the existence of solution to the following mixed $\mathcal{H}_2/\mathcal{H}_{\infty}$ /pole-placement control problem is proposed

$$\begin{array}{ll} \mathcal{H}_2 \text{ objective:} & \sup_{\Delta} \|L_2 T_{cl}^{\Delta}(z) R_2\|_2^2 < \gamma_2, \\ \mathcal{H}_{\infty} \text{ objective:} & \sup_{\Delta} \|L_{\infty} T_{cl}^{\Delta}(z) R_{\infty}\|_{\infty}^2 < \gamma_{\infty}, \\ \text{Pole-placement:} & \lambda (A_{cl}^{\Delta}) \in \mathcal{D}, \ \forall \Delta. \end{array}$$

given any $\gamma_2>0$, and $\gamma_\infty>0$, where $T_{cl}^\Delta(z)$ is denoted the closed-loop transfer function, Δ denotes the (structured) uncertainty in the system, and the matrices L_2 , R_2 , L_∞ , and R_∞ , are used to select the desired input-output channels in the mixed control objective above. The superscript Δ denotes dependence on the uncertainty. The complex region \mathcal{D} , in which the closed-loop eigenvalues, denoted as $\lambda(A_{cl}^\Delta)$, are required to lie, is assumed to have the form

$$\mathcal{D} = \{ z \in C : L + zM + \bar{z}M^T < 0, L = L^T \}.$$

Due to the fact that the system of LMIs, which implies the constraints (1), is affine in both γ_2 and γ_{∞} , one may also wish to consider the optimization problem

$$\min_{\gamma_2,\gamma_{\infty}} \alpha_2 \gamma_2 + \alpha_{\infty} \gamma_{\infty} \text{ subject to (1)}.$$

for given positive numbers α_2 and α_{∞} . The approach has been tested on a case study with an aircraft model with six uncertain parameters.

References

[1] S. Kanev and M. Verhaegen, An LMI Approach to Multiobjective Robust Dynamic Output-Feedback Control for Uncertain Discrete-Time Systems, *submitted to Automatica*, December 2001.

Interior Point Method for Reduced Order Controller Synthesis of Electro-Mechanical Servo-Systems

Camile W.J. Hol
Department of Mechanical Engineering
Delft University of Technology
Mekelweg 2, 2628 CD Delft
The Netherlands
Email: C.W.J.Hol@wbmt.tudelft.nl

Carsten Scherer

Department of Mechanical Engineering
Delft University of Technology
Mekelweg 2, 2628 CD Delft
The Netherlands
Email: C.W.Scherer@wbmt.tudelft.nl

1 Introduction

One of the reasons that H_{∞} synthesis has not yet been widely used in industry is the high order (i.e. the Mc Millan degree) of the resulting controller. The order equals the order of the dynamical model plus the order of the weighting functions. The computation of the controller action becomes more expensive with increasing controller order. In view of real-time implementation on electro-mechanical systems with a very high sampling rate, the need for low-order controllers is obvious. This research aims at facilitating the implementation of H_{∞} controllers by developing a direct synthesis method for reduced-order controllers. Although lot of work has been published on this topic in the literature [2], [3], [4], there is no method that works well for high-order models, i.e. order > 50.

2 Fixed-order control problem

We consider the following problem:

Problem 1 (fixed-order \mathcal{H}_{∞} synthesis) Given a transfer matrix P of the plant, find a controller with transfer matrix K of order n_c such that the closed loop inter-connection is asymptotically stable and satisfies $\|S(P,K)\|_{\infty} < \gamma$, where S(P,K) denotes the lower linear fractional transformation of P and K and $\|\cdot\|_{\infty}$ denotes the \mathcal{H}_{∞} -norm.

Problem 1 is equivalent to the following minimization problem:

Problem 2 (BMI formulation)

$$\min_{X,K,\gamma} \gamma$$

subject to:

$$\begin{bmatrix} A_{cl}^{T} X_{cl} + X_{cl} A_{cl} & X_{cl} B_{cl} & C_{cl}^{T} \\ B_{cl}^{T} X_{cl} & -\gamma I & D_{cl}^{T} \\ C_{cl} & D_{cl} & -\gamma I \end{bmatrix} < 0$$

$$X_{cl} > 0$$

where the quadruple $[A_{cl}, B_{cl}, C_{cl}, D_{cl}]$ is the closed loop state-space system description.

The first inequality constraint in Problem 2 is a bilinear inequality in the unknown Lyapunov matrix X_{cl} and the state space matrices of the controller. These bilinear couplings make the problem nonconvex.

3 Interior point method

We propose to use an Interior Point method to solve Problem 2 as suggested by Goh *et.al.* [5]. The approach is based on the predictor-corrector method for nonconvex semidefinite programming of Jarre [1]. This method uses a curved line-search in the corrector to deal with the nonconvexity. Because the \mathcal{H}_{∞} -norm is invariant under similarity transformations of the controller, we can reduce the number of decision variables by keeping a part of the Lyapunov matrix X_{cl} fixed.

- [1] F. Jarre, "An Interior Method for Nonconvex Semidefinite Programs", Tecnical report, Institut für Mathematik, 2001.
- [2] L. El Ghaoui, F. Oustry and M. AitRami, "A Cone Complementarity Linearization Algorithm for Static Output-Feedback and Related Problems", *IEEE transactions on automatic control*, 42: 1171-1176, 1997.
- [3] T. Iwasaki, "The Dual Iteration for Fixed-order Control", *IEEE transactions on automatic control*, 44: 783-788, 1999.
- [4] K.M. Grigoriadis and R.E. Skelton, "Fixed-Order Control Design for LMI Control Problems Using Alternating Projection Methods", *Proceedings of the 33th Conference on Decision and Control*, Lake Buena Vista, Florida, 2003-2008, 1994.
- [5] K.C. Goh, L. Turan, M.G. Safonov, G.P. Papavas-silopoulos and J.H. Ly, "Biaffine Mtarix Inequality Properties and Computational Methods", *Proceedings of the American Conference*, Baltimore, Maryland, 850-855, 1994.

Application of \mathcal{H}_{∞} feedback control: Reference tracking on a half-axle test rig

David Vaes¹ and Jan Swevers KULeuven, Dep. of Mechanical Engineering Celestijnenlaan 300B, 3001 Heverlee, Belgium david.vaes@mech.kuleuven.ac.be Joris De Cuyper and Wouter Dehandschutter LMS International Interleuvenlaan 68, 3001 Haasrode, Belgium joris.decuyper@lms.be

1 Introduction

In automotive industry, durability tests are used to investigate whether a vehicle endures a long sequence of repeated cyclic loading. On a so-called "half-axle" test rig, a suspension is mounted and loaded in vertical and lateral direction. In order to subject the suspension to a realistic loading, one tries to reproduce the vertical and lateral forces measured on the suspension during a test drive on a special test track. The reproduction of these forces on the rig, by controlling the excitation, is a multivariable tracking problem.



Figure 1: Half-axle test rig, with suspension.

The present-day solution for this tracking problem applies only feedforward, which is generated in an off-line iterative process, based on the measured open loop Frequency Response Function (FRF) of the test rig. An iterative process is necessary due to the nonlinear dynamics of the suspension: the measured FRF can't exactly predict the response of the test rig. Based on the difference between the target signal and the measured response, the feedforward control signal for the next iteration is updated, until the desired accuracy is obtained. [2] explains this method, and determines its convergence properties. Current research tries to introduce a feedback controller to accelerate this process. In [2] it is shown that the convergence is faster when a performant feedback controller is used.

Nonlinearities, measurement noise and spill-over result in modeling errors, which necessitates a robust feedback control design. This research considers \mathcal{H}_{∞} -control design.

2 \mathcal{H}_{∞} feedback control and results on the test rig

The design method used is the so-called "Mixed sensitivity loop shaping" design method described in [1], which mini-

mizes:

$$\left\| \begin{bmatrix} W_1 S & W_2 T & W_3 K S \end{bmatrix}^T \right\|_{\infty} \tag{1}$$

with K the controller, S, T and KS the sensitivity, the complementary sensitivity and the input sensitivity function respectively. W_1 , W_2 and W_3 are user-defined weighting functions. A good choice of the weighting functions tries to meet the performance, robustness and input-limitation requirements as good as possible.

This presentation discusses the design of a robust and performant multivariable controller for the test setup. The use of this controller yields a reduction of the number of iterations from 7 (without feedback) to 3 (with feedback). Figure 2 shows these results by means of the evolution of the damage ratio as a function of the iteration number. The damage ratio is a measure for the difference (in per cent) between the damage caused to the suspension during the test and by the desired loading. It is an important evaluation criterion for durability tests.

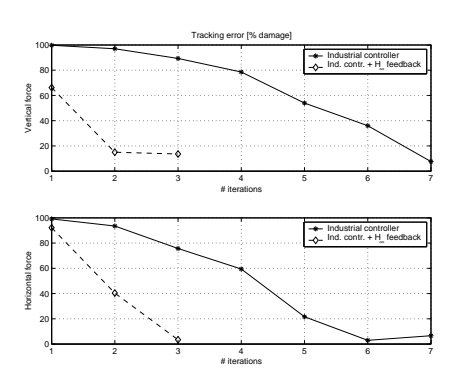


Figure 2: Evolution of the damage-ratio over the iterations.

- [1] S. Skogestad, and I. Postlethwaite, "Multivariable Feedback Control, Analysis and design." John Wiley & Sons, 1996
- [2] J. De Cuyper, M. Verhaegen, and J. Swevers, "Offline Feed-forward and \mathcal{H}_{∞} Feedback Control for improved Tracking on an industrial vibration test rig." submitted to *Journal of Control Engineering Practice* (also internal report nr. 01pp117 at KULeuven, Dep. of Mech. Engineering)

¹David Vaes is Research Assistant of the F.W.O. - Flanders (Belgium)

Auto-tuning of chemical processes using adaptive λ -tracking control

Michiel E. van Wissen, J. Pieter Schmal and Johan Grievink
Department of Chemical Technology
Delft University of Technology
Julianalaan 136, 2628 BL Delft
The Netherlands
E-mail:{m.e.vanwissen,j.p.schmal,j.grievink}@tnw.tudelft.nl

1 Introduction

In many chemical plants, the use of P and PI control is still widely used. Tuning of these controllers is a time consuming matter, because a detailed process model or extensive plant tests are needed. For this reason, we propose a new tuning method based on adaptive control and we use it to determine the parameters in the P and PI controllers. Our purpose in this paper is twofold. First, we investigate the needs in process industry and based on that, we develop our adaptive controller. For a number of examples, the usefulness of the developed controller is illustrated. Second, we use this controller for tuning and derive a set of tuning-rules. The obtained tuning-parameters are used in a model of an industrial plant. We emphasize that the developed controller is only used for tuning and after that replaced by the conventional P or PI controller.

2 Adaptive λ -tracking control

In adaptive λ -tracking, the main goal is to keep some variables within bounds. The basic structure (Allgöwer and Ilchmann [1]) is that of a P-controller (a PI-structure is also possible) with a time-varying gain $k(\cdot)$:

$$u(t) = -\beta k(t) [y(t) - y_{ref}(t)] + \delta$$

$$\dot{k}(t) = \begin{cases} \gamma(y(t) - y_{ref}(t))^{2} &, ||y(t) - y_{ref}(t)|| \ge \lambda \\ 0 &, ||y(t) - y_{ref}(t)|| < \lambda. \end{cases}$$
(1)

In this controller, the gain $k(\cdot)$ is strictly monotonically increasing as long as the difference between the output $y(\cdot)$ and the reference signal $y_{ref}(\cdot)$ is larger than the given λ . If this difference enters the λ -strip the adaptation is switched off and the gain is kept constant. The parameters β , δ , $\lambda > 0$ and $\gamma > 0$ are left to the choice of the designer. The assumptions on the plant and the proof that the gain $k(\cdot)$ converges to a constant value and that $y(\cdot) - y_{ref}(\cdot)$ converges to the λ -strip are given in [1]. We make plausible that the assumptions on the plant are satisfied in many practical cases. Investigating the needs of process industry, we concluded that λ-tracking within prespecified time and with input saturation is needed. We incorporated the combination of these two in the controller (1) and we were able to proof that $\lim_{t\to T} k(t) = k_T \in \mathbb{R}_{\geq 0}$ and $\lim_{t\to T} [y(t) - y_{ref}(t)] = 0$, in which T is the prespecified time.

3 Tuning and results

Here, we used the modified λ -tracking controller (1) for tuning purposes on three different cases. The reasons to use this controller for tuning are

- A process model or plant tests are not required and the tuning of the parameters is done on-line.
- The controller itself does not require much tuning, is very robust and is easy to implement.

First, we compared the results of Vrančić *et al.* [4] with our controller and concluded that the results were only slightly worse, but much faster obtained because of the reasons above. We also derived a set of tuning-rules. An activated sludge process (Georgieva and Ilchmann [2]) that not fulfilled the assumptions completely, has been controlled and tuned by the proposed λ -tracking controller. In this case, we also incorporated the modifications proposed by Polderman and Mareels [3] in our controller. Finally, because all of the examples above were single-input, single-output, we tested the λ -tracking controller in multiple-input, multiple-output setting on a model of an industrial plant.

- [1] F. Allgöwer and A. Ilchmann (1995), 'Multivariable adaptive λ -tracking for nonlinear chemical processes', *Proc.* of the 3rd European Control Conference, Rome, pp. 1645-1651.
- [2] P. Georgieva and A. Ilchmann (2001), 'Adaptive λ -tracking control of activated sludge processes', *Int. J. of Control*, **74**, pp. 1247-1259.
- [3] J.W. Polderman and I.M.Y. Mareels (2000), 'Robustification of high gain adaptive control', *Invited session of the 39th IEEE Conf. Decision and Control*, Sydney.
- [4] D. Vrančić, Youbin Peng and S. Strmčnik (1999), 'A new PID controller tuning method based on multiple integrations', Control Engineering Practice, **7**, pp. 623-633.

Model Reduction by Proper Orthogonal Decomposition

Patricia Astrid
Department of Electrical Engineering
Control Systems Group
Eindhoven University of Technology
P.O.Box 513
5600 MB Eindhoven
The Netherlands
p.astrid@tue.nl

Siep Weiland
Department of Electrical Engineering
Control Systems Group
Eindhoven University of Technology
P.O.Box 513
5600 MB Eindhoven
The Netherlands
s.weiland@tue.nl

1 Abstract

REGLA project deals with the control and optimization of glass melting furnaces. The desired applied control scheme for the glass melting furnace is the Model-Based Predictive Control. Currently, a simulating first-principle based model has been built in a software package and considered as a good model that approximates the real furnace behaviour. Since the model of the glass melting furnace comprises mainly of nonlinear partial differential equations, numerical implementation of this model will require discretisation of the computation domain in enormous amount of grid cells that leads to a slow model. Model reduction becomes an inevitable need to provide a good simulating model for the controller that employs much less computational effort, yet provides a good agreement with the original model. Currently the Proper Orthogonal Decomposition technique is investigated for feasibility and after analyzing the results for some test cases, this method offers an extremely promising tool for model reduction of glass melting furnaces.

2 Proper Orthogonal Decomposition

It is well-known that the dynamics of a system can be approximated as linear combinations of its basic modes. This has been employed for example in the Fourier and Taylor series.

Consider a general form of a PDE [2]:

$$\frac{\partial u}{\partial t} = D(u) \tag{1}$$

In the Proper Orthogonal Decomposition (POD) technique, the solution of the PDE in Eq. 1 can be expressed as [2]:

$$\hat{u} = \sum_{i=1}^{N} a_i(t)\varphi(x) \tag{2}$$

The basic modes in POD are the corresponding eigenvectors obtained from the Singular Value Decomposition of the

empirical data collection [4],[1]. The degree of the reduction is determined from the number of eigenvectors taken. An error minimization criteria is applied to determine the time-varying coefficients for each eigenvectors $a_i(t)$.

To test the feasibility of this approach, several test cases have been built, among others Navier Stokes Equation for 2-D flow and a heat conduction problem. Despite of the nonlinearity of these physical phenomena, the reduced model shows good agreement with the original model although the number of modes taken is very few compared to the original order of the model. In many examples, the POD method adapts quite well with the changing of working points.

In the near future, mathematical properties of the POD method are going to be investigated and application to the rigorous software is planned.

- [1] M.Kirby. *Geometric Data Analysis*. John Wiley and Sons, Inc.2001
- [2] Glavaski, S. Marsden, J.E., Murray, R.M. Model Reduction, Centering, and the Karhunen-Loeve Expansion.
- [3] Kunisch,K, S. Volkwein, Control of Burger's Equation by a Reduced Order Approach Using Proper Orthogonal Decomposition. JOTA, 1998
- [4] Volkwein,S. Proper Orthogonal Decomposition and Singular Value Decomposition.1998

Oscillation Diagnosis in Control Loops - a Survey

V. Grosfils, M. Kinnaert
Service d'Automatique et d'Analyse des Systèmes,
Université Libre de Bruxelles,
CP 165/55, 50, Av. F. D. Roosevelt, B-1050 Brussels, Belgium
vgrosfil@labauto.ulb.ac.be,kinnaert@ulb.ac.be

1 Abstract

In industrial plants, many control loops have poor performance which implies a decrease of the product quality, unnecessary high energy consumption, waste of raw material... An important indication of deterioration of the control performance is the presence of oscillations in the control error especially due to friction in valve, oscillating load disturbances, or badly tuned controller. In this work, a review of existing approaches, that help to distinguish oscillations due to valve stiction from oscillations due to other causes, is performed. These methods only use the set point, the process output and the control signal.

Many methods rely on the shape of the output signal and of the control signal to determine the origin of an oscillation. Indeed, usually, in case of stiction, the control signal is always triangular and the output signal is rectangular for non-integrating processes and triangular for integrating processes.

The method described in [3] compares the output signal with a set of primitives representing the trends that can appear in a signal (linear increasing, linear decreasing, curved increasing...). Another method [1], dedicated to self-regulating processes, is based on the shape of the correlation function between process output and controller output. In [2], diagnostic is performed using the shape of the probability density function of the first or of the second derivative of the output signal. In cascade loops, some hardware problems can be diagnosed by studying the plots of the set point against the output signal [5].

Other methods that do not use the shape of the signals have also been developed. Such an approach is proposed in [5] and in [6] where the presence of a nonlinarity inside a control loop is detected and in [6] where diagnosis of the root cause of plant-wide oscillations caused by a nonlinearity is performed.

The results obtained with some of these approaches are illustrated via simulations. To this end, a typical model of a control loop including a phenomenological model of a control valve [4] is used. The latter is a nonlinear first-order model including non-linearities like dead zone, dead time and velocity saturation. This model allows one to simulate a control valve in healthy condition and to introduce stic-

tion and hysteresis. Possible limitations of the methods are pointed out.

- [1] Horch A., A simple method for detection of stiction in control valve, *Control Engineering Practice*, 7(10): 1221 1231, 1999
- [2] Horch A. and A.J. Isaksson, Detection of valve stiction in integrating processes, *Proceedings of the ECC 2001*, Porto, Portugal, pp. 1327 1332, 2001.
- [3] Rengaswamy R., T. Hägglund, and V. Venkatasubramanian, A Qualitative shape analysis formalism for monitoring control loop performance, *Engineering Applications of Artificial Intelligence*, 14, pp. 23-33, 2001.
- [4] Riihilahti J., Control Valve Simulation Models for process simulators, *Proceedings of the 1997 ISA TECH/EXPO Technology Update (Future Technology for Measurements and Control)*, Part 1/5 (of 5); Oct 7-9 1997, Anaheim, CA, USA, 1997.
- [5] Thornhill N.F. and T. Hägglund, Detection and Diagnosis of Oscillation in Control Loops, *Control Engineering Practice*, Vol. 5, No. 10, pp. 1343-1354, 1997.
- [6] Thornhill N. F., S.L. Shah and B. Huang, Detection of distributed oscillations and root-cause diagnosis, *Proceedings of the 4th IFAC workshop on On-line fault detection and supervision in the chemical process industries*, Jejudo Island, Korea, pp. 167 172, 2001.

Modeling and predictive control of cement grinding circuits

Renato Lepore, Alain Vande Wouwer and Marcel Remy Laboratoire d'Automatique, Faculté Polytechnique de Mons, 7000 Mons, Belgium (lepore@autom.fpms.ac.be)

Clinker and raw material grinding is a fundamental step in cement manufacturing. This highly energyconsuming operation is usually performed in closedloop grinding circuits, including a ball mill and an air classifier [4].

Modeling of industrial grinding circuits is a delicate task due to the lack of reliable measurements of some key variables, such as material hold-up and particle size distribution inside the mill, which are function of space and time [1].

In previous studies [2, 3], the authors have developed and validated a first-principle model of a closed-loop grinding circuit of the cement manufacturer CBR (Belgium). This first-principle model, which consists of sets of partial differential equations (PDEs) and algebraic equations (AEs), can be used as a tool to investigate process dynamics, to study the effect of changes in material properties, and to test control schemes.

Even though this approach has proved quite successful, the resulting model is too complex in nature to allow model-based control to be readily implemented. As a next step, it is therefore required to develop simplified models and, in [5], a reduced-order model is proposed for a laboratory-scale fed-batch process.

The objective of the present study is twofold:

- to extend the results presented in [5] to a full-scale closed-loop grinding circuit. This objective involves the development of a low-order distributed-parameter model for a continuous ball mill, which would allow the description of the particle size distribution along the mill axis, the estimation of the unknown model parameters, and the validation of this model with respect to the previously developed, more complex, first-principle model.
- to design a nonlinear predictive control (NMPC) based on the low-order distributed-parameter model.

The main advantage of the proposed modeling approach – which is still based on elementary mass balances for

several particle size intervals – is that it enables the description of the particle size distribution inside the grinding circuit, whereas black-box approaches often refer to some global variables only (such as the material flow rates or the total mass content of the mill).

- [1] Austin, L.G., R.R. Klimpel and P.T. Luckie (1984). *Process engineering of size reduction: ball milling*, Soc. of Mining Engineers, New York.
- [2] Boulvin M., C. Renotte, A. Vande Wouver, M. Remy, S. Tarasiewicz and P. César (1999). Modeling, simulation and evaluation of control loops for a cement grinding process, *European Journal of Control* 5, 10-18.
- [3] Boulvin, M. (2000). Contribution à la modélisation dynamique, à la simulation et à la conduite des circuits de broyage à boulets utilisés en cimenterie, Ph.D. thesis. Faculté Polytechnique de Mons, Mons (Belgium).
- [4] Labahn, O. and B. Kohlhaas (1991). Cement engineer's handbook, Bauverlag GmbH, Wiesbaden and Berlin.
- [5] Lepore, R., A. Vande Wouwer, Ph. Bogaerts and M. Remy (2001). Control-oriented modeling in grinding circuits: a new approach, *European Control Conference* (ECC '01), Porto, Portugal.

Optimal Errors-in-Variables Smoothing

Ivan Markovsky, Bart De Moor, and Sabine Van Huffel K. U. Leuven, ESAT/SISTA, Kasteelpark Arenberg 10, B-3001 Leuven-Heverlee, Belgium {Ivan.Markovsky, Bart.DeMoor, Sabine.VanHuffel}@esat.kuleuven.ac.be

1 Abstract

We consider an estimation problem for dynamical system described with an errors-in-variables model (see Figure 1). We give a recursive solution of the smoothing problem, i.e., the estimation problem when all data is available beforehand. The problem statement is given in Section 2 and the solution is given in Section 3.

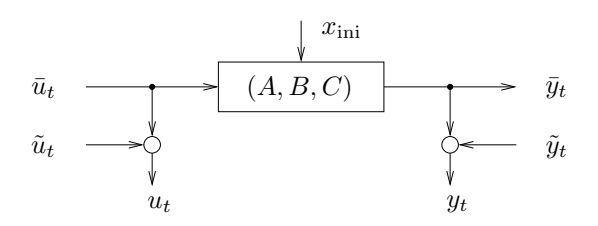


Figure 1: Errors-in-variables model

2 Optimal EIV smoothing problem

Given is a discrete-time LTI state-space system

$$\begin{array}{rcl} \bar{x}_{t+1} & = & A\bar{x}_t + B\bar{u}_t \\ \bar{y}_t & = & C\bar{x}_t, \end{array}$$

for $t=0,1,\ldots,T-1$, and with given initial condition $\bar{x}_0=x_{\rm ini}$. The signals \bar{u} and \bar{y} are not measurable. The measured signals are

$$u_t = \bar{u}_t + \tilde{u}_t$$
 and $y_t = \bar{y}_t + \tilde{y}_t$,

where \tilde{u} and \tilde{y} are white, centered, and uncorrelated random processes with known covariance matrices $\operatorname{var}(\tilde{u}_t) \triangleq R^{-1} > 0$ and $\operatorname{var}(\tilde{y}_t) \triangleq Q^{-1} > 0$, for $t = 1, \dots, T$.

The optimal EIV smoothing problem is: find sequences $\{\hat{u}_t\}_{t=0}^{T-1}$, $\{\hat{y}_t\}_{t=0}^{T-1}$, and $\{\hat{x}_t\}_{t=0}^{T}$ that solve the following optimization problem

$$\begin{split} \min_{\substack{\hat{u}_0, \dots, \hat{u}_{T-1} \\ \hat{y}_0, \dots, \hat{y}_{T-1} \\ \hat{x}_0, \dots, \hat{x}_T}} \sum_{\tau=0}^{T-1} \left(\left(u_{\tau} - \hat{u}_{\tau} \right)^T R \left(u_{\tau} - \hat{u}_{\tau} \right) + \right. \\ \left. + \left(y_{\tau} - \hat{y}_{\tau} \right)^T Q \left(y_{\tau} - \hat{y}_{\tau} \right) \right) \quad \text{(P)} \\ \text{s.t.} \quad \hat{x}_{t+1} &= A \hat{x}_t + B \hat{u}_t \\ \hat{y}_t &= C \hat{x}_t, \end{split}$$

for $t=0,1,\ldots,T-1$, and with initial condition $\hat{x}_0=x_{\rm ini}$.

3 Solution

Let $\{P_t\}_{t=0}^{T-1}$ be the solution of the Riccati difference equation

$$P_{t} = -A^{T} P_{t+1} B (B^{T} P_{t+1} B + R)^{-1} B^{T} P_{t+1} A + A^{T} P_{t+1} A + C^{T} Q C,$$

for $t=T-1,\ldots,0$, with final condition $P_T=0$, and let $\{s_t\}_{t=0}^{T-1}$ be the solution of the recursion

$$s_t = -A^T P_{t+1} B (B^T P_{t+1} B + R)^{-1} (B^T s_{t+1} - R u_t) + A^T s_{t+1} - C^T Q y_t,$$

for t = T - 1, ..., 0, with final condition $s_T = 0$. Then the optimal smoothed signals solving problem (P) are obtained from the forward recursion

$$\hat{x}_{t+1} = A\hat{x}_t + B\hat{u}_t, \qquad \hat{y}_t = C\hat{x}_t,$$

$$\hat{u}_t = -(B^T P_{t+1} B + R)^{-1} \times \times (B^T P_{t+1} A\hat{x}_t + B^T s_{t+1} - Ru_t).$$

for t = 0, ..., T - 1, with initial condition $\hat{x}(0) = x_{\text{ini}}$.

4 Acknowledgments

All authors are with the Katholieke Universiteit Leu-Ivan Markovsky is a doctoral student, Bart De Moor is a full professors, and S. Van Huffel is an associate professors. Our research is supported by grants from the following sources: IUAP P4-02 and P4-24, TMR Programme project CHRX-CT97-0160, Thematic Network BRRT-CT97-5040 'Niconet', Concerted Research Action (GOA) projects of the Flemish Government MEFISTO-666 (Mathematical Engineering for Information and Communication Systems Technology), IDO/99/03 project (K.U.Leuven), FWO projects G.0078.01 and G.0200.00, Flemish Government: Fund for Scientific Research Flanders G.0256.97, IWT Soft4s (softsensors), STWW-Genprom GBOU-McKnow (Knowledge management algorithms), Eureka-Impact (MPC-control), Eureka-FLiTE (flutter modeling)), Belgian Federal Government: DWTC (IUAP IV-02 (1996-2001) and IUAP V-10-29 (2002-2006): Dynamical Systems and Control: Computation, Identification and Modelling), Program Sustainable Development PODO-II (Traffic Management Systems), Direct contract research: Verhaert, Electrabel, Elia, Data4s, and IP-COS.

Real-Time Control using Interactive Sensing and Classification

Ronald L. Westra
Mathematics Department, Universiteit Maastricht
P.O.Box 616, 6200 MD Maastricht, The Netherlands
westra@math.unimaas.nl

1 Abstract

In this paper we study systems that can occur in a finite number of partly overlapping states, where the state directly defines the (set of) appropriate control action(s) required to bring the system back in its ground or equilibrium state. We describe an approach for the real-time control of such systems, based on the concurrent aggregation and classification of numerous heterogeneous noisy sensor data. Starting point for the approach is a large set of empirical observations of the given system, represented in the space of the sensor parameters. The relevant states of the system are identified with parametric clustering techniques like Gaussian mixture decomposition. Using this parametric representation, a hypothesis on the actual state of the system can be expressed in terms of the currently obtained sensor data. The realtime control approach is based on determining the state of the system as fast as possible. This is realized by iteratively determining the most informative sensor-parameter, and consequently reading the associated sensor. The newly collected information will give rise to a new hypothesis on the system state. This iteration is continued until a specified confidence level has been met, or all sensors have been red. Central in our approach is the notion of the most informative parameter. This entity is defined as the parameter which has the highest potency for deciding between the competing hypotheses. This parameter is computed with dynamic parameter selection, using the optimization of functionals that express relative state separation and relative parameter relevance, involving the actual hypothesis on the system. The approach is analysed theoretically, and an application is described on real-time production quality control using computational vision.

- [1] Efficient On-line Classification based on Fuzzy Multivariate Class Membership Functions for Clustering and Optimal Parameter Selection, R.L. Westra, 7th UK conference on Fuzzy Systems, Sheffield, October 2000
- [2] Real-Time Quality Control using Interactive Vision, R.L. Westra, Ph.D.Thesis Universiteit Maastricht 2001, ISBN 90.5278.326.8

Coverage control for distributed sensing networks

Jorge Cortés
Faculty of Mathematical Sciences
University of Twente
P.O. Box 217 7500 AE Enschede
The Netherlands
j.cortes@imaff.cfmac.csic.es

Sonia Martínez Departamento de Matemáticas IMAFF-CSIC Serrano 123, Madrid 28006, Spain s.martinez@imaff.cfmac.csic.es

Timur Karatas Francesco Bullo Coordinated Science Laboratory University of Illinois, Urbana-Champaign Urbana, IL 61801, United States {tkaratas,bullo}@uiuc.edu

1 Abstract

We describe decentralized control laws for the coordination of multiple vehicles performing spatially distributed tasks. The control laws are based on a gradient descent scheme applied to a class of decentralized navigation functions that encode optimal coverage and sensing policies. The approach exploits the computational geometry of Voronoi diagrams.

Our central motivation in this note is provided by distributed sensing networks in scientific exploration or surveillance missions. The motion coordination problem is to maximize the information provided by a swarm of vehicles taking measurement of some process.

1.1 Setting up the coverage control

Let $\{p_1,\ldots,p_n\}$ be the location of n sensors moving in a Riemannian manifold (with boundary) Q. Let $\phi:Q\to\mathbb{R}_+$ be a distribution density function. The measure ϕ plays the role of an "information density". Assume each vehicle has a sensor that provides accurate local measurements and whose performance degrades with distance. Formally, let $f(\operatorname{dist}(q,p_i))$ (with 'dist' the distance defined through the Riemmanian metric) describe the performance degradation, e.g., noise, loss of resolution, etc, of the measurement at the point $q\in Q$ taken from the ith sensor at position p_i . The function $f:\mathbb{R}_+\to\mathbb{R}_+$ is monotone increasing.

The overall "sensing performance" is given by,

$$U(p_1, ..., p_n) = \int_{Q} \min_{i \in \{1, ..., n\}} f(\text{dist}(q, p_i)) \phi(q) dq.$$
 (1)

This function (common in geographical optimization science [1]) measures the ability of a collection of vehicles to provide accurate distributed sensing. The locational optimization problem is to minimize U.

1.2 Voronoi diagrams

Let the Voronoi region $V_i = V(p_i)$ be the set of all points $q \in Q$ such that $\operatorname{dist}(q,p_i) \leq \operatorname{dist}(q,p_j)$ for all $j \neq i$. The set of regions $\{V_1,\ldots,V_n\}$ is called the Voronoi diagram for the generators $\{p_1,\ldots,p_n\}$. When the two Voronoi regions V_i and V_j are adjacent, p_i is called a (Voronoi) neighbor of p_j (and vice-versa).

1.3 Decentralized control protocols

We propose the gradient descent as a decentralized control law that achieve "uniform coverage" of Q,

$$\dot{p}_i(t) = -\frac{\partial U}{\partial p_i}.$$
 (2)

The following result [2, 3] shows that indeed the control law is decentralized, in the sense that only depends on local information, i.e. the location of p_i and of its neighbors,

$$\frac{\partial U}{\partial p_i} = \int_{V_i} \frac{\partial}{\partial p_i} f\left(\operatorname{dist}(q, p_i)\right) d\phi(q). \tag{3}$$

Hence, U provides us with a decentralized navigation function [4] in the setting of multiple vehicle networks.

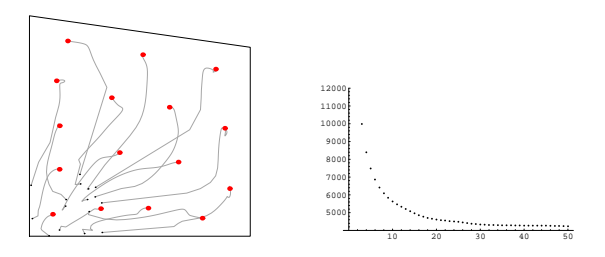


Figure 1: Distribution of sensors obtained by 16 vehicles in a polygon. The vehicles' initial positions are in a tight group in the lower left corner and their final positions are optimally distributed.

- [1] A. Okabe, B. Boots, K. Sugihara, and S. N. Chiu, Spatial Tessellations: Concepts and Applications of Voronoi Diagrams, John Wiley & Sons, New York, NY, 2 edition, 2000.
- [2] Q. Du, V. Faber, and M. Gunzburger, "Centroidal Voronoi tessellations: applications and algorithms," SIAM Review 41 (4), 637–676, 1999.
- [3] J. Cortés, S. Martínez, T. Karatas, and F. Bullo, "Coverage control for mobile sensing networks," in IEEE Conf. on Robotics & Automation, Arlington, VA, May 2002, submitted.
- [4] E. Rimon and D. E. Koditschek, "Exact robot navigation using artificial potential functions," IEEE Trans. Robotics & Automation 8 (5), 501–518, 1992.

Global H_2 -approximation in state-space: a case study

Ralf Peeters
Dept. Mathematics
Universiteit Maastricht
P.O. Box 616
6200 MD Maastricht
The Netherlands
ralf.peeters@math.unimaas.nl

Bernard Hanzon
Dept. Econometrics, FEWEB
Vrije Universiteit
De Boelelaan 1105
1081 HV Amsterdam
The Netherlands
bhanzon@feweb.vu.nl

Dorina Jibetean CWI P.O. Box 94079 1090 GB Amsterdam The Netherlands d.jibetean@cwi.nl

Abstract

In state-space, the discrete-time H_2 -approximation problem can be stated as follows. Let Σ be a given (linear time-invariant causal) stable system with m inputs and p outputs and an associated minimal state-space realization (A, B, C, D) of order n. For k < n, find an approximating stable system $\hat{\Sigma}$ and an associated minimal state-space realization $(\hat{A}, \hat{B}, \hat{C}, \hat{D})$ of order k which minimizes the H_2 -distance between Σ and $\hat{\Sigma}$, specified by

$$\begin{split} \|\Sigma - \hat{\Sigma}\|_{H_2}^2 &= \operatorname{tr}\left\{ (D - \hat{D})(D - \hat{D})^* \right\} + \\ &+ \operatorname{tr}\left\{ \left(\begin{array}{cc} C & -\hat{C} \end{array} \right) \left(\begin{array}{cc} P_1 & P_2 \\ P_2^* & P_3 \end{array} \right) \left(\begin{array}{cc} C^* \\ -\hat{C}^* \end{array} \right) \right\}, \end{split}$$

where P_1 , P_2 and P_3 are the (unique) solutions of the discrete-time Lyapunov and Sylvester equations

$$P_1 - AP_1A^* = BB^*,$$

 $P_2 - AP_2\hat{A}^* = B\hat{B}^*,$
 $P_3 - \hat{A}P_3\hat{A}^* = \hat{B}\hat{B}^*.$

This criterion is quadratic with respect to the each of the entries of both \hat{C} and \hat{D} , so that unique optimal values for \hat{C} and \hat{D} corresponding to a *fixed* choice for \hat{A} and \hat{B} , are easily computed as

$$\hat{D}_{\text{opt}} = D,$$

$$\hat{C}_{\text{opt}} = C P_2 P_3^{-1}.$$

Substitution of these values into the H_2 -criterion to be minimized yields the following 'concentrated H_2 -criterion'

$$\|\Sigma - \hat{\Sigma}\|_{H_2}^2 = \operatorname{tr}\left\{CP_1C^*\right\} - \operatorname{tr}\left\{CP_2P_3^{-1}P_2^*C^*\right\}.$$

which is to be minimized over all controllable input pairs (\hat{A}, \hat{B}) with \hat{A} asymptotically stable of size $k \times k$ and \hat{B} of size $k \times m$. Note that the first term of this expression is equal to the H_2 -norm squared of the given system Σ and provides an upper bound for the expression $V_c(\hat{A}, \hat{B}) := \operatorname{tr}\left\{CP_2P_3^{-1}P_2^*C^*\right\}$ to be maximized.

In this paper we present a case study of a nontrivial multivariable example of a given system Σ of order 4 with 2 inputs and 2 outputs together with an accompanying approximating system $\hat{\Sigma}$ of order 2. This example was designed

in a systematic way such that the entries in the matrices of the state-space realizations of both Σ and $\hat{\Sigma}$ are available in exact rational format. This makes the example suitable for testing recently developed exact algebraic methods that can be employed to decide on global optimality of the approximant. The property of stationarity of the approximant $\hat{\Sigma}$ for the concentrated H_2 -criterion is part of the design procedure, but local optimality has to be verified explicitly. For the case of our example this is achieved by establishing positive definiteness of the Hessian at the approximant.

To establish global optimality of $\hat{\Sigma}$, the algebraic form of the concentrated H_2 -criterion, involving 4 free parameters, still happens to be far too complicated to be handled directly by available state-of-the-art algebraic methods and software, despite the seemingly low values of m, p, n and k. (This illustrates the intrinsic complexity of the problem, which may indicate to some extent why a general method to compute global H_2 -approximants is still lacking in the literature.)

However, by means of a 'second concentration step', consisting of an (unsuccessful) attempt to rewrite the concentrated H_2 -criterion into a form which allows for a general characterization of all optimal matrices \hat{B} for a *fixed* given matrix \hat{A} , we are able to derive a function $W(\hat{A})$ which acts as an upper bound on the achievable value of $V_c(\hat{A}, \hat{B})$ when keeping \hat{A} fixed and varying only \hat{B} . These computations involve the use of so-called Faddeev reachability matrices, which allow one to express the solution of a discrete-time Lyapunov or Sylvester equation as a finite sum of matrices. The upper bound $W(\hat{A})$ turns out to be rational in the entries of \hat{A} . Since \hat{A} can be chosen to be in canonical (companion) form, the number of free parameters is reduced to 2, and the complexity of W becomes considerably less than that of V_c .

We are finally in a feasible position to apply algebraic techniques for global optimization of rational functions. We then will show, for the case at hand, that: (i) the upper bound $W(\hat{A})$ is *sharp* at the approximant $\hat{\Sigma}$, and (ii) the upper bound has a global maximum at the approximant $\hat{\Sigma}$. This leads us to conclude global optimality of the H_2 -approximant, providing (to the best of our knowledge) the first nontrivial multivariable instance of this nature described in the literature.

Performance and Convergence of Iterative Learning Control

Mark H.A. Verwoerd and Theo J.A. de Vries
Control Laboratory
Faculty of Electrical Engineering
University of Twente
P.O. Box 217
7500 AE Enschede
The Netherlands
m.h.a.verwoerd@el.utwente.nl

Gjerrit Meinsma
Systems and Control group
Faculty of Applied Mathematics
University of Twente
P.O. Box 217
7500 AE Enschede
The Netherlands
g.meinsma@math.utwente.nl

1 Abstract

Iterative Learning Control (ILC) [1] deals with the problem of finding the optimal input u^* to an unknown plant P by utilizing information from previous trials. The optimal input is defined in terms of the plant's output in the sense that it minimizes the distance between the actual output y and some desired output y_d . From a mathematical point of view, the problem boils down to defining a recursion relation on the space of inputs \mathcal{U} . This relation should define a convergent sequence and moreover it is generally required that $\lim_{k\to\infty} u(k) = u^*$.

At first sight, this seems like a difficult, if not impossible problem to solve. Nevertheless, many papers on ILC have addressed this problem and a variety of 'solutions' has been proposed [2]. The main idea that is common to all these solutions can easily be explained by means of a simple example.

Consider a recursion of the following type

$$u(k+1) = u(k) + e(k) \tag{1}$$

where e is defined as $y_d - y$. Assume there exists a $u_d \in \mathcal{U}$ such that $Pu_d = y_d$. If this sequence is convergent, then necessarily $\lim_{k \to \infty} e(k) = 0$. Assuming that P is bounded on \mathcal{U} , it is not hard to show that a necessary and sufficient condition for convergence is given by

$$||I - P|| < 1 \tag{2}$$

This implies that P^{-1} exists and is bounded. In fact, if this condition holds, the recursion defined by (1) can be shown to converge to the fixed point $\bar{u} = P^{-1}y_d = P^{-1}\left(Pu_d\right) = u_d$. In the context of linear systems this means that, as a necessary condition for convergence, P should be invertible in \mathcal{RH}^{∞} . Clearly only a very limited subclass of LTI plants satisfies this condition. This makes us wonder whether in general there exists at all a scheme that converges to the optimal input $u^* = u_d$. If the answer would turn out to be negative, the limits of performance have to be taken into account from the start, which means that aiming for perfect tracking is not a good idea.

In its full generality, there is no way we can answer this question. One way to constrain the problem is to consider only recursions that are linear in u.

In this presentation, we will propose a framework for the analysis of linear recursions of arbitrary order. Within this framework, the Iterative Learning Control problem reduces to a discrete time controller design problem on an infinite dimensional state space. Then, using the internal model principle, we are able to show that a zero steady state error can only be achieved if the controller has some integral action. This is illustrated in Figure 1 for the recursion defined by (1). We will elaborate on the implications of this result.

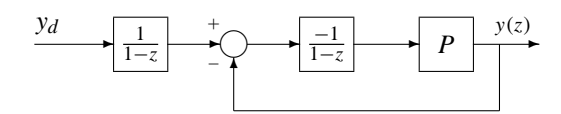


Figure 1: The internal model principle for ILC. The controller contains a model of the reference input.

- [1] Kevin L. Moore, "Iterative Learning Control for Deterministic Systems," Springer-Verlag, 1993.
- [2] Kevin L. Moore, J.-X. Xu (eds.), *International Journal of Control*, 73 (10), 2000. (Special issue on Iterative Learning Control)

A behavioral approach to decoding

Jan Willem Polderman¹

Margreta Kuijper²

1 Abstract

In this paper we present a behavioral interpretation of the list decoding approach that was proposed in [1]. We concentrate on the behavioral elements and keep the coding details to a minimum that is just sufficient to appreciate the lines of thought. A more elaborate treatment will be presented in a forthcoming paper. The paper is a follow up of [2] and works out the suggestion made there to put list decoding in the perspective of multivariable behavioral interpolation.

Briefly, an (n, κ) Reed-Solomon code is defined as follows. Let \mathbb{F} be a finite field, say $\mathbb{F} = \{\xi_1, \dots, \xi_n\}$. The message word is a κ -tuple $(m_0, m_1, \dots, m_{\kappa-1}) \in \mathbb{F}^{\kappa}$. With this κ -tuple we associate the polynomial $m(\xi) = m_0 + m_1 \xi + \dots + m_{\kappa-1} \xi^{\kappa-1} \in \mathbb{F}[\xi]$. The codeword \mathbf{c} is then the n-tuple of the evaluations of $m(\xi)$ in the elements of \mathbb{F} : $\mathbf{c} = (m(\xi_1), \dots, m(\xi_n))$. The codeword \mathbf{c} is transmitted through a channel where errors may occur so that the received word \mathbf{r} is not necessarily equal to the transmitted codeword \mathbf{c} . The decoding problem consists of reconstructing the original polynomial $m(\xi)$ from the received word \mathbf{r} .

In a recent paper, [1], a list decoding scheme based on bi-variate interpolation was proposed. In list decoding a list of possible polynomials $m(\xi)$ is derived from the received word. Subsequently a unique member is selected on the basis of secondary criteria. This second step is not discussed in the present paper.

The idea put forward in [1] is as follows. Denote the received word by $\mathbf{r} = (\eta_1, \dots, \eta_n)$. Let $Q(\xi, \eta) \in \mathbb{F}[\xi, \eta]$ be a bivariate polynomial of $(1, \kappa - 1)$ weighted degree, defined below, such that $Q(\xi_i, \eta_i) = 0$ for $i = 1, \dots, n$.

1.1 Definition

Let $Q(\xi, \eta) \in \mathbb{F}[\xi, \eta]$, say $Q(\xi, \eta) = \sum_{i \in I, j \in J} q_{ij} \xi^i \eta^j$. The (w_{ξ}, w_{η}) weighted degree of $Q(\xi, \eta)$ is defined as

wdeg
$$Q(\xi, \eta) = \max_{i \in I, j \in J} \{iw_{\xi} + jw_{\eta} \mid q_{ij} \neq 0\}$$
 (1)

In fact, in most but not all cases, the weighted degree is just the normal degree of $Q(\xi^{w_{\xi}}, \xi^{w_{\eta}})$. In the sequel we

are only concerned with the $(1, \kappa - 1)$ weighted degree and therefore we refer to it as just the weighted degree. Let $\ell = \operatorname{wdeg} Q(\xi, \eta)$. Suppose now that the received word contains less than $n-\ell$ errors. Then there exists a polynomial $\tilde{m}(\xi)$ of degree less than κ such that $\tilde{m}(\xi_i) = \eta_i$ for at least $\ell+1$ values of i. In fact, the original polynomial $m(\xi)$ does this, but there can be more. We conclude that $Q(\xi, \tilde{m}(\xi))$ has at least $\ell+1$ zeros. On the other hand, $\deg Q(\xi, \tilde{m}(\xi))$ cannot exceed ℓ since by assumption wdeg $Q(\xi, \eta) = \ell$ so that deg $Q(\xi, \tilde{m}(\xi)) \leq \ell$. Since a polynomial of degree not exceeding ℓ can only have more than ℓ roots if it is the zero polynomial, it follows that $Q(\xi, \tilde{m}(\xi))$ is indeed the zero polynomial. But this implies that $\eta - \tilde{m}(\xi)$ divides $Q(\xi, \eta)$. In particular $\eta - m(\xi)$ divides $Q(\xi, \eta)$. The list decoding now consists of constructing a polynomial $Q(\xi, \eta)$ such that $Q(\xi, \eta_i) = 0$ and such that $\deg Q(\xi, \xi^{\kappa-1})$ is minimal. Once $Q(\xi, \eta)$ has been constructed all factors of the form $\eta - \tilde{m}(\xi)$ are extracted thus producing a list of candidate polynomials $\tilde{m}(\xi)$. Roughly, our approach is structured as follows. We write the polynomial $Q(\xi, \eta)$ to be constructed as $Q(\xi, \eta) = \sum_{j=0}^{M-1} d_j(\xi) \eta^j$ for an appropriate choice of M. With the data (ξ_i, η_i) we associate n trajectories $\mathbf{w}_i : \mathbb{Z}_+ \to \mathbb{F}^M$. We then determine the Most Powerful Unfalsified Model \mathfrak{B} of these n trajectories. Then we construct a weighted degree row reduced matrix $R(\xi) \in \mathbb{F}[\xi]$ that represents \mathfrak{B} . From $R(\xi)$ we select a row $d(\xi)$ of minimal weighted row degree and finally we define $Q(\xi, \eta) = \sum_{j=0}^{M-1} d_j(\xi) \eta^j$, where, of course, the $d_i(\xi)$ s are the entries of $d(\xi)$. It turns out that $Q(\xi, \eta)$ constructed is this way is a bivariate polynomial of minimal $(1, \kappa - 1)$ weighted degree that interpolates the data points (ξ_i, η_i) .

- [1] M. Sudan. Decoding of Read-Solomon codes beyond the error correction bound. *Journal of Complexity*, 13:180–193, 1997.
- [2] M. Kuijper. Behavioral interpolation for coding and control. In *Proc. 39th IEEE Conf. Decision and Control*, pages 2488–2493, Sydney, Australia, 2000.

¹Faculty of Mathematical Sciences, University of Twente, P.O.Box 217, 7500 AE Enschede, The Netherlands. E-mail: J.W.Polderman@math.utwente.nl

²Department of Electrical and Electronics Engineering, The University of Melbourne, VIC 3052, Australia. E-mail: m.kuijper@unimelb.edu.au

Principal angles in system theory, information theory and signal processing

Katrien De Cock and Bart De Moor¹
K.U.Leuven
Dept. of Electrical Engineering (ESAT), Research Group SCD
Kasteelpark Arenberg 10, B-3001 Leuven, Belgium
{decock,demoor}@esat.kuleuven.ac.be

Abstract

We establish relations between system theory, information theory and signal processing by computing the principal angles between linear subspaces. Our main result is the equivalence of a weighted cepstral norm of a Gaussian autoregressive moving average (ARMA) process and the mutual information of its past and future.

1 Principal angles between subspaces

Principal angles between linear subspaces were defined by Camille Jordan [3] in the nineteenth century and statistically interpreted by Hotelling as canonical correlations [2]. In systems and control, the principal angles occur in subspace identification methods [5] and also in damage location [1]. We start with the definition of the principal angles between linear subspaces and show how the canonical correlations of two stochastic processes can be interpreted as principal angles.

2 Principal angles between input and output spaces of a linear model

We obtain expressions for the canonical correlations of the past and future input and output processes of a linear stochastic model, in terms of the model parameters. From these parametric expressions, the relations between the different sets of principal angles can easily be deduced, which are also corroborated by geometric insights.

For single-input single-output (SISO) models, we give a new characterization for the canonical correlations of the input and the output: the canonical correlations of the input and output process of a SISO ARMA model are equal to the cosines of the principal angles between the row spaces of the infinite controllability matrix of the model and the infinite controllability matrix of the inverse model.

3 A cepstral norm for ARMA models and the mutual information of past and future

We treat one particular cepstral norm for ARMA models, derived from a metric in [4]. We show that the cepstral norm of a model can be characterized as a function of the principal angles between the row spaces of the controllability matrix of the model and the controllability matrix of the inverse model. By using the insights of the first part of the talk, the norm is related to the canonical correlations of the past and the future of the output process and hence to the mutual information of these processes.

References

- [1] M. I. Friswell, J. E. T. Penny and S.D. Garvey, Parameter subset selection in damage location, Inverse Problems in Engineering 5 (1997) 189–215.
- [2] H. Hotelling, Relations between two sets of variates, Biometrika 28 (1936) 321–372.
- [3] C. Jordan, Essai sur la géométrie à n dimensions, Bulletin de la Société Mathématique 3 (1875) 103–174.
- [4] R. J. Martin, A metric for ARMA processes, IEEE Transactions on Signal Processing 48 (2000) 1164–1170.
- [5] P. Van Overschee and B. De Moor, Subspace Identification for Linear Systems: Theory Implementation Applications, Kluwer Academic Publishers, Boston, 1996.

Acknowledgements

Our research is supported by several sources: Research Council KUL: Concerted Research Action GOA-Mefisto 666, IDO, several PhD/postdoc & fellow grants; Flemish Government: Fund for Scientific Research Flanders (several PhD/postdoc grants, projects G.0256.97 (subspace), G.0115.01, G.0240.99, G.0197.02, G.0407.02, research communities ICCoS, ANMMM), AWI (Bil. Int. Collaboration Hungary/ Poland), IWT (Soft4s, STWW-Genprom, GBOU-McKnow, Eureka-Impact, Eureka-FLiTE); Belgian Federal Government: DWTC (IUAP IV-02 (1996-2001) and IUAP V-10-29 (2002-2006)), Program Sustainable Development PODO-II; Direct contract research: Verhaert, Electrabel, Elia, Data4s, IPCOS.

¹ Katrien De Cock is a research assistant at the K.U.Leuven. Dr. Bart De Moor is a full professor at the K.U.Leuven.

Bang-bang Control of Underactuated Mechanical Systems

M. Gerard

Université de Liège, Institut Montefiore Bât. B28, Sart-Tilman 4000 Liège, Belgique gerard@montefiore.ulg.ac.be

R. Sepulchre

Université de Liège, Institut Montefiore Bât. B28, Sart-Tilman 4000 Liège, Belgique sepulchre@montefiore.ulg.ac.be

Abstract

This paper describes the design of a control structure based on bang-bang control laws in order to generate acrobatic trajectories. As an illustration, we consider the swinging-up of the free pendulum of the pendubot system and the cart-pole system.

The goal is to get simple control laws allowing analytical approximations while minimizing the computation efforts in practical implementations.

Swing-up specifications

We are interested in swinging-up the free pendulum of the cart-pole system and the pendubot system by controlling respectively the acceleration of the cart and the angular acceleration of the actuated arm.

By choosing an appropriate bang-bang law, we obtain the following parametrised bang-bang control law:

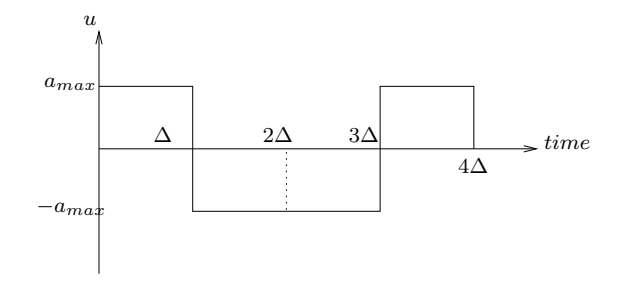


Figure 1: Control law: acc. of the cart/actuated arm

The shape is chosen symetric in order to satisfy an additional constraint: we want the cart or the actuated arm to come back to their initial position. Note also that the acceleration is bounded.

Design methodology

The system equations are of the form:

$$\dot{x} = f(t, x, u) \tag{1}$$

where $x \in \mathbb{R}^n$, $u \in \{-a_{max}, +a_{max}\}$ is the control law described in figure 1.

The energy of the free pendulum is equal to:

$$E_{pdl} = \frac{1}{2}J\omega^2 - mgl(1 + \cos\theta)$$
 (2)

where m is the mass of the pendulum, l is its length and J its moment of inertia. The energy level -2mgl corresponds to the vertical down position of the pendulum (at rest) and the energy level 0 corresponds to the vertical up position of the pendulum (at rest). The goal to reach is to supply the free pendulum a quantity of energy equal to 2mgl. We decide to fix the maximum value a_{max} of the acceleration and we play only on the switching time parameter. Then we derive an $analytical\ relation$ between the energy level E_{pdl} and Δ :

$$E_{pdl} = E(\Delta)$$

To obtain this relation, we proceed as follow:

- 1. We approximate non-linear function f of equation (1) by an integrable one; we consider different system approximations over successive time intervals.
- 2. We solve the approximated systems and find analytic approximations of $\theta(t), \omega(t)$ over the interval $[0, 4\Delta]$ which are Δ dependent.
- 3. We introduce the result in expression (2) and find the minimum value of Δ which zeroes it at time $t=4\Delta$, i.e. when the end of the energy transfer is reached.

References

[ARS] P.A. Absil, R. Sepulchre, "A Hybrid Control Scheme for Swing-up Acrobatics.

[AF96] K.J. Astrom, K. Furuta, "Swinging up a pendulum by energy control", Proceedings of IFAC 13th World Congress, San Francisco, Pergamon, 1996.

Point stabilization of the extended chain form with robustness to model uncertainties

David A. Lizárraga, Edo Aneke and Henk Nijmeijer Mechanical Engineering, Eindhoven University of Technology Den Dolech 2, Postbus 513 5600 MB Eindhoven, The Netherlands Email: {D.Lizarraga | N.P.I.Aneke | H.Nijmeijer}@tue.nl

1 Introduction

Consider the extended chained form system (ECF)

$$\ddot{x}_1 = u_1, \quad \ddot{x}_2 = u_2, \quad \ddot{x}_3 = u_1 x_2,$$
 (1)

which can also be written as $\dot{x}=b_0(x)+u_1b_1(x)+u_2b_2(x)$ with $b_0(x_0)=x_2\frac{\partial}{\partial x_1}+x_4\frac{\partial}{\partial x_3}+x_6\frac{\partial}{\partial x_5},\ b_1(x)=\frac{\partial}{\partial x_2}+x_3\frac{\partial}{\partial x_6}$ and $b_2(x)=\frac{\partial}{\partial x_4}$. This canonical form can be used to model the dynamics of several mechanical underactuated systems, for instance the PPR manipulator with unactuated third joint, the planar VTOL system in the absence of gravity, and the planar, parallel-drive RRR manipulator with any two joints actuated. Asymptotic *stabilization* of the ECF to the origin is a challenging problem solved in [1] by means of time-varying, homogeneous feedback. A limitation of controllers of this class, however, is the lack of robustness with respect to unmodeled dynamics. Uncertainties in the physical parameter values, for example, may introduce additive disturbance vector fields in the actual system, and these may cause instability of the origin. We are thus led to consider the *perturbed* system

$$\dot{x} = b_0(x) + h_0^{\varepsilon}(x) + \sum_{i=1}^{2} u_i(b_i(x) + h_i^{\varepsilon}(x)),$$
 (2)

where the disturbance vector fields h_i^{ε} —analytic both in $x \in \mathbb{R}^6$ and $\varepsilon \in \mathbb{R}$ —satisfy $h_i^0(\cdot) = 0$ (their magnitudes tend to zero as $\varepsilon \to 0$) and $h_0^{\varepsilon}(0) = 0$ (the origin is an equilibrium for the perturbed system). Roughly stated, a feedback law $(x,t) \mapsto \alpha(x,t)$ is considered robust if, for any family of disturbances $(h_i^{\varepsilon})_{i=0,1,2}$ of a given class, the origin of (2) with $u_i = \alpha_i(x,t)$ is locally asymptotically stable whenever $|\varepsilon|$ is small enough. Obviously, this notion of "robustness" is limited since more general sources of disturbance cannot be modelled by (2).

2 Robust control law for the ECF

Inspired by existing results, we propose a hybrid *openloop/feedback* approach. The principle is simple and based on a time-varying (indeed T-periodic) feedback-law $(x,t)\mapsto \alpha(x,t)$. α is designed so that $u=\alpha(x_0,t), t\in [0,T)$, drives the system's state from $x(0)=x_0$ to a point x(T) that is "closer" to the origin (in some particular metric). The control is *periodically* updated in terms of x_0 and

used to steer the system. Under appropriate conditions, this iterative scheme stabilizes the origin of a dynamic extension to (2), and is robust to a class of perturbations. System (2) is thus controlled by applying $u(t) = \alpha(x(kT), t)$, for $t \in [kT, (k+1)T)$ and $k \in \mathcal{K} = \{\lfloor t_0/T \rfloor, \lfloor t_0/T \rfloor + 1, \ldots \}$. This can be represented by complementing (2) with a dynamic extension whose solution $y(\cdot)$ coincides with x(t) at the sampling instants $(kT)_{k \in \mathcal{K}}$, and by controlling the system with $u(t) = \alpha(y(t), t)$, namely

$$\dot{x} = b_0(x) + h_0^{\varepsilon}(x) + \sum_{i=1}^{2} \alpha_i(y, t) (b_i(x) + h_i^{\varepsilon}(x))
\dot{y} = \sum_{k=\lfloor t_0/T \rfloor + 1}^{\infty} \delta(t - kT) x(t).$$
(3)

This system is initialized by choosing $(x_0, y_0) \in \mathbb{R}^6 \times \mathbb{R}^6$ and then setting $(x(t_0), y(t_0))$ equal to (x_0, x_0) if $t \mod T = 0$, or equal to (x_0, y_0) otherwise. We propose the following feedback law

$$\begin{array}{rcl} \alpha_1(x,t) & = & a_1x_1 + a_2x_2 + b\rho(x)\cos(\omega t) \\ \alpha_2(x,t) & = & a_3x_3 + a_4x_4 - \frac{2\omega^2}{b\rho(x)}(a_5x_5 + a_6x_6)\cos(\omega t) \end{array}$$

where b>0 and $\rho(x)=(\sum_{i=1}^6|x_i|^{\frac{2}{r_i}})^{\frac{1}{2}}$ with r=(1,1,1,1,2,2). One checks easily that when (1) is initialized at x_0 and controlled by $u(t)=\alpha(x_0,t),\ t\in[0,T),$ the solution satisfies $x(T)=Ax_0+\mathrm{o}(\|x_0\|)$. In the sequel we assume that $A\in\mathbb{R}^{6\times 6}$ is discrete-stable, i.e., $\sigma(A)\subset\{z\in\mathbb{C}:|z|<1\}$. This can be achieved by a proper choice of the gains $a=(a_1,\ldots,a_6)$.

Proposition 1 For any family of disturbances $(h_i^{\varepsilon})_{i=0,1,2}$ such that $h_{0,k}^{\varepsilon}(x) = O(\|x\|^2)$, k = 1..., 6, the origin of (3) is locally exponentially stable for $|\varepsilon|$ small enough.

The proof of this, our main result, is rather elaborate in part because it requires the Chen-Fliess series expansion of the solution $x(t),\ t\in [0,T)$. We show that the influence of the potentially "destabilizing" perturbation terms in the expansion can be made negligible by considering initial values x_0 sufficiently near the origin, and disturbance parameters ε sufficiently near zero. This control strategy has been verified in simulation; experiments on a real PPR manipulator with passive third joint are currently underway at our research group.

References

[1] N.P.I. Aneke, D.A. Lizárraga, and H. Nijmeijer. Homogeneous stabilization of the extended chained form system (*Submitted*). In *IFAC World Congress*, Barcelona, Spain, 2002.

Drive actuation in active control of centrifugal compressors

Jan Tommy Gravdahl and Olav Egeland Department of Engineering Cybernetics Norwegian University of Science and Technology N-7491 Trondheim NORWAY

Corresponding author Email: Tommy.Gravdahl@itk.ntnu.no

Svein Ove Vatland ABB Corporate Research Bergerveien 12 N-1375 Billingstad NORWAY

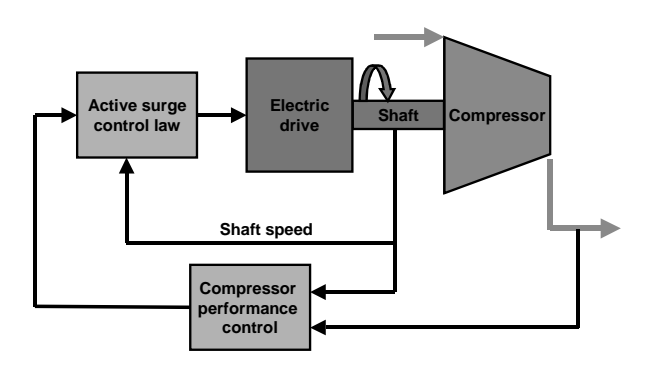


Figure 1: Active surge control using drive

1 Introduction

Traditionally, centrifugal compressor surge has been avoided using surge avoidance schemes that use various techniques to keep the operating point of the compressor away from the surge line. Typically, a surge control line is drawn at a specified distance from the surge line, and the surge avoidance scheme ensures that the operating point does not cross this line. Usually a recycle valve around the compressor is used as actuation. This method works well, as has been proved by numerous installations. However, due to the presence of the surge margin, the method restricts the operating range of the machine, and achievable efficiency is limited. In this study, which is on compressors with electrical drives, we propose to use the electrical drive as a means of active surge control, as depicted in Fig. 1. The advantage of this is that the drive is already present, and no additional actuation device is required. This means that the compressor can be operated at low flows without recycling, and there is a potential for reduced energy consumption of the compressor.

2 Modeling

A Greitzer model with varying speed [1] is used:

$$\hat{p} = a_{01}^2 V_p^{-1} (\hat{m} - \hat{m}_t)$$
(1a)

$$\dot{\hat{m}} = A_1 L_c \left(\hat{\Psi}_c \left(\hat{\omega}, \hat{m} \right) p_{01} - \hat{p}_p \right), \qquad (1b)$$

$$\dot{\hat{\omega}} = J^{-1} (\hat{\tau}_d - \hat{\tau}_c). \tag{1c}$$

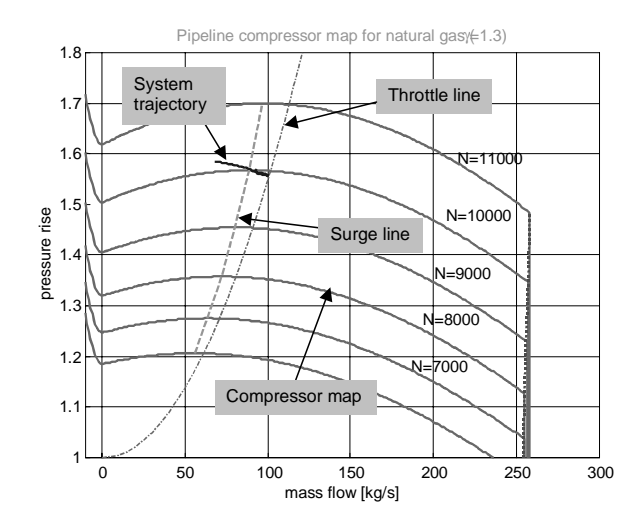


Figure 2: Stabilized operating point using torque.

3 Control

The control is derived in two steps. First, the angular speed, $\hat{\omega}$, is used as control, and then the drive torque $\hat{\tau}_d$, with its additional dynamics (1c) is used.

Theorem: Using the speed as control, the control law

$$\hat{\omega} = -c\hat{m},\tag{2}$$

where the gain c is chosen according to $c > \frac{\partial \Psi_c/\partial m}{\partial \Psi_c/\partial \omega}$ makes the origin of (1a) and (1b) globally exponentially stable. **Sketch of proof:** Consider the Lyapunov function candidate

 $V = \frac{V_p}{2a_{01}^2}\hat{p}^2 + \frac{L}{2A}\hat{m}^2 > 0, \forall \, (\hat{m},\hat{p}) \neq (0,0)$.Using (2) it can be shown that $\dot{V} < -k_p\hat{p}^2 - k_m\hat{m}^2 < -kV, \forall \, (\hat{m},\hat{p}) \neq (0,0)$ and the result follows.

A simulation of active surge control on a industrial size natural gas pipeline compressor using drive torque is shown in Fig. 2. The complete analysis and additional simulations can be found in [2]

References

[1] J.T. Gravdahl and O. Egeland, *Compressor surge and rotating stall: modeling and control*, Advances in Industrial Control. Springer-Verlag, London, 1999.

[2] ," http://www.itk.ntnu.no/ansatte/Gravdahl_Jan.Tommy/papers/automatica2002.pdf.

Improved Disturbance Rejection in a DVD Player using Switching Control

Marcel Heertjes
Philips CFT
Mechatronics Research
P.O. Box 218 / SAQ-1135
5600 MD Eindhoven, The Netherlands
marcel.heertjes@philips.com

Frank Cremers
Philips CFT
Mechatronics Research
P.O. Box 218 / SAQ-1131
S600 MD Eindhoven, The Netherlands
f.l.m.cremers@philips.com

Frank Sperling
Philips CFT
Mechatronics Research
P.O. Box 218 / SAQ-2118
5600 MD Eindhoven, The Netherlands
frank.sperling@philips.com

1 Abstract

Nowadays CD/DVD players are mainly controlled by linear feedback based on the concept of bandwidth. Depending on the type of disturbance, the bandwidth is set to meet certain specifications. Within the automotive industry, this imposes a trade-off. Namely in case of shocks, for example due to road excitation, increasing the bandwidth commonly results in an increased low-frequency disturbance rejection. However the playability [1], a performance measure related to deteriorated error signals during disc deficiencies like scratches or fingerprints, decreases due to sensor noise tracking. To overcome this trade-off, the merits of nonlinear control design will be studied. Nonlinear control enables a different amount of disturbance rejection, or playability, depending on: 1) the amount of disturbance, and 2) the type of disturbance.

Ideally a nonlinear controller may offer the ability of improving both disturbance rejection and playability within a single control design. Here, it will be shown that improvements in disturbance rejection can be obtained without necessarily affecting the playability. Hereto a hardening control strategy is presented that switches to a higher value for the controller gain beyond a pre-defined radial error level. As a result, large shocks correspond to a large amount of additional control effort giving improved disturbance rejection while, at the same time, small shocks hardly correspond to additional control thus leaving the playability unaffected.

The nonlinear control design is discussed regarding stability and performance. Closed-loop stability is derived on the basis of the circle criterion [3]. Especially the graphical representation of the circle criterion will serve as a tool for nonlinear design. Performance is quantified using a generalization of the linear sensitivity function. Based on the ampli-

tude part, the maximum absolute values of the periodic nonlinear responses subjected to harmonic excitations are depicted within a frequency range of interest. These responses are obtained numerically using efficient periodic solvers [2]. With this amplitude measure, improvements in disturbance rejection are studied for varying parameter values.

Experimental results performed on a lab-scale setup of a DVD (video) drive subjected to additional vibration excitation are shown to illustrate the possibilities of the nonlinear control design within a real-life application. The results largely correspond to the numerical results obtained with the simplified lens model and, therefore, provide a sufficient basis for further research.

- [1] Baggen, C.P.M.J., and Nijhof, J.E., *A Compact Disc IC Concept Enhancing Playability*, Proc. Conference on Consumer Electronics, IEEE, pp. 48-49, 1985.
- [2] Heertjes, M.F., Sperling, F.B., and van de Molengraft, M.J.G., Computing Periodic Solutions for a CD-Player with Impact using Piecewise Linear Shooting, *Proc. 40th IEEE Conference on Decision and Control*, WeP03-4, 2001.
- [3] Sastry, S., *Nonlinear Systems; Analysis, Stability, and Control*, Springer-Verlag, New York, 1999.
- [4] Stan, S.G., *The CD-ROM Drive; A Brief System Description*, Kluwer, Boston, 1998.

Robust Trajectory Tracking Control with Discrete-Time Sliding-Mode Controller and Feedforward Controller

Jian Wang¹, Jan Swevers, Hendrik Van Brussel Division PMA, Dept. Mechanical Engineering Katholieke Universiteit Leuven Celestijnenlaan 300B, B-3001 HEVERLEE, Belgium Tel: +32-16-322833 Fax: +32-16-322987 jian.wang@mech.kuleuven.ac.be

1 Abstract

A discrete time sliding-mode controller is designed with the reaching law method. To build up a tracking controller, a feedforward part is added outside the closed-loop sliding-mode controller. The robust performance of this tracking controller in the presence of plant model uncertainty and input disturbance is proved theoretically, and verified on the X-Y table driven by linear motors.

In continuous-time sliding-mode controller design, a switching surface is defined as a function of the system state:

$$s(t) = C_{sl} \cdot x(t). \tag{1}$$

A continuous-time sliding-mode controller can be designed such that the evaluation of the scalar *s* satisfy a prescribed differential equation:

$$\dot{s}(t) = -q \cdot s(t). \tag{2}$$

Discretizing the continuous-time reach law in Equation (2) yields:

$$s(k+1) = (1 - q \cdot T) \cdot s(k).$$
 (3)

Given a plant mode as:

$$\begin{cases} x(k+1) = (A + \Delta A) \cdot x(k) + B \cdot u(k) + P \cdot d(k); \\ y(k) = C \cdot x(k). \end{cases}$$
(4)

Calculating the command signal with reaching law (3):

$$u(k) = K \cdot x(k) - (C_{sl}B)^{-1} \cdot C_{sl} \cdot [\Delta A \cdot x(k) + P \cdot d(k)]$$
 (5)

Where

$$K = (C_{sl}B)^{-1}[(1 - q \cdot T) \cdot C_{sl} - C_{sl} \cdot A].$$
 (6)

The command in (5) is not implementable, because ΔA and d(k) are unknown. But if we know the boundary of the

model uncertainty ΔA and the input disturbance d(k) such that:

$$\begin{aligned} |C_{sl} \cdot [\Delta A \cdot x(k) + P \cdot d(k)]| &< U_d \cdot T, \\ U_d &> 0 \end{aligned} \tag{7}$$

and modify the command (5) as:

$$u(k) = K \cdot x(k) - (C_{sl}B)^{-1} \cdot U_d \cdot T \cdot sign(s)$$
 (8)

The command in (8)is implementable now, and it can be proved that a quasi-sliding-mode bound under this command satisfies:

$$|s(k)| < \frac{2U_d \cdot T}{1 - q \cdot T}.\tag{9}$$

Outside this bound, the plant state trajectory moves monotonously towards this bound. Inside this bound, the zigzag motion of the system state around the switching line is not guaranteed because the reaching law in (3) is changed to:

$$s(k+1) = (1 - q \cdot T) \cdot s(k) + C_{sl} \cdot [\Delta A \cdot x(k) + P \cdot d(k)] - U_d \cdot T \cdot sign(s).$$

$$(10)$$

The closed-loop system can be derived by substituting Equation (8) into Equation (4), which yield:

$$x(k+1) = A_w \cdot x(k) + \Delta Ax(k) + P \cdot d(k) - B \cdot (C_{sl}B)^{-1} \cdot U_d \cdot T \cdot sign(s).$$
(11)

$$A_w = A + B \cdot (C_{sl}B)^{-1} [(1 - q \cdot T) \cdot C_{sl} - C_{sl}A] \quad (12)$$

Notice that if the plant system matrix A is written in the controller canonic form, it can be proved that A_w is only dependent on the switching line parameter C_{sl} and the reaching law parameter q. This property allow us to build a tracking controller by adding a robust feedforward part based on the closed-loop system matrix A_w .

New Passivity Properties for Electro-Mechanical Systems¹

Dimitri Jeltsema*, Jesus Clemente-Gallardo*, Romeo Ortega**
Jaquelien Scherpen* and Ben Klaassens*

*Control Systems Engineering Group Delft University of Technology, P.O. Box 5031, 2600 GA Delft, The Netherlands.

**Laboratoire des Signaux et Systémes Supélec, Plateau de Moulon 91192 Gif-sur-Yvette, France

Motivation

It is well-known that the Port-Hamilton [4] equations form a very suitable and natural framework to describe the dynamics of a broad class of nonlinear electrical, mechanical and electro-mechanical systems. In this presentation we present a dual formulation of the dynamics of nonlinear electromechanical systems in terms of the power variables. The method is based on the classical Brayton-Moser [1] equations parameterized by the generalized mechanical configuration coordinates (positions). The main ingredients are the kinetic, magnetic and electric co-energy and the definition of a mixed-potential function. Originally, this framework stems from the early sixties and is very little known in the systems and control community. In the new setting the mixed-potential function exists of power preserving potentials and the mechanical, magnetic and electric applied power and dissipated power. The main advantage of a well-defined dual formulation is that essential and important properties can be translated from one framework to another. One of these useful properties is that the mixed-potential function is used as a starting point to derive a new family of storage functions. Instead of using the total stored energy as a storage function, as with Port-Hamiltonian (PH) systems, we use the dissipative structure. This will lead to the power balance:

$$\int_0^t \left[F(\tau) + \Phi(x(\tau)) \right]^\top \dot{x}(\tau) d\tau \ge Q(x(t)) - Q(x(0)),$$

where x is the state, Q(x) the dissipated power, F the external forces and $\Phi(x)$ reflects the interconnection variables of the different subsystems. Consequently, the system defines a passive port with respect to the port variables $\{F, \Phi(x), \dot{x}\}$.

The motivation behind the use of the generalized Brayton-Moser (BM) framework is the following. In the context of electrical circuits it is shown in [2] that the BM equations bear a marked similarity in structure to the PH equations. The most trivial duality between the two frameworks is that PH systems assume the circuit elements to be flux and

charge controlled, while the BM equations impose the restriction that the elements are current and voltage controlled. One reason to work with PH systems is that the equations are formulated in natural physical variables. However, the inclusion of static elements, like sources and resistors seems not so natural in this framework. In principal, the constitutive relations of voltage sources, current sources and resistive elements are rather considered in terms of currents or voltages (Ohm's law), instead of fluxes or charges. It seems therefore more natural to use the BM equations. In the context of feedback controller design for electro-mechanical systems, an additional advantage of using the BM equations for the electrical part of the system is that the dynamics are directly expressed in measurable quantities. Similar arguments hold for the mechanical part of the system, where it is more common to measure velocity instead of momenta.

Contribution

The results of this research are very useful to overcome the dissipation obstacle in electro-mechanical systems that cannot be stabilized by the energy-balancing technique as recently proposed in [3]. At a more general level, our objective is to put forth the mixed-potential function and the dissipative structure as a new building block for analysis and controller design.

- [1] R.K. Brayton, J.K. Moser, "A theory of nonlinear networks I and II", Quart. Appl. Math. Vol. 12, No. 1 and 2, pp. 1-33, pp. 81-104, April 1964 and July 1964.
- [2] D. Jeltsema, J.M.A. Scherpen, "On nonlinear RLC networks: Port-Controlled Hamiltonian systems dualize the Brayton-Moser equations", *Submitted for publication 2001*.
- [3] R. Ortega, A.J. van der Schaft, I. Mareels, B.M. Maschke, "Putting energy back in control", IEEE Control Syst. Mag., Vol. 21, No. 2, April 2001, pp. 18–33.
- [4] A.J. van der Schaft, \mathcal{L}_2 -Gain and Passivity Techniques in Nonlinear Control, Springer-Verlag, 2000.

¹Sponsered by Marie Curie Control Training Site (CTS)

Controllers for hybrid isolation of structure borne sound in a demonstrator set-up

H. Super

University of Twente, Faculty of Engineering Laboratory of Mechanical Automation P.O. Box 217, 7500 AE Enschede The Netherlands Email: h.super@ctw.utwente.nl

Abstract

The joint research program in cooperation with TNO-TPD called "Hybrid Isolation of Structure Borne Noise" studies the possibilities of reducing the sound radiation at certain locations in a structure, due to the presence of a vibration source. A ship engine is such an example of a vibration source, which causes noise annoyance due to the vibration transmission through its carrier structure.

The existing passive isolation methods (e.g. rubber mounts) are insufficient to achieve the desired sound reduction. A promising approach for this type of applications is the use of so called hybrid isolation techniques, being a combination of passive (spring, damper) and active (controlled actuator) isolation methods. Important issues are optimal performance and integration in the existing construction.

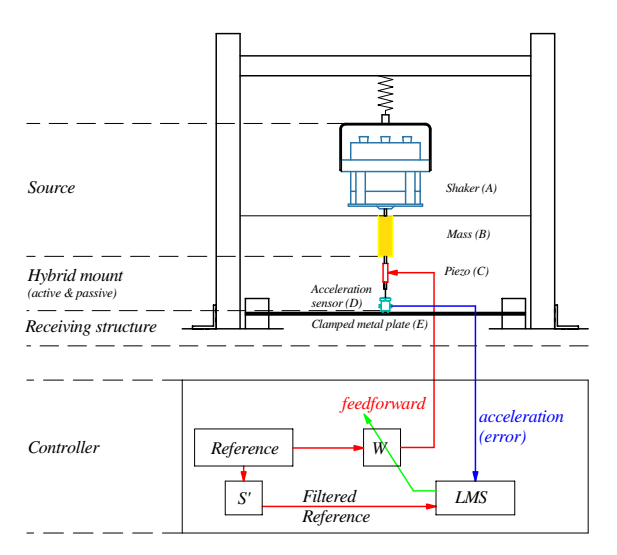


Figure 1: Schematic of 1-DOF demonstrator set-up

The experiments are performed with an experimental set-up for a one degree of freedom (1-DOF) system (see fig. 1). An electrodynamic shaker(A) serving as a vibration source excites a mass(B) with an unknown (harmonic) disturbance. The mass is mounted on a clamped metal plate(E) by a piezoelectric actuator(C) which operates as a hybrid isolation mount. Setting the frequency of the disturbance close

J. van Dijk University of Twente, Faculty of Engineering Laboratory of Mechanical Automation

P.O. Box 217, 7500 AE Enschede
The Netherlands

Email: j.vandijk@ctw.utwente.nl

to the 1^{st} or 3^{rd} eigenfrequency of the receiver construction results in significant sound radiation from the metal plate. Remark that the mount is designed to transfer only forces perpendicular to the plate. This means that the mount can completely isolate the source from the receiver by ensuring that the external force in the mount-plate interconnection point equals zero. Effectively the hybrid mount needs to generate an internal force to counteract the force induced by the mount stiffness and the displacement of the vibration source. As a consequence the source vibration remains unchanged while the receiver remains silent.

An adaptive feedforward LMS controller is used for online calculation of the optimal piezo force which minimizes the signal measured with the acceleration sensor(D). The two filter coefficients in the vector \bar{w} are updated according to the LMS weight update equation[1,2]

$$\bar{w}(n+1) = \bar{w}(n) + \mu \bar{x}a \tag{1}$$

in which n is the current sample number, μ the convergence step size, \bar{x} the filtered reference signal and a the measured acceleration (error signal). The reference signal needs to be filtered by an estimation of the transfer function from the piezo force to the measured acceleration in order to compensate for the mechanical delays in this transfer path. Without this, the controller may exhibit slow convergence or may even show divergent behavior, even for appropriate selection of the step size μ . In general, a smaller μ results in lower convergence speed but diminishes the residual error and therefore the radiated sound levels.

For the presented configuration the source is almost completely isolated for the frequency of the harmonic disturbance.

- [1] C.R. Fuller, S.J. Elliott, P.A. Nelson, "Active Control of Vibration", 1996.
- [2] S.M. Kuo, D.R. Morgan, "Active Noise Control Systems, Algorithms and DSP Implementations", 1996

Decoupling of collocated actuator-sensor-pairs for active vibration control

Jan Holterman, Theo J.A. de Vries
Drebbel Institute for Mechatronics, University of Twente
P.O. Box 217, 7500 AE Enschede
The Netherlands

Email: j.holterman@utwente.nl, t.j.a.devries@utwente.nl

Frank Auer
ASM Lithography
De Run 1110, 5503 LA Veldhoven
The Netherlands

Email: frank.auer@asml.com

1 Introduction

High-precision machines typically suffer from small but persistent vibrations. As it is difficult to damp these vibrations by passive means, research at the Drebbel Institute is aimed at the development of an *active structural element* that can be used for vibration control. The active structural element, popularly referred to as 'Smart Disc', is based on a piezoelectric position actuator and a piezoelectric force sensor.

One of the main problems in active control is to ensure stability. In this respect it is often advantageous to consider the use of so-called *collocated* actuator-sensor-pairs, as this enables to actively implement a passive control law, which is robustly stable, irrespective of structural modeling errors. Within the context of vibration control for lightly damped structures, collocated actuator-sensor-pairs are known to be well-suited to obtain robust active damping [1, 2].

2 Example: wafer stepper lens vibrations

A wafer stepper, i.e., the advanced microlithography system that is at the heart of Integrated Circuit manufacturing, is an excellent example of a high-precision machine the performance of which is limited by the lack of damping within the machine frame. Badly damped vibrations of the lens of the wafer stepper limit the attainable line width of the circuit patterns.

The lens of the wafer stepper is conventionally suspended by means of three (passive) lens support blocks, constituting a kinematically well-designed interface to the so-called metroframe of the wafer stepper. In order to perform Smart Disc experiments, the lens support blocks have been equipped with two piezoelectric stacks, both comprising a position actuator and a collocated force sensor. Each of the resulting 'Piezo Active Lens Mounts' has two perpendicular active degrees of freedom.

By applying collocated control to the individual piezoelectric stacks, all six 'suspension modes' of the lens can be damped. Due to the passivity of the control laws, unmodeled flexible modes of the lens and the metroframe are also stabilized.

3 Collocated control versus modal analysis

Control based on collocated actuator-sensor-pairs is inherently in terms of *local* coordinates. Vibration problems however are usually analyzed in terms of *modal* coordinates, corresponding to a limited number of vibration modes, as captured in a simplified model of the mechanical structure.

In terms of the wafer stepper example: we are primarily interested in the six suspension modes of the lens. From a modal analysis point of view, it is therefore desirable to have six SISO control problems, each one directly related to a single suspension mode. However, due to the symmetry in the set-up, the frequency response functions from a single actuator to the collocated sensor are all similar. Tuning of the local control laws, such that damping for the individual modes is optimal, is therefore not straightforward.

4 Modal control through decoupling

The above-mentioned problem can be solved by realizing that decoupling of collocated actuator-sensor-pairs, i.e, the transformation of the original control problem into modal coordinates, yields control loops that again enable the implementation of a passive control law. Stability of 'decoupled collocated control' does not depend on the accuracy of the model that has been used for decoupling.

This implies that, for the case of the wafer stepper, a simple 'rigid-body' model may be used for decoupling of the six collocated control loops. Obviously, in contrast to stability, the *performance* of active damping based on 'decoupled collocated control' *does* depend on the accuracy of the model.

- [1] S.M. Joshi, "Control of Large Flexible Space Structures", Lecture Notes in Control and Information Sciences, Vol.131, Springer-Velag, Berlin, Germany, 1989.
- [2] A. Preumont, "Vibration Control of Active Structures, An Introduction", Kluwer Academic Publishers, Dordrecht, The Netherlands, 1997.

Model based control of a passenger car using an active suspension

Christophe Lauwerys
K.U.Leuven
christophe.lauwerys@mech.kuleuven.ac.be

Jan Swevers
K.U.Leuven
jan.swevers@mech.kuleuven.ac.be

Paul Sas K.U.Leuven paul.sas@mech.kuleuven.ac.be

1 Abstract

In classic passive suspension design, comfort and road handling are conflicting design criteria. An active or semi-active suspension offers the possibility to vary the damper characteristics along with the road profile. Such systems have discrete settings or are limited in bandwidth up to 10Hz. This paper discusses the development of a controller for a passenger car using a recently developed active shock absorber, were two current controlled valves continuously vary the damper characteristics. The aim is to control the cars rigid body modes heave, roll and pitch, as well as wheelhop and the first bending and torsion modes. The control design is based on damper and car models that are valid up to these frequencies. Since the shock absorber is a highly nonlinear hydraulic system, several nonlinear modeling techniques, such as neural networks and Wiener-Hammerstein models are derived. Using the active shock absorber as an actuator, the car itself is identified using linear ide! nt! ification techniques based on random multisine excitations to find the best linear approximation of its dynamic behavior. Based on the identified linear car model, linear controllers are derived. These controllers calculate the actuator forces that have to be generated by the active shock absorber. Based on the nonlinear damper models, these desired forces are converted into appropriate currents to be applied at the damper valves. This requires a nonlinear model inversion. The paper presents experimental results of the proposed controllers on a quarter car test setup. The performance of several linear car controllers in combination with nonlinear damper model inversion strategies are compared.





Control design in restraint systems

Rogier J. Hesseling
Control Systems Technology Group, Department of Mechanical Engineering,
Eindhoven University of Technology, P.O. Box 513, 5600 MB, Eindhoven, The Netherlands
R.J.Hesseling@tue.nl

Introduction

In the past ten years, vehicle safety becomes more and more important. Passive safety refers to the components of a vehicle reducing the occupant injuries when an accident occurs. These components can be divided in two groups; components which do have contact with the occupant during a crash and components which do not have contact with the occupant during the crash. The latter group is referred to as restraint system, e.g. the airbag. Currently, restraint systems are adaptive only in the sense that the most appropriate setting for the actuators of the restraint system is chosen once, directly after a crash has been detected. Obviously, occupant injuries will be less severe if it is possible to manipulate the restraint system during the crash. The goal of this project is to set up a method to control the occupant injuries by manipulating the restraint system online. The method is set up using models in the finite element and multibody package MADYMO, see Figure 1.

Problem statement

The problem to start with is to develop a design method to control and minimize the chest acceleration by online manipulation of the beltforce in one standardized crash test. The control algorithm will be based on feedback. The adopted injury measure is the maximal value of the chest acceleration, i.e. $J = \max |\ddot{x}(t)|$. An appropriate reference trajectory is set up, based on a simple representation of a crash.

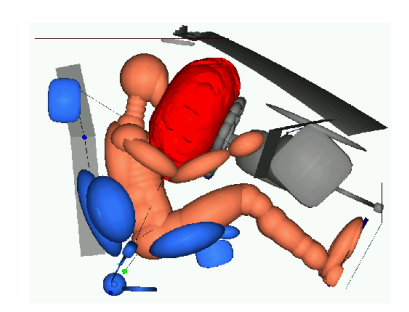


Figure 1: Numerical model of a BMW

Approach

The numerical model in Figure 1 is complex and non linear. The problem is how to get insight into the behaviour of this model, such that it is possible to design a controller. Two problems arise. The first has to do with the complexity of the restraint system. This problem is partly solved by excluding the airbag. The second has to do with MADYMO. MADYMO has no facilities for model reduction or linearization.

Therefore, it is chosen to identify the transfer function from beltforce to chest acceleration by analyzing the disturbed chest acceleration to a step wise perturbation in the beltforce. The transfer function of a LTI SISO system is identified on the difference between the original chest acceleration and the disturbed chest acceleration. The identified SISO system has the beltforce as input and the chest acceleration as output. Based on this SISO system, a controller can be set up and then be validated in the complex and non linear MADYMO model.

Results

Application of the controller in the non linear MADYMO model results in a reduction of the injury measure of approximately 60% with respect to the non controlled situation.

Estimation of an N-L-N Hammerstein-Wiener Model

Yucai Zhu
Control Systems Section, Faculty of Electrical Engineering
Eindhoven University of Technology
P.O. Box 513, 5600 MB Eindhoven, The Netherlands

Also with: Tai-Ji Control Grensheuvel 10, 5685 AG Best, The Netherlands

Abstract: Estimation of a single-input single-output block-oriented model is studied. The model consists of a linear block embedded between two static nonlinear gains. Hence it is called N-L-N Hammerstein-Wiener model. First the model structure is motivated and the disturbance model is discussed. The paper then concentrates on parameter estimation. A relaxation iteration scheme is proposed by making use of a model structure in which the error is bilinear-in-parameters. This leads to a simple algorithm which minimizes the original loss function. The convergence and consistency of the algorithm are studied. In order to reduce the variance error, the obtained linear model is further reduced using frequency weighted model reduction. Simulation study will be used to illustrate the method.

Key words: Identification, nonlinear process, block-oriented model, parameter estimation, relaxation algorithm

Identification of composite local linear state-space models using a projected gradient search

Vincent Verdult
Faculty of Information Technology and Systems
Delft University of Technology
P. O. Box 5031, 2600 GA Delft
The Netherlands

Email: V. Verdult@its.tudelft.nl

Local linear modeling is one of the many possibilities to approximate a nonlinear dynamical system. It is based on partitioning the whole operating range of the nonlinear system into multiple, smaller operating regimes and modeling the system for each of these regimes by a linear model. By making a weighted combination of these linear models, one hopes to describe the complete nonlinear behavior sufficiently accurately. In this talk, the following weighted combination of local linear models is considered:

$$x_{k+1} = \sum_{i=1}^{s} p_i(\phi_k) \Big(A_i x_k + B_i u_k + O_i \Big)$$

$$y_k = C x_k,$$

where s is the number of local models, $x_k \in \mathbb{R}^n$ represents the unknown state, $u_k \in \mathbb{R}^m$ is the input, $y_k \in \mathbb{R}^\ell$ is the output, and $p_i(\phi_k) \in \mathbb{R}$ is the weighting for the ith model. The weighting vectors p_i are unknown functions of the scheduling vector $\phi_k \in \mathbb{R}^q$. This scheduling vector corresponds to the operating point of the system, typically it will depend on the input and the state. The weighting functions can be interpreted as model validity functions: they indicate which model or combination of models is active for a certain operating regime of the system. A weighted combination of local linear models can be used to approximate a smooth nonlinear system up to arbitrary accuracy, by increasing the number of local models.

The identification of local linear model structures has been studied mainly for input-output systems and for state-space systems of which the full state vector is measured. The case where only part of the state is measured is of course of more general interest. This talk addresses the identification of local linear state-space systems where the state is not measured directly; only an observable linear combination of some of the states is available as an output. Normalized radial basis functions are used as weighting functions that combine the local state-space models to obtain a global description of the input-output behavior.

For the local linear model structure, an optimization-based identification procedure has been developed. The system matrices of the local models are fully parameterized. An

Michel Verhaegen
Faculty of Information Technology and Systems
Delft University of Technology
P. O. Box 5031, 2600 GA Delft
The Netherlands

Email: M. Verhaegen@its.tudelft.nl

iterative projected gradient search method is used to identify the local models and the centers and widths of the radial basis functions. The method deals with the nonuniqueness of the fully parameterized state-space representation by first calculating at every iteration the directions in which a change of parameters does not influence the input-output behavior of the model, and subsequently projecting these directions out of the parameter update.

Because of the recurrent nature of the local linear models, the gradient calculations needed in the projected gradient search method are governed by dynamic equations. For successful identification, these gradient calculations need to be stable. The stability is discussed for two special cases of scheduling. When the scheduling is based only on the input signals, stability of the dynamic gradient calculations can be guaranteed, and hence the training is well-behaved. In the more general case where scheduling is also based on the output signals, two training methods are possible, each having their own advantages and disadvantages. One training method is based on scheduling with the measured outputs; this method behaves well during training, but the resulting model can perform poorly when simulated in free run. The other training method that uses the model output for scheduling, does not have this problem, but can suffer from stability problems during training.

Because the identification procedure is based on solving a nonlinear optimization problem, an initial estimate of the local linear models is required. It is proposed to estimate a global linear model, and use it to initialize all the local models; in addition the weighting functions are uniformly distributed over the operating range of the scheduling vector.

References

[1] V. Verdult, L. Ljung and M. Verhaegen (2001). Identification of composite local linear state-space models using a projected gradient search. Accepted for publication in *International Journal of Control*.

[2] V. Verdult (2002). *Nonlinear System Identification: A State-Space Approach.* Ph. D. thesis, Faculty of Applied Physics, Twente University, Enschede, The Netherlands.

Identification of whole-body glutamine kinetics

Natal van Riel Department of Electrical Engineering Eindhoven University of Technology P.O. Box 513, 5600 MB Eindhoven The Netherlands

Email: n.a.w.v.riel@tue.nl

1 Introduction

Glutamine is a nonessential amino acid which supports the function of the gut and the immune system. Several organs and tissues can both synthesise and degrade glutamine, dependent on the physiological condition. Skeletal muscle is considered to be the main glutamine producing tissue in man. Quantitative assessment of glutamine kinetics is required to understand its physiology and to diagnose pathology. Tracer dilution experiments with infusion of stable isotope amino acids are used to study in vivo transport and metabolic processes in human subjects. Experimental enrichment data are interpreted in context of (linear) compartment models to yield synthesis and degradation rates. Under steady-state assumption for both tracee and tracer the calculations reduce to algebraic equations only requiring measurement of the steady-state plateau enrichment. In literature experiments have been reported with tracer infusion periods of 8 [2] and 6 or 11 [3] hours. The obtained rates have caused controversy identifying skeletal muscle either as net producer or consumer of glutamine. In this paper it is shown that, based on non-steady-state identification of new data, the tracer steady-state assumption cannot be valid for the reported experiments.

2 Model

The tracee and tracer (*) are assumed to be homogenously mixed in two compartments: a blood plasma (p) and Whole-Body Free (WBF) pool (b)). The mass balances of tracee and tracer have the same structure (2 sets of 2 differential equations):

$$\dot{\mathbf{x}} = \mathbf{A}\mathbf{x} + \mathbf{B}\mathbf{u} \qquad \dot{\mathbf{x}}^* = \mathbf{A}\mathbf{x}^* + \mathbf{B}\mathbf{u}^* \tag{1}$$

with $\mathbf{x} = [\lceil g \ln \rceil_p, \lceil g \ln \rceil_b]^T$ and $\mathbf{x}^* = [\lceil g \ln^* \rceil_p, \lceil g \ln^* \rceil_b]^T$ [μ mol·kg⁻¹·h⁻¹] contains the fluxes which are independent of the model states. Tracee inflow is assumed to be constant $\mathbf{u} = [r_{inflow}, 0]$. The tracer infusion r_{infuse}^* is experimentally set: $\mathbf{u}^* = [r_{infuse}, 0]$. For the other fluxes a first–order exchange between the compartments is assumed, described by rate constants k_{ij} [h⁻¹], which are the same for tracer and tracee:

$$\mathbf{A} = \begin{bmatrix} -k_{12} - k_{10} & k_{21} \\ k_{12} & -k_{21} \end{bmatrix} \qquad \mathbf{B} = \begin{bmatrix} 1 & 1 \end{bmatrix}^T \tag{2}$$

Stationarity constraints In tracer experiments it is usually assumed that the tracee pool concentrations remain constant throughout the experiment, i.e. $\dot{\mathbf{x}} = \mathbf{0}$. The tracee

Ad Damen
Department of Electrical Engineering
Eindhoven University of Technology
P.O. Box 513, 5600 MB Eindhoven
The Netherlands

Email: a.a.h.damen@tue.nl

submodel reduces to a static representation and the plasma and WBF tracee concentrations become constants $\mathbf{V} = [V_I, V_2]$ [μ mol·kg⁻¹]. The stationarity condition for the tracee yields a set of algebraic equations which set the values of V_I and V_2 , given a specific realisation for the parameters $\theta = [r_{inflow}, k_{10}, k_{12}, k_{21}]$:

$$\mathbf{A}(\mathbf{q})\mathbf{V} + \mathbf{B}\mathbf{u}(\mathbf{q}) = \mathbf{0} \quad \Leftrightarrow \quad \mathbf{V} = -\mathbf{A}(\mathbf{q})^{-1}\mathbf{B}\mathbf{u}(\mathbf{q}) \tag{3}$$

To estimate the unknown parameters θ the remaining model states \mathbf{x}^* need to be linked to experimental data. The model outputs \mathbf{y} are the same quantities as experimentally accessible: plasma pool enrichment. $\mathbf{y} = \mathbf{C}\mathbf{x}^*$ with

$$\mathbf{C} = diag\left(\frac{1}{V_i} \quad 0\right) \tag{4}$$

3 Identification

During 24 h a [5-¹⁵N]-glutamine tracer was supplied to 7 healthy, male subjects by a continuous intravenous infusion in the arm, $r_{infuse} = 0.68 \, [\mu \text{mol kg}^{-1} \cdot \text{h}^{-1}]$. During 36 h 46 blood samples have been taken from the artery femoralis (leg) at non-equidistant times. Since the tracer infusion is started at t = 0, the initial values $\mathbf{x}_0^* = \begin{bmatrix} 0 & 0 \end{bmatrix}^T$. For each subject the parameters $\theta \in \mathbb{R}^+$ have been estimated with a weighted least squares output error criterion using SAAM II (software for identification of compartment models based on tracer data [1], [4]) and Matlab. The datasets contained both the infusion (load) period and the wash-out curve (N=46). The average time constants of the 2 pools for the 7 subjects are $t_1 = 32\pm12$ min and $t_2 = 18.1\pm2.2$ hour. The stationarity condition of the tracee pools was verified.

4 Conclusion

The traditional calculations applied to tracer data are usually not based on time series data and system identification. The model realisation obtained here, shows that the required tracer steady-state is not reached during the reported experiments. Instead, an infusion of at least 90h is required to apply traditional calculations, which is hardly feasible with human subjects. The tracer steady-state calculations are not applicable.

- [1] Bell et al. Comput. Statist. Data Anal. 22: 119-135, 1996.
- [2] Mittendorfer et al. Am. J. Physiol.), 280: E323-E333, 2001.
- 3] Van Acker, et al. Clin. Sci. 95: 339-346, 1998.
- [4] www.saam.com

Identification of the SIMONA Research Simulator motion system

Maria Isabel Parra Calvache
Mechanical Engineering, Systems and Control Group
Delft University of Technology
Mekelweg 2, 2628 CD Delft, The Netherlands
Email: m.i.parra@wbmt.tudelft.nl

1 Abstract

Current advanced controller synthesis methods are based on a mathematical representation of the system to be controlled. Clearly there is a strong correlation between the performance achieved by the designed controllers and the accuracy of the essential-dynamics model [1].

The approximation of real systems by means of models can be applied in any process or mechanism. This approximation is done by a representation of the relationships between variables of interest, usually physical quantities that can be measured or manipulated. The system identification techniques look for a representation based in the real plant to be modelled. In general these techniques estimate a best-fit model based on measurements from the real system. This approach allows the simplification of the representation of systems whose theoretical model is excessively complex or uncertain to describe.

Moreover, non-linear mechanical systems with several mechanical degrees of freedom that require high dynamical performance over their whole operating envelope must be based on dynamic models that carefully represent both the global non-linear dynamic behavior, the representation of dominant structural flexible modes and the inclusion of relevant other parasitic dynamic phenomena.

Within this framework, the objective of the SIMONA research Simulator project (SIMONA stands for the Institute for research in SImulation, MOtion and NAvigation) is the research in the field of simulation with an advanced flight-simulator. The SIMONA Research simulator is a lightweight multi-vehicle-re-configurable cockpit mounted over a six-degrees-of-freedom motion platform. It is desired that this simulator work with a wider bandwidth, from 10 Hz to 15 Hz, (actual simulators work in the range of 3 to 5 Hz) that would allow the simulation of special conditions [2]. The simulation of special conditions make necessary the high dynamical performance over the flight simulator work space, which is achieved by means of a model based controller. At present, an approximation of the real system considering only the motion platform dynamics has been used for an initial control design. A better approximation of the dynamics of the whole system is necessary for increasing the performance in all the working envelope and fulfill bandwidth requirements [3].

In the case of the SIMONA research simulator project, system identification procedures are applied to the motion system that can be described as a Stewart Platform with 6 DOF (Degrees of Freedom). The objective is to provide a linear simplified model of the motion of the Stewart Platform. The proposed model can be used to design a multi variable control or a Linear Parameter Varying Control of the complete motion system, the last would require the modelling of the parameter dependence over the global operating domain.

In order to obtain an adequate model with system identification procedures attention should be given to the experiment design. The proper excitation of the system is crucial in order to obtain measurements with enough information over the relevant dynamics of the system for the subsequent use in identification routines. For the particular system of the SIMONA Research Simulator motion system, subspace identification techniques provide state space models with a straightforward application to Multi Input Multi Output (MIMO) Systems. The Subspace Techniques are used in combination with optimization routines [4] to obtain models with good characteristics in terms of analysis of residuals and prediction of signals in the time domain.

- [1] M. Gevers, B.D.O. Anderson, B. Dorons, "Issues in modelling for control," American control conference, 1998.
- [2] S.J.W. Bettendorf, "Static Calibration of the SI-MONA Motion System," Faculty of Mechanical Engineering and Maritime Technology, Delft University of Technology, 1997.
- [3] S.H. Koekebakker, "Model based control of a flight simulator motion system," Delft University of Technology, 2001.
- [4] P. van Overschee, B. de Moor, "Closed Loop Subspace System Identification," Proceedings of the 36th Conference in Decision and Control, 1997.

Robot Identification for Accurate Dynamic Simulation

R.R. Waiboer
Netherlands Institute for Metals Research
University of Twente
Laboratory of Mechanical Automation
r.r.waiboer@utwente.nl

Introduction

Robotised laser welding, figure 1, is an application which requires high speed combined with high precision. Off-line programming is used to reduce the expensive downtime while programming the accurate and high-speed motion. Unfortunately, the robot will deviate from the programmed trajectory due to dynamic limitations at the high welding speed.



Figure 1: Robotised Laser Welding.

Goal

In order to *a priory* predict the dynamic performance of the robot during laser welding of a specific product, realistic dynamic simulations are combined with Off-line Programming. Realistic dynamic simulations require realistic models of the robot and controller. Robot identification techniques will be used to find the unknown model parameters.

Robot Identification

A 3 degree of freedom (3DOF) robot model has been formulated which includes lumped inertia parameters, stiffness parameters of the gravity compensation spring and a -three parameter- friction model to describe joint friction. The equations of motion are expressed in the vector of generalised coordinates \boldsymbol{q} and the vector of model parameters \boldsymbol{p}

$$\underline{\tau} = M(q, p)\ddot{q} + C(q, \dot{q}, p)\dot{q} + K(q, p)q + g(q, p),$$

where $M(\underline{q},\underline{p})$ is the reduced mass matrix, $C(\underline{q},\underline{\dot{q}},\underline{p})\underline{\dot{q}}$ represents the Coriolis and the centrifugal forces as well as the friction model, $K(\underline{q},\underline{p})\underline{q}$ includes stiffness properties and $\underline{g}(\underline{q},\underline{p})$ is the vector with external nodal forces, including gravity, and the driving torques are expressed by vector $\underline{\tau}$. The model parameters \underline{p} are estimated using experimental parameter identification. The set of model parameters is

R.G.K.M. Aarts University of Twente Laboratory of Mechanical Automation P.O. Box 217, 7500 AE, Enschede r.g.k.m.aarts@utwente.nl

found using a linear least squares method. This linear least squares method requires that the robot dynamic model is rewritten in a parameter linear form

$$\underline{\tau} = \Phi(\underline{q}, \underline{\dot{q}}, \underline{\ddot{q}})\underline{p},$$

where $\Phi(\underline{q},\underline{\dot{q}},\underline{\ddot{q}})$ is known as the regression matrix. Evaluation of the dynamic model in a number of samples $i=1\dots n$ along the trajectory (q,\dot{q},\ddot{q}) yields the data-set

$$\underline{b} = Ap \,,$$

where

$$\underline{b} = \left[\begin{array}{c} \underline{\tau}_1 \\ \vdots \\ \underline{\tau}_n \end{array} \right] \qquad \text{and} \qquad A = \left[\begin{array}{c} \Phi_1(\underline{q}_1, \underline{\dot{q}}_1, \underline{\ddot{q}}_1) \\ \vdots \\ \Phi_n(\underline{q}_n, \underline{\dot{q}}_n, \underline{\ddot{q}}_n) \end{array} \right] \,,$$

The least squares solution is given by:

$$\underline{p}_{LS} = (A^T A)^{-1} A^T \underline{b} = A^+ \underline{b}.$$

To be able to apply a least squares fit, A should have full rank. Consequently, the regression matrix should also have full rank. This is obtained when the set of parameters \underline{p} that will be estimated is minimal.

The quality of the least squares fit depends strongly on the condition of matrix A. Using excitation trajectories $(\underline{q}, \underline{\dot{q}}, \underline{\ddot{q}})$ consisting of a Fourier series with 5 frequencies, this condition can be manipulated by choosing the phases and amplitudes. Non-linear optimisation techniques are used to find the best phase and amplitude combination while obeying motion constraints.

Results & Conclusion

A parameter estimation for a 3DOF model has been performed. The torques are obtained by measuring the servo currents and transforming them to joint torques. The trajectories are programmed in the robot control software. All experiments are done without modifications to the original industrial robot. The simulations are performed using SPACAR and MATLAB. Simulation of the 3DOF robot model shows good agreement with the experimental results. The identified model parameters closely match the values given by the robot manufacturer. The end goal is a realistic 6DOF robot model which enables the accurate and realistic simulations needed with off-line programming for laser welding.

Disturbance detection on cd players using wavelets

M.G.E. Schneiders m.g.e.schneiders@tue.nl

M.J.G. van de Molengraft m.j.g.v.d.molengraft@tue.nl

M. Steinbuch m.steinbuch@tue.nl

Control Systems Technology
Department of Mechanical Engineering
Eindhoven University of Technology
P.O. Box 513, 5600 MB Eindhoven
The Netherlands

Abstract

In general it can be useful to identify disturbances that deteriorate the closed-loop behaviour of a control system. Often the only way to detect disturbances is using a measurement that is also used in the closed-loop. We can design the controller in a way to effectively deal with disturbances, but in some cases this will not be enough. When large disturbances corrupt the measurement, a supervisory control strategy is sometimes used which adapts the closed-loop controller in order to cancel the effect of the disturbances. In that case fast detection of the disturbance is beneficial in minimizing performance losses.

Feature detection is a technique to extract or isolate information from a signal that is important to a certain application. It is well known in the field of image processing were algorithms to detect edges (one dimensional feature detection) and corners (two dimensional feature detection) are used. Wavelet analysis [1] shows good results in isolating features (time-patterns in signals), especially short-living events. Therefore wavelets are already used in several fields for this purpose, even in engineering [2]. However, applications found in literature are not time critical: the signals are processed off-line or quasi on-line in a delayed security loop.

The need for an on-line feature detector is born within research to improve playability of compact discs. A CD-player is a complex system in which high-tech mechanical, control and digital signal processing techniques are combined. In the playback process of discs two servo-loops are involved: one for focusing and one for radial positioning of the laser-unit. The radial positioning loop controls the following of the track and receives input from a reflected laser beam, which is also used for reconstructing the data on the disc. Scratches on the disc have much influence on this measurement and disturb the radial-positioning servo-loop. Since the actual mechanical system is not disturbed, the controller gets the wrong information: disc-scratches imply radial tracking errors, which are not present in real. It would

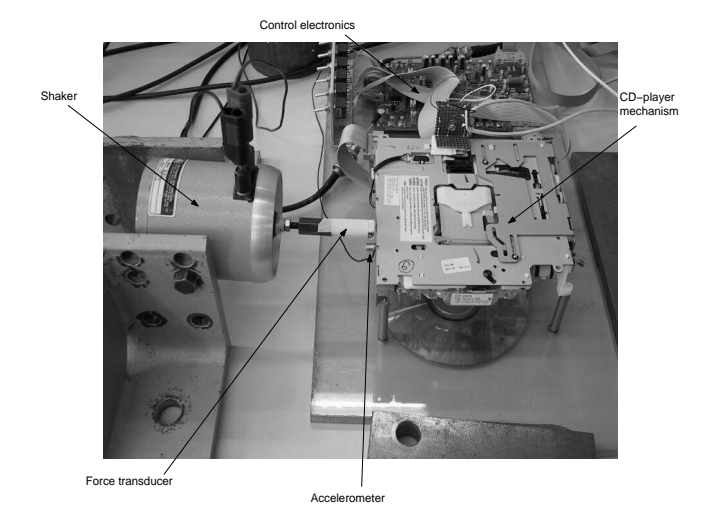


Figure 1: CD-player setup used for feature detection

be beneficial to detect this kind of disturbances in an early stage to adapt the servo-loop to cancel the consequences of these effects. For this purpose wavelets are used to build an on-line feature detector.

References

- [1] Olivier Rioul and Martin Vetterli. Wavelets and Signal Processing. *IEEESPM*, 8(4):14–38, 1991.
- [2] Fahmida N. Chowdhury and Jorge L. Aravena. A Modular Methodology for Fast Fault Detection adn Classification in Power Systems.

IEEE Trans. on Control Systems Technology, 6(5):623–634, September 1998.

[3] Gilbert Strang and Truong Nguyen. *Wavelets and Filter Banks*. Wellesley-Cambridge Press, Wellesley, MA, 1996.

One approach for the detection and estimation of a jump in discrete time LTI systems

Ichiro Jikuya and Michel Verhaegen SCE Division, Department of Applied Physics University of Twente P.O. Box 217, 7500 AE Enschede, The Netherlands Email: I.Jikuya@tn.utwente.nl

1 Abstract

A deadbeat observer based generalized likelihood ratio (GLR) test is proposed for the detection and estimation of a jump in discrete time linear time invariant (LTI) systems. The proposed approach overcomes the difficulty in the choice of the window size for the online detection procedure. The marginalized GLR test is also discussed as the offline procedure to overcome the difficulty in the choice of the threshold.

2 Problem Formulation

The problem is to detect and estimate the jump ν and the jump time t_0 from the given sequence of observations $\{y(t)\}$ of the discrete time LTI system

$$x(t+1) = Ax(t) + Gw(t) + \delta_{t_0,t} \nu$$

$$y(t) = Cx(t) + v(t)$$

where x(t) is the state, y(t) is the observation, and $\{w(t)\}$ and $\{v(t)\}$ are independent, zero mean, Gaussian sequences with variance $\mathbf{E}[w(t)w(t)^T] = W > 0$ and $\mathbf{E}[v(t)v(t)^T] = V > 0$. The term $\delta_{t_0,t} \nu$ represents a jump in the state. Here t_0 is an unknown positive integer, which assumes a value if a jump occurs and takes the value $+\infty$ if there is no jump. Also $\delta_{i,j}$ is the Kronecker delta and ν is the unknown size of the jump (see [2, 8, 4, 3] for surveys).

One of the most powerful methods for the jump detection is the GLR test proposed in [7]. The key points of the GLR test are summarized as follows. Based on the state estimation of the Kalman filter, the residual can be computed at each time instant. It does not depend on the initial state and becomes independent Gaussian sequence with/without the jump. If no jump has occurred, the mean value of the residual is 0. Once a jump occurs, the mean value of the residual is linearly dependent on the jump at each time instant. This linear dependence of the mean value together with the variance of the residual can be computed utilizing the Kalman filter gain. Since the log likelihood ratio (LLR) becomes a function of the unknown jump and the unknown jump time, they can be estimated by maximizing the LLR over a fixed interval. The choices of the window size and that of the threshold have been recognized as key problems.

3 Solution

This paper proposes a deadbeat observer based GLR test to detect and estimate the unknown jump in discrete time LTI systems, *i.e.* we apply the deadbeat observer to generate the residual as a substitute for the Kalman filter [7] and estimate the unknown jump and the unknown jump time. Compared with the Kalman filter based approach, it can be shown that we can follow the same procedure of the GLR test, and furthermore the small window size at most the McMillan degree of the LTI system is enough for the detection and estimation. Assuming the noninformative prior information for the size of the noise variance, the marginalized GLR test is discussed as an offline procedure to overcome the difficulty in the choice of the threshold (cf. [5, 6]).

- [1] I. Jikuya and M. Verhaegen, "Deadbeat observer based detection and estimation of a jump in LTI systems", to appear in *IFAC* 2002
- [2] M. Basseville and I.V. Nikiforov, *Detection of Abrupt Changes, Theory and Applications*, Prentice-Hall, 1993
- [3] T. Kerr, "Decentralized Filterling and Redundancy Management for Multisensor Navigation", *IEEE Transaction on Aerospace and Electronic Systems*, pp. 83–119, vol. 23, 1987
- [4] R. Isermann, "Process Fault Detection Based on Modeling and Estimation Methods—A Survey", *Automatica*, pp. 387–404, vol. 20, 1984
- [5] F. Gustafsson, "The marginalized Likelifood Ratio Test for Detectiong Abrupt Changes", *IEEE Transactions on Automatic Control*, pp. 66-78, vol. 41, 1996
- [6] F. Gustafsson, *Adaptive Filtering and Change Detection*, John Wiley & Sons Ltd, 2000
- [7] A. S. Willsky and H. L. Jones, "A Generalized Likelihood Ratio Approach to the Detection and Estimation of Jumps in Linear Systems", *IEEE Transaction on Automatic Control*, pp. 108–112, vol. 21, 1976
- [8] A. S. Willsky, "A survey of design methods for failure detection in dynamics systems", *Automatica*, pp. 601–611, vol. 12, 1976

Multiphase Adaptive Control based on Strong Robustness

M.Cadic
Faculty of Mathematical Sciences
University of Twente
P.O. Box 217, 7500 AE Enschede
m.cadic@math.utwente.nl

1 abstract

Most adaptive control systems have been derived from the certainty equivalence principle: at each new iteration of the design, a model of the plant is obtained from the previous model, and a new controller is designed on the basis of this updated model. Unfortunately, in case the uncertainty about the system parameters is too large, the stability of the real plant controlled by the model-based controller can not be guaranteed. However, if the uncertainty about the true system is such that no matter where we believe that the true system is and no matter where it actually is, the controller based on the model stabilizes the actual plant, then we can safely apply a certainty equivalence type of strategy.

Therefore, we propose to build a test checking at each iteration whether the parameter uncertainty set is such that for any models P_1 , P_2 in this set, the controller based on P_1 stabilizes P_2 . If this condition holds, the uncertainty set is then said to be strongly robust [?]. Hence, our adaptive scheme splits in two phases depicted in Figure 1. In the first phase, we put effort on identification of the system to be controlled, and once the condition of Strong Robustness is verified, we switch to the second phase where the emphasis is gradually put on control.

Our objective is to present the general structure of our algorithm, irrespectively of computational issues. In particular, we show that, for the class of systems we specify, if we can compute an input sequence such that the parameter uncertainty set is converging to the point set $\{\theta^0\}$, where $\{\theta^0\}$ denotes the true parameter vector, then there exists a finite time at which the condition of strong robustness is fulfilled, dismissing the situation where we would stay in the first phase indefinitely. Next, assuming that the condition of Strong Robustness is verified in finite time, since the stability of the controlled system is now guaranteed, we can proceed as in classical adaptive control, i.e. we can design the controller on the basis of the updated model. At each new data measurement, the model is updated into a new model closer to the real system, leading to an updated controller expected to show better performance. Although this is still under investigation, the J.W. Polderman
Faculty of Mathematical Sciences
University of Twente
P.O. Box 217, 7500 AE Enschede
j.w.polderman@math.utwente.nl

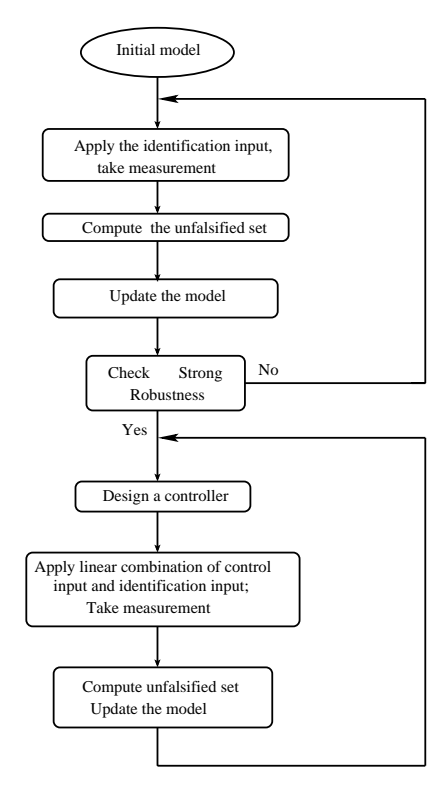


Figure 1: Iterative scheme.

main improvement brought by the introduction of our multiphase adaptive control system is expected to be the decrease of undesired transients of the control system.

References

[1] M.Cadic, J.W.Polderman, Strong Robustness in Adaptive Control, Proc.~4th~NCN~Workshop,~Sheffield,~UK,~2001.

Robust Linear and Nonlinear PID Tuning based on Identification¹

Yucai Zhu
Control Systems Section, Faculty of Electrical Engineering
Eindhoven University of Technology
P.O. Box 513, 5600 MB Eindhoven, The Netherlands

Also with: Tai-Ji Control Grensheuvel 10, 5685 AG Best, The Netherlands

Abstract: In this work, identification based PID tuning is studied. The proposed approach consists of the identification of linear or nonlinear process model and model based control design. The identification test can be performed in both open loop and closed-loop. The so-called ASYM method is used to solve the identification problem. The method can identify a low order process model with a quantification of model errors (uncertainty). The PID tuning is based on the internal model control (IMC) tuning rules. Two case studies will be performed to demonstrate the proposed methodology. The first one is the adaptive control of the dissolved oxygen (DO) of a bioreactor; the second one is the nonlinear PID control of a pH process. Practical problems will be discussed and new research topics are highlighted.

Key words: PID control, adaptive control, identification, performance, robustness

-

¹ This work is partly funded by Senter, The Netherlands, under project name BTS98083

Optimal Finite time ILC design, with application to a waferstage.

B.G.Dijkstra¹
Mechanical Engineering
Systems and Control Group,
Delft University of Technology
Mekelweg 2, 2628 CD Delft,
The Netherlands
B.G.Dijkstra@wbmt.tudelft.nl

O.H.Bosgra
Mechanical Engineering
Systems and Control Group,
Delft University of Technology
Mekelweg 2, 2628 CD Delft,
The Netherlands
O.H.Bosgra@wbmt.tudelft.nl

1 abstract

In many servo control application the same task is repeatedly performed in the same way. Iterative learning control has been shown to be a very effective way to obtain control signals to greatly reduce the errors during these tasks by using the knowledge of similarity between the tasks ([1],[2],[3],[4]). In 1988 Phan and Longman [5] presented a setting describing the design of and ILC as a finite time problem where the input and output vectors of a plant are considered as discrete finite vectors. This setting is known as a lifted system description. Some research has been done towards reducing the calculation complexity of the lifted system ILC design problem through the use of basis functions [6] but it has only recently been shown that classical feedback design methods can quite easily be applied to the lifted system description [7]. In ILC design methods that are based on infinite time considerations (like transfer functions,([1])) the nonzero value of the error to be used by the ILC at the start and end of the trajectory (which can be caused by system noise), causes problems that need to be handled separately often resulting in rather heuristic approaches. Design in the finite time lifted system setting has as a main advantage that the solution explicitly takes into account states of the plant at the beginning and end of the trajectory, resulting in a time varying operation that can be applied without any extra effort. In addition clear feedback layout of the lifted system setting enables us to design the ILC using classical feedback design methods, taking into account the effects of noise and convergence in a single design.

One drawback however is that these design methods are based on a fixed size of the lifted system, which essentially means that the ILC will be calculated for a fixed length of the trajectory under consideration and the application to a trajectory of different length will change the design and require a recalculation of the ILC. In this presentation is shown that, for LTI systems, it is very well possible to express the optimal lifted system ILC in the parameters of the underlying LTI plant. Effectively creating a finite time optimal ILC

design.

This finite time ILC design has been applied to an industrial grade wafer stage, showing the value of this extrapolated solution.

- [1] Dick de Roover. *Motion Control of a Wafer Stage.* A Design Approach for Speeding Up IC Production. PhD thesis, Delft University of Technology, 1997. ISBN: [90-407-1562-9].
- [2] S.P. Bhattacharyya Kevin L. Moore, Mohammed Dahled. Iterative learning for trajectory control. *Proceedings on the 28th Conference on Decision and Control, Tampa Florida*, pages 860–865, December 1989.
- [3] Mikael Norrlöf. *Iterative Learning Control Analysis, Design and Experiments*. PhD thesis, Department of Electrical Engineering, LinköpingUniversity, Division of Autmomatic Control, Department of Electrical Engineering, Linköpings universitet, SE-581 83 Linköping, Sweden, 2000.
- [4] Badrinath Viswanathan Jian-Xin Xu. On the integrated learning control method. *Proceedings of the 14th IFAC*, pages 495–500, 1999.
- [5] Minh Phan and Richard W. Longman. A mathematical theory of learning control, of linear discrete multivariable systems. *Proceedings of the AIAA/AAS Astrodynamics Specialist Conference, Minneapolis*, pages 740–746, 1988.
- [6] Minh Q. Phan and James A. Frueh. System identification and learning control. In X Xu J. Bien, editor, *Recent Advances in Iterative Learning Control*, chapter 15. Kluwer Academic Publisers, Boston, 1998.
- [7] Rob Tousain and Eduard Van der Meché. Design strategies for iterative learning control based on optimal control. *Selected Topics in Identification, Modelling and Control*, 12, December 2001. www.ocp.tudelft.nl/sr/ (short version:CDC 2001).

¹This research project is being sponsored by Philips CFT

Application of Learning Feed-Forward Control to Cam-Follower Systems

B. Demeulenaere and J. Swevers
Katholieke Universiteit Leuven
Department of Mechanical Engineering
Division of Production Engineering, Machine Design and Automation (PMA)
Celestijnenlaan 300B, B-3001 Heverlee, Belgium
Email: bram.demeulenaere@mech.kuleuven.ac.be

1 Abstract

Cam-follower mechanisms are often used for realizing fast, periodical motions, as they occur in e.g. car engines and weaving machines. Traditionally, cam profiles are synthesized based on the assumption that the camshaft speed is constant. Nevertheless, many cam-follower systems, especially high-speed systems, exhibit substantial camshaft speed fluctuation, due to the high inertial torques that result from the exchange of kinetic energy between the flywheel on the camshaft and the follower inertia. The fluctuation of the camshaft speed causes the follower motions to be inaccurate, since the cams are designed for constant camshaft speed. As a result, the follower accelerations exhibit undesired harmonics that may excite machine resonances, causing vibrations, noise and wear.

Two fundamentally different approaches exist to obtain accurately realized follower motions. The first, more traditional approach consists of taking measures in order to reduce the camshaft speed fluctuation. Several methods have been proposed. First of all, the flywheel size can be increased. The main disadvantage of this method is the resulting bad start/stop behaviour of the machine. A better method is the application of an advanced control technique to keep the camshaft speed as constant as possible, see e.g. [1]. This works fine, but has the disadvantage that the motor has to deliver large (mainly inertial) torques in high-speed systems. These torques can however be drastically reduced by adding an extra mechanism that compensates for the inertial torques, see e.g. [2]. The second, recently developed approach [3] doesn't aim at reducing the camshaft speed variation but explicitly takes it into account when designing the cam profiles. These inertially compensated cams yield accurately realized follower motions, even for small flywheel sizes. Moreover, the motor has to deliver no inertial torque, despite the fact that no compensating mechanism is present.

Both the second approach and the (second method of the) first approach require advanced control strategies in order to accurately impose the desired constant (first approach) or fluctuating (second approach) camshaft speed. As cam-

follower systems are nonlinear systems performing repetitive motions, Repetitive Control (RC), Iterative Learning Control (ILC) and (Time-Indexed) Learning Feed-Forward Control (LFFC) [4] seem applicable. This paper reports on the application of LFFC to an experimental set-up, consisting of a DC motor driving a cam-follower system. The camfollower system is strongly nonlinear, that is, it cannot be accurately modeled as an underlying linear system with nonlinear distortions. Consequently the LFFC stability analysis presented in [4] is not applicable as it is based on the transfer function of the underlying linear system. Nevertheless, simulation and experimental results point out that controlling the set-up using LFFC yields satisfactory results.

Acknowledgement

Bram Demeulenaere is research assistant with the Fund for Scientific Research-Flanders (Belgium) (F.W.O.). This work also benefits from the Belgian Interuniversity Poles of Attraction Programme, initiated by the Belgian State, Prime Minister's Office, Science Policy Programming. Its authors assume the scientific responsibility.

- [1] Tao, Jian and Sadler, J.P., 1995, Constant Speed Control of a Motor Driven Mechanism System, Mechanism and Machine Theory, Vol. 30, No. 5, pp.737–748.
- [2] Dooner, D. B., 1997, Use of Noncircular Gears to Reduce Torque and Speed Fluctuations in Rotating Shafts, ASME J. of Mech. Design, Vol.119, pp. 299–306.
- [3] Demeulenaere B. and De Schutter, J., 2001, Dynamically Compensated Cams for Rigid Cam-Follower Systems with Fluctuating Cam Speed and Dominating Inertial Forces, Proc. of IEEE/ASME Int. Conf. on Advanced Intelligent Mechatronics, Como, Italy, pp. 763-768 (extended version submitted to ASME J. of Mech. Design)
- [4] Velthuis, W.J.R., 2000, Learning Feed-Forward Control: Theory, Design and Applications, Ph.D. Thesis, Department of Electrical Engineering, University of Twente, Enschede, The Netherlands.

¹Only the camshaft speed variation due to *inertial* forces is taking into account.

Evaluation of (unstable) non-causal systems for iterative learning

M.J.G. van de Molengraft, M.G.E. Schneiders, M. Steinbuch

Eindhoven University of Technology
Faculty of Mechanical Engineering
Group Dynamics and Control Technology
Section Control Systems Technology
P.O. Box 513
5600 MB Eindhoven
The Netherlands

{M.J.G.v.d.Molengraft, M.G.E.Schneiders, M.Steinbuch}@tue.nl

This paper presents a new approach towards the design of iterative learning control (ILC, Moore, 1993). ILC improves the tracking accuracy of a (closed-loop) control system by learning from previous experience prescribing the same trajectory. This is done by updating the feedforward signal in an iterative way according to a learning law. This process makes use of a learning filter that is optimal if it equals the inverse model of the process sensitivity. In linear motion control systems the design is often complicated by the inverse plant sensitivity being non-causal and unstable. We assume that we have a reliable (linear) model of the inverse process sensitivity. To evaluate such non-causal system we split it up in a causal and a non-causal part. The non-causal part can be written as a linear combination of differentiating filters. Since in ILC the whole input series is known, we can use high-performance differentiating filters for this part (Carlsson, 1989). The output of this non-causal part serves as the input for solving the causal part. By choosing a solver for mixed boundary value problems we can put extra constraints on begin and end values of the output signal. The advantages of this new approach over the existing techniques are demonstrated by examples. First, the new approach is applied on an academic non-minimum phase system. At this point, contrary to another widely used technique (ZPETC, Tomizuka, 1986), the new approach succeeds in calculating inverse responses of non-minimum phase systems. Next, both the new approach and ZPETC are applied to an industrial motion system, i.e. an H-drive. Using a tenth order model of the process sensitivity, the resulting tracking error for both methods is of the same order of magnitude. Further exploring the use of mixed boundary value constraints will be a major issue for future research. In particular, creating cyclic feedforward signals seems a very attractive option in motion control. Furthermore, research will focus on optimizing the numerical implementation of the solver to make this method more efficient and suitable for higher order systems.

References

[1] B. Carlsson, Digital differentiating filters, Model based fault detection, Dissertations from the faculty of sci-

ence 28, 215pp., Acta Univ. Ups. Uppsala., 1989

- [2] K. Moore, Iterative learning control for deterministic systems, Springer Verlag, London, 1993
- [3] M. Tomizuka, Zero phase error tracking algorithm for digital control, ASME Journal of Dynamic Systems, Measurement and Control, 109, 65-68, 1986

Reinforcement learning algorithms for continuous state-spaces

D. Ernst[†]

Department of Electrical and Computer Engineering - Institut Montefiore University of Liège - Sart-Tilman B28 - B4000 Liège - Belgium † Research Fellow F.N.R.S.

Email: ernst@montefiore.ulg.ac.be

1 Abstract

Reinforcement learning (RL) takes its origin in the optimal control theory and the dynamic programming. It consists of a collection of methods for approximating by experience optimal solutions to problems of unknown dynamics [3].

We focus on how to apply these methods to discrete time optimal control of systems with continuous state-spaces. The main idea of the approach used is to tranform the discrete time control problem into a Markov Decision Process (MDP) by discretizing the state-space (the discretization technique we use is known as triangularisation [2]) and then to solve the MDP by means of classical dynamic programming techniques.

First we concentrate on how a MDP structure can effectively represent the discrete time optimal control problem and how to compute this structure through the knowledge of the dynamics of the system. Then we explain how to estimate this structure by interacting with the system. Validity of the approximations and convergence of the methods are discussed. Moreover an application of these reinforcement learning methods to power system control is used as illustration [1].

- [1] D. Ernst. Reinforcement Learning Applied to Power System Oscillations Damping. In *Proceedings of 40th IEEE Conference on Decision and Control*, Orlando, USA, December 2001.
- [2] R. Munos. A study of reinforcement learning in the continuous case by the means of viscosity solutions. *Machine Learning*, 40:265–299, 2000.
- [3] R.S. Sutton and A.G. Barto. *Reinforcement Learning, an introduction*. The MIT Press, 1998.

Allowed sloppy magnet placement due to learning control

Bas J. de Kruif University of Twente Drebbel Institute of Mechatronics b.j.dekruif@utwente.nl

1 Introduction

Linear motors are typically used in applications that require high speed, high force and high precision actuation. A linear synchronous motor consists of two parts, the moving part and the stationary part. The motor we investigated had permanent magnets fixed on the stationary part. To generate a force, a three phase current has to be applied with a certain phase depending on the position. To increase this force, iron-core coils are used that bundle the flux. The permanent magnets in the stationary part attract these iron which results in cogging forces. The motor has preference positions due to this attraction. By skewing the permanent magnets this effect can be minimized [1], however, at the cost of a smaller peak force. If the magnets are placed with small tolerance and the generated magnetic field would be equal, the cogging force would be periodic. This would mean that the cogging force is known before-hand and can be compensated for. However this would require a set of tightly toleranced magnets that are placed accurately.

The downside of precise placement and a good set of permanent magnets is that it is costly. It would be advantageous to use a set of inferior magnets and place them with a large tolerance. This would result in a cogging force that cannot be calculated beforehand, thus introducing a disturbance force that depends on the position of the moving part. Tracking errors will be introduced by this force and these are unwanted in scanning motions that are performed in semiconductor manufacturing.

By identifying the current that is required to compensate for the cogging force as a function of the position and by applying this as a feedforward signal, precise magnet placement is not necessary and a set of less costly magnets can be used.

2 Method

Identification of the required compensating currents can be done with Learning Feed-Forward Control [2]. By moving the translator over the stationary part, the extent of the cogging force can be determined. This force can be stored in a linear neural network or in a different function approximator

This method has been applied on a linear motor in which the set of magnets could be exchanged. First, the cogging force Theo J.A. de Vries
University of Twente
Drebbel Institute of Mechatronics
t.j.a.devries@utwente.nl

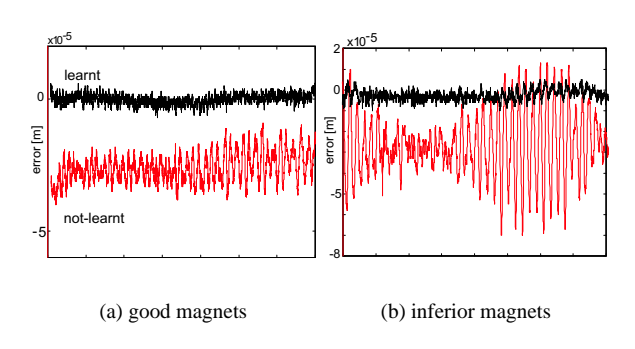


Figure 1: Error on evaluation path with constant velocity.

of the linear motor with a high quality magnetic field was determined. This force was stored in a B-spline network as a function of position and used for compensating the cogging force in the next run. Next the same procedure was applied for the set of magnets with inferior specifications.

The result are given in figure 1. The scales of the inferior magnets are slightly larger. From these figures it is clear that the tracking error of the configuration with inferior magnets is worse than the tracking with the good magnets. After the learning of the individual cogging force, they can be compensated for. The tracking error after the learning is about equal for both set of magnets.

3 Conclusion

The tracking error of a linear synchronous motor stems among others form cogging forces. These forces can be limited by precise construction. However by identifying and compensation for these forces, it is shown to be possible that the tolerances on the construction can be loosened without introducing larger tracking errors. By investing time identification and control, the construction becomes less costly.

- [1] J.F. Gieras and Z.J. Piech. *Linear Synchronous Motors, Transportation and Automation Systems*. CRC Press, Boca Raton, Florida, 2000.
- [2] W.J.R. Velthuis. *Learning Feed-Forward Control, Theory, Design and Applications*. PhD thesis, University of Twente, Enschede, Febuary 2000.

Robust stabilization of linear time-delay systems

W. Michiels P. Vansevenant D.Roose Katholieke Universiteit Leuven Department of Computer Science Celestijnenlaan 200 A B-3001 Leuven, Belgium

Email: {Wim.Michiels, Patrick.Vansevenant, Dirk.Roose}@cs.kuleuven.ac.be

In previous work [1], we developed a new numerical stabilization procedure for linear time-delay systems, called the continuous pole placement method, which can be considered as an extension of the classical pole placement method for ordinary differential equations. One of its applications is the calculation of a stabilizing feedback gain for linear systems with an input delay,

$$\dot{x}(t) = Ax(t) + Bu(t - \tau), \quad u = K^{T}x(t),$$

Since the closed-loop system has infinitely many eigenvalues, the procedure consists of controlling only the rightmost or unstable eigenvalues, which are moved to the left half plane in a quasi-continuous way by applying small changes to the feedback gain K and meanwhile monitoring the other eigenvalues with a large real part. The rightmost eigenvalues can be computed with the method described in [2]. The procedure ends when the rightmost eigenvalues cannot be further shifted to the left using the available controller parameters; for stabilizable systems this means that the exponential decay rate of the solutions is maximal.

However, the resulting controller is often not very robust.

For this reason, we consider in this talk some perturbations on the parameters of the (stabilizable) system and discuss a numerical procedure to determine the value of the feedback gain, which maximizes some robust stability measures. These measures are quantitively expressed by stability radii, which can be interpreted as the size of the smallest destabilazing perturbations. The procedure consists of two steps. First the continuous pole placement method is applied until stability is reached. In case of complex perturbations, we then optimize complex stability radii based on shaping of some frequency response plots.

The talk consists of three parts. First we motivate the importance of robustness considerations in the stabilization of delay equations with the analysis of a scalar and a two-dimensional example. Thereby, it turns out that the feedback gain and the configuration of the eigenvalues can be completely different in the cases where some robust stability measures are maximal and where the exponential decay rate of the solutions is maximal. Moreover, in the latter case, robustness can be poor. Secondly we describe the numerical procedure in detail and finally we apply it to a realistic ex-

ample.

- [1] W. Michiels, K. Engelborghs, P. Vansevenant and D. Roose, "Continuous pole placement for delay equations," *Automatica*, accepted, 2001.
- [2] K. Engelborghs and D. Roose, "Numerical computation of stability and detection of hoph bifurcations of steady state solutions of delay differential equations," *Advances in Computational Mathematics*, 10(3-4):271-289, 1999.

Using Genetic Programming for finding Lyapunov functions

Iris Soute, Georgo Angelis Philips Centre for Industrial Technology {iris.soute, georgo.angelis}@philips.com René van de Molengraft Eindhoven University of Technology m.j.g.v.d.molengraft@tue.nl

1 Abstract

Genetic programming (GP) is the technique for finding solutions to problems by imitating processes as seen in nature during the evolution. Starting with a population (i.e. a set of random generated solutions, also called individuals) operations as crossover, mutation and reproduction are applied to create new generations, until a suitable solution is found. To make this process converge to a suitable solution, the individuals need to be evaluated for their 'fitness', i.e. how well they are able to solve the problem. Individuals with a good fitness are allowed to evolve, individuals with a bad fitness are not. In a way this is similar to breeding. Lyapunov's theory provides a way of proving stability of equilibrium points for all kinds of systems. If a Lyapunov function exists for a system, one can draw conclusions regarding the stability. However, the difficult part is to *find* such a function, as there exists no universal method for finding a Lyapunov function. On the other hand, it is a well known fact that for the systems that we study, stability of the system implies that a Lyapunov function exists that proves it. Consider the set of (non)linear differential equations represented as $\dot{\mathbf{x}} = \mathbf{f}(\mathbf{x})$, with \mathbf{f} locally Lipschitz. The Lyapunov theorem for local stability states that the equilibrium at the origin is locally asymptotically stable when two conditions are met.

Theorem 1 (Local stability) If, in a ball B_{R_0} , there exist a scalar function $V(\mathbf{x})$ with continuous first partial derivatives such that

- $V(\mathbf{x})$ is positive definite (locally in \mathbf{B}_{R_0})
- $\dot{V}(\mathbf{x})$ is negative semi-definite (locally in \mathbf{B}_{R_0})

then the equilibrium point $\mathbf{0}$ is locally stable. If actually the derivative $\dot{V}(\mathbf{x})$ is locally negative definite in \mathbf{B}_{R_0} , then the stability is asymptotic.

Merging the theories above, we present an algorithm that helps finding Lyapunov function in many cases. Besides stability, also performance issues such as the region of attraction of an equilibrium point can be addressed within this framework. To find a Lyapunov function using GP, an assessment of the *likeliness* of the function of evolving into a Lyapunov function needs to be made. To assign the fitness value (quantification of likeliness) a grid is created in the search space. The individuals are evaluated on every point

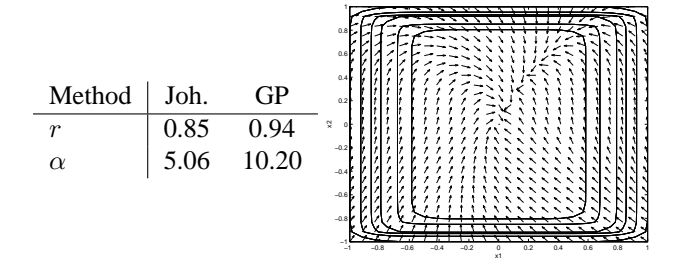
of the grid, while checking if the inequalities of Theorem 1 hold. The best function is the function with fitness value zero. The fitness of a GP-generated Lyapunov function candidate can be conceptually evaluated as follows:

- 1. Evaluate $V(\mathbf{x})$ and $\dot{V}(\mathbf{x})$ for all fitness cases \mathbf{p} . Increase the fitness value for every \mathbf{p} where $V(\mathbf{x}) \leq 0$ and/ or $\dot{V}(\mathbf{x}) \geq 0$.
- 2. Evaluate performance (i.e. the region of attraction). Increase the fitness value according to how well the performance criteria are met (a small value being good performance).

This way, the individuals are graded to the likeliness of them becoming a Lyapunov function. Individuals that fail in most points on the grid, will end up with a high fitness value. Whereas individuals that fail on few points, i.e. individuals that are near being a Lyapunov function, receive a low fitness value. As a benchmark problem, the problem posed by Johansen [1] is used. For the system:

$$\dot{x}_1 = -3x_1 + x_2
\dot{x}_2 = \frac{2x_1^2}{0.3 + (x_2 + 0.4)(x_2 - 0.6)} - 2x_2$$
(1)

Lyapunov functions are to be found. The Lyapunov functions found by Johansen and by GP are compared in terms of the region of attraction r or the decay rate α . Contour curves of the Lyapunov function found by GP together with a vector plot of Eq. (2) are shown in the figure below. As



the table shows, GP succeeds in finding better values for r and α .

References

[1] Johansen, T. A. (1999). Computation of Lyapunov Functions for Smooth Nonlinear Systems using Convex Optimization.

Tuning Rules for Passivity-Based Controllers

Dimitri Jeltsema and Jaquelien M. Scherpen

Control Systems Engineering Group Delft University of Technology, P.O. Box 5031, 2600 GA Delft, The Netherlands. d.jeltsema/j.m.a.scherpen@its.tudelft.nl

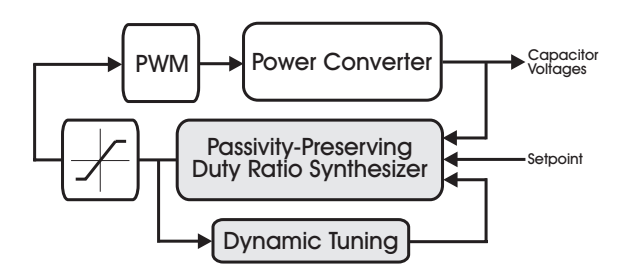
Motivation

Nonlinear passivity-based control (PBC) algorithms for power converters have proven to be an interesting alternative for other, mostly linear, control techniques. The control objective is usually achieved through an energy reshaping process and by injecting damping to modify the dissipation structure of the system. However, a key question that arises during the implementation of the controller is how to tune the various parameters. The first attempt to develop some guidelines to adjust the damping parameters is to study the disturbance attenuation properties using \mathcal{L}_2 -gain analysis techniques [5]. Unfortunately, the necessary calculations become quite complex, especially when dealing with large converter structures. In previous works, see e.g. [4], the location where to add the damping is mainly motivated by the form of the dissipation structure, in the sense that damping is added to those states that do not contain any damping terms a priori. For example, in the boost converter case this means that only damping is injected on the input current, as the output voltage already contains a damping term due to the load resistance. However, this leads to a PBC regulated circuit that is highly sensitive to load variations and also needs an expensive current sensor to measure the inductor current. This disadvantage holds for many other (switching) networks too. Another disadvantage is that in general more states have to be measured than is strictly necessary, resulting in a more expensive controller from both a financial and computational point of view.

Contribution

In this presentation a solution to these problems is provided. The method uses the classical Brayton-Moser equations [1] stemming from the early sixties. First, these equations are accommodated to include controllable switches. Due to the passive nature and their close relation with Lagrangian and Port-Hamiltonian dynamics [3], the Brayton-Moser equations appear to be naturally suited for application of passivity-based control. Secondly, because the PBC design is based on the energy and the interconnection structure of the circuit, it is not surprising that this allows an interpretation in similar physical terms of the controlled closed-loop system. From a circuit-theoretic point of view, as is discussed in [2], the controller produces a computed duty ratio function (switch control) which forces the closed-loop dynamics to act as if there are *virtual* resistors connected in se-

ries and/or in parallel to the real circuit elements. In this way the characteristic impedance(s) of the filter elements can be matched dynamically by the controller [2]. However, this method is quite conservative and not easy to extend to general circuits with nonlinear elements. In this talk we present an alternative methodology to tune the various control parameters based on modified versions of the stability theorems developed in [1]. These fairly sharp criteria following from these theorems form a systematic and straight forward tool for solving the tuning problem for a general class of PBC controlled power electronic circuits. Both criteria are compared and tested using the elementary single switch buck and boost converters. Interestingly enough, the idea of dynamic parallel damping injection (see figure) provides a method to control non-minimum phase circuits based on the corresponding non-minimum phase output(s) only.



- [1] R.K. Brayton, J.K. Moser, "A theory of nonlinear networks I and II", Quart. Appl. Math. Vol. 12, No. 1 and 2, pp. 1-33, pp. 81-104, April 1964 and July 1964.
- [2] D. Jeltsema, J.M.A. Scherpen, J.B. Klaassens, "Energy control of multi-switch power supplies an application to the three-phase buck rectifier with input filter", in Proc. IEEE 32nd Power Electr. Spec. Conf., Vancouver, Canada, June 2001.
- [3] D. Jeltsema, J.M.A. Scherpen, "On nonlinear RLC networks: Port-Controlled Hamiltonian systems dualize the Brayton-Moser equations", *Submitted for publication 2001*.
- [4] R. Ortega, A. Loría, P.J. Nicklasson and H. Sira-Ramírez, *Passivity-Based Control of Euler-Lagrange Systems; Mechanical, Electrical and Electromechanical Applications*, Springer-Verlag London Limited, 1998.
- [5] J.M.A. Scherpen, R. Ortega, "On nonlinear control of Euler-Lagrange systems: Disturbance attenuation properties", System & Control Letters 30, pp.49–56, 1997.

Regular implementability, stabilization and pole placement of behaviors

Madhu N. Belur
Institute for Mathematics
University of Groningen
P.O. Box 800, 9700 AV Groningen
The Netherlands
Email: M.N.Belur@math.rug.nl

The Netherlands Email: H.L.Trentelman@math.rug.nl

Harry L. Trentelman

Institute for Mathematics

University of Groningen

P.O. Box 800, 9700 AV Groningen

In the behavioral approach, a system is studied as the set of trajectories that the system allows. We call this set as the *behavior* of the system. There is no a priori distinction among the system variables as inputs and outputs. Details of this general approach of studying systems can be found in [2]. Further, in this context, control of a given system is viewed as interconnection of this system with another system (called the controller) such that the interconnection brings about a (desired) restriction on the set of allowable trajectories. This view of treating control problems has been introduced in [5].

In contrast to [5], where the problems of stabilization and pole placement were considered for the case that *all* system variables are available for interconnection (the so-called full information case), we work in the generality that we are allowed to use only some of the system variables for the purpose of interconnection. These variables are called the control variables. Restricting oneself to using only the control variables for interconnection brings in the notion of *implementability* into the control problem. Necessary and sufficient conditions for implementability of a behavior have been obtained and they can be found in [4] and [3].

Another important role is played by the notion of *regular* interconnection. This too was introduced in [5]. We deal with interconnections that are regular in this paper. Regular interconnections turn out to be precisely the interconnections that bring about a restriction on *only* the controllable part of a behavior and thus do not interfere with the autonomy within a plant. This captures the intuitive idea that a plant's autonomy must not be interfered upon by a controller.

We combine these notions of regular interconnection with that of implementability and establish necessary and sufficient conditions for the existence of a *regularly implementable* subbehavior. This result is then applied to solve the problems of stabilization and pole placement by interconnection.

A noteworthy feature here (like in most other literature on behaviors) is that the results have been formulated in terms of properties of the behaviors themselves and *not* in terms of any particular set of equations that the behaviors are repre-

sented by. The above results along with the proofs can also be found in [1].

- [1] M.N. Belur and H.L. Trentelman, Stabilization, pole placement and regular implementability, to appear in *IEEE Transactions on Automatic Control*.
- [2] J.W. Polderman and J.C. Willems, *Introduction to Mathematical Systems Theory: A Behavioral Approach*, Springer Verlag, 1997.
- [3] J.W. Polderman and I. Mareels, A behavioral approach to adaptive control, in: *Mathematics of System and Control* J.W. Polderman and H.L. Trentelman eds., Festschrift on the occasion of the 60th birthday of J.C. Willems, Groningen, 1999.
- [4] J.C. Willems and H.L. Trentelman, Synthesis of dissipative systems using quadratic differential forms, Part I, to appear in *IEEE Transactions on Automatic Control*.
- [5] J.C. Willems, On interconnections, control and feedback, *IEEE Transactions on Automatic Control*, volume 42, pages 326-337, 1997.

On the optimization of satellite orbit plane changes subject to time constraints and its applications ¹

Valery Moreno Vega SYSTeMS Research Group Ghent University, Belgium E-mail: valery@ensmain.rug.ac.be Dirk Aeyels SYSTeMS Research Group Ghent University, Belgium E-mail:Dirk.Aeyels@rug.ac.be

1 Abstract

In this article the authors deal with the optimization of the fuel burned during orbit plane change corrections under time constrained situations. A necessary and sufficient condition for which a three impulse maneuver burns less propellant than the standard non-coplanar Hohmann transfer (the single impulse plane change maneuver) is given. For the case when the condition is satisfied, the authors derive the (optimal) value of the transfer orbit semi-major axis for which the fuel expenditure during the maneuvering is minimized. Some practical applications of these results are delineated in the contribution as well.

2 Introduction

The majority of investigations carried out on satellite orbital plane changes have been concentrated on techniques that minimize the fuel consumption. This is an optimization problem, which, to this day, has *only* been posed considering as a cost function the *expenditure of fuel* regardless of the *time* needed to perform the maneuver. However, in a number of situations, it might be desirable to optimize the maneuver fuel consumption subject to time constraints.

3 Results

The fuel burned during an orbital maneuver is often expressed in terms of the *change in velocity* needed to achieve the new location and conditions. It can be easily proved that this ΔV is a direct measure of such propellant consumption. In this contribution the authors use the same criterion.

Although the standard orbit plane change maneuver is the so-called simple impulse maneuver (or the non-coplanar extension to Hohmann transfer maneuver) in the paper the authors propose to make use of another type of maneuver, the so-called Bi-elliptic plane change maneuver (see [1]). We apply the latter to obtain better results regarding less fuel consumption when compared with the standard manuever. The problem we solved can be formulated as follows:

Problem: Minimization of the fuel consumption applying bi-elliptic transfers subject to time constraints:

Minimize
$$\Delta V = f(r_1, \theta, n)$$
 subject to
$$g(r_1, n) \le t_{max} \tag{1}$$

with θ the plane change angle, r_1 the radius of the orbit in which the satellite is coasting, $n = \frac{r_2}{r_1}$, n > 1, $\frac{r_2 + r_1}{2}$ the semi-major axis of the transfer orbits and g a function that expresses the duration of the orbit plane change transfer maneuver in terms of r_1 and n.

The optimization problem is solvable iff $t_{max} > P_{r_1}$, with P_{r_1} the period of the orbit of radius r_1 .

- 1. For $\theta \geq 48.94^{\circ}$ the ratio $n = \frac{r_2}{r_1}$ is determined **only** by the time constraint inequality $n \leq \frac{\alpha}{r_1}(\sqrt[3]{t_{max}} 1)$ with $\alpha = \sqrt[3]{\frac{2\mu_e}{\pi^2}}$. The optimal value of n, denoted by n^* , is $n^* = \frac{\alpha}{r_1}(\sqrt[3]{t_{max}} 1)$.
- 2. For $\theta < 48.94^{\circ}$ we have:

$$n^* = \frac{2\lambda - 1 - \lambda^2}{2\lambda^2 + 4\lambda - 2} \tag{2}$$

where n^{\star} is the solution that maximizes the difference in ΔV when performing a three-impulse maneuver instead of an one-impulse maneuver $(\lambda = \sin(\frac{\theta}{2}))$. The optimal value of n is given by (2) if $n^{\star} < \frac{\alpha}{r_1}(\sqrt[3]{t_{max}} - 1)$, otherwise it is $n^* = \frac{\alpha}{r_1}(\sqrt[3]{t_{max}} - 1)$.

4 Applications

Orbiting satellites need orbit corrections several times during their lifetime. We studied some satellite formation flights guaranteeing that at each time one of the satellites is operational while the others are in stand-by to replace the operational one. The maneuver needed to put in the operational orbit one of the stand-by satellites is cost inexpensive if the time for doing this operation is long enough. This procedure can be repeated several times giving as a result a better overall performance.

References

[1] J. E. Prussing and B. A. Conway, "Orbital mechanics", Oxford University Press, 1993.

¹This paper presents research results of the Belgian Programme on Inter-University Poles of Attraction, initiated by the Belgian State, Prime Minister's Office for Science, Technology and Culture. The scientific responsibility rests with its authors.

Cessna Citation II Aircraft Aerodynamic Model Parameter Identification

Sinar Juliana
PhD student, Dept. of Control and Simulation
s.juliana@lr.tudelft.nl

Q.P. Chu
Assistant Professor, Dept. of Control and Simulation
q.p.chu@lr.tudelft.nl

J.A. Mulder
Professor, Dept. of Control and Simulation
j.a.mulder@lr.tudelft.nl

Faculty of Aerospace Engineering TU Delft, The Netherlands

1 Abstract

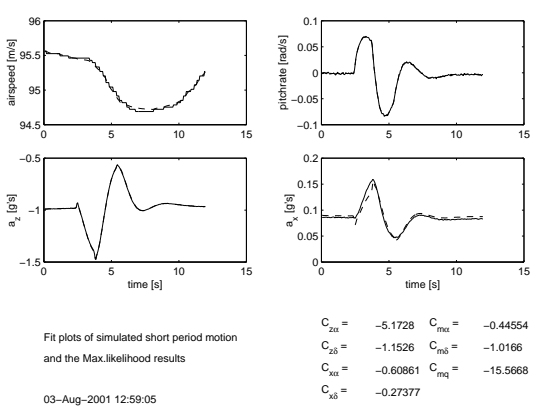
Dynamic system such as an aircraft is best described with non-linear stochastic models, possibly with correlation between process and measurement noise. Estimation of aero-dynamic parameter of aircraft from this kind of model gives closer approximation to reality of the system. The objective of this work is therefore to develop an algorithm of parameter and state estimation for non-linear stochastic systems, considering correlation of process and measurement noise into account.

Investigation of the nature of noise has been conducted for aircraft dynamic model. Correlation can happen if control input measurement is noisy, hence corrupts both state- and measurement equations. By taking a similar approach to Sage and Melsa[1], an extended Kalman filter has been developed to obtain state estimates for this system. Furthermore, Maximum Likelihood parameter estimation algorithm was established to identify aerodynamic parameters of the system.

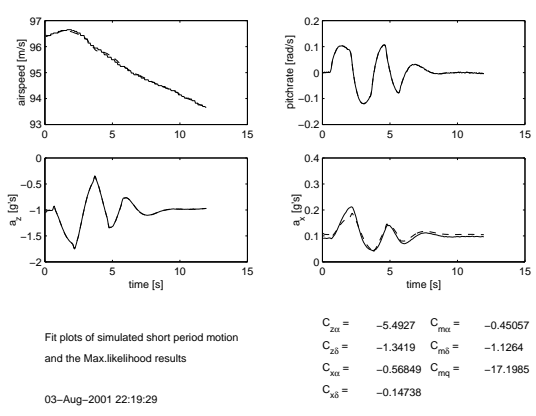
The algorithm is implemented in MATLAB environment. It has been validated by using Citation II short period motion simulation and gave a desired performance in identifying the aerodynamic parameters. Applying the algorithm to flight test data completed the validation of the software. The results shows superior performance compared to linear Maximum Likelihood algorithm. Further improvement can be obtained as non-linear aerodynamic model is implemented to the algorithm, especially in the estimation of x-axis aerodynamic parameters.

References

[1] A.P. Sage and J.L. Melsa "Estimation Theory with application to communication and control," McGraw-Hill, 1971.



maneuver with doublet input



maneuver with 3211 input

Figure 1: Plots of flight maneuvers with doublet and 3211 control inputs on elevator and the proof of match

The range-dependence problem of clutter spectrum for non-sidelooking monostatic STAP radars

Fabian D. Lapierre Signal Processing Group Montefiore Department University of Liege Belgium

Email: f.lapierre@ulg.ac.be

Jacques G. Verly
Signal Processing Group
Montefiore Department
University of Liege
Belgium

Email: jacques.verly@ulg.ac.be

Problem formulation

The problem of slow moving targets detection by means of a moving pulsed radar is examined for monostatic radars, where the transmitter and the receiver are co-localized. The radar uses a linear antenna and transmits a train of coherent pulses. Combining this space (antenna) and time (train of pulses) informations can enhance target detection.

The signal received from reflexions on the ground is divided in range gates. For a given range gate, the signal is a spacetime snapshot. Applying a 2D FOURIER transform to the snapshot allows us to determine the spatial and DOPPLER frequencies f_s and f_d of the scatterer under interest.

The most important challenge is the rejection of interferences coming from the fixed background (clutter). The space-time repartition of the clutter power is found by plotting the clutter DOPPLER frequency as a function of the clutter spatial frequency. (direction-DOPPLER trajectories).

The optimum clutter rejection is provided using Space-Time Adaptive Processing (STAP) [1, 3]. For each range gate r, a new processor is applied. The optimum processor (OP) for a given r is [1]

$$\underline{\boldsymbol{w}}_{opt}(r)(f_s, f_d) = \underline{\underline{\boldsymbol{Q}}}^{-1}(r)\underline{\boldsymbol{v}}(r)(f_s, f_d),$$

where $\underline{\underline{Q}}$ is the space-time clutter-plus-noise covariance matrix and $\underline{\underline{v}}$, the space-time steering vector. The construction of the OP implies the estimation of $\underline{\underline{Q}}$, based on information contained in neighboring snapshots [3]. The estimator $\underline{\underline{\hat{Q}}}(r)$ for the range gate r is obtained by using N_r snapshots centered about r, i.e.,

$$\underline{\underline{\hat{Q}}}(r) = \frac{1}{N_r} \sum_{k} \underline{y}(r_k) \underline{y}^{\dagger}(r_k)$$

for $r-\frac{N_r-1}{2}\leq k\leq r+\frac{N_r-1}{2}$ and $k\neq r$. $\underline{\boldsymbol{y}}(r_k)$ is the received snapshot for the r_k th range gate.

 $\underline{y}(r_k)$ being a random process, the clutter spectrum is the 2D FOURIER transform of $\widehat{\underline{Q}}(r)$ (or $\underline{y}(r_k)\underline{y}^\dagger(r_k)$) for a

given r. An accurate estimator is found by applying the MVE to $\underline{y}(r_k)\underline{y}^{\dagger}(r_k)$ [1]. The resulting clutter spectrum is composed of a clutter ridge that has the same shape as the corresponding direction-DOPPLER trajectory. A non-biaised estimator is obtained only if the clutter spectrum is range-independant in the N_r range gates. This is not the case for non-sidelooking monostatic radars. The only existing method to compensate for this range-dependence is the DOPPLER warping [2]. However, the performance decreases as the crab angle of the antenna increases.

Proposed solution

This method appies to each $\underline{y}(r_k)\underline{y}^{\dagger}(r_k)$ a non-linear transformation that fit the clutter ridge of each $\underline{y}(r_k)\underline{y}^{\dagger}(r_k)$ to that of the range gate of interest, before application of STAP. The deformation studied here is a 2D dilatation.

After estimation of \underline{Q} , the OP must be applied in the space-time domain. However, the clutter spectrum is found by a non-linear power spectrum estimator that has no inverse transformation. The dilatation must then be done in the space-time domain. Working with discrete snapshots, 2D replicas of the clutter spectrum must first be suppressed in the space-time domain by applying a 2D interpolation filter to $y(r_k)y^{\dagger}(r_k)$.

The optimum trade-off between low sidelobes and reduction of high frequencies amplitudes is the 2D-KAISER window. This solution is examined and compared to the DOPPLER warping technique.

- [1] R. Klemm, *Space-Time Adaptive Processing: Principles and Applications*, IEE Radar, Sonar, Navigation and Avionics 9, 2000.
- [2] G.K. Borsari, *Mitigating effects on STAP processing caused by an inclined array*, IEEE National Radar Conference, Dallas, 1998, pp 135-140.
- [3] J. Ward, *Space-time adaptive processing for airborne radar*, Technical Report 1015, Lincoln Laboratory MIT, 1994.

Optimal Input Design for the Estimation of Kinetic Parameters

K.J. Keesman and J.D. Stigter Systems and Control Group, Wageningen University and Research Centre THE NETHERLANDS

karel.keesman@user.aenf.wau.nl

1 OPTIMAL PARAMETRIC SENSITIVITY CONTROL: AN EXAMPLE

In bioprocess modelling substrate limitation is usually modelled in terms of the well-known Monod kinetics with unknown coefficients μ_{max} and K_S , that is $\mu(C_S) =$ $\mu_{\max} \frac{C_S}{K_S + C_S}, \qquad \text{where } \mu_{\max} \, (1/\min) \, \text{is the maximum spe-}$ cific growth rate, K_S (g/l) the half-saturation coefficient and C_S (g/l) the substrate concentration. A natural question is how the input sequence should be chosen in such a way that the parameters can be optimally estimated. This is the well known problem of 'optimal' input design, which is a classical problem in the identification literature. Recently, Stigter and Keesman (2001) [1] have shown how a closely related problem for a fed-batch reactor can be solved analytically using the minimum principle of Pontryagin. In that paper only the simplest case, i.e. input design for either K_S or $\mu_{\rm max}$ in a fed-batch reactor using direct state measurements, has been considered.

In this presentation the emphasis is now on finding a 'feedback' control law that maximizes the parameter sensitivity $y_{\theta}\triangleq \frac{\partial y}{\partial \theta_k}$ for the *specific* parameter θ_k from the set $\{\theta_i, i=1,\ldots,p\}$ related to the model structure (f,g), to allow more or less simple analytical solutions, under indirect state measurements, continuous flow in the bioreactor and input or state weighting.

Define the following simple cost function, with y=x, that has to be maximized: $J=\int_{t=0}^{t_f}x_{\theta}^2(\tau)d\tau$ under the dynamic constraints given by state equation: $\dot{x}(t)=f(x(t),\theta)+bu(t)$ and related sensitivity equation. Using Pontryagin's minimum principle [2] the singular arc condition (or interior boundary condition) can be derived as $x_{\theta}(t)=-\frac{f_{x\theta}}{f_{xx}}$. Under the interior boundary condition the optimal input is found from $u^*(t)=-\frac{[f_{\theta}f_{xx}+ff_{xx\theta}+x_{\theta}(t)(f_xf_{xx}+ff_{xxx})\}]}{b[f_{xx\theta}+x_{\theta}(t)f_{xxx}]}$, where $f_{\theta}=\frac{\partial f}{\partial \theta}$, $f_{x}=\frac{\partial f}{\partial x}$, ...

Let us illustrate the procedure for estimating K_S in a practical context using the dilution rate for compensating the growth in the biomass to avoid growth effects. Hereto, the following equations of the fed-batch reactor are introduced:

$$\frac{\frac{dC_S}{dt} = -\frac{\mu(C_S)}{Y_{X/S}}C_X + \frac{F}{V}(u - C_S)}{\frac{dC_X}{dt} = \mu(C_S)C_X - \frac{F}{V}C_X} \tag{1}$$

$$\frac{dV}{dt} = F$$

where $Y_{X/S}$ (-) is the yield coefficient, F (l/min) the flow

rate, V (1) the volume of the reactor and $u=C_{S,in}$ (g/l) the variable substrate concentration in the influent. The biomass concentration C_X is kept constant at C_X^* , the biomass setpoint, by selecting $F=\mu(C_S)V$. Consequently,

$$\frac{dC_S}{dt} = \mu(C_S)[-C_S - \frac{C_X^*}{Y_{X/S}} + u]$$
 (2)

The following singular arc condition is found: $x_{\theta}(t) = \frac{C_S}{K_S}$. The corresponding simple optimal control law is: $u^*(t) = \frac{C_X^*}{Y_{X/S}}$. Hence, an experiment could be organized as:

- (i) Apply an impulsive input at t=0, such that $C_{S,0}=20$ g/l. From the first measurements of C_S , given $Y_{X/S}$ and C_X^* , the unknown parameter μ_{\max} , can be estimated.
- (ii) Keep u(t)=0, so that pure water is fed into the reactor with flow $F(t)=\mu_{\max}\frac{C_S(t)}{K_S+C_S(t)}V(t)$ using initial estimates of both μ_{\max} and K_S and measured substrate concentrations and volumes. Observe whether the singularity condition $x_{\theta}(t)=\frac{C_S}{K_S}$ with $x_{\theta}(0)=0$ holds.
- (iii) Once the singularity condition is satisfied, switch to the control $u^*(t) = C_{S,in}^* = \frac{C_X^*}{Y_{X/S}}$, $\iota.e.$ feed the reactor with a flow $F_2 = \frac{1}{Y_{X/S}} \frac{C_X^*}{C_S} F$ (l/min) from a buffer with constant concentration C_S (g/l) and a pure water flow $F_1 = F F_2$ (l/min), such that the substrate concentration in the continuously stirred buffer tank is $C_{S,in}^*(=u^*)$ and estimate K_S .

2 CONCLUDING REMARKS

Analytical solutions to the general *one-dimensional* optimal parameter sensitivity problem have been found. For the estimation of the Monod constant K_S , under fed-batch conditions with regulated biomass concentration C_X^* , the simple control law: $u^*(t) = \frac{C_X^*}{Y_{X/S}}$ has been derived. Solutions with input or state weighting or with nonlinear output relationships and under different flow conditions can be derived in a similar way.

- [1] J.D. Stigter, K.J. Keesman, Optimal parametric sensitivity control of a fed batch reactor. In: Proc. ECC 2001, Porto, Portugal, 4-7 Sep., 2001, pp. 2841-2844.
- [2] A.E. Bryson (Jr.), Dynamic Optimization, Addison Wesley, pp. 434, 1999.

Hybrid extended Luenberger - asymptotic observer for bioprocess state estimation

Ph. Bogaerts¹, X. Hulhoven¹ and A. Vande Wouwer²

¹Service d'Automatique et d'Analyse des Systèmes, Université Libre de Bruxelles, CP 165/55, 50, Av. F. D. Roosevelt, B-1050 Brussels, Belgium Philippe.Bogaerts@ulb.ac.be, xhulhove@labauto.ulb.ac.be

²Faculté polytechnique de Mons, Control Engineering Department. Bld. Dolez, 31 B-7000 Mons, Belgium vdw@autom.fpms.ac.be

1 Abstract

The measurements of the main component concentrations in bioprocesses are useful for on-line monitoring and control of the process. But in most cases, hardware sensors involve several problems (cost, sterilization, sample destruction, time delay, discrete time measurements, etc.). These problems encourage the use of software sensors which give on-line measurement estimates (in continuous time) based, on the one hand, on the available hardware sensors signals and, on the other hand, on a mathematical model. The algorithm is called a state observer whose goal is thus to provide a state estimate converging towards the true state of the process.

Many state observer techniques have been applied to bioprocesses, trying to deal with the nonlinear models involved in this field. Bastin and Dochain [1] distinguish the exponential state observers from the asymptotic observers. The former ones allow to handle a tuning parameter for the rate of convergence towards the true state. The main drawback is that the results are strongly dependent on the model quality. The extended Kalman filter, extended Luenberger observer and high gain observer are exponential observers. On the other hand, the rate of convergence of the Bastin and Dochain's asymptotic observer [1] is completely determined by the experimental conditions (namely the dilution rate) and does not own any tuning parameter. This may lead to a very slow convergence in the case of a low dilution rate or even, in the limit case of a batch process, to a constant state estimation error. However, the main advantage is that the kinetic model is not necessary anymore, this model being most of time badly known.

In order to combine both advantages of exponential observers (i.e., fast convergence with a good model) and asymptotic observers (i.e., convergence without any knowledge on the kinetic model), hybrid observers have been developed. They estimate the state of the bioprocess together with a confidence parameter δ w.r.t. the kinetic model quality. The structure of the hybrid observer evolves continu-

ously between the two limit cases, namely $\delta=1$ (100% confidence in the kinetic model) which then corresponds rigorously to the exponential observer and $\delta=0$ (0% confidence in the kinetic model) which then corresponds rigorously to the asymptotic observer. Two cases of such hybrid observers have already been proposed, the former using an extended Kalman filter as exponential observer [2] and the latter using a full horizon (or optimization based) observer [3]. This contribution tackles the case of a hybrid observer based on the extended Luenberger observer. Its basic principle and properties are given and the performances are illustrated in simulation in the case of a bacterial fed-batch fermentation with substrate measurement and no biomass measurement.

- [1] G. Bastin and D. Dochain, On-line state estimation and adaptive control of bioreactors, Elsevier, 1990
- [2] Ph. Bogaerts, A hybrid asymptotic Kalman observer for bioprocesses, Bioprocess Engineering, 20 (n3), pp. 249-255, 1999
- [3] X. Hulhoven and Ph. Bogaerts, Hybrid full horizon-asymptotic observer for bioprocesses, submitted to the IFAC World Congress, Barcelona (Spain), 21-26/7/2002

Sensitivity function based model reduction: a bacterial gene expression case study

Ilse SMETS¹

Kristel BERNAERTS¹
Jos VANDERLEYDEN³

Kathleen MARCHAL²
Jan VAN IMPE^{1*}

Jun SUN³

¹BioTeC - Katholieke Universiteit Leuven Kasteelpark Arenberg 22 B-3001 Leuven (Belgium) e-mail: jan.vanimpe@agr.kuleuven.ac.be * Corresponding author

²ESAT - Katholieke Universiteit Leuven

³CMPG - Katholieke Universiteit Leuven

Abstract

To qualify and quantify the influence of external signals on bacterial gene expression, continuous culture steady-state experiments have been performed throughout the past [1, 2]. These costly, labor-intensive and time consuming experiments can be reduced to a minimum with the aid of a mathematical model that describes the intrinsic properties of the dynamic bioprocess.

Although the advantages of model based optimization and control of *fermentations* (e.g., baker's yeast production processes and biological wastewater treatment systems) are well established, the introduction of mathematical modeling in the field of genetic engineering is fairly recent. The scarce, knowledge based models that have been developed are usually characterized by complex kinetic expressions involving a high number of parameters.

In this contribution it is illustrated that sensitivity function analysis is a powerful tool to reduce the complexity of a knowledge based model.

As a vehicle to present the model reduction methodology and the results obtained, a bacterial gene expression case study is considered in which the influence of dissolved oxygen concentration on the expression of the *cytN* gene in *Azospirillum brasilense* Sp7 is modeled.

In a first approach available physiological knowledge is incorporated into a mass balance equation model with 3 states and 14 parameters.

The large differences in order of magnitude of the identified parameter values, is a clear indication that not all these parameters are significant. A careful sensitivity function analysis revealed that a reduced model with only 6 parameters is almost as accurate as the original model.

Acknowledgments

Work supported in part by grants from the Flemish Government (GOA) and the Fund for Scientific Research Flanders, Project OT/99/24 of the Research Council of the Katholieke Universiteit Leuven and the Belgian Program on Interuniversity Poles of Attraction initiated by the Belgian State, Prime Minister's Office for Science, Technology and Culture. The scientific responsibility is assumed by its authors.

- [1] Chao, G., Shen, J., Tseng, C.P., Park, S.-J., and Gunsalus, R.P. (1997). Aerobic regulation of isocitrate dehydrogenase gene (*icd*) expression in *Escherichia coli* by the *arcA* and *fnr* gene products. *Journal of Bacteriology*, **179**:4299-4304.
- [2] Kasimoglu, E., Park, S.-J., Malek, J., Tseng, C.P. and Gunsalus, R.P. (1996). Transcriptional regulation of the proton-translocating ATPase (*atpIBEFHAGDC*) operon of *Escherichia coli*: control by cell growth. *Journal of Bacteriology*, **178**:5563-5567.
- [3] Sun, J., Smets, I., Bernaerts, K., Van Impe, J., Vanderleyden, J. and Marchal K. (2001). Quantitative analysis of bacterial gene expression by using the *gusA* reporter gene system. *Applied and Environmental Microbiology*, **67**:3350-3357.

Systematic model reduction for complex bioprocesses described by metabolic pathways

Jens E. Haag, Alain Vande Wouwer and Marcel Remy
Laboratoire d'Automatique
Faculté Polytechnique de Mons
Boulevard Dolez 31,
B-7000 Mons

e-mail: haag@fpms.ac.be

1 Abstract

Much effort has been put towards the mathematical description of mammalian cell cultures during the last few decades. Early attempts revealed a very global view of the cells acting as biocatalysts that reproduce themselves, excrete metabolites and often overexpress proteins of interest, e.g. for pharmaceutical purposes. Simple models have been developed, which give a phenomenological representation of the cell activities. Their validity for describing eucaryotic cells is, however, limited to a relatively small range of culture conditions.

Nevertheless, simple models have been successfully used for process design [1]. A survey on unstructured models for hybridoma cell growth and metabolite production is given by Pörtner and Schäfer [2]. The authors also discuss the structured kinetic model of Batt and Kompala [3] distinguishing four compartments inside the cell. The major substrates (glucose and amino acids) and metabolites (lactate and ammonia) are considered. Glutamine is distinguished from the other amino acids to emphasize its important role in the metabolism, since it additionally serves as a carbon source besides a nitrogen source typical for amino acids.

During the last decade, mass balancing techniques have been used for Metabolic Flux Analysis to calculate the specific reaction rates in a considered metabolic pathway network in steady-state cultures [4, 5]. Bonarius *et al.* [6] discuss the problem of underdetermined networks and the choice of additional constraints.

Recently, Biener [7] formulated a dynamic model based on the major metabolic pathways including amino acid metabolism. This model allows several limiting influences to be described, e.g. energy limitation, and accounts for irreversible reaction pathways.

In this contribution, a class of dynamic models based on metabolic reaction pathways is analysed, showing that systems with complex intracellular reaction networks can be represented by macroscopic reactions relating extracellular components only. Based on rigorous assumptions, the model reduction procedure is systematic and allows an equivalent 'input—output' representation of the system (i.e. a representation in terms of extracellular components, such as substrates and products) to be derived. The resulting macroscopic reaction scheme can be useful for system analysis as well as for the development of model-based optimisation, sensor and control techniques.

2 Acknowledgements

This work is supported by the *Directorate General for Technologies*, *Research & Energy* of the Wallonia Region (Belgium) and the company *4C Biotech S.A.*, Seneffe (Belgium)

- [1] Dhir, S., J. Morrow Jr., R. R. Rhinehart and T. Wiesner (2000). Dynamic optimization of hybridoma growth in a fed-batch bioreactor. *Biotechnol. Bioeng.* **67**(2), 197–205.
- [2] Pörtner, R. and T. Schäfer (1996). Modelling hybridoma cell growth and metabolism a comparison of selected models and data. *J. Biotechnol.* **49**, 119–135.
- [3] Batt, B. C. and D. S. Kompala (1989). A structured kinetic modeling framework for the dynamics of hybridoma growth and monoclonal antibody production in continuous suspension cultures. *Biotechnol. Bioeng.* **34**, 515–531.
- [4] Zupke, C. and G. Stephanopoulos (1995). Intracellular flux analysis in hybridomas using mass balances and in vitro ¹³C NMR. *Biotechnol. Bioeng.* **45**(4), 292–303.
- [5] Bonarius, H. P. J., V. Hatzimanikatis, K. P. H. Meesters, C. D. de Gooijer, G. Schmid and J. Tramper (1996). Metabolic flux analysis of hybridoma cells in different culture media using mass balances. *Biotechnol. Bioeng.* **50**(3), 299–318.
- [6] Bonarius, H. P. J., G. Schmid and J. Tramper (1997). Flux analysis of underdetermined metabolic networks: the quest for the missing constraints. *TIBTECH* **15**, 308–314.
- [7] Biener, R. (1998). Modellbildung und modellgestützte Prozeßführung bei tierischen Zellkulturen. Vol. 178 of Fortschritt-Berichte VDI, Reihe 17. VDI Verlag. Düsseldorf.

Optimal Control with Imprecise Gain through Dynamic Programming

Gert de Cooman SYSTeMS Research Group Universiteit Gent, Belgium gert.decooman@rug.ac.be

Matthias Troffaes
SYSTeMS Research Group
Universiteit Gent, Belgium
matthias.troffaes@ruq.ac.be

Abstract

We generalise the optimisation technique of dynamic programming for discrete-time systems with an uncertain gain function. The main objective in optimal control is to find out how a system can be influenced, or controlled, in such a way that it its behaviour satisfies certain requirements, while at the same time maximising a given gain function. A very effective method for solving such problems, is the well-known recursive *dynamic programming* method, introduced by Richard Bellman [1].

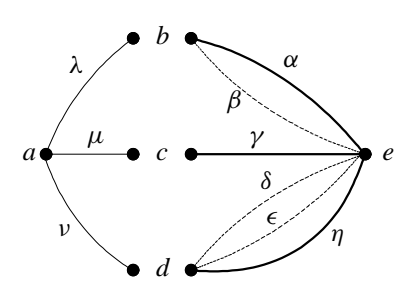


Figure 1: A Simple Example

To explain the ideas behind this method, we refer to Figure 1. If the optimal paths from b, c and d to the final state e are known to be α , γ and η , respectively, then to find the optimal path from a to e, we only need to compare the paths $\lambda\alpha$, $\mu\gamma$ and $\nu\eta$. This follows from Bellman's *principle of optimality*, by which $\lambda\beta$, $\nu\delta$ and $\nu\epsilon$ cannot be optimal, since in that case β , δ and ϵ would be optimal. Based on these observations, an efficient recursive algorithm can be constructed to calculate optimal paths.

We now wish to weaken the assumption that the gain associated with every path is exactly known. This problem is most often treated by modelling the uncertainty about the gain function by means of a probability measure, and by maximising the *expected gain* under this probability measure, rather than the (unknown) gain itself—we could call this the Bayesian approach. It turns out that, due to the linearity of the expectation operator, this approach does not change the nature of the optimisation problem, and the usual dynamic programming method can therefore still be applied to find the 'optimal' controls.

But it has often been argued that uncertainty cannot always

be modelled adequately by probability measures, because, roughly speaking, there will in certain cases not be enough information in order to identify a single probability measure. In those cases, the available information can be represented through so-called *imprecise probability models* (see [3] and references therein), such as comparative probability orderings, Choquet capacities, belief functions, possibility measures, lower previsions, sets of desirable gambles, or convex sets of probability distributions.

This approach naturally gives rise to a strict preference order on paths. But, in contradistinction to the Bayesian approach, this order is only partial. This means that two paths will not always be comparable and that there may be no maximally preferred path, i.e., there may be no path that is strictly preferred or equivalent to all other paths. However, we have shown [2] that the principle of optimality still holds, if we look for *undominated paths*, these are paths for which there is no other path that is strictly preferred to it. An efficient recursive dynamic programming-like algorithm follows. It turns out that as imprecision increases, more paths become undominated, and consequently, decisions based on the model also become more indeterminate. As imprecision decreases, we recover the classical theory of dynamic programming as a special case.

- [1] Richard Bellman. *Dynamic Programming*. Princeton University Press, 1957.
- [2] Gert de Cooman and Matthias C. M. Troffaes. Dynamic programming for discrete-time systems with uncertain gain. In preparation.
- [3] Peter Walley. *Statistical Reasoning with Imprecise Probabilities*. Chapman and Hall, London, 1991.

Linear Matrix Inequalities for Optimization of Rational Functions

Dorina Jibetean CWI, P.O. Box 94079, 1090 GB Amsterdam d.jibetean@cwi.nl

1 Introduction

Many problems in system theory can be reformulated as optimization problems where the criterion function is a polynomial or rational function. For example in system identification of linear systems, one may try to estimate the transfer function of a system, which is a rational function, from the data by the least squares method. The function to be estimated depends in general on some parameters that need to be identified. This procedure is nothing else that minimization of a rational function.

Another application area is the model reduction of the order of a system. There one tries to approximate a given transfer function by one of a lower degree which reduces again to optimization of a rational function.

We believe however that the applications are much more numerous.

In this paper we study unconstrained global optimization of rational functions. We give first few theoretical results. Then we give a relaxation of the initial problem which can be solved using LMI techniques. Therefore, in general our procedure will produce a lower bound of the infimum of the original problem. However, under no degeneracies, it is possible to check whether the relaxation was in fact exact.

2 Main results

Lemma 1 Let a(x)/b(x) be a rational multivariate function, with a(x), b(x) relatively prime polynomials. If $a(x)/b(x) \ge 0$, $\forall x \in \mathbf{R}^n \setminus \{x \in \mathbf{R}^n \mid b(x) = 0\}$, then one of the two following statements holds:

- $a(x) \ge 0$, $b(x) \ge 0 \ \forall x \in \mathbf{R}^n$,
- $a(x) \le 0$, $b(x) \le 0 \ \forall x \in \mathbf{R}^n$.

Next, we discuss the application of Lemma 1 to rational optimization problems.

Consider the problem

$$\min_{x \in \mathbf{R}^n} \frac{p(x)}{q(x)}, \text{ with } p(x), q(x) \in \mathbf{R}[x] \text{ relatively prime.}$$

Theorem 2 Let p(x)/q(x) be a rational function with p(x), q(x) relatively prime. If p(x)/q(x) is bounded from below, then q has constant sign on \mathbb{R}^n .

Corollary 3 Let p(x)/q(x) be a rational function with p(x), q(x) relatively prime polynomials. If q(x) changes sign on \mathbb{R}^n then $\min_{x \in \mathbb{R}^n} p(x)/q(x) = -\infty$.

Note that the reciprocal is not true. However, we can reformulate now the problem (1). Suppose that $q(x) \ge 0 \ \forall x \in \mathbf{R}^n$. Then problem (1) is equivalent to

max
$$\alpha$$

s.t. $p(x) - \alpha q(x) \ge 0$, $\forall x \in \mathbf{R}^n$. (2)

Obviously the largest α satisfying the condition is the infimum of p(x)/q(x).

Note that the feasibility domain of (2) may be the empty set. That is, there is no $\alpha \in \mathbf{R}$ satisfying the polynomial inequality for every $x \in \mathbf{R}^n$. In this case the maximum will be $-\infty$.

Using the technique described in [2], [1], one can construct a relaxation of (2)

$$\max_{\text{s.t. }} \alpha$$
s.t. $Q(\alpha, \lambda) \succeq 0$. (3)

Here $Q(\alpha, \lambda)$ is a symmetric matrix, affine in $\alpha \in \mathbf{R}$ and $\lambda \in \mathbf{R}^k$ and k+1 is the dimension of the affine space (see [1]). Therefore (3) is a standard LMI problem. The solution of (3) is in general a lower bound on (2). However, in general, there are ways to check whether the relaxation was exact.

3 Conclusions

The rational optimization problem is rewritten as constrained polynomial optimization. A relaxation of the latter problem can be subsequently solved using LMI's.

- [1] D. Jibetean, Global optimization of rational multivariate functions, CWI Report PNA-R120 October 2001.
- [2] P. Parrilo, Semidefinite programming relaxations for semialgebraic problems, submitted

The Newton method for invariant subspace computation

Pierre-Antoine Absil Université de Liège, Belgium absil@montefiore.ulg.ac.be Rodolphe Sepulchre Université de Liège, Belgium R.Sepulchre@ulg.ac.be

1 Abstract

We consider the Newton method on Riemannian manifolds and its application to the particular case of finding a stationary point of the (generalized) Rayleigh quotient on the Grassmann manifold of p-dimensional subspaces of \mathbb{R}^n . This yields an iterative method that cubically converges to the p-dimensional invariant subpaces of a symmetric n-by-n matrix. Emphasis will be laid in the presentation on the intuitive meaning of the Newton method, and illustrations will be given in the case p = 2, n = 3.

In \mathbb{R}^n , the kth iteration of the Newton method for a smooth cost function $f: \mathbb{R}^n \to \mathbb{R}$ computes $x^{(k+1)} \in \mathbb{R}^n$ from $x^{(k)} \in \mathbb{R}^n$ in the following way (see e.g. [2]):

(a) solve
$$H^{(k)}N = -\operatorname{grad} f(x^{(k)})$$
 for $N \in \mathbb{R}^n$ (1a)

(b) set
$$x^{(k+1)} = x^{(k)} + N$$
 (1b)

where $\operatorname{grad} f(\hat{x})$ denotes the Euclidean gradient of f at $\hat{x} \in \mathbb{R}^n$, namely $\operatorname{grad} f(\hat{x}) = (\partial f/\partial x_1(\hat{x}), \ldots, \partial f/\partial x_n(\hat{x}))^T$, and $H^{(k)}$ is the Hessian of f at $x^{(k)}$, that is $H^{(k)} = (\partial \operatorname{grad} f/\partial x_1(x^{(k)}), \ldots, \partial \operatorname{grad} f/\partial x_n(x^{(k)}))$. Note that the term $H^{(k)}N$ appearing in (1a) is nothing else than the directional derivative of $\operatorname{grad} f$ in the direction of N. An intuitive interpretation of (1) is that we compute by (1a) a "direction of motion" N in which the gradient varies as the opposite of $\operatorname{grad} f(x^{(k)})$, and then make a step in this direction (1b), the aim being to find a new point $x^{(k+1)}$ where the gradient approximately vanishes. And indeed, it can be proved (see e.g. [2]) that, under mild hypotheses on f, the Newton method is well defined and quadratically converges to a stationary point of f, i.e. a point x^* such that $\operatorname{grad} f(x^*) = 0$.

The following generalization of the Newton method to a Riemannian manifold M is due to Smith [5]:

(a) solve
$$\nabla_N \operatorname{grad} f = -\operatorname{grad} f(x^{(k)})$$
 (2a) for $N \in T_{x^{(k)}}M$

(b)
$$set x^{(k+1)} = ExpN$$
 (2b)

where T_xM denotes the tangent space to M at x, ∇ the Riemannian (also called Levi-Civita) connection, and Exp the exponential mapping. All these differential geometric concepts are explained in introductory books on Riemannian geometry (see e.g. [3]). The term $\nabla_N \operatorname{grad} f$ can be thought of as the variation of $\operatorname{grad} f$ in the direction of N, while the exponential generalizes the concept of step in the direction of N. Again, this iteration quadratically converges to stationary points of f, provided f does not behave too badly.

We will show how this applies to the following case. The manifold M is the Grassmann manifold $\operatorname{Gr}(p,n)$, i.e. the set of the p-dimensional subspaces of \mathbb{R}^n . Note that any element \mathcal{Y} of $\operatorname{Gr}(p,n)$ can be represented as the column span of an n-by-p matrix Y with full rank. Let A be a symmetric n-by-n matrix. The cost function considered is the generalized Rayleigh quotient $\rho_A(\operatorname{span}(Y)) := \operatorname{trace}[(Y^TY)^{-1}Y^TAY]$. This cost function has the interesting proprety that its stationary points are the p-dimensional invariant subspaces of A. The Newton iteration in this case maps a subspace \mathcal{X} to a new subspace \mathcal{X}_+ according to the following procedure [4]: (a) Pick an orthonormal n-by-p matrix X such that $\operatorname{span}(X) = \mathcal{X}$.

(b) Solve the following Sylvester equation

$$X_{\perp}^{T}AX_{\perp}K - KX^{T}AX = -X_{\perp}^{T}AX \tag{3}$$

for $K \in \mathbb{R}^{(n-p)\times p}$, where X_{\perp} is any orthonormal n-by-(n-p) matrix such that $X^T X_{\perp} = 0$.

(c)
$$\mathfrak{X}_+ := \operatorname{span}(X + X_{\perp}K)$$
.

We will show how this iteration compares to the generalized Rayleigh quotient iteration we presented last year [1].

- [1] P.-A. Absil, R. Mahony, R. Sepulchre, P. Van Dooren, A Grassmann-Rayleigh quotient iteration for computing invariant subspaces, to appear in SIAM Review, Vol. 44, No. 1, 2002.
- [2] D. P. Bertsekas, *Nonlinear programming*, Athena Scientific, 1995.
- [3] W. B. Boothby, An introduction to differentiable manifolds and Riemannian geometry, Academic Press, 1975.
- [4] A. Edelman, T. A. Arias, S. T. Smith, *The geometry of algorithms with orthogonality constraints*, SIAM J. Matrix Anal. Appl., Vol. 20, No. 2, pp. 303-353, 1998.
- [5] S. T. Smith, *Optimisation techniques on Riemannian manifolds*, in Hamiltonian and Gradient Flows, Algorithms and Control, A. Bloch, ed., Fields Institute Communications 3, AMS, pp. 113-136, 1994.

Conjectures for exact observability for infinite-dimensional systems

Hans Zwart
Faculty of Mathematical Sciences
University of Twente
Email: h.j.zwart@math.utwente.nl

1 Introduction

Consider the infinite-dimensional system

$$\dot{x}(t) = A(x(t), \quad y(t) = Cx(t),$$

with initial condition $x(0) = x_0$ on the infinite-dimensional state space H (Hilbert space). We assume that A is the infinitesimal generator of a C_0 -semigroup T(t) on the Hilbert space Z, and that C is a bounded operator from the domain of A to another Hilbert space Y. Furthermore, we assume that for every initial condition x_0 the output y is square integrable.

We want to derive necessary and sufficient conditions for exact observability. The above system is (by definition) exactly observable if and only if $\int_0^\infty \|y(t)\|^2 dt \ge m \|x_0\|^2$, for some positive m.

2 Conjecture

Some ten years ago, Russell and Weiss posed the following conjecture: The system is exactly observable if and only if

$$||(s-A)x||^2 + |Re(s)||Cx||^2 \ge m_1 Re(s)^2 ||x||^2$$

for some $m_1 > 0$, all x in the domain of A, and all complex s with negative real part.

We show that in general this conjecture is not true. Furthermore, we show that this conjecture should be reformulated. This new conjecture is still open.

Control of Variable Profiles in a Distributed Parameter System using Reduced Models

Leo Huisman
Eindhoven University of Technology
P.O. Box 595, 5600 AN Eindhoven
The Netherlands
l.huisman@tue.nl

A.C.P.M. Backx Eindhoven University of Technology IPCOS Technology The Netherlands

1 Motivation

This presentation describes the control of temperature profiles using model predictive control (MPC) based on reduced models obtained by proper orthogonal decomposition (POD). A simple heat transfer problem will be used as an example. The basic ideas will in future be extended to (parts of) glass melting furnaces, where the behaviour of physical variables, such as temperature, is described by partial differential equations (PDE). The main processes taking place in the glass melt (melting, fining and mixing) must take place in different parts of the domain. This results in requirements on the temperature profile in the glass melt.

Numerical models that are used to simulate the temperature behaviour are based on discretisation of the spatial domain. The number of state variables in these models is high ($^{\sim}10^5$) to achieve acceptable accuracy. Therefore reduced models are nescessary for controller design. Next it is explained how these by POD reduced models are used in a controller.

2 Strategy

Consider the following partial differential equation:

$$\frac{\partial x\left(\xi,t\right)}{\partial t} = \mathcal{D}\left(x\left(\xi,t\right),u\left(\xi_{a},t\right)\right) \tag{1}$$

where $x\left(\xi,t\right)$ is the state, $\mathcal{D}\left(\cdot\right)$ is an operator (e.g. partial derivatives of $x\left(\xi,t\right)$) and ξ_a is a finite dimensional vector of actuator positions. Suppose the control problem is given by:

$$u(\xi_a, t) = \arg\min||r(\xi, t) - x(\xi, t)||^2$$
 (2)

that is, track a reference profile $r(\xi, t)$ as close as possible. If (1) is discretised with respect to space, then:

$$\frac{d\bar{x}(t)}{dt} = f(\bar{x}(t), \bar{u}(t)) \tag{3}$$

where $\bar{x} \in \mathbb{R}^n$, $u \in \mathbb{R}^m$ and $f : \mathbb{R}^n \times \mathbb{R}^m \to \mathbb{R}^n$. Through the snapshot method a set of orthogonal basis vectors $\{\varphi_i\}_{i=1}^l$ is found (POD basis, [1], [3], [2]) to approximate the state:

$$\bar{x}(t) = \sum_{i=1}^{l} a_i(t) \varphi_i + \varepsilon_x(t)$$
 (4)

where the coefficients $a_i(t)$ are calculated by $a_i(t) = \langle \bar{x}(t), \varphi_i \rangle$. Define $\Phi = \begin{bmatrix} \varphi_1 & \varphi_2 & \cdots & \varphi_l \end{bmatrix}$ and $a = \begin{bmatrix} a_1 & a_2 & \cdots & a_l \end{bmatrix}^T$ to find an approximate model for the coefficients $a_i(t)$:

$$\dot{a}(t) = \Phi^{T} f(\Phi a(t), \bar{u}(t)) \tag{5}$$

Furthermore, assume a finite number of measurements at locations that are given in ξ_m , $y(\xi_m,t)=g(x(\xi_m,t))$ which gives $\bar{y}(t)=g(\Phi a(t))$. A reduced control problem is formulated using a discretised reference trajectory $\bar{r}(t)$:

$$\bar{u}(t) = \arg\min ||a_{ref}(t) - a(t)||^{2}$$

where $a_{ref,i}\left(t\right) = \langle \bar{r}\left(t\right), \varphi_i \rangle$ or $a_{ref}\left(t\right) = \Phi^T \bar{r}\left(t\right)$ and $a_{ref}, a \in \mathbb{R}^l$. An observer is used to estimate the vector of coefficients $a\left(t\right)$ rather than the state \bar{x} . To demonstrate the approach a 1D heat transfer example will be presented with a considerable reduction of state space dimension in the controller, l << n.

3 Conclusions

The original control problem (2) in \mathbb{R}^n can be translated into a reduced control problem on \mathbb{R}^l . Results achieved up to now are promising and the strategy may also be feasible for more difficult 3D problems.

Future work on this subject will be done on the incorporation of equality and inequality contraints and the effects of modeling errors (e.g. $\varepsilon_x(t)$).

- [1] P. Astrid. Model reduction by proper orthogonal decomposition. Submitted to Benelux meeting on Systems and Control, December 2001.
- [2] J. A. Atwell and B. B. King. Proper orthogonal decomposition for reduced basis feedback controllers for parabolic equations. *Mathematical and Computer Modelling*, 33:1–19, 2001.
- [3] K. Kunisch and S. Volkwein. Control of burgers' equation by a reduced order approach using proper orthogonal decomposition. *Journal of Optimization Theory and Applications*, 102(2):345–373, 1999.

Spectral Factorization of Meromorphic Functions of Finite Order for Distributed Parameter Systems

Frank M. CALLIER, Joseph J. WINKIN University of Namur (FUNDP), Department of Mathematics 8 Rempart de la Vierge, B–5000 NAMUR, BELGIUM frank.callier@fundp.ac.be, joseph.winkin@fundp.ac.be

Spectral factorization is a paramount problem in feedback control system design, see e.g. [10], [7] and the references therein. In particular, the spectral factorization problem of the so-called Popov function constitutes an essential step in the solution of the Linear-Quadratic optimal control problem for infinite-dimensional state-space systems, see e.g. [1], [3], [6], [9], [11] and the references therein.

This contribution is devoted to the analysis of the spectral factorization problem for a large class of distributed parameter system transfer functions, [4]. More specifically, this question is studied for (coercive) spectral densities which are meromorphic functions of finite order, see e.g. [8], in the framework of the Callier-Desoer algebra of distributed parameter system transfer functions, see e.g. [2],[5].

In particular, criteria for the elementary rational factor infinite product representation of a coercive spectral density and for the convergence of the spectral factorization procedure based on such representation are developed. These criteria are based on the knowledge of the comparative asymptotic behavior of the spectral density poles and zeros, i.e. on the pole-zero absolute and relative errors.

- [1] F.M. Callier and J. Winkin, "LQ-optimal control of infinite-dimensional systems by spectral factorization", *Automatica*, Vol. 28, No. 4, 1992, pp.757–770.
- [2] F.M. Callier and J. Winkin, "Infinite dimensional system transfer functions", in *Analysis and optimization of systems: state and frequency domain approaches to infinite-dimensional systems*, R.F. Curtain, A. Bensoussan and J.L. Lions (eds.), Lecture Notes in Control and Information Sciences, Springer–Verlag, Berlin, New York, 1993, pp. 72–101.
- [3] F.M. Callier and J. Winkin, "The spectral factorization problem for multivariable distributed parameter systems", *Integral Equations and Operator Theory*, Vol. 34, 1999, pp. 270–292.
- [4] F.M. Callier and J. Winkin, "Spectral factorization by symmetric extraction for distributed parameter systems",

- University of Namur (FUNDP), Belgium, *Internal Report*, 2002; in preparation.
- [5] R.F. Curtain and H. Zwart, "An introduction to infinite-dimensional linear systems theory", Springer-Verlag, New York, 1995.
- [6] P. Grabowski, "The LQ controller problem: An example", *IMA Journal of Mathematical Control and Information*, Vol. 11, 1994, pp. 355–368.
- [7] B. Jacob, J. Winkin and H. Zwart, "Continuity of the spectral factorization on a vertical strip", *Systems & Control Letters*, Vol. 37, 1999, pp. 183-192.
- [8] R. Nevanlinna, "Analytic functions", Springer-Verlag, Berlin Heidelberg, 1970.
- [9] O.J. Staffans, "Quadratic optimal control through coprime and spectral factorizations", *Abo Akademi Reports on Computer Science and Mathematics*, Vol. 29, 1996, pp. 131–138.
- [10] M. Vidyasagar, "Control system synthesis: A factorization approach", MIT Press, Cambridge, MA, 1985.
- [11] M. Weiss and G. Weiss, "Optimal control of stable weakly regular linear systems", *Math. Control Signals Systems*, Vol. 10, 1997, pp. 287–330.

The sub-optimal Hankel norm approximation problem for the Wiener class

Orest V. Iftime
Department of Applied Mathematics
University of Twente
P.O. Box 217 7500AE Enschede
The Netherlands
o.v.iftime@math.utwente.nl

Amol J. Sasane
Department of Applied Mathematics
University of Twente
P.O. Box 217 7500AE Enschede
The Netherlands
a.j.sasane@math.utwente.nl

1 Abstract

The sub-optimal Hankel norm approximation problems have been studied extensively in the literature and we have nothing to add in this direction. The new contribution of this paper is to present an elementary derivation of the reduction of the sub-optimal Hankel norm approximation problem to a J-spectral factorization problem. We do this for the Wiener class of matrix-valued functions. The solution of this J-spectral factorization problem can then be obtained solving two equations involving projection operators, hence obtaining an explicit parameterization of all solutions to the sub-optimal Hankel norm approximation problem.

The first source of the connection between the sub-optimal Hankel norm approximation problem and a J-spectral factorization problem is Ball and Helton [1], although it is not stated explicitly there. Various corollaries of this abstract paper have been stated, but there is a gap between the abstract theory in [1] and the elementary looking corollaries. This motivated the search for an elementary self-contained proof in many papers. These elementary proofs were important steps along the way to solving the sub-optimal Nehari problem or the sub-optimal Hankel norm approximation problem for specific classes of

infinite-dimensional systems. Consequently, there were several slightly different versions presented.

The results presented in this paper refines and/or generalizes the preceding lemmas in Sasane and Curtain [4] and Iftime and Zwart [2]. We use in an essential way the notion of equalizing vectors, introduced by G. Meinsma [3].

- [1] J.A. Ball and J.W. Helton, A Beurling-Lax Theorem for the Lie Group U(m, n) which contains most Classical Interpolation Theory, Journal of Operator Theory, 9:107-142, 1983.
- [2] O.V. Iftime and H.J. Zwart, *J-spectral factorization and equalizing vectors*, System and Control Letters, 43:321-327, 2001.
- [3] G. Meinsma, *J-spectral factorization and equalizing vectors*, Systems and Control Letters, 25, 243-249, 1995.
- [4] R.F. Curtain and A.J. Sasane, Sub-optimal Hankel Norm Approximation for the Pritchard-Salamon Class of Infinite-Dimensional Systems, Integral Equations and Operator Theory, 2001

Convergence criteria for nonlinear feedback controlled Euler-Lagrange systems

Liesbeth Luyckx

Dept. of Electrical Energy, Systems and Automation, Ghent University Technologiepark - Zwijnaarde 9, B-9052 Zwijnaarde, Belgium liesbeth@autoctrl.rug.ac.be

Mia Loccufier

Dept. of Electrical Energy, Systems and Automation, Ghent University Technologiepark - Zwijnaarde 9, B-9052 Zwijnaarde, Belgium mia@autoctrl.rug.ac.be

Erik Noldus

Dept. of Electrical Energy, Systems and Automation, Ghent University Technologiepark - Zwijnaarde 9, B-9052 Zwijnaarde, Belgium noldus@autoctrl.rug.ac.be

Abstract

We address the design of nonlinear feedback controllers for the set point control of Euler-Lagrange (EL) systems

$$\frac{\partial \mathcal{L}}{\partial q}(q,\dot{q}) - \frac{d}{dt} \left[\frac{\partial \mathcal{L}}{\partial \dot{q}}(q,\dot{q}) \right] - \frac{\partial \mathcal{F}}{\partial \dot{q}}(\dot{q}) + Mu = 0 \quad (1)$$

with vector of generalized coordinates $q \in R^m$ and input $u \in R^r$. $\mathcal{L}(q, \dot{q})$ is the Lagrangian and $\mathcal{F}(\dot{q})$ is Rayleigh's dissipation function, which satisfies

$$\dot{q}' \frac{\partial \mathcal{F}}{\partial \dot{q}} (\dot{q}) \ge 0 \; ; \quad \forall \dot{q} \in R^m$$
 (2)

We consider the case of collocated actuator-sensor control. This implies that the output is

$$w = M'q \in R^r \tag{3}$$

We study controllers for EL systems that allow the existence of several closed loop equilibrium points. We rely on principles from dissipativity and Liapunov theory. The controllers contain a linear dynamic output feedback component and several nonlinear components. They have the general form

$$\dot{z} = Az - Bf(\sigma) + \eta(w) \tag{4}$$

$$\sigma = C'z \tag{5}$$

$$u = \psi(z, w) \tag{6}$$

in the case of displacement feedback, while the controller's input and output read $\eta(\dot{w})$ and $u=\psi(z,\dot{w})$ in the case of velocity feedback. The controller state $z\in R^n$; $A\in R^{n\times n}$ is nonsingular; $B, C\in R^{n\times s}$ and (A,B) is controllable; $f(\sigma)=\operatorname{col}[f_i(\sigma_i);\ i=1\ldots s];\ \sigma=\operatorname{col}[\sigma_i;\ i=1\ldots s].$ $\eta\in R^n$ and $\psi\in R^r$ are suitably designed nonlinearities.

Our approach is to find conditions that ensure the convergence of every bounded solution to one of the closed

loop equilibria. Systems having this property behave in a nonoscillating way: As time increases every solution either tends to infinity or it converges to an equilibrium state. If all solutions remain bounded then the set of the equilibria is globally convergent. The results constitute a basis for control systems synthesis in such cases where the existence of several stable closed loop equilibria is acceptable or desirable.

The conditions for convergence of the closed loop involve a frequency domain criterion on the tranfer matrix G(s) of the controller's linear component and some restrictions on the nonlinear amplifier characteristics. Several possibilities are investigated: First we consider velocity feedback, using controllers with sector-type bounds on the amplifier characteristics and a corresponding Popov-type criterion on G(s). A second class of controllers is characterized by slope restrictions on the nonlinearities resulting in a modified frequency condition on G(s). Subsequently we consider displacement feedback instead of velocity feedback. Finally we develop controllers possessing hard constraints on the control force amplitude. The four proposed types of controllers are compared w.r.t. their conditions of applicability and the local and global dynamic behaviour of the closed loop. They are applied to the example of a rotational-translational proof mass actuator which has been proposed as a benchmark problem for nonlinear control systems design.

Symmetry results in partial synchronization

A. Pogromsky, G. Santoboni, H. Nijmeijer
Department of Mechanical Engineering
Eindhoven University of Technology
P.O.Box 513, 5600MB, Eindhoven, The Netherlands
{A.Pogromsky, G.Santoboni, H.Nijmeijer}@tue.nl

Abstract

The proliferation of scientific contributions in the field of synchronization of coupled dynamical systems reflects the importance of this subject. The reason for this importance appears to be threefold: synchronization is common in nature, it displays a very rich phenomenology, and, finally, synchronization may be useful in applications [1].

In this paper we study the existence and stability of linear invariant manifolds in a network of k diffusively coupled dynamical systems:

$$\begin{cases} \dot{x}_j = f(x_j) + Bu_j \\ y_j = Cx_j \end{cases} \tag{1}$$

where j = 1, ..., k, $x_j(t) \in \mathbb{R}^n$ is the state of the j-th system, $u_j(t) \in \mathbb{R}^m$ and $y_j(t) \in \mathbb{R}^m$ are, respectively, the input and the output of the j-th system, and B, C are constant matrices of appropriate dimension. The coupling between the systems is assumed to be in the form of static relation between systems' inputs and outputs:

$$u_i = -\gamma_{i1}(y_i - y_1) - \gamma_{i2}(y_i - y_2) - \dots - \gamma_{ik}(y_i - y_k)$$
 (2)

where $\gamma_{ij} = \gamma_{ji} \ge 0$ are constants such that $\sum_{j \ne i}^{k} \gamma_{ji} > 0$ for all i = 1, ..., k. Let us rewrite the collection of the dynamics of the elements (1),(2) in the more compact form

$$\dot{x} = F(x) + Gx \tag{3}$$

where we denoted $x = \operatorname{col}(x_1, \dots, x_k)$, $F(x) = \operatorname{col}(f(x_1), \dots, f(x_k)) \in \mathbb{R}^{kn}$ and $G = -\Gamma \otimes BC$ with the coupling matrix defined as follows:

$$\Gamma = \begin{pmatrix} \sum_{i=2}^{k} \gamma_{1i} & -\gamma_{12} & \cdots & -\gamma_{1k} \\ -\gamma_{21} & \sum_{i=1, i \neq 2}^{k} \gamma_{2i} & \cdots & -\gamma_{2k} \\ \vdots & \vdots & \ddots & \vdots \\ -\gamma_{k1} & -\gamma_{k2} & \cdots & \sum_{i=1}^{k-1} \gamma_{ki} \end{pmatrix}$$
(4)

where $\gamma_{ij} = \gamma_{ji} \ge 0$ and all row sums are zero.

Let us recall here that given a dynamical system as (3), the linear manifold $A_M = \{x \in \mathbb{R}^{kn} : Mx = 0\}$, with $M \in \mathbb{R}^{kn \times kn}$, is *invariant* if $M\dot{x} = 0$ whenever Mx = 0, that is, if at a certain time t_0 a trajectory is on the manifold, $x(t_0) \in A_M$, then it will remain there for all time, $x(t) \in A_M$ for all

t. The problem can be summarized in the following terms: given G and $F(\cdot)$ find M a solution to

$$MF(x(t_0)) + MGx(t_0) = 0$$
 (5)

for all $x(t_0)$ for which $Mx(t_0) = 0$. There is no general solution to this, however, if these objects satisfy certain properties, it is possible to find a class of matrices M that solve (5). A natural way to do this is to exploit the symmetry of the network.

For this sort of systems we are able to prove the following result related [2] to the existence of linear invariant manifolds: i) given a permutation matrix Π that commutes with Γ , the set $\ker(I_{kn} - \Pi \otimes I_n)$ is a linear invariant manifold for system (3) and ii) suppose there is a permutation matrix Π commuting with Γ , and an $n \times n$ constant matrix J satisfying Jf(x) = f(Jx) for $f(\cdot)$ in (1), with J commuting with the $n \times n$ matrix BC. Then the set $\ker(I_{kn} - \Pi \otimes J)$ is a linear invariant manifold for system (3).

Once the existence of the linear invariant manifolds is established it is possible to study its stability. We preent sufficient conditions guaranteeing the existence of globally asymptotically stable invariant compact subset of the invariant manifold. The stability criterion is formulated in terms of eigenvalues of the coupling matrix Γ [3].

The consequences of the stability test are discussed by a number of examples.

Acknowledgements

G. Santoboni wishes to thank NWO for financial support.

- [1] I. Blekman, Synchronization in science and technology, ASME Press, New York (1988).
- [2] A. Yu. Pogromsky, G. Santoboni and H. Nijmeijer, "Partial synchronization through permutation symmetry,", submitted to 15th IFAC World Congress, Barcelona, Spain (2002).
- [3] A. Yu. Pogromsky and H. Nijmeijer, "Cooperative oscillatory behaviour of mutually coupled dynamical systems," *IEEE Trans. Circ. Sys. I* **48**,152-162(2001).

Energy functions and balancing for nonlinear discrete-time systems: an application example

Ricardo Lopezlena Control Systems Engineering Group, ITS Delft University of Technology P.O. Box 5031, 2600 GA Delft, The Netherlands E-mail: R.Lopezlena@ITS.TUDelft.nl

Jacquelien M.A. Scherpen
Control Systems Engineering Group, ITS
Delft University of Technology
P.O. Box 5031, 2600 GA Delft, The Netherlands
E-mail: J.M.A.Scherpen@ITS.TUDelft.nl

1 Abstract

The study of systematic tools for model reduction of dynamic systems has been an early topic of interest in the systems and control fields. Model approximation based on the Hankel norm and the balancing method have shown to be useful tools for model reduction for linear systems. Today singular values-based balancing, LQG balancing and \mathcal{H}_{∞} balancing are important practical tools for linear model reduction. Therefore the study of model reduction for linear systems can be considered a mature topic.

For nonlinear systems, there has been important progress with the continuous nonlinear extensions of systematic methods of balancing (singular-value-based, LQG and \mathcal{H}_{∞}), mainly based on the controllability and observability functions [2], [3]. Rougly speaking, in such procedure a Hamilton-Jacobi equation and a Lyapunov-like partial differential equation have to be solved in order to determine the energy functions. Then a nonlinear transformation transforms the system in balanced form. The mathematical complexity in solving such partial differential equations has stimulated the search for alternative methods to determine the energy functions [4].

In [1] energy functions for stable nonlinear discrete-time systems are discussed with the purpose of extending the continuous-time theory exposed in [2], [3]. Since the determination of such energy functions are a fundamental condition for nonlinear balancing and model reduction, the importance of this results lies on the establishment of firm steps towards a methodology suitable for computer implementation for the reduction of nonlinear discrete-time systems.

Consider the following discrete-time nonlinear system,

$$\begin{array}{rcl}
x_{k+1} & = & f(x_k, u_k), \\
y_k & = & h(x_k),
\end{array}$$
 $k \in \mathbb{Z}$

The energy functions of this system are naturally defined:

$$L_c(x_0) = \min_{\substack{u \in \ell_2(-\infty,0), \\ x(-\infty) = 0, \ x(0) = x_0}} \frac{1}{2} \sum_{k=-\infty}^{0} \| u_k \|^2,$$

as the controllability function and

$$L_o(x_0) = \frac{1}{2} \sum_{k=0}^{\infty} ||y_k||^2, x(0) = x_0, u_k = 0, k \in \mathbb{Z}^+,$$

as the observability function. These discrete time versions of the energy functions are discussed and analized, providing necessary existence conditions. Instead of looking for the solution of a Hamilton-Jacobi-Isaacs and a Lyapunov-like partial differential equations as in the continuous-time case, an optimization approach and an iterative algorithm are proposed to find L_c and L_o respectively.

Moreover, since the resulting energy functions are continuous in its arguments, several tools originally developed for balancing of continuous-time systems are directly applicable to discrete-time systems.

Although the applicability of one of these methods depends on the invertibility of an associated nonlinear map, this is not really a strong restriction since discrete-time systems that result from discretization of continuous-time systems are invertible. The relevance of these results lies on its applicability to model reduction and system identification for discrete-time nonlinear systems.

Furthermore, with the availability of nonlinear discretization procedures, such methods may provide alternative balancing algorithms for continuous-time systems. This is presented with an *ad hoc* application example consisting on the nonlinear balancing of a *universal* motor.

- [1] Lopezlena R., J.M.A. Scherpen,"Energy functions and Balancing for nonlinear discrete-time systems," submitted for publication, 2001.
- [2] Scherpen J. M. A., *Balancing for Nonlinear Systems*, Doctoral Dissertation, University of Twente, 1994.
- [3] Scherpen J. M. A., *Balancing for Nonlinear Systems*, Syst & Contr. Let.,21, pp.143-153, 1993.
- [4] Newman A.J., Krishnaprasad P.S., "Computation for Nonlinear Balancing," *Proc.*37th *IEEE Conf. on Dec. & Control*, Tampa Fl. U.S.A., 1998.

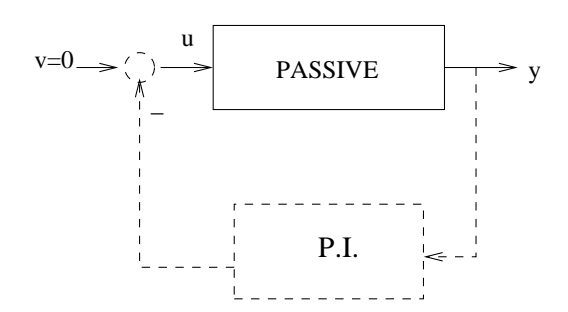
Passivity as a tool for analysis of limit cycles

STAN Guy-Bart
Systèmes et Automatique,
Université de Liège
Institut Montefiore B28,
Sart Tilman, B-4000 LIEGE 1, BELGIUM
Email:gb.stan@ulg.ac.be

SEPULCHRE Rodolphe
Systèmes et Automatique,
Université de Liège
Institut Montefiore B28,
Sart Tilman, B-4000 LIEGE 1, BELGIUM
Email:r.sepulchre@ulg.ac.be

Abstract

This paper studies the feedback interconnection of a passive system with the nonlinear proportional-integral block $u(t) = -k_i \int y(t) dt - k_p((\int y(t) dt)^2 - 1)y(t)$.



In the particular case where the passive system is an integrator, the feedback interconnection reduces to the Van der Pol equation.

For any $k_i > 0$, this equation is well known to possess a limit cycle in the phase plane for $k_p > 0$. This limit cycle is globally asymptotically stable (all solutions converge to the limit cycle except for the unstable zero equilibrium).

In this paper we prove that for any $k_i > 0$, there exists a stable limit cycle for a broad range of values for the parameter k_p in the general case of a linear passive system which is controllable, observable, of relative degree one and whithout any purely imaginary zero.

The paper discusses some implications of this result for robotic applications.

An Autonomous Robot for Harvesting of Cucumbers in Greenhouses

E.J. Van Henten, J. Hemming, B.A.J. Van Tuijl, J.G. Kornet, J. Bontsema

Institute of Agricultural and Environmental Engineering (IMAG B.V.),
Department of Advanced Systems, Plant and Energy,
P.O. Box 43, NL-6700 AA Wageningen, The Netherlands,
Email of corresponding author: E.J.vanHenten@imag.wag-ur.nl

Abstract

In the Netherlands, soft fruit vegetables such as tomatoes, cucumbers and sweet pepper are produced at large quantities in greenhouses. The total production area for these three vegetables is 3000 ha. The average size of the nursery has increased throughout the last decades to more than 1 ha and large production facilities of around 5 ha are quite common today.

Today, labour is the largest cost factor of a modern greenhouse holding. More than 30% of the total production costs are spent on wages for the grower and his employees. Obviously, to cope with saturating market demands and increasing competition, the grower is looking for ways to improve the over-all efficiency of the production process. Improving the efficiency of human labour or even reducing the amount of human labour seems to be a key issue.

Therefore, in 1996, IMAG began research on the development of an autonomous cucumber harvesting robot supported by the Dutch Ministry of Agriculture, Food and Fishery ([1]). The task of designing robots for agricultural applications raises issues not encountered in other industries. The robot has to operate in a highly unstructured environment in which no two scenes are the same. Both crop and fruit are prone to mechanical damage and should be handled with care. The robot has to operate under adverse climatic conditions, such as high relative humidity and temperature as well as changing light conditions. Finally, to be cost effective, the robot needs to meet high performance characteristics in terms of speed and success rate of the picking operation. In this project these challenging issues have been tackled by an interdisciplinary approach in which mechanical engineering, sensor technology (computer vision), systems and control engineering, electronics, software engineering, logistics, and, last but not least, horticultural engineering partake.

This paper describes the concept of an autonomous robot for harvesting vegetable fruit in greenhouses. To facilitate automatic harvesting a new cultivation system was adopted, the so-called high wire cultivation system. A description is given of the working environment of the robot and the logistics of harvesting. It is concluded that for a 2 ha Dutch nursery, 4 harvest robots and one docking station are needed during the peak season. Based on these preliminaries, the design specifications of the harvest robot are defined. The main requirement is that a single harvest operation may take at most 10 s. Then, the paper focuses on the individual hardware and software components of the robot. They include the autonomous vehicle, the manipulator, the end-effector, the two computer vision systems for detection and 3D imaging of the fruit and the environment, high-level control of the manipulator including collision-free path planning and low-level control of the whole robot. A task analysis revealed the sufficiency of a 7DOF manipulator. The endeffector handles soft fruit without loss of quality. The thermal cutting device used prevents transport of viruses through the greenhouse. The computer vision system is able to detect up to 95% of the cucumbers in a greenhouse. Using geometric models the volume (ripeness) of the cucumbers can be estimated with an accuracy of 97%. A motion planner based on the A*search algorithm assures collision-free eye-hand coordination. For more details refer to [2].

In 2001 system integration took place and the robot was tested in an experimental greenhouse. With a success rate of 80%, field tests in the experimental greenhouse at IMAG b.v confirmed the ability of the robot to pick cucumbers without human interference.

References

[1] Gieling, Th.H., Van Henten, E.J., Van Os, E.A., Sakaue, O. and Hendrix, A.T.M., 1996. Conditions, demands and technology for automatic harvesting of fruit vegetables. *Acta Horticulturae* 440: 360-365.

[2] Van Henten, E.J., Van Kollenburg-Crisan, L.M., Hemming, J., Van Tuijl, B.A.J., Kornet, J., Meuleman, J., Bontsema, J. and Van Os, E.A., 2002. An autonomous robot for harvesting of cucumber fruit. *Autonomous Robots*, accepted for publication.

LPV System Identification for Electromechanical Systems

Eduard van der Meché Department of Mechanical Engineering Delft University of Technology Mekelweg 2, 2628 CD, Delft The Netherlands

Email: E.G.vanderMeche@wbmt.tudelft.nl

Okko Bosgra
Department of Mechanical Engineering
Delft University of Technology
Mekelweg 2, 2628 CD, Delft
The Netherlands
Email: O.H.Bosgra@wbmt.tudelft.nl

1 Introduction

At Philips CFT controllers for electromechanical positioning systems, such as wafer stages and component mounters, traditionally have been designed manually in a loop-shaping fashion, even for multivariable systems. However, in order to meet the increasingly stringent specifications for controller performance, a lot of research has been conducted towards model based design of multivariable controllers. Robust controller design was investigated initially to cope with position dependent dynamics, but very recently modern LMI based synthesis mehtods [1] are used to design multivariable LPV controllers. At present however, the theory of system identification of LPV models is still underdeveloped.

2 Project goal

The main objective of this research project is to develop theory for LPV identification that is applicable in the first place to electromechanical positioning systems. First, the research is focussed on frequency domain identification, which is common practice for electromechanical systems. Frequency domain identification can be viewed as the problem of interpolating complex valued numbers in a set of frequency points, using a real rational function of given order. The observation that the closely related problem of real valued interpolation with real rational functions can be translated to a linear program (LP) motivates a convex programming approach. Analysis of the \mathcal{L}_{∞} optimal frequency domain identification problem has shown that the solution set is nonconvex. However, we propose a relaxation that renders the solution set convex, at the expense of conservatism. Using this relaxation the frequency domain identification problem can be translated to a so-called conic quadratic program [2] that can be solved efficiently using interior point (IP) solvers. The method can be directly extended to multivariable, frequency weighted identification for some classes of LPV models.

- [1] C. Scherer, *LPV control and full block multipliers*, Automatica, Vol.37, pp.361-375, 2001
- [2] A. Ben-Tal, A. Nemirovski, *Convex Optimization in Engineering: Modeling, Analysis, Algorithms*, Technion-Israel Institute of Technology

Non-linear Control of Active Magnetic Bearings for Ultra High Precision Applications

L. Jabben
Mechanical Engineering
Delft University of Technology
Email: L.Jabben@wbmt.tudelft.nl

D. Hobbelen Mechanical Engineering Delft University of Technology

J. van Eijk Mechanical Engineering Delft University of Technology

Introduction

At the group Advanced Mechatronics we are investigating the possibilities of using Active Magnetic Bearings (AMBs) in a so-called CD-mastering device. These machines make the master CD (DVD), used in the (mass) production of the CDs. The most restricting factor for further increasing the data density of CD and DVD mastering systems is the so-called Non-Repetitive Run Out (NRRO) of the rotor.

For the next generation of optical storage devices, the pitch of the tracks will further decrease. With a pitch of 300 nm the NRRO needs to be around 1 nm. The currently used air bearings have a NRRO of about 10 nm (at 6000 rpm), which seems to be the limit of the current technology.

Also, the decrease in pitch distance, might well require vacuum production of the master CD. These two reasons make AMBs an attractive candidate.

Reduce Bias Flux

The force a single standard E-core actuator generates, is described by the following equation:

$$F = 3Dk_{amb}\frac{i^2}{x_o^2},\tag{1}$$

where k_{amb} represents some properties of the AMB, i is the current through the coil, and x_g the air gap. Common practise in operating the AMBs is to linearise around a working point, using two opposite AMBs which preload the rotor with a bias current (i_0). This gives:

$$F = 3Dk_{x}x + k_{i}i,$$
 (2) where $k_{x} = 3D4k_{amb}\frac{i_{0}^{2}}{x_{g}^{3}}$, and $k_{i} = 3D4k_{amb}\frac{i_{0}}{x_{g}^{2}}$.

In machines with extreme positioning demands, the accuracy is limited because of the vibrations in the frame. Separation of the measurement and force frames is then used to further increase the positioning accuracy.

In these kind of machines the use of actuators like (2) has two disadvantages. First, the position dependent term introduces disturbances to the rotor, since in practise the machine frame is not without vibrations. Secondly, the preloading introduces a bias flux through the rotor. When rotating this introduces Eddy-currents. This will heat up the rotor (deformation) and will introduce (velocity) coupling between the frame and the rotor.

Non-Linear Compensation

If we want to reduce the position coupling, we have two options; increase the airgap and/or decrease the bias current. It follows from (1) that the air gap cannot be increased too much, which leaves reducing the bias current.

Ideally we would have no bias current. This forces us to deal with the zero gain around i = 3D0. From (1) it is suspected that a square root should be used in the drive. Indeed, the square root function shows an infinite gain at i = 3D0, compensating the zero gain of the actuator.

If the current to the AMB would be set to:

$$i = 3Dx_g\sqrt{\alpha},\tag{3}$$

with α the output of the controller, then the actuator would reduce to $F = 3Dk\alpha$.

The method described above has two disadvantages. Thirst, the infinite gain of the square root function at i=3D0 is implemented on a discrete system, which does not have infinite gain. Secondly, since an AMB always has attracting forces (1), two opposite AMB are used. This implies a switching behaviour, which could limit the position accuracy.

A practical preliminary investigation was performed using a 1 DoF AMB. The performance of 3 different methods are compared in terms of achievable bandwidth and accuracy.

Linear Parameter Varying Control of a Wafer Stage

Matthijs Groot Wassink, Marc van de Wal, Carsten Scherer Philips Centre for Industrial Technology (CFT), Mechatronics Research PO Box 218 / SAQ-2, 5600 MD Eindhoven, The Netherlands matthijs.groot.wassink@philips.com

1 Background

For the production of Integrated Circuits (ICs), wafer scanners are used. Positioning of the wafer with respect to the imaging optics is accomplished with a so called wafer stage. Keeping the servo errors within nanometer accuracy is crucial for obtaining satisfactory overall performance of a wafer scanner.

As often in servo systems, varying (anti)-resonances are present. In the case of the wafer stage, plant dynamics alter with different operating points. Therefore, this effect is referred to as "position dependent dynamics". Making the controller robust against position dependent effects can be used to tackle this problem, yet at the expense of performance. However, for the next generation wafer scanners, performance specifications become even tighter and this robust control strategy might fail to accomplish the desired performance level.

Therefore, more advanced controller techniques are investigated, among others Linear Parameter-Varying (LPV) control. Based on a system description which accurately captures the position dependent dynamics of a system, LPV control offers a framework to compute a controller which adjusts its dynamics to the operating position, thereby avoiding the conservatism which is present with robust control. Guarantees for stability and performance for each position can be given as well. However, conservatism due to technical assumptions necessary for the LPV controller synthesis and numerical problems therein could prevent achieving the expected performance improvement compared to robust control. Another major issue is LPV modeling which is still at its infancy. Generating an LPV model is therefore not a straightforward task.

2 Approach

To implement LPV control for an experimental wafer scanner, the following steps are taken. First of all, an accurate LPV model has to be obtained. To use this model for LPV controller synthesis, it is transformed into the so called LFT structure: a structure similar to that used for μ -synthesis. Second, an LPV controller is designed. To investigate the effect of numerical problems and conservatism, various algorithms are used and results are compared. Finally, the LPV controller is implemented for the wafer stage and its performance is compared to a standard PID-like LTI con-

troller.

3 LPV modeling

For LPV modeling, a rather custom-made approach is chosen. For a finite number of positions, frequency response functions are measured and transfer functions are fitted and transformed into a canonical form. By the specific arrangements of the varying elements in that form, an LFT model can be constructed. For intermediate positions, an interpolation technique is used and consequently this pragmatic approach does not lead to a model with guaranteed validity for all positions. Besides, if more positions were used the resulting LPV model would become more complex, which is a serious threat for the synthesis algorithms. To deal with these two effects, as an extra ingredient physical knowledge of the setup is used. First of all, the "smoothness" assumption for interpolation is justified. Second, taking into account that mode shapes cause the position dependent effects might reduce the number of parameters needed to describe the phenomenon resulting in an LPV model with fewer parameters.

4 Synthesis

Numerical problems and conservatism play an important role in LPV synthesis algorithms. Numerical problems are handled mainly by trial and error. Unfortunately, a generic systematic approach is currently unavailable. There is a trade-off between conservatism and complexity of the LPV controller synthesis inequalities. For example, the rate of parameter variations can assumed to be unbounded to limit the complexity of LPV controller synthesis, although it might cause conservatism for most practical applications. Research on reducing conservatism and complexity might involve extensions and alterations of the currently used design inequalities.

5 Presentation

The stepwise approach to implement LPV control for the wafer stage will be discussed and illustrated with experimental results. Shortcomings in LPV modeling and problems in the LPV synthesis step will be given special attention.

Potential benefits of ramp metering on motorways

Tom Bellemans, Sven Maerivoet and Bart De Moor ESAT/SISTA, K.U.Leuven Kasteelpark Arenberg 10 B-3001 Heverlee (Belgium)

{Tom.Bellemans, Sven.Maerivoet, Bart.DeMoor}@esat.kuleuven.ac.be http://www.esat.kuleuven.ac.be/sista-cosic-docarch

Bart De Schutter
Control Systems Eng., Fac. ITS, TU Delft
P.O. Box 5031
2600 GA Delft (The Netherlands)
b.deschutter@its.tudelft.nl

Keywords

Ramp metering, Traffic control, Traffic flow models, Fundamental diagram

Abstract

Ramp metering is an advanced traffic management system that can be implemented quickly and easily on motorways in Belgium as well as in the Netherlands. It consists of a traffic light that is placed at the on-ramp of a motorway. Vehicles are allowed to enter the motorway in a controlled way, avoiding 'bursts' of cars that would disrupt the traffic flow on the motorway too much.

In this talk we start with the discussion of the potential benefits of ramp metering on a qualitative level. What is ramp metering and how is it implemented? Why does ramp metering work and what can be expected of it? We answer these questions using the notion of the fundamental diagram, a well known concept in traffic theory.

After the qualitative approach, we quantify the performance of the motorway system under study by defining a cost function corresponding to the traffic state. The motorway system is simulated using a second order traffic flow model that is discretised in time and space [1], [2] and [4]. The cost function that we study in this talk is the total time spent by all the vehicles in the network and can be calculated based on the simulated traffic density on the motorway. The cost function can then be minimized by optimizing the metering rate at the on-ramp or, stated otherwise, by temporarily limiting the number of vehicles allowed to enter the motorway through the on-ramp [3]. This boils down to a non-linear optimization problem with constraints. In order to illustrate the potential benefits of ramp metering, we simulate a motorway stretch with an on-ramp without control and compare this to a simulation with a ramp metering set-up in a model predictive control

framework.

References

- [1] T. Bellemans, B. De Schutter and B. De Moor, "Models for traffic control," Accepted for publication in *Journal A*.
- [2] M. Papageorgiou, "Some remarks on macroscopic traffic flow modelling," *Transportation Research Part A*, vol. 32, no. 5, pp. 323–329, Sept. 1998.
- [3] M. Papageorgiou, J.M. Blosseville, and H. Haj-Salem, "Modelling and real-time control of traffic flow on the southerm part of Boulevard Périphérique in Paris Part I: Modelling," *Transportation Research Part A*, vol. 24, pp. 345–359, 1990.
- [4] H.J. Payne, "Models of freeway traffic and control," in *Mathematical Models of Public Systems* (G.A. Bekey, ed.), vol. 1, no. 1 of *Simulation Council Proceedings Series*, pp. 51–61, La Jolia California, 1971.

Acknowledgments

Dr. Bart De Moor is a full professor at the Katholieke Universiteit Leuven, Belgium. Our research is supported by grants from several funding agencies and sources: Research Council KUL: Concerted Research Action GOA-Mefisto 666 (Mathematical Engineering), IDO (Oncology, Genetic networks), several PhD/postdoc & Fellow grants; Flemish Government: Fund for Scientific Research Flanders (several PhD/postdoc grants, projects G.0256.97(subspace), G.0115.01 (bio-i and microarrays), G.0240.99 (multilinear algebra), G.0197.02 (power islands), G.0407.02 (support vector machines), research communities ICCoS, ANMMM), AWI (Bil. Int. Collaboration Hungary Poland), IWT (Soft4s (softsensors), STWW-Genprom (gene promotor prediction), GBOU-McKnow (Knowledge management algorithms), Eureka-Impact (MPC-control), Eureka-Impact (Fultret modeling)); Belgian Federal Government: DWTC (I/2P IV-02 (1996-2001) and IUAP V-10-29 (2002-2006): Dynamical Systems and Control: Computation, Identification & Modelling), Program Sustainable Development PODO-II (Traffic Management Systems); Direct contract research: Verhaert, Electrabel, Elia, Data-4s, IPCOS.

Model Predictive Control for Optimal Coordination of Ramp Metering and Variable Speed Control

Andreas Hegyi

Control Systems Engineering, Faculty of Information Technology and Systems

Delft University of Technology

P.O. Box 5031, 2600 GA Delft, The Netherlands Phone: +31-15-278 20 87, Fax: +31-15-278 66 79 email: A.Hegyi@ITS.TUDelft.nl

Bart De Schutter

Control Systems Engineering, Faculty of Information Technology and Systems
Delft University of Technology

P.O. Box 5031, 2600 GA Delft, The Netherlands Phone: +31-15-278 51 13, Fax: +31-15-278 66 79 email: B.DeSchutter@ITS.TUDelft.nl

Hans Hellendoorn

Control Systems Engineering, Faculty of Information Technology and Systems
Delft University of Technology

P.O. Box 5031, 2600 GA Delft, The Netherlands Phone: +31-15-278 90 07, Fax: +31-15-278 66 79 email: J.Hellendoorn@ITS.TUDelft.nl

1 Abstract

The steadily increasing number and length of traffic jams on motorways has led to the use of several dynamic traffic management measures all over the world such as ramp metering, incident warning, and route information. Usually these measures operate based on local data (occupancy or intensity measurements). However, recently more and more researchers and practitioners have started to recognize that considering the effect of the measures on the network level has many advantages compared to local control. We apply model predictive control to optimally coordinate variable speed limits and ramp metering. It is clear that ramp metering is only useful when traffic is not too light (otherwise ramp metering is not needed) and not too dense (otherwise breakdown will happen anyway). The basic idea is that speed limits can increase the range in which ramp metering is useful. For the prediction we use a slightly adapted version of the METANET [1] traffic flow model that takes the variable speed limits into account. The optimal control signals aim at minimizing the total time that vehicles spend in the network. The coordinated control results in a network with less congestion, a higher outflow, and a lower total time spent. In addition, the receding horizon approach of model predictive control results in an adaptive, on-line control strategy that can take changes in the system automatically into account. We illustrate our approach using a simple network for which we compare the cases 'ramp me-



Figure 1: Ramp metering at the A13 near Delft.

tering only' and 'coordinated ramp metering and speed limits' for a typical demand scenario.

References

[1] A. Kotsialos, M. Papageorgiou, A. Messmer, *Integrated optimal control of motorway traffic Networks*, Proceedings of the 18th American Control Conference, pp. 2183-2187, 1999.

MPC as a tool for optimal process operation of MSW combustion plants

M. Leskens
Department of Energy Systems
TNO Environment, Energy and Process Innovation
Laan van Westenenk 501, P.O. Box 342, 7300 AH Apeldoorn
The Netherlands
M.Leskens@mep.tno.nl

Mechanical Engineering Systems and Control Group /
(Applied Physics) Signals, Systems and Control Group
Delft University of Technology
Delft, The Netherlands

1 Introduction

Throughout the world, combustion of municipal solid waste (MSW), better known as household waste, is used for the reduction of its volume, otherwise being disposed of by means of landfilling, and for the production of energy. An MSW combustion plant, see figure 1, is subject to both economic operational objectives and environmental requirements being enforced by law. In the fulfillment of these objectives, the control system plays an essential role.

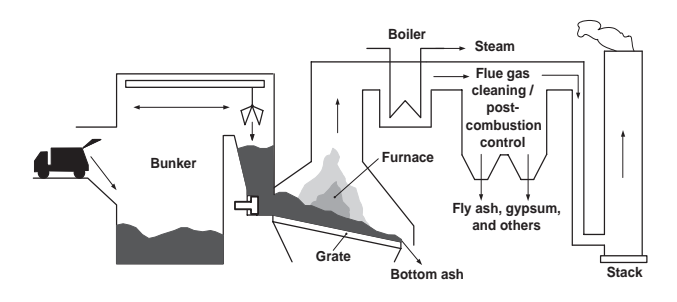


Figure 1: Schematic view of an MSW combustion plant.

Among many MSW combustion plant managers there is a need to optimize the process operation performance. This is due to the ever becoming more stringent environmental regulations and ever growing higher energy efficiency demands. As a result, research is being carried out in order to improve this operation performance. One important research direction aims at improving this performance by investigating the feasibility of advanced control strategies of which fuzzy control and Model Predictive Control (MPC) are at present the main representatives. The motivation for this research is that the conventional (PI(D)) combustion control systems are not able to fulfill properly the present and future energy efficiency and environmental needs of an MSW

combustion plant.

2 Outline of the talk

A feasibility study is presented on the application of MPC as a tool for obtaining an improved operation performance for MSW combustion plants. First, the main operational and control objectives for these plants are identified. Subsequently, a specific MSW control problem is selected. On the basis of this control problem a comparison is made between the control performance of a conventional (PI(D)) control system, as determined by measurements, and that obtained with a linear model predictive controller, as determined through simulations. The latter were performed using an estimated process and disturbance model. These were obtained from a large scale MSW combustion plant in The Netherlands via a specific system identification procedure which is discussed in [1].

The presented results are also discussed in [2]

- [1] Leskens, M., Van Kessel, L.B.M. & Van den Hof, P.M.J. (2002). MIMO closed-loop identification of an MSW incinerator, *Control Engineering Practice*, Vol. 10, No. 3, pp. 315-326.
- [2] Leskens, M., Van Kessel, L.B.M. & Bosgra, O.H. (2002). Model predictive control as a tool for optimal process operation of MSW combustion plants, submitted to *Control Engineering Practice*.

Model predictive control algorithm with multiple linear models

A. Tiagounov, S. Weiland, A.C.P.M. Backx Department of Electrical Engineering, Technische Universiteit Eindhoven P.O. Box 513, 5600 MB Eindhoven, The Netherlands email: a.tiagounov@tue.nl

J. Buijs
Department of Electrical Engineering
Katholieke Universiteit Leuven
Kardinaal Mercierlaan 94
B-3001 Heverlee (Leuven), Belgium

email: jeroen.buijs@esat.kuleuven.ac.be

1 Introduction

Model Predictive Control (MPC), also known as moving or receding horizon control, has originated in industry as a real-time computer control algorithm to solve linear multivariable problems that have constraints and time delays. The various MPC algorithms differ mainly in the type of model used to represent the process and its disturbances, as well as the cost functions to be minimized, with or without constraints. The on-line optimization can be typically reduced to either a linear program or a quadratic program. The MPC controller solves on-line a constrained optimization problem and determines an optimal control input over a fixed future time-horizon, based on the predicted future behaviour of the process, and based on the desired reference trajectory.

2 MPC algorithm

In this presentation we consider a nonlinear MPC scheme where the predicted future process behaviour is represented as a cumulative effect of a nonlinear prediction component and a component based on linear time-varying models defined along the predicted trajectory ([4]). The first component constitutes a future output prediction using nonlinear simulation models, given past process inputs and measured disturbance history. The second component uses linearized models for prediction of future process outputs as required for calculation of optimum future process input manipulations that bring the process behavior closest to the desired behavior (see, for example [1, 2]).

The constrained optimization problem leads to the quadratic programming problem, which can be split into a steady state and a dynamic optimization. The MPC module solves a constrained optimization problem on-line and determines optimal control inputs over a fixed future time-horizon, based on the predicted future behavior of the process using a time variant linear model (a set of linear time invariant models over the prediction horizon). Although more than one control move is generally calculated, only the first one is imple-

mented. At the next sampling time, the optimization problem is reformulated and solved with new measurements obtained from the system. Given the initial status of the process, estimates of disturbances and the reference trajectories, the optimizer in the MPC module produces the manipulated variable such that input and output trajectories follow the reference trajectories as close as possible subject to the constraints imposed in the optimization.

To reduce computational complexity quadratic programming problem is solved using a structured interior-point method (see [3]). The described above MPC problem was properly reformulated to apply this optimization algorithm. The cost of this approach is linear in the horizon length, compared with the cubic growth for the standard approach. A discrete Riccati recursion is used to solve the linear equations efficiently at each iteration of the interior-point method. We can expect this recursion to be numerically stable although it was motivated originally by structural rather than numerical considerations. The effectiveness of this approach will be demonstrated in the presentation by applying this MPC algorithm to a distillation process.

- [1] J.H. Lee, N.L. Ricker, "Extended Kalman filter based nonlinear model predictive control", Ind. Eng. Chem. Res. 33:1530–1541, 1994.
- [2] N.L. Ricker, J.H. Lee, "Nonlinear model predictive control of the Tennessee Eastman challenge process", Computers and Chemical Engineering 19(9):961–981, 1995.
- [3] C.V. Rao, S.J. Wright, and J.B. Rawlings, "Application of interior-point methods to model predictive control", Journal of Optimization Theory and Applications 99:723–757, 1998.
- [4] R. de Keyser, "A gentle introduction to model based predictive control", Plenary paper, EC-PADI2 Int. Conference on Control Engineering and Signal Processing, Peru, 1998.

Optimal topology and geometry of controllable tensegrity systems

Bram de Jager

Department of Mechanical Engineering, Eindhoven University of Technology P.O. Box 513, 5600 MB Eindhoven, The Netherlands A.G.de.Jager@wfw.wtb.tue.nl

Milenko R. Masic & Bob Skelton
Department of Mechanical and Aerospace Engineering, University of California at San Diego
La Jolla, California, 92093-0411
mmasic@mae.ucsd.edu & bobskelton@ucsd.edu

Abstract

Tensegrity systems are composed of tensile members (tendons) and compressive members (bars) [1]. These structures have been studied for a long time, see, e.g., [2], whose terminology consisted of ties and struts instead of tendons and bars. In a class 1 tensegrity structure, as considered here, the bar endpoints, or nodal points, are only connected to tendons, not to other bars. The integrity (stability) of a tensegrity structure is due to pre-stress with tensile forces in the tendons, hence the name tensegrity.

Because bars are connected by tendons, and not directly, the stiffness of the structure may be diminished: tendons are elastic. Furthermore, pre-stress gives rise to heavier members, to avoid yield or buckling when forces are increased due to pre-stress. On the other hand, a proper choice of material for these systems is easier to achieve and stiffness can be improved by controlling the tendon or bar lengths. Changing member lengths also enables shape control. The net result of disadvantages and advantages may make tensegrity systems the systems of choice for a reasonable wide class of applications.

We discuss how a balanced choice of topology and geometry improves the stiffness and stiffness-to-mass properties of tensegrity systems. We also incorporate controllability requirements, by constraining the tendon length, that should exceed a certain minimum length, so there is room for the joint structures and for installation of a mechanism used to change the tendon length in the case closed loop tendon length control is applied.

Optimization of topology and geometry of structures has been studied for a long time. One of the results is the formulation of Optimality Criteria [3]. Furthermore, several approaches for numerical optimization are known [4], while recent approaches are, *e.g.*, free material modeling [5, 6], or optimization of trusses starting from a fully populated grid [7]. In practice we encounter problems that require to

- incorporate constraints (nonlinear) for failure of the structure, like yield and buckling,
- tackle a wide class of geometries and boundary and loading conditions, which excludes approaches using linear models,
- stabilize the system by requiring pre-stress in the structure.

Although there are approaches that address some of these issues, none of these combines all of them.

Our goal is to reduce this gap in the knowledge base, and to

- incorporate requirements for static equilibria for prestressed mechanical structures, both loaded and unloaded,
- show the influence of incorporating nonlinear failure constraints,
- investigate the handling of requirements of installing actuating devices to control the length of the tendons.

To illustrate our approach we apply it on a tensegrity system build up from several elementary stages and compare it to an approach from literature.

The computations are done with a nonlinear programming approach and most design aspects (static equilibrium, yield and buckling limits, force directionality, *etc.*, both for the unloaded and loaded cases) can be, and are, incorporated. By using an efficient and robust solver, by employing the structure of the Jacobian of the nonlinear constraints, and/or by providing analytical expressions for the Jacobian, this approach appears to be feasible.

From this work it becomes clear that certain topologies are clearly advantageous, especially the ones that are built up from a mix of class one (each nodal point is connected to one bar only) and class two (where in a nodal point up to two bars can connect) systems.

- [1] R. Adhikari, R. Skelton, and W. Helton, "Mechanics of tensegrity structures," Feb. 1998. Report 1998-01 UCSD Structural Systems and Control Lab.
- [2] J. C. Maxwell, *The Scientific Papers of James Clerk Maxwell*. New York: Dover, Forew. 1890.
- [3] M. Save, W. Prager (eds.), and G. Sacchi, Structural Optimization, Volume 1, Optimality Criteria, vol. 34 of Mathematical Concepts and Methods in Science and Engineering. New York: Plenum Press, 1985.
- [4] M. Save, W. Prager (eds.), A. Borkowski, S. Jendo, and M. I. Reitman, *Structural Optimization, Volume 2, Mathematical Programming*, vol. 40 of *Mathematical Concepts and Methods in Science and Engineering*. New York: Plenum Press, 1990.
- [5] M. P. Bendsøe, "Optimial shape design as a material distribution problem," *Struct. Optim.*, vol. 1, pp. 193–202, 1989.
- [6] O. Sigmund, "A 99 line topology optimization code written in Matlab," *Struct. Multidisc. Optim.*, vol. 21, pp. 120–127, Feb. 2001.
- [7] F. Jarre, M. Kočvara, and J. Zowe, "Optimal truss design by interior-point methods," *SIAM J. Optimization*, vol. 8, pp. 1084–1107, Nov. 1998.

A MILP approach to the optimization of emulsification

M. Stork
Mechanical Engineering Systems and Control Group
Delft University of Technology
Mekelweg 2
2628 CD Delft
m.stork@wbmt.tudelft.nl

R. L. Tousain
Philips CFT
Mechatronics Research
SAQ-2115
5600 MD Eindhoven
rob.tousain@philips.com

1 Abstract

Emulsification is an essential manufacturing technology in the food industry. Examples of emulsions are mayonnaise and all kind of dressings. For profit maximization it is desirable to decrease the production time of emulsions while maintaining the product quality specifications. In this project we focus on the model-based optimization of emulsification. The quality of emulsions is strongly influenced by the drop size distribution (DSD). For the aim of this study models that predict the course of the DSD in time are used.

This work addresses the model-based computation of stirrer profiles for reaching a certain predefined DSD in minimal time. The model involved describes the evolution of the DSD as a function of time in a vessel that is operated in a fed-batch way. The model consists of compartment models and for each compartment a population balance equation is formulated to model the DSD. For simulation purposes the model was discretized using the method of [1]. Each state corresponds to the number of drops with a certain drop size in a certain compartment.

The breakage phenomena (the breakage condition, the breakage frequency, the number and the sizes of the formed drops) depend heavily on the stirrer speed and exhibit discrete events. A very small increase of the stirrer speed may already lead to the breakage of certain drop sizes that did not break with the slightly lower stirrer speed. Comparable behavior is observed for the formation of certain drop sizes; until some stirrer speed they are not formed whereas they are formed very rapidly at a stirrer speed that is only slightly higher. A further increase of the stirrer speed may suddenly lead to the non-formation or even breakage of these drop sizes. These phenomena make the model strongly non-linear and in fact almost discontinuous. Gradient based optimization techniques like SQP will fail because of this behavior. Also non-gradient based methods like genetic algorithms do not guarantee satisfactory behavior. It is unsure if the global optimum will be reached and even if a feasible solution will be found.

In this work we suggest an approach that approximates the original non-linear optimization problem as a Mixed Integer Linear Program (MILP). This method does enable to solve the optimization problem and if the global optimum of the

MILP is found, then this is also a good solution to the original minimal time optimization problem. The method is derived as follows. First, by model analysis it can be shown that the strong nonlinearity is only in the dependence on the stirrer speed. Further, in small intervals of the stirrer speed the dynamics are approximately linear. These intervals form the *modes* of the system. At any given time, the system finds itself in exactly one mode; its mathematical behavior is then described by a given set of evolution ODE equations. A transition from one mode to another is triggered when the stirrer speed passes a certain critical value. Hence, the stirrer speed determines completely in which mode the system is and when the transitions occur. This suggests that the model can be reformulated as a state-transition network [2] where linear dynamics describe the behavior in a certain interval of the stirrer speed and where transitions between different modes are modeled using integer decision variables. The objective, being to reach a certain end point condition in minimum time, can be enforced through the introduction of another set of integer decision variables. This way, the minimum time optimization problem can be reformulated as a MILP, which can be solved using well-proven, standard optimization codes. The feasibility of the approach is illustrated by means of an example, the computation of stirrer profiles for reaching a certain predefined DSD in a minimal amount of time.

- [1] S. Kumar and D. Ramkrishna. On the solution of population balance equations by discretization-I. A fixed pivot technique. Chem. Eng. Sci., 51: 1311-1332, 1996.
- [2] Avraam, M. P., Shah, N. and Pantelides, C. C. Modelling and optimisation of general hybrid systems in the continuous time domain. Comp. Chem. Eng., 22: S221-S228, 1998.

SOFT-CONSTRAINED FEEDBACK NASH EQUILIBRIA

J.C. Engwerda, W.A. van den Broek, and J.M. Schumacher

Tilburg University, Department of Econometrics P.O. Box 90153, 5000 LE Tilburg, The Netherlands email: engwerda@kub.nl

Keywords:

Robustness, Indefinite linear quadratic games, feedback Nash equilibrium, solvability conditions, Riccati equations

Abstract

In this paper we consider feedback Nash equilibria in a disturbed differential game. Like in H_{∞} theory, we assume that the uncertainty is modeled as an additive deterministic disturbance term entering the system. That is, we consider the system

$$\dot{x} = Ax + B_1u_1 + B_2u_2 + Ew, x(0) = x_0$$

where $w \in L_2^q(0, \infty)$ represents the unknown disturbance, x denotes the state of the system and u_i is the control of player i. We assume that the information structure of the players is a feedback pattern and that the control functions are of the form $u_i = F_i x$, where (F_1, F_2) are such that they stabilize the system.

We assume that the performance criterion J_i the individual players like to minimize is given by an indefinite linear quadratic function, i.e.

$$J_i := \int_0^\infty \{x^T(t)Q_i x(t) + u_i^T R_i u_i(t) - w^T V_i w\} dt,$$

where Q_i are only assumed to be symmetric; R_i and V_i positive definite. V_i expresses the risky attitude of player i. Sufficient conditions for existence of feedback Nash equilibria for such a game are given. Furthermore, the one player case is elaborated to show the consequences of the stabilizing feedback assumption in this context.

References:

- 1. Başar T. and Olsder G.J., 1999, Dynamic Noncooperative Game Theory, SIAM, Philadelphia.
- 2. Engwerda J.C., 2000, Feedback Nash equilibria in the scalar infinite horizon LQ-game, Automatica 36, pp.135-139.
- 3. Engwerda J.C., 2000, The solution set of the N-player

scalar feedback Nash algebraic Riccati equation, I.E.E.E. Trans. Aut. Contr., no.12

- 4. Lukes D.L., 1971, Equilibrium feedback control in linear games with quadratic costs, SIAM Journal on Control and Optimization, vol.9, no.2, pp.234-252.
- 5. Mageirou E.F., 1976, Values and strategies for infinite time linear quadratic games, I.E.E.E. Transactions on Automatic Control AC-21, pp.547-550.
- 6. Weeren A.J.T.M, Schumacher J.M. and Engwerda J.C., 1999, Asymptotic analysis of linear feedback Nash equilibria in nonzero-sum linear-quadratic differential games, JOTA, 101: 693-723.
- 7. Willems J.C., 1971, least squares stationary optimal control and the algebraic Riccati equation, I.E.E.E. Transactions on Automatic Control, vol. AC-16, no.6, pp.621-634.

Closed-loop stochastic economic optimization under state and input constraints

D.H. van Hessem
Mech. Eng. Syst.& Contr.
Delft Univ. of Tech.
Mekelweg 2, 2628 CD, Delft
The Netherlands
d.h.vanhessem@wbmt.tudelft.nl

C.W. Scherer
Mech. Eng. Syst.& Contr.
Delft Univ. of Tech.
Mekelweg 2, 2628 CD, Delft
The Netherlands
c.w.scherer@wbmt.tudelft.nl

O.H. Bosgra
Mech. Eng. Syst.& Contr.
Delft Univ. of Tech.
Mekelweg 2, 2628 CD, Delft
The Netherlands
o.h.bosgra@wbmt.tudelft.nl

Introduction

Objective functions in economic steady-state optimization for chemical processes are often determined by linear terms, for instance corresponding to maximization of feed- or product flows. This leads to optimal steady-states close to the constraints on process variables, controlled variables (c.v.'s) and manipulated variables (m.v.'s). Due to process disturbances and plant-model mismatch, one is forced to keep some distance to the constraints. This problem of selecting a suitable back-off is a trade-off between avoiding frequent constraint violation and concessions on the profit rate of the process. The hard part in solving this problem consists of the interaction between the tuning of the model predictive controllers and the selection of the optimal steady-state. Better tuning leads to profitable reduction of the back-off from the constraints. In [5] this problem is addressed for a plantmodel mismatch case in which the back-off is selected for randomly distributed model parameters, biases and worstcase parameter variations. These results incorporate control in the back-off selection, but the operating condition is optimized for a fixed controller and fixed back-off. Only in [3, 2], the authors solve a nonlinear back-off problem in which they iterate between computation of optimal operating conditions and controller parameters and worst-case disturbances.

A new approach to the problem

In this work, we will formulate a different optimization problem in which the optimal operating condition, the controller parameters and the back-off are optimized simultaneously. The control configuration corresponding to our strategy is depicted schematically in figure 1 and is discussed in [1] for the LQG problem. The objective is to find an optimal linear controller and an optimal steady-state operating condition which maximize the profit rate of a chemical process while guaranteeing a bound on the probability that the state and/or input constraints are not violated. In [4] we show that we can globally solve this problem using a two step approach in which we borrow techniques from multi-objective control [6, 7]. Due to the computational burden of these techniques, we also propose an suboptimal but fast iterative

procedure relying on the linearization of certain constraints. The LTI-design is justified by viewing it as an important first step for closed-loop MPC design.

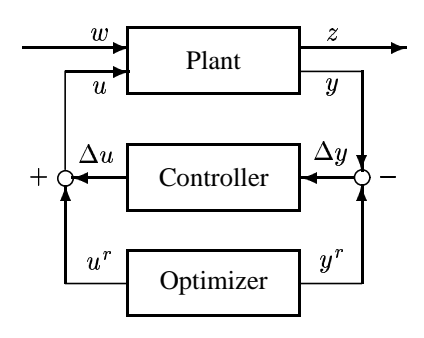


Figure 1: The control configuration

- [1] M. Athans. The role and use of the stochastic Linear-Quadratic-Gaussian problem in control system design. *IEEE Trans. Automatic Control*, 16(6):529–552, 1971.
- [2] P.A. Bahri, J.A. Bandoni, G.W. Barton, and J.A. Romagnoli. Back-off calculations in optimizing control: A dynamic approach. *Computers and Chemical Engineering*, 19(Suppl.):S699–S708, 1995.
- [3] J.L. Gigueroa, P.A. Bahri, J.A. Bandoni, and J.A. Romagnoli. Economic impact of disturbances and uncertain parameters in chemical processes- a dynamic back-off analysis. *Computers and Chemical Engineering*, 20(4):453–461, 1996.
- [4] D.H. van Hessem, C.W. scherer, and O.H. Bosgra. LMI-based closed-loop economic optimization of stochastic process operation under state and input constraints *Conf. Decision and Control*, 2001.
- [5] C. Loeblein and J.D. Perkins. Analysis and structural design of integrated on-line optimization and regulatory control systems. *Aiche Journal*, 45(5):1030–1040 1999.
- [6] C.W. Scherer. Multiobjective $\mathcal{H}_2/\mathcal{H}_{\infty}$ control. *IEEE Trans. Automatic Control*, 40:1054–1062, 1995.
- [7] C.W. Scherer. Lower bounds in multi-objective $\mathcal{H}_2/\mathcal{H}_{\infty}$ problems. *Conf. Decision and Control*, 1999.

Part 2 Plenary Lectures

An Introduction to Nonlinear Model Predictive Control

Rolf Findeisen, Frank Allgöwer, Institute for Systems Theory in Engineering, University of Stuttgart, 70550 Stuttgart, Germany, {findeise,allgower}@ist.uni-stuttgart.de

Abstract

While linear model predictive control is popular since the 70s of the past century, the 90s have witnessed a steadily increasing attention from control theoretists as well as control practitioners in the area of nonlinear model predictive control (NMPC). The practical interest is driven by the fact that today's processes need to be operated under tighter performance specifications. At the same time more and more constraints, stemming for example from environmental and safety considerations, need to be satisfied. Often these demands can only be met when process nonlinearities and constraints are explicitly considered in the controller. Nonlinear predictive control, the extension of well established linear predictive control to the nonlinear world, appears to be a well suited approach for this kind of problems. In this note the basic principle of NMPC is reviewed, the key advantages/disadvantages of NMPC are outlined and some of the theoretical, computational, and implementational aspects of NMPC are discussed. Furthermore, some of the currently open questions in the area of NMPC are outlined.

1 Principles, Mathematical Formulation and Properties of Nonlinear Model Predictive Control

Model predictive control (MPC), also referred to as moving horizon control or receding horizon control, has become an attractive feedback strategy, especially for linear processes. Linear MPC refers to a family of MPC schemes in which linear models are used to predict the system dynamics, even though the dynamics of the closed-loop system is nonlinear due to the presence of constraints. Linear MPC approaches have found successful applications, especially in the process industries. A good overview of industrial linear MPC techniques can be found in [64, 65], where more than 2200 applications in a very wide range from chemicals to aerospace industries are summarized. By now, linear MPC theory is quite mature. Important issues such as online computation, the interplay between modeling/identification and control and system theoretic issues like stability are well addressed [41, 52, 58].

Many systems are, however, in general inherently nonlinear. This, together with higher product quality specifications and increasing productivity demands, tighter environmental regulations and demanding economical considerations in the process industry require to operate systems closer to the boundary of the admissible operating region. In these cases, linear models are often inadequate to describe the process dynamics and nonlinear models have to be used. This motivates the use of nonlinear model predictive control.

This paper focuses on the application of model predictive control techniques to nonlinear systems. It provides a review of the main principles underlying NMPC and outlines the key advantages/disadvantages of NMPC and some of the theoretical, computational, and implementational aspects. Note, however, that it is not intended as a complete review of existing NMPC techniques. Instead we refer to the following list for some excellent reviews [4, 16, 22, 52, 58, 68]. In Section 1.1 and Section 1.2 the basic underlying concept of NMPC is introduced. In Section 2 some of the system theoretical aspects of NMPC are presented. After an outline of NMPC schemes that achieve stability one particular NMPC formulation, namely quasi-infinite horizon NMPC (QIH-NMPC) is outlined to exemplify the basic ideas to achieve stability. This approach allows a (computationally) efficient formulation of NMPC while guaranteeing stability and performance of the closed-loop.

Besides the basic question of the stability of the closed-loop, questions such as robust formulations of NMPC and some remarks on the performance of the closed-loop are given in Section 2.3 and Section 2.2. Section 2.4 gives some remarks on the output-feedback problem in connection with NMPC. After a short review of existing approaches one

specific scheme to achieve output-feedback NMPC using high-gain observers for state recovery is outlined. Section 3 contains some remarks and descriptions concerning the numerical solution of the open-loop optimal control problem. The applicability of NMPC to real processes is shown in Section 4 considering the control of a high purity distillation column. This shows, that using well suited optimization strategies together with the QIH-NMPC scheme allow real-time application of NMPC even with todays computing power. Final conclusions and remarks on future research directions are given in Section 5.

In the following, $\|\cdot\|$ denotes the Euclidean vector norm in \mathbb{R}^n (where the dimension n follows from context) or the associated induced matrix norm. Vectors are denoted by boldface symbols. Whenever a semicolon ";" occurs in a function argument, the following symbols should be viewed as additional parameters, i.e. $f(x;\gamma)$ means the value of the function f at x with the parameter γ .

1.1 The Principle of Nonlinear Model Predictive Control

In general, the model predictive control problem is formulated as solving on-line a finite horizon open-loop optimal control problem subject to system dynamics and constraints involving states and controls. Figure 1 shows the basic principle of model predictive control. Based on measurements obtained at time t, the controller predicts the future

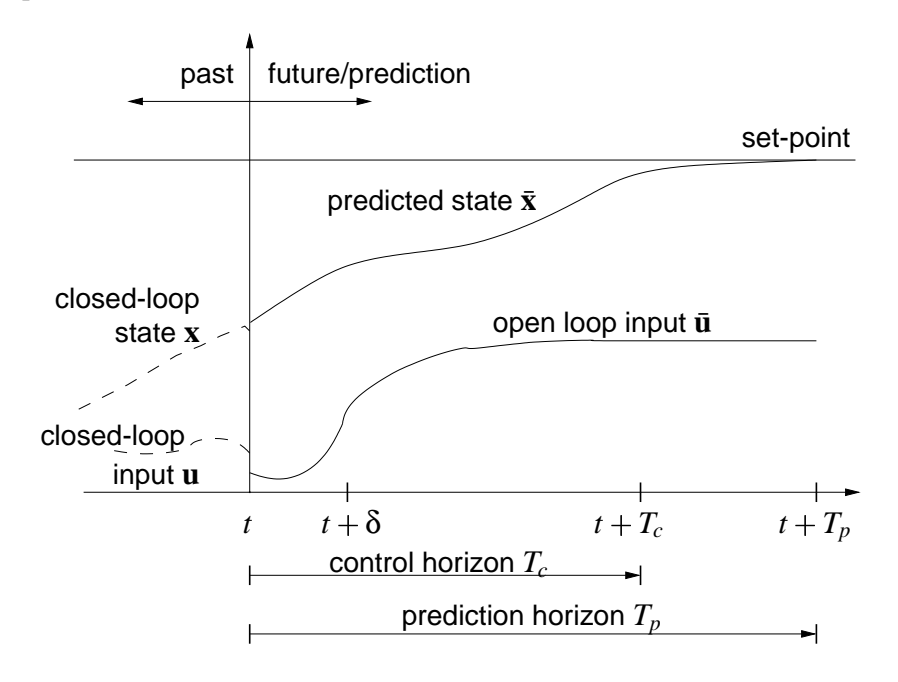


Figure 1: Principle of model predictive control.

dynamic behavior of the system over a prediction horizon T_p and determines (over a control horizon $T_c \leq T_p$) the input such that a predetermined open-loop performance objective functional is optimized. If there were no disturbances and no model-plant mismatch, and if the optimization problem could be solved for infinite horizons, then one could apply the input function found at time t=0 to the system for all times $t\geq 0$. However, this is not possible in general. Due to disturbances and model-plant mismatch, the true system behavior is different from the predicted behavior. In order to incorporate some feedback mechanism, the open-loop manipulated input function obtained will be implemented only until the next measurement becomes available. The time difference between the recalculation/measurements can vary, however often it is assumed to be fixed, i.e the measurement will take place every δ sampling time-units. Using the new measurement at time $t+\delta$, the whole procedure – prediction and optimization – is repeated to find a new input function with the control and prediction horizons moving forward.

Notice, that in Figure 1 the input is depicted as arbitrary function of time. As shown in Section 3, for numerical solutions of the open-loop optimal control problem it is often necessary to parameterize the input in an appropriate way. This is normally done by using a finite number of basis functions, e.g. the input could be approximated as piecewise constant over the sampling time δ .

As will be shown, the calculation of the applied input based on the predicted system behavior allows the inclusion of constraints on states and inputs as well as the optimization of a given cost function. However, since in general

the predicted system behavior will differ from the closed-loop one, precaution must be taken to achieve closed-loop stability.

1.2 Mathematical Formulation of NMPC

We consider the stabilization problem for a class of systems described by the following nonlinear set of differential equations¹

$$\dot{\mathbf{x}}(t) = \mathbf{f}(\mathbf{x}(t), \mathbf{u}(t)), \quad \mathbf{x}(0) = \mathbf{x}_0 \tag{1}$$

subject to input and state constraints of the form:

$$\mathbf{u}(t) \in \mathcal{U}, \ \forall t \ge 0 \quad \mathbf{x}(t) \in \mathcal{X}, \ \forall t \ge 0,$$
 (2)

where $\mathbf{x}(t) \in \mathcal{X} \subseteq \mathbb{R}^n$ and $\mathbf{u}(t) \in \mathcal{U} \subseteq \mathbb{R}^m$ denotes the vector of states and inputs, respectively. The set of feasible input values is denoted by \mathcal{U} and the set of feasible states is denoted by \mathcal{X} . We assume that \mathcal{U} and \mathcal{X} satisfy the following assumptions:

Assumption 1 $\mathcal{U} \subset \mathbb{R}^p$ is compact, $\mathcal{X} \subseteq \mathbb{R}^n$ is connected and $(0,0) \in \mathcal{X} \times \mathcal{U}$.

In its simplest form, \mathcal{U} and \mathcal{X} are given by box constraints of the form:

$$\mathcal{U} := \{ \mathbf{u} \in \mathbb{R}^m | \mathbf{u}_{min} \le \mathbf{u} \le \mathbf{u}_{max} \}, \tag{3a}$$

$$\mathcal{X} := \{ \mathbf{x} \in \mathbb{R}^n | \mathbf{x}_{min} < \mathbf{x} < \mathbf{x}_{max} \}. \tag{3b}$$

Here \mathbf{u}_{min} , \mathbf{u}_{max} and \mathbf{x}_{min} , \mathbf{x}_{max} are given constant vectors.

With respect to the system we additionally assume, that:

Assumption 2 The vector field $\mathbf{f}: \mathbb{R}^n \times \mathbb{R}^m \to \mathbb{R}^n$ is continuous and satisfies $\mathbf{f}(\mathbf{0}, \mathbf{0}) = \mathbf{0}$. In addition, it is locally Lipschitz continuous in \mathbf{x} .

Assumption 3 The system (1) has an unique continuous solution for any initial condition in the region of interest and any piecewise continuous and right continuous input function $\mathbf{u}(\cdot):[0,T_p]\to\mathcal{U}$.

In order to distinguish clearly between the real system and the system model used to predict the future "within" the controller, we denote the internal variables in the controller by a bar (for example \bar{x}, \bar{u}).

Usually, the finite horizon open-loop optimal control problem described above is mathematically formulated as follows:

Problem 1 Find

$$\min_{ar{\mathbf{u}}(\cdot)} J(\mathbf{x}(t), ar{\mathbf{u}}(\cdot); T_c, T_p)$$

with

$$J(\mathbf{x}(t), \bar{\mathbf{u}}(\cdot); T_p, T_c) := \int_t^{t+T_p} F(\bar{\mathbf{x}}(\tau), \bar{\mathbf{u}}(\tau)) d\tau$$
(4)

subject to:

$$\dot{\bar{\mathbf{x}}}(\tau) = \mathbf{f}(\bar{\mathbf{x}}(\tau), \bar{\mathbf{u}}(\tau)), \quad \bar{\mathbf{x}}(t) = \mathbf{x}(t)$$
 (5a)

$$\bar{\mathbf{u}}(\tau) \in \mathcal{U}, \quad \forall \tau \in [t, t + T_c]$$
 (5b)

$$\bar{\mathbf{u}}(\tau) = \bar{\mathbf{u}}(\tau + T_c), \quad \forall \tau \in [t + T_c, t + T_p]$$
 (5c)

$$\bar{\mathbf{x}}(\tau) \in \mathcal{X}, \quad \forall \tau \in [t, t + T_p]$$
 (5d)

where T_p and T_c are the prediction and the control horizon with $T_c \leq T_p$.

The bar denotes internal controller variables and $\bar{\mathbf{x}}(\cdot)$ is the solution of (5a) driven by the input $\bar{\mathbf{u}}(\cdot):[t,t+T_p]\to\mathcal{U}$ with initial condition $\mathbf{x}(t)$. The distinction between the real system and the variables in the controller is necessary, since the predicted values, even in the nominal undisturbed case, need not, and in generally will not, be the same as the actual closed-loop values, since the optimal input is recalculated (over a moving finite horizon T_c) at every sampling

¹In this paper only the continuous time formulation of NMPC is considered. However, notice that most of the presented topics have dual counterparts in the discrete time setting.

instance.

The function F, in the following called stage cost, specifies the desired control performance that can arise, for example, from economical and ecological considerations. The standard quadratic form is the simplest and most often used one:

$$F(\mathbf{x}, \mathbf{u}) = (\mathbf{x} - \mathbf{x}_s)^T Q(\mathbf{x} - \mathbf{x}_s) + (\mathbf{u} - \mathbf{u}_s)^T R(\mathbf{u} - \mathbf{u}_s),$$
(6)

where \mathbf{x}_s and \mathbf{u}_s denote given setpoints; Q and R denote positive definite, symmetric weighting matrices. In order for the desired reference $(\mathbf{x}_s, \mathbf{u}_s)$ to be a feasible solution of Problem 1, \mathbf{u}_s should be contained in the interior of \mathcal{U} . As already stated in Assumption 2 we consider, without loss of generality that $(\mathbf{x}_s, \mathbf{u}_s) = (\mathbf{0}, \mathbf{0})$ is the steady state that should be stabilized. Note the initial condition in (5a): The system model used to predict the future in the controller is initialized by the actual system state; thus they are assumed to be measured or must be estimated. Equation (5c) is not a constraint but implies that beyond the control horizon the predicted control takes a constant value equal to that at the last step of the control horizon.

In the following an optimal solution to the optimization problem (existence assumed) is denoted by $\bar{\mathbf{u}}^*(\cdot; \mathbf{x}(t), T_p, T_c)$: $[t, t+T_p] \to \mathcal{U}$. The open-loop optimal control problem will be solved repeatedly at the sampling instances $t=j\delta, j=0,1,\cdots$, once new measurements are available. The *closed-loop* control is defined by the optimal solution of Problem 1 at the sampling instants:

$$\mathbf{u}^*(\tau) := \bar{\mathbf{u}}^*(\tau; \mathbf{x}(t), T_p, T_c) , \tau \in [t, \delta].$$
(7)

The optimal value of the NMPC open-loop optimal control problem as a function of the state will be denoted in the following as value function: $V(\mathbf{x}; T_p, T_c) = J(\mathbf{x}, \bar{\mathbf{u}}^*(\cdot; \mathbf{x}(t)); T_p, T_c). \tag{8}$

The value function plays an important role in the proof of the stability of various NMPC schemes, as it serves as a Lyapunov function candidate.

1.3 Properties, Advantages, and Disadvantages of NMPC

In general one would like to use an infinite prediction and control horizon, i.e. T_p and T_c in Problem 1 are set to ∞ . 5case) to minimize the performance objective determined by the cost However as mentioned, the open-loop optimal control Problem 1, that must be solved on-line, is often formulated in a finite horizon manner and the input function is parameterized finitely, in order to allow a (real-time) numerical solution of the nonlinear open-loop optimal control problem. It is clear, that the shorter the horizon, the less costly the solution of the on-line optimization problem. Thus it is desirable from a computational point of view to implement MPC schemes using short horizons. However, when a finite prediction horizon is used, the actual closed-loop input and state trajectories will differ from the predicted open-loop trajectories, even if no model plant mismatch and no disturbances are present [4]. This fact is depicted in Figure 2 where the system can only move inside the shaded area as state constraints of the form $\mathbf{x}(\tau) \in \mathcal{X}$ are assumed. This makes the key difference between standard control strategies, where the feedback law is obtained a priori and

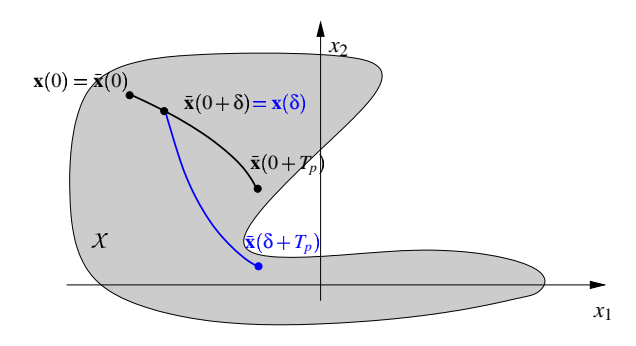


Figure 2: The difference between open-loop prediction and closed-loop behavior.

NMPC where the feedback law is obtained on-line and has two immediate consequences. Firstly, the actual goal to compute a feedback such that the performance objective over the *infinite horizon* of the closed loop is minimized is not achieved. In general it is by no means true that a repeated minimization over a *finite horizon objective* in a receding horizon manner leads to an optimal solution for the infinite horizon problem (with the same stage $\cos F$) [10]. In fact, the two solutions differ significantly if a short horizon is chosen. Secondly, if the predicted and the actual trajectories

differ, there is no guarantee that the closed-loop system will be stable. It is indeed easy to construct examples for which the closed-loop becomes unstable if a (small) finite horizon is chosen. Hence, when using finite horizons in standard NMPC, the stage cost cannot be chosen simply based on the desired physical objectives.

The overall basic structure of a NMPC control loop is depicted in Figure 3. As can be seen, it is necessary to estimate

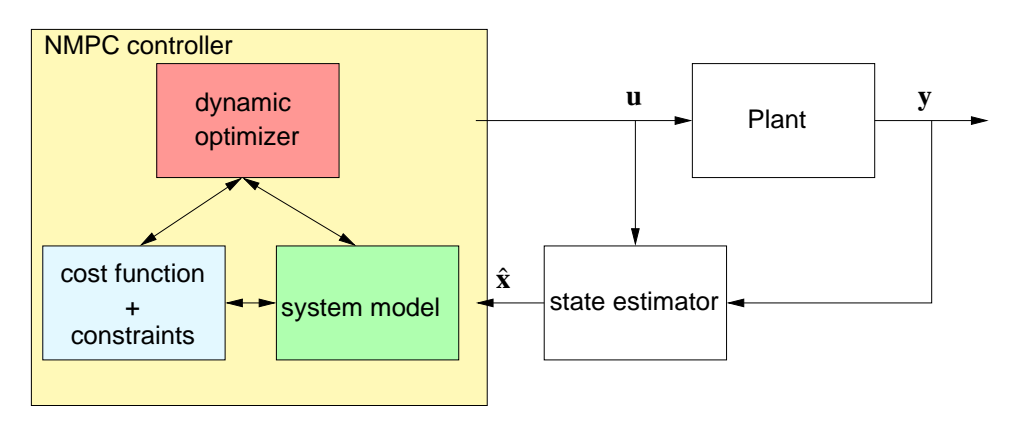


Figure 3: Basic NMPC control loop.

the system states from the output measurements. Summarizing the basic NMPC scheme works as follows:

- 1. obtain measurements/estimates of the states of the system
- 2. compute an optimal input signal by **minimizing** a given **cost function** over a certain **prediction horizon** in the future using a **model of the system**
- 3. **implement the first part of the optimal input signal** until new measurements/estimates of the state are available
- 4. continue with 1.

From the remarks given so far and from the basic NMPC setup, one can extract the following key characteristics of NMPC:

- NMPC allows the use of a nonlinear model for prediction.
- NMPC allows the explicit consideration of state and input constraints.
- In NMPC a specified performance criteria is minimized on-line.
- In NMPC the predicted behavior is in general different from the closed loop behavior.
- The on-line solution of an open-loop optimal control problem is necessary for the application of NMPC.
- To perform the prediction the system states must be measured or estimated.

In the remaining sections various aspects of NMPC regarding these properties will be discussed. The next section focuses on system theoretical aspects of NMPC. Especially the questions on closed-loop stability, robustness and the output feedback problem are considered.

2 System Theoretical Aspects of NMPC

In this section different system theoretical aspects of NMPC are considered. Besides the question of nominal stability of the closed-loop, which can be considered as somehow mature today, remarks on robust NMPC strategies as well as the output-feedback problem are given.

2.1 Stability

One of the key questions in NMPC is certainly, whether a finite horizon NMPC strategy does lead to stability of the closed-loop. As pointed out, the key problem with a finite prediction and control horizon stems from the fact that the predicted open and the resulting closed-loop behavior is in general different. Ideally one would seek for a NMPC strategy that achieves closed-loop stability independent of the choice of the performance parameters in the cost functional and, if possible, approximates the infinite horizon NMPC scheme as good as possible. A NMPC strategy that achieves closed-loop stability independent of the choice of the performance parameters is usually referred to a NMPC approach with guaranteed stability. Different possibilities to achieve closed-loop stability for NMPC using finite horizon length have been proposed. After giving a short review about these approaches we exemplary present on specific approach that achieves guaranteed stabilit, the so called quasi-infinite horizon approach to NMPC (QIH-NMPC). This approach achieves guaranteed closed loop stability while being computationally feasible.

Here only the key ideas are reviewed and no detailed proofs are given. Furthermore notice, that we will not cover all existing NMPC approaches, instead we refer the reader to the overview papers [4, 22, 52].

For all the following sections it is assumed that the prediction horizon is set equal to the control horizon, $T_p = T_c$.

2.1.1 Infinite Horizon NMPC

The most intuitive way to achieve stability is the use of an infinite horizon cost [10, 39, 54], i.e. T_p in Problem 1 is set to ∞ . In the nominal case feasibility at one sampling instance also implies feasibility and optimality at the next sampling instance. This follows from Bellman's Principle of Optimality [7], i.e. the input and state trajectories computed as the solution of the NMPC optimization Problem 1 at a specific instance in time, are in fact equal to the closed-loop trajectories of the nonlinear system, i.e. the remaining parts of the trajectories after one sampling instance are the optimal solution at the next sampling instance. This fact also implies closed-loop stability.

Key ideas of the stability proof: Since nearly all stability proofs for NMPC follow along the same basic steps as for the infinite horizon proof, the key ideas are shortly outlined. In principle the proof is based on the use of the value function as a Lyapunov function. First it is shown, that feasibility at one sampling instance does imply feasibility at the next sampling instance for the nominal case. In a second step it is established that the value function is strictly decreasing and by this the state and input converge to the origin. Utilizing the continuity of the value function at the origin and the monotonicity property, asymptotic stability is established in the third step. As feasibility thus implies asymptotic stability, the set of all states, for which the open-loop optimal control problem has a solution does belong to the region of attraction of the origin.

2.1.2 Finite Horizon NMPC Schemes with Guaranteed Stability

Different possibilities to achieve closed-loop stability for NMPC using a finite horizon length have been proposed, see for example [3, 17, 20, 23, 34, 35, 38, 39, 44, 51, 53, 55, 56, 60, 62, 63, 70]. Most of these approaches modify the NMPC setup such that stability of the closed-loop can be guaranteed independently of the plant and performance specifications. This is usually achieved by adding suitable equality or inequality constraints and suitable additional penalty terms to the cost functional. These additional constraints are usually not motivated by physical restrictions or desired performance requirements but have the sole purpose to enforce stability of the closed-loop. Therefore, they are usually termed *stability constraints* [49, 50, 52].

The simplest possibility to enforce stability with a finite prediction horizon is to add a so called *zero terminal equality constraint* at the end of the prediction horizon [39, 51, 53], i.e. to add the equality constraint

$$\bar{\mathbf{x}}(t+T_p;\mathbf{x}(t),t,\bar{\mathbf{u}}) = \mathbf{0}$$
(9)

to Problem 1. This leads to stability of the closed-loop, if the optimal control problem possesses a solution at t = 0, since the feasibility at one time instance does also lead to feasibility at the following time instances and a decrease in the value function. One disadvantage of a zero terminal constraint is that the system must be brought to the origin in finite time. This leads in general to feasibility problems for short prediction/control horizon lengths, i.e. a small region of attraction. Additionally, from a computational point of view, an exact satisfaction of a zero terminal equality constraint does require an infinite number of iterations in the nonlinear programming problem [17]. On the other hand, the main advantages are the straightforward application and the conceptual simplicity.

Many schemes have been proposed (i.e. [17, 20, 34, 38, 51, 56, 60, 63]), that try to overcome the use of a zero terminal constraint of the form (9). Most of them either use a so called *terminal region constraint*

$$\bar{\mathbf{x}}(t+T_p) \in \Omega \subseteq \mathcal{X} \tag{10}$$

and/or a terminal penalty term $E(\bar{\mathbf{x}}(t+T_p))$ which is added to the cost functional:

$$J(\mathbf{x}(t), \bar{\mathbf{u}}(\cdot); T_p) = \int_t^{t+T_p} F(\bar{\mathbf{x}}(\tau), \bar{\mathbf{u}}(\tau)) d\tau + E(\bar{\mathbf{x}}(t+T_p)). \tag{11}$$

Note that the terminal penalty term is not a performance specification that can be chosen freely. Rather E and the terminal region Ω in (10) are determined off-line such that stability is "enforced". We do not review all these methods here. Instead we exemplify the basic idea considering one specific approach, the so called quasi-infinite horizon NMPC approach [17].

2.1.3 Quasi-Infinite Horizon NMPC

In the quasi-infinite horizon NMPC method [15, 17] a terminal region constraint of the form (10) and a *terminal* penalty term $E(\bar{\mathbf{x}}(t+T_p))$ as in (11) are added to the standard setup. As mentioned the terminal penalty term is not a performance specification that can be chosen freely. Rather E and the terminal region Ω are determined off-line such that the cost functional with terminal penalty term (11) gives an upper approximation of the infinite horizon cost functional with stage cost F. Thus closed-loop performance over the infinite horizon is addressed. Furthermore, as is shown later, stability is achieved, while only an optimization problem over a finite horizon must be solved. The resulting open-loop optimization problem is formulated as follows:

Problem 2 [Quasi-infinite Horizon NMPC]:

Find

$$\min_{\bar{\mathbf{u}}(\cdot)} J(\mathbf{x}(t), \bar{\mathbf{u}}(\cdot); T_p) \tag{12}$$

with:

$$J(\mathbf{x}(t), \bar{\mathbf{u}}(\cdot); T_p) := \int_t^{t+T_p} F(\bar{\mathbf{x}}(\tau), \bar{\mathbf{u}}(\tau)) d\tau + E(\bar{\mathbf{x}}(t+T_p)). \tag{13}$$

subject to:

$$\dot{\bar{\mathbf{x}}}(\tau) = \mathbf{f}(\bar{\mathbf{x}}(\tau), \bar{\mathbf{u}}(\tau)), \quad \bar{\mathbf{x}}(t) = \mathbf{x}(t)$$
(14a)

$$\bar{\mathbf{u}}(\tau) \in \mathcal{U}, \ \forall \tau \in [t, t + T_p]$$
 (14b)

$$\bar{\mathbf{x}}(\tau) \in \mathcal{X}, \ \forall \tau \in [t, t + T_p]$$
 (14c)

$$\bar{\mathbf{x}}(t+T_p) \in \Omega. \tag{14d}$$

If the terminal penalty term E and the terminal region Ω are chosen suitably, stability of the closed-loop can be guaranteed. To present the stability results we need that the following holds for the stage cost-function.

Assumption 4 The stage cost $F: \mathbb{R}^n \times \mathcal{U} \to \mathbb{R}$ is continuous in all arguments with $F(\mathbf{0}, \mathbf{0}) = 0$ and $F(\mathbf{x}, \mathbf{u}) > 0 \ \forall (\mathbf{x}, \mathbf{u}) \in \mathbb{R}^n \times \mathcal{U} \setminus \{\mathbf{0}, \mathbf{0}\}.$

Given this assumption, the following result, which is a slight modification of Theorem 4.1 in [14], can be established:

Theorem 1 Suppose

- (a) that Assumptions 1-4 are satisfied,
- (b) E is C^1 with $E(\mathbf{0},\mathbf{0}) = 0$, $\Omega \subseteq X$ is closed and connected with the origin contained in Ω and there exists a continuous local control law $\mathbf{k} : \mathbb{R}^n \to \mathbb{R}^m$ with $\mathbf{k}(\mathbf{0}) = \mathbf{0}$, such that:

$$\frac{\partial E}{\partial \mathbf{x}} f(\mathbf{x}, \mathbf{k}(\mathbf{x})) + F(\mathbf{x}, \mathbf{k}(\mathbf{x})) \le 0, \quad \forall \mathbf{x} \in \Omega$$
 (15)

with $\mathbf{k}(\mathbf{x}) \in \mathcal{U} \ \forall \mathbf{x} \in \Omega$

(c) the NMPC open-loop optimal control problem has a feasible solution for t = 0.

Then for any sampling time $0 < \delta < T_p$ the nominal closed-loop system is asymptotically stable with the region of attraction \mathcal{R} , being the set of states for which the open-loop optimal control problem has a feasible solution.

A formal proof of Theorem 1 can be found in [14, 16] and for a linear local controller as described below in [17]. Loosely speaking E is a local Lyapunov function of the system under the local control $\mathbf{k}(\mathbf{x})$ in Ω . As will be shown, Equation (15) allows to upper bound the optimal infinite horizon cost inside Ω by the cost resulting from a local feedback $\mathbf{k}(\mathbf{x})$.

Notice, that the result in Theorem 1 is nonlocal in nature, i.e. their exists a region of attraction \mathcal{R} of at least the size of Ω . The region of attraction is given by all states for which the open-loop optimal control problem has a feasible solution.

Obtaining a terminal penalty term E and a terminal region Ω that satisfy the conditions of Theorem 1 is not easy. If the linearized system is stabilizable and the cost function is quadratic with weight matrices Q and R, a locally *linear* feedback law $\mathbf{u} = K\mathbf{x}$ can be used and the terminal penalty term can be approximated as quadratic of the form $E(\mathbf{x}) = \mathbf{x}^T P \mathbf{x}$. For this case, a procedure to systematically compute the terminal region and a terminal penalty matrix *off-line* is available [17]. Assuming that the Jacobian linearization (A, B) of (1) is stabilizable, where $A := \frac{\partial \mathbf{f}}{\partial \mathbf{x}}(\mathbf{0}, \mathbf{0})$ and $B := \frac{\partial \mathbf{f}}{\partial \mathbf{u}}(\mathbf{0}, \mathbf{0})$, this procedure can be summarized as follows:

Step 1: Solve the linear control problem based on the Jacobian linearization (A,B) of (1) to obtain a locally stabilizing linear state feedback $\mathbf{u} = K\mathbf{x}$.

Step 2: Choose a constant $\kappa \in [0, \infty)$ satisfying $\kappa < -\lambda_{max}(A_K)$ and solve the Lyapunov equation

$$(A_K + \kappa I)^T P + P(A_K + \kappa I) = -(Q + K^T R K)$$
(16)

to get a positive definite and symmetric P, where $A_K := A + BK$.

Step 3: Find the largest possible α_1 defining a region

$$\Omega_1 := \{ \mathbf{x} \in \mathbb{R}^n \, | \, \mathbf{x}^T P \mathbf{x} \le \alpha_1 \} \tag{17}$$

such that $K\mathbf{x} \in \mathcal{U}$, for all $\mathbf{x} \in \Omega_1 \subseteq \mathcal{X}$.

Step 4: Find the largest possible $\alpha \in (0, \alpha_1]$ specifying a terminal region

$$\Omega := \{ \mathbf{x} \in \mathbb{R}^n \, | \, \mathbf{x}^T P \mathbf{x} \le \alpha \} \tag{18}$$

such that the optimal value of the following optimization problem is non-positive:

$$\max_{\mathbf{x}} \{ \mathbf{x}^T P \mathbf{\phi}(\mathbf{x}) - \kappa \cdot \mathbf{x}^T P \mathbf{x} \mid \mathbf{x}^T P \mathbf{x} \le \alpha \}$$
 (19)

where $\varphi(\mathbf{x}) := \mathbf{f}(\mathbf{x}, K\mathbf{x}) - A_K\mathbf{x}$.

This procedure allows to calculate E and Ω if the linearization of the system at the origin is stabilizable. If the terminal penalty term and the terminal region are determined according to Theorem 1, the open-loop optimal trajectories found at each time instant approximate the optimal solution for the *infinite* horizon problem.

The following reasoning make this plausible: Consider an infinite horizon cost functional defined by

$$J^{\infty}(\mathbf{x}(t), \bar{\mathbf{u}}(\cdot)) := \int_{t}^{\infty} F(\bar{\mathbf{x}}(\tau), \bar{\mathbf{u}}(\tau)) d\tau$$
 (20)

with $\bar{\mathbf{u}}(\cdot)$ on $[t,\infty)$. This cost functional can be split up into two parts

$$\min_{\bar{\mathbf{u}}(\cdot)} J^{\infty}(\mathbf{x}(t), \bar{\mathbf{u}}(\cdot)) = \min_{\bar{\mathbf{u}}(\cdot)} \left(\int_{t}^{t+T_{p}} F(\bar{\mathbf{x}}(\tau), \bar{\mathbf{u}}(\tau)) d\tau + \int_{t+T_{p}}^{\infty} F(\bar{\mathbf{x}}(\tau), \bar{\mathbf{u}}(\tau)) d\tau \right).$$
(21)

The goal is to upper approximate the second term by a terminal penalty term $E(\bar{\mathbf{x}}(t+T_p))$. Without further restrictions, this is not possible for general nonlinear systems. However, if we ensure that the trajectories of the closed-loop system remain within some neighborhood of the origin (terminal region) for the time interval $[t+T_p,\infty)$, then an upper bound

on the second term can be found. One possibility is to determine the terminal region Ω such that a local state feedback law $\mathbf{u} = \mathbf{k}(\mathbf{x})$ asymptotically stabilizes the nonlinear system and renders Ω positively invariant for the closed-loop. If an additional terminal inequality constraint $\mathbf{x}(t+T_p) \in \Omega$ (see (14d)) is added to Problem 1, then the second term of equation (21) can be upper bounded by the cost resulting from the application of this local controller $\mathbf{u} = \mathbf{k}(\mathbf{x})$. Note that the predicted state will not leave Ω after $t+T_p$ since $\mathbf{u} = \mathbf{k}(\mathbf{x})$ renders Ω positively invariant. Furthermore the feasibility at the next sampling instance is guaranteed dismissing the first part of $\bar{\mathbf{u}}$ and replacing it by the nominal open-loop input resulting from the local controller. Requiring that $\mathbf{x}(t+T_p) \in \Omega$ and using the local controller for $\mathbf{\tau} \in [t+T_p,\infty)$ we obtain:

$$\min_{\bar{\mathbf{u}}(\cdot)} J^{\infty}(\mathbf{x}(t), \bar{\mathbf{u}}(\cdot)) \leq \min_{\bar{\mathbf{u}}(\cdot)} \left(\int_{t}^{t+T_{p}} F(\bar{\mathbf{x}}(\tau), \bar{\mathbf{u}}(\tau)) d\tau + \int_{t+T_{p}}^{\infty} (\bar{\mathbf{x}}(\tau), \mathbf{k}(\bar{\mathbf{x}}(\tau))) d\tau \right).$$
(22)

If, furthermore, the terminal region Ω and the terminal penalty term are chosen according to condition b) in Theorem 1 (as for example achieved by the procedure given above), integrating (15) leads to

$$\int_{t+T_p}^{\infty} F\left(\bar{\mathbf{x}}(\tau), \mathbf{k}\left(\bar{\mathbf{x}}(\tau)\right)\right) d\tau \le E\left(\bar{\mathbf{x}}(t+T_p)\right). \tag{23}$$

Substituting (23) into (22) we obtain

$$\min_{\bar{\mathbf{u}}(\cdot)} J^{\infty}(\mathbf{x}(t), \bar{\mathbf{u}}(\cdot)) \le \min_{\bar{\mathbf{u}}(\cdot)} J(\mathbf{x}(t), \bar{\mathbf{u}}(\cdot); t + T_p).$$
(24)

This implies that the optimal value of the finite horizon problem bounds that of the corresponding infinite horizon problem. Thus, the prediction horizon can be thought of as extending *quasi* to infinity which gives this approach its name. Equation (24) can be exploited to prove Theorem 1.

Like in the dual-mode approach [56], the use of the terminal inequality constraint gives the quasi-infinite horizon nonlinear MPC scheme computational advantages. Note also, that as for dual-mode NMPC, it is not necessary to find optimal solutions of Problem 1 in order to guarantee stability. Feasibility also implies stability here [17, 70]. In difference to the dual-mode controller, however, the local control law $\mathbf{u} = \mathbf{k}(\mathbf{x})$ is never applied. It is only used to compute the terminal penalty term E and the terminal region Ω .

Many generalizations and expansions of QIH-NMPC exist. For example discrete time variants can be found in [21, 33]. If the nonlinear system is affine in **u** and feedback linearizable, then a terminal penalty term can be determined such that (23) is exactly satisfied with equality [14], i.e. the infinite horizon is recovered exactly. In [18, 19, 44] robust NMPC schemes using a min-max formulation are proposed, while in [27] an extension to index one DAE systems is considered. A variation of QIH-NMPC for the control of varying setpoints is given in [28, 30].

2.2 Performance of Finite Horizon NMPC Formulations

Ideally one would like to use an infinite horizon NMPC formulation, since in the nominal case, the closed-loop trajectories do coincide with the open-loop predicted ones (principle of optimality). The main problem is, that infinite horizon schemes can often not be applied in practice, since the open-loop optimal control problem cannot be solved sufficiently fast. Using finite horizons, however, it is by no means true that a repeated minimization over a *finite horizon objective* in a receding horizon manner leads to an optimal solution for the infinite horizon problem (with the same stage cost *F*). In fact, the two solutions will in general differ significantly if a short horizon is chosen.

From this discussion it is clear that short horizons are desirable from a computational point of view, but long horizons are required for closed-loop stability and in order to achieve the desired performance.

The QIH-NMPC strategy outlined in the previous section allows in principle to recover the performance of the infinite horizon scheme without jeopardizing the closed-loop stability. The value function resulting from Problem 2 can be seen as an upper bound of the infinite horizon cost. To be more precise, if the terminal penalty function E is chosen such that a corresponding local control law is a good approximation of the control resulting from the infinite horizon control law in a neighborhood of the origin, the performance corresponding to Problem 2 can recover the performance of the infinite horizon cost even for short horizons (assuming the terminal region constraint can be satisfied).

2.3 Robustness

So far only the nominal control problem was considered. The NMPC schemes discussed before do require that the actual system is identical to the model used for prediction, i.e. that no model/plant mismatch or unknown disturbances are present. Clearly this is a very unrealistic assumption for practical applications and the development of a NMPC framework to address robustness issues is of paramount importance. In this note the nonlinear uncertain system is assumed to be given by:

$$\dot{\mathbf{x}}(t) = \mathbf{f}(\mathbf{x}(t), \mathbf{u}(t), \mathbf{d}(t)) \tag{25}$$

where the uncertainty $\mathbf{d}(\cdot)$ satisfies $\mathbf{d}(\tau) \in \mathcal{D}(x,u)$ and \mathcal{D} is assumed to be compact. Like in the nominal stability and performance case, the resulting difference between the predicted open-loop and actual closed-loop trajectory is the main obstacle. As additional problem the uncertainty \mathbf{d} hitting the system now leads not only to one single future trajectory in the prediction, instead a whole tree of possible solutions must be analyzed.

Even though the analysis of robustness properties in *nonlinear* NMPC must still be considered as an unsolved problem in general, some preliminary results are available. In principle one must distinguish between two approaches to consider the robustness question. Firstly one can examine the robustness properties of the NMPC schemes designed for nominal stability and by this take the uncertainty/disturbances only indirectly into account [40, 47]. Secondly one can consider to design NMPC schemes that directly take into account the uncertainty/disturbances.

2.3.1 Inherent Robustness of NMPC

As mentioned above, inherent robustness corresponds to the fact, that nominal NMPC can cope with input model uncertainties without taking them directly into account. This fact stems from the close relation of NMPC to optimal control. Assuming that the system under consideration is of the following (input affine) form

$$\dot{\mathbf{x}}(t) = \mathbf{f}(\mathbf{x}(t)) + \mathbf{g}(\mathbf{x}(t))\mathbf{u}(t), \quad \mathbf{x}(0) = \mathbf{x}_0$$
 (26)

and the cost function takes the form:

$$J(\mathbf{x}(t), \bar{\mathbf{u}}(\cdot); T_p) := \int_t^{t+T_p} \frac{1}{2} ||\mathbf{u}||^2 + \mathbf{q}(\mathbf{x}) d\tau + E(\bar{\mathbf{x}}(t+T_p))$$
(27)

where \mathbf{q} is positive definite, that there are no constraints on the state and the input and the resulting control law and the value function satisfies further assumptions (\mathbf{u}^* being continuously differentiable and the value function being twice continuously differentiable). Then one can show [47] that the NMPC control law is inverse optimal, i.e. it is also optimal for a modified optimal control problem spanning over an infinite horizon. Due to this inverse optimality, the NMPC control law inherits the same robustness properties as infinite horizon optimal control assuming that the sampling time δ goes to zero. In particular, the closed-loop is robust with respect to sector bounded input uncertainties; the nominal NMPC controller also stabilizes systems of the form:

$$\dot{\mathbf{x}}(t) = \mathbf{f}(\mathbf{x}(t)) + \mathbf{g}(\mathbf{x}(t))\phi(\mathbf{u}(t)), \tag{28}$$

where $\phi(\cdot)$ is a nonlinearity in the sector $(1/2, \infty)$.

2.3.2 Robust NMPC Schemes

At least three different robust NMPC formulations exist:

• Robust NMPC solving an open-loop min-max problem [18, 45]:

In this formulation the standard NMPC setup is kept, however now the cost function optimized is given by the worst case disturbance "sequence" occurring, i.e.

$$J(\mathbf{x}(t), \bar{\mathbf{u}}(\cdot); T_p) := \max_{\bar{\mathbf{d}}(\cdot)} \int_t^{t+T_p} F(\bar{\mathbf{x}}(\tau), \bar{\mathbf{u}}(\tau)) d\tau + E(\bar{\mathbf{x}}(t+T_p)).$$
(29)

subject to

$$\dot{\bar{\mathbf{x}}}(t) = \mathbf{f}(\bar{\mathbf{x}}(t), \bar{\mathbf{u}}(t), \bar{\mathbf{d}}(t)), \quad \bar{\mathbf{x}}(t) = \mathbf{x}(t). \tag{30}$$

The resulting open-loop optimization is a min-max problem. The key problem is, that adding stability constraints like in the nominal case, might lead to the fact that no feasible solution can be found at all. This mainly stems from the fact, that one input signal must "reject" all possible disturbances and guarantee the satisfaction of the stability constraints.

• H_{∞} -NMPC [11, 18, 45, 46]: Another possibility is to consider the standard H_{∞} problem in a receding horizon framework. The key obstacle is, that an infinite horizon min-max problem must be solved (solution of the nonlinear Hamilton-Jacobi-Isaacs equation). Modifying the NMPC cost functions similar to the H_{∞} problem and optimizing over a sequence of control laws robustly stabilizing finite horizon H_{∞} -NMPC formulations can be achieved. The main obstacle is the prohibitive computational time necessary. This approach is in close connection to the first approach.

• Robust NMPC optimizing a feedback controller used during the sampling times [45]:

The open-loop formulation of the robust stabilization problem can be seen as very conservative, since only open-loop control is used during the sampling times, i.e. the disturbances are not directly rejected in between the sampling instances. To overcome this problem it has been proposed not to optimize over the input signal. Instead of optimizing the open-loop input signal directly, a feedback controller is optimized, i.e. the decision variable $\bar{\mathbf{u}}$ is not considered as optimization variable instead a "sequence" of control laws $\mathbf{u}_i = \mathbf{k}_i(\mathbf{x})$ applied during the sampling times is optimized. Now the optimization problem has as optimization variables the parameterizations of the feedback controllers $\{\mathbf{k}_1, \dots, \mathbf{k}_N\}$. While this formulation is very attractive since the conservatism is reduced, the solution is often prohibitively complex.

2.4 Output Feedback NMPC

So far it was assumed, that the system state necessary for prediction is (perfectly) accessible through measurements. In general this is not the case and a state observer, as already shown in Figure 3 must be implicitly or explicitly included in the control loop. Two main questions arise from the use of a state observer. Firstly the question occurs, if the closed-loop including the state observer possesses the same stability properties as the state feedback contribution alone. Secondly the question arises, what kind of observer should be used to obtain a good state estimate and good closed loop performance. The second point is not considered in detail here. It is only noted, that a dual of the NMPC approach for control does exist for the state estimation problem. It is formulated as an on-line optimization similar to NMPC and is named moving horizon estimation (MHE). It is dual in the sense, that a moving window of old measurement data is used to obtain an optimization based estimate of the system state, see for example [1, 57, 66, 67, 69, 75].

2.4.1 Possible Solutions to the Output Feedback NMPC Problem

The most often used approach for output-feedback NMPC is based on the "certainty equivalence principle". The estimate state $\hat{\mathbf{x}}$ is measured via a state observer and used in the model predictive controller. Even assuming, that the observer error is exponentially stable, often only local stability of the closed-loop is achieved [42, 43, 71], i.e. the observer error must be small to guarantee stability of the closed-loop and in general nothing can be said about the necessary degree of smallness. This is a consequence of the fact that no general valid separation principle for nonlinear systems exists. Nevertheless this approach is applied successfully in many applications.

To achieve non-local stability results of the observer based output-feedback NMPC controller, different possibilities to attack the problem exist:

- **Direct consideration of the observer error in the NMPC controller**: One could in principle consider the observer error as disturbance in the controller and design a NMPC controller that can reject this disturbance. The hurdle of this approach is the fact, that so far an applicable robust NMPC scheme is not available.
- Separation of observer error from the controller [31,37,57]: In this approach the observer error is "decoupled"/separated from the controller by either a time scale separation, i.e. making the observer much faster than the other system parts or by projection of the observer error. For example using special separation principles based on high-gain observers, semi-regional stability results for the closed-loop can be established. The key component is, that the speed of the observer can be made as fast as necessary.
- Usage of I/O models [65]: One could use suited I/O models that have no internal states for prediction.

In the following we shortly review one possible approach for output-feedback NMPC using a time-scale separation of the observer and controller.

2.4.2 Output Feedback NMPC using High-Gain Observers

We propose to combine high-gain observers with NMPC to achieve semi-regional stability. I.e. if the observer gain is increased sufficiently, the stability region and performance of the state feedback is recovered. The closed loop system is semi-regionally stable in the sense, that for any subset $\mathcal S$ of the region of attraction $\mathcal R$ of the state-feedback controller (compare Theorem 1, Section 2.1.3) there exists an observer parameter (gain), such that $\mathcal S$ is contained in the region of attraction of the output-feedback controller.

The results are based on "nonlinear separation principles [6,72]" and it is assumed, that the NMPC feedback is instantaneous (see below). We will limit the presentation to a special SISO systems class and only give the main result. The more general MIMO case considering the NMPC inherent open loop control parts (i.e. no instantaneous feedback) can be found [31,37].

In the following we consider the stabilization of SISO systems of the following form:

$$\dot{\mathbf{x}} = A\mathbf{x} + \mathbf{b}\phi(\mathbf{x}, u) \tag{31a}$$

$$y = x_1. (31b)$$

with $u(t) \in \mathcal{U} \subset \mathbb{R}$ and $y(t) \in \mathbb{R}$. The output y is given by the first state x_1 . The $n \times n$ matrix A and the $n \times 1$ vector \mathbf{b} have the following form:

$$A = \begin{bmatrix} 0 & 1 & 0 & \cdots & 0 \\ 0 & 0 & 1 & \cdots & 0 \\ \vdots & & & \vdots \\ 0 & \cdots & \cdots & 0 & 1 \\ 0 & \cdots & \cdots & \cdots & 0 \end{bmatrix}_{n \times n}, \quad \mathbf{b} = \begin{bmatrix} 0 & \cdots & 0 & 1 \end{bmatrix}_{n \times 1}^{T},$$
(32a)

Additional to the Assumptions 1-4 we assume, that:

Assumption 5 The function $\phi : \mathbb{R}^n \times \mathcal{U} \to \mathbb{R}$ is locally Lipschitz in its arguments over the domain of interest. Furthermore $\phi(\mathbf{0},0) = 0$ and ϕ is bounded in \mathbf{x} everywhere.

Note that global boundedness can in most cases be achieved by saturating ϕ outside a compact region of \mathbb{R}^n of interest. The proposed output feedback controller consists of a high-gain observer to estimate the states and an instantaneous variant of the full state feedback QIH-NMPC controller as outlined in Sect. 2.1.3. By instantaneous we mean that the system input at *all* times (i.e. not only at the sampling instances) is given by the instantaneous solution of the open-loop optimal control problem:

$$u(\mathbf{x}(t)) := u^{\star}(\tau = 0; \mathbf{x}(t), T_p). \tag{33}$$

This feedback law differs from the standard NMPC formulation in the sense that no open-loop input is implemented over a sampling time δ . Instead u(t) is considered as a "function" of $\mathbf{x}(t)$.

To allow the subsequent result to hold, we have to require that the feedback resulting from the QIH-NMPC is locally Lipschitz.

Assumption 6 The instantaneous state feedback (33) is locally Lipschitz.

The observer used for state recovery is a high-gain observer [6, 72, 73] of the following form:

$$\dot{\hat{\mathbf{x}}} = A\hat{\mathbf{x}} + \mathbf{b}\phi(\hat{\mathbf{x}}, u) + H(x_1 - \hat{x}_1) \tag{34}$$

where $H^{\top} = [\alpha_1/\epsilon, \ \alpha_2/\epsilon^2, \dots, \alpha_n/\epsilon^n]$. The α_i 's are chosen such that the polynomial

$$s^n + \alpha_1$$
 $s^{n-1} + \cdots + \alpha_{n-1}s + \alpha_n = 0$,

is Hurwitz. Here $\frac{1}{\varepsilon}$ is the high-gain parameter and can be seen as a time scaling for the observer dynamics (34). A, \mathbf{b} and ϕ are the same as in (31).

Notice that the use of an observer makes it necessary that the input also be defined (and bounded) for (estimated) states that are outside the feasible region of the state feedback controller. We simply define the open-loop input for $\mathbf{x} \notin \mathcal{R}$ as fixed to an arbitrary value $u_f \in \mathcal{U}$:

$$u(\mathbf{x}) = u_f, \qquad \forall \mathbf{x} \notin \mathcal{R}. \tag{35}$$

This together with the assumption that \mathcal{U} is bounded separates the peaking of the observer from the controller/system [26]. Using the high-gain observer for state recovery, the following result, which establishes semi-regional stability of the closed-loop can be obtained [36, 37]:

Theorem 2 Assume that the conditions a)-c) of Theorem 1 and Assumption 5-6 hold. Let S be any compact set contained in the interior of R (region of attraction of the state feedback). Then there exists a (small enough) $E^* > 0$ such that for all $0 < E \le E^*$, the closed-loop system is asymptotically stable with a region of attraction of at least S. Further, the performance of the state feedback NMPC controller is recovered as E decreases.

By performance recovery it is meant that the difference between the trajectories of the state feedback and the output feedback can be made arbitrarily small by decreasing ε . The results show that the performance of the state feedback scheme can be recovered in the output feedback case, if a state observer with a suitable structure and a fast enough dynamics is used.

Figure 5 shows the simulation result for an illustrative application of the proposed output feedback scheme to a two dimensional pendulum car system as depicted in Figure 4 and presented in [36]. The angle between the pendulum

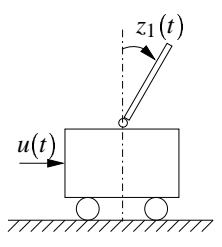


Figure 4: Sketch of the inverted pendulum/car system

and the vertical is denoted by z_1 , while the angular velocity of the pendulum is given by z_2 . The input u is the force applied to the car. The control objective is to stabilize the upright position of the pendulum. To achieve this objective, a QIH-NMPC scheme with and without (state-feedback case) a high-gain observer is used. For the results shown in Figure 5 the pendulum is initialized with an offset from the upright position, while the high-gain observer is started with zero initial conditions. The figure shows the closed loop trajectories for state feedback QIH-NMPC controller and the output-feedback controller with different observer gains. The gray ellipsoid around the origin is the terminal region of the QIH-NMPC controller. The outer "ellipsoid" is an estimate of the region of attraction of the state-feedback controller. As can be seen for small enough values of the observer parameter ε the closed loop is stable. Furthermore the performance of the state feedback is recovered as ε tends to zero. More details can be found in [36].

Furthermore the recovery of the region of attraction and the performance of the state-feedback is possible up to any degree of exactness. In comparison to other existing output-feedback NMPC schemes [42, 71] the proposed scheme is thus of non-local nature. However, the results are based on the assumption that the NMPC controller is time continuous/instantaneous. In practice, it is of course not possible to solve the nonlinear optimization problem instantaneously. Instead, it will be solved only at some sampling instants. A sampled version of the given result, in agreement with the "usual" sampled NMPC setup can be found in [31]. Notice also, that the use of a high gain observer is critical, if the output measurements are very noise, since the noise will be amplified due to the high gain nature of the observer.

3 Computational Aspects of NMPC

NMPC requires the repeated on-line solution of a *nonlinear* optimal control problem. In the case of linear MPC the solution of the optimal control problem can be cast as the solution of a (convex) quadratic program and can be solved

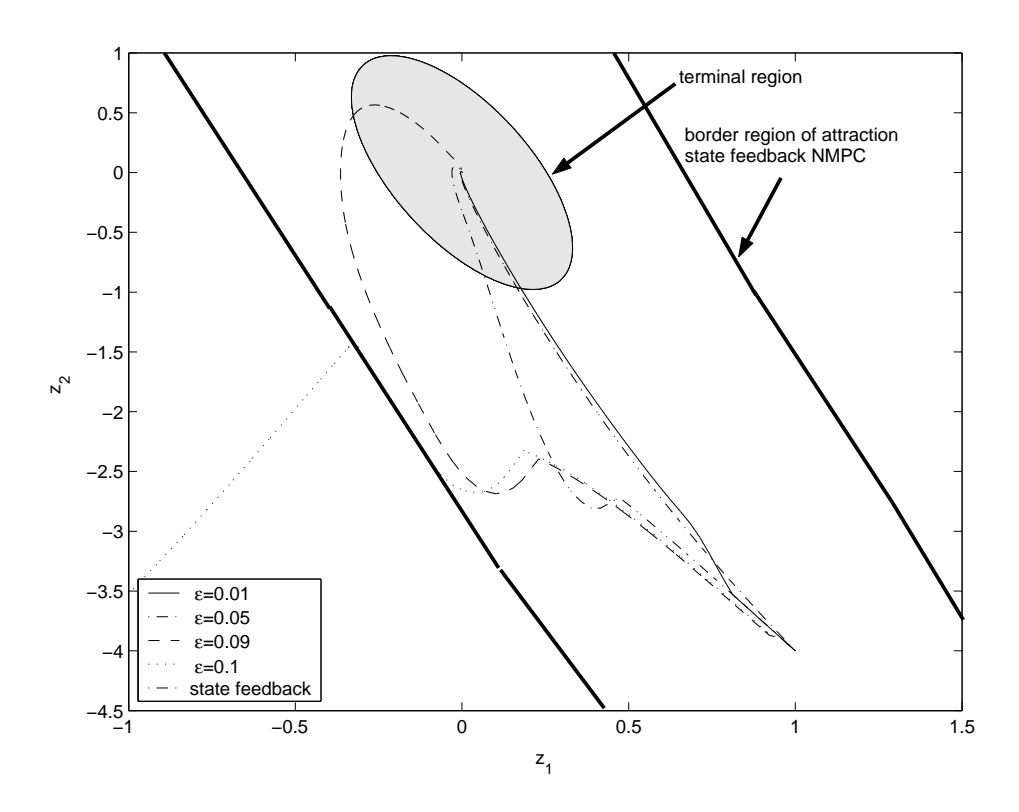


Figure 5: Phase plot of the pendulum angle (z_1) and the angular velocity (z_2)

efficiently even on-line. This can be seen as one of the reasons why linear MPC is widely used in industry. For the NMPC problem the solution involves the solution of a *nonlinear* program, as is shown in the preceding sections. In general the solution of a nonlinear (non-convex) optimization problem can be computational expensive. However in the case of NMPC the nonlinear program shows special structure that can be exploited to still achieve a real-time feasible solution to the NMPC optimization problem.

For the purpose of this Section the open-loop optimal control Problem 2 of Section 2.1.2 will be considered in a more optimization focused setting. Especially it is considered, that the state and input constraints $\mathbf{x} \in \mathcal{X}$, $\mathbf{u} \in \mathcal{U}$ can be recasted as a nonlinear inequality constraint of the form $\mathbf{l}(\mathbf{x}, \mathbf{u}) \leq 0$. Furthermore for simplicity of exposition it is assumed that the control and prediction horizon coincide and that no final region constraint is present, i.e. we consider the following deterministic optimal control problem in Bolza form that must be solved at every sampling instance:

Problem 3: Find

subject to:

$$\min_{\bar{\mathbf{u}}(\cdot)} J(\mathbf{x}(t), \bar{\mathbf{u}}(\cdot); T_p) \tag{36}$$

with
$$J(\mathbf{x}(t), \bar{\mathbf{u}}(\cdot); T_p) := \int_t^{t+T_p} F(\bar{\mathbf{x}}(\tau), \bar{\mathbf{u}}(\tau)) d\tau + E(\bar{\mathbf{x}}(t+T_p))$$
 (37)

 $\dot{\bar{\mathbf{x}}}(\tau) = \mathbf{f}(\bar{\mathbf{x}}(\tau), \bar{\mathbf{u}}(\tau)), \quad \bar{\mathbf{x}}(t) = \mathbf{x}(t)$ (38a)

 $\mathbf{l}(\bar{\mathbf{u}}(\tau), \bar{\mathbf{x}}(\tau)) \le \mathbf{0}, \ \forall \tau \in [t, t + T_p]. \tag{38b}$

3.1 Solution Methods for the Open-Loop Optimal Control Problem

In principle three different approaches to solve the optimal control Problem 3 exist (see for example [9, 48]):

• Hamilton-Jacobi-Bellmann partial differential equations/dynamic programming: This approach is based on the direct solution of the so called Hamilton-Jacobi-Bellmann partial differential equations. Rather than just seeking for the optimal $\mathbf{u}(\tau)$ trajectory the problem is approach as finding a solution for all $\mathbf{x}(t)$. The solution derived is a state feedback law of the form $\mathbf{u}^* = \mathbf{k}(\mathbf{x})$ and is valid for every initial condition. The key obstacle of this approach is, that since the "complete" solution is considered at once, it is in general computationally

intractable and suffers from the so called curse of dimensionality, i.e. can be only solved for small systems. Ideally one would like to obtain such a closed loop state feedback law. In principle the intractability of the solution can be seen as the key motivation of receding horizon control.

- Euler-Lagrange differential equations/calculus of variations/maximum principle: This method employs classical calculus of variations to obtain an explicit solution of the input as a function of time $\mathbf{u}(\tau)$ and not as feedback law. Thus it is only valid for the specified initial condition $\mathbf{x}(t)$. The approach can be thought of as the application of the necessary conditions for constrained optimization with the twist, that the optimization is infinite dimensional. The solution of the optimal control problem is cast as a boundary value problem. Since an infinite dimensional problem must be solved, this approach can normally not be applied for on-line implementation.
- **Direct solution using a finite parameterization of the controls and/or constraints:** In this approach the input and/or the constraints are parametrized finitely, thus an approximation of the original open-loop optimal control problem is seeked. The resulting finite dimensional dynamic optimization problem is solved with "standard" static optimization techniques.

For an on-line solution of the NMPC problem only the last approach is normally used. Since no feedback is obtained, the optimization problem must be solved at every sampling instance with the new state information. In the following only the last solution method is considered in detail.

3.2 Solution of the NMPC Problem Using a Finite Parameterization of the Controls

As mentioned the basic idea behind the direct solution using a finite parameterization of the controls is to approximate/transcribe the original infinite dimensional problem into a finite dimensional nonlinear programming problem. In this note the presentation is limited to a parameterization of the input signal as piecewise constant over the sampling times. The controls are piecewise constant on each of the $N = \frac{T_p}{\delta}$ predicted sampling intervals: $\bar{\mathbf{u}}(\tau) = \bar{\mathbf{u}}_i$ for $\tau \in [\tau_i, \tau_{i+1})$, $\tau_i = t + i\delta$, compare also Figure 6. Thus in the optimal control problem the "input vector" $\{\bar{\mathbf{u}}_1, \dots \bar{\mathbf{u}}_N\}$ is

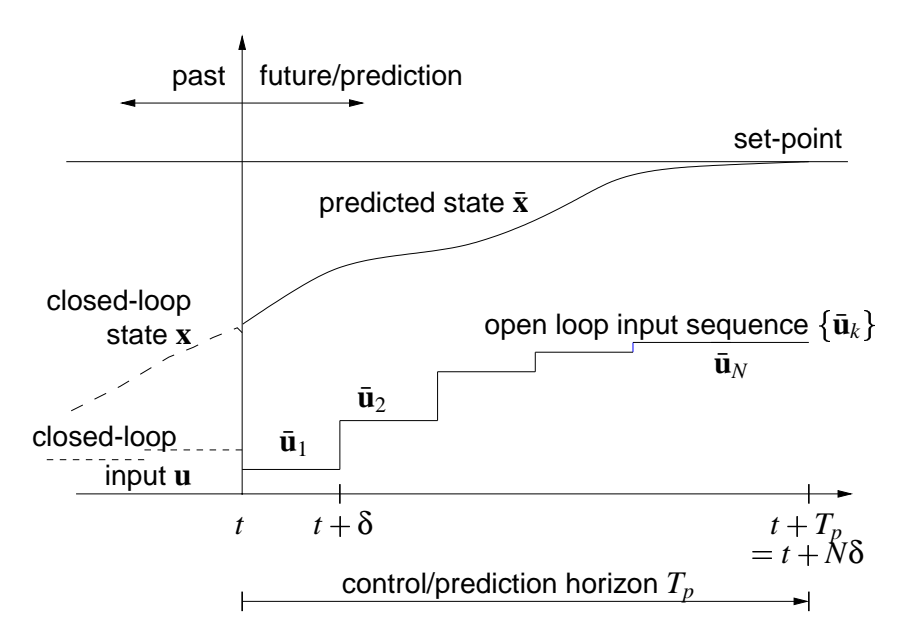


Figure 6: Piecewise constant input signal for the direct solution of the optimal control problem.

optimized, i.e. the optimization problem takes the form

$$\min_{\{\bar{\mathbf{u}}_1,\dots\bar{\mathbf{u}}_N\}} J(\mathbf{x}(t), \{\bar{\mathbf{u}}_1,\dots\bar{\mathbf{u}}_N\}; T_p)$$
(39)

subject to the state and input constraints and the system dynamics. Basically two different solution strategies to this optimization problem exist [8, 9, 13, 48, 74]:

- **Sequential approach:** In this method in every iteration step of the optimization strategy the differential equations (or in the discrete time case the difference equation) are solved exactly by a numerical integration, i.e. the solution of the system dynamics is implicitly done during the integration of the cost function and only the input vector $\{\bar{\mathbf{u}}_1, \dots \bar{\mathbf{u}}_N\}$ appears directly in the optimization problem.
- **Simultaneous approach:** In this approach the system dynamics (38a) at the sampling points enter as nonlinear constraints to the optimization problems, i.e. at every sampling point the following equality constraint must be satisfied:

$$\bar{\mathbf{s}}_{i+1} = \bar{\mathbf{x}}(t_{i+1}; \bar{\mathbf{s}}_i, \bar{\mathbf{u}}_i). \tag{40}$$

Here $\bar{\mathbf{s}}_i$ is introduced as additional degree in the optimization problem and describes the "initial" condition for the sampling interval i, compare also Figure 7. This constraint requires, once the optimization has converged,

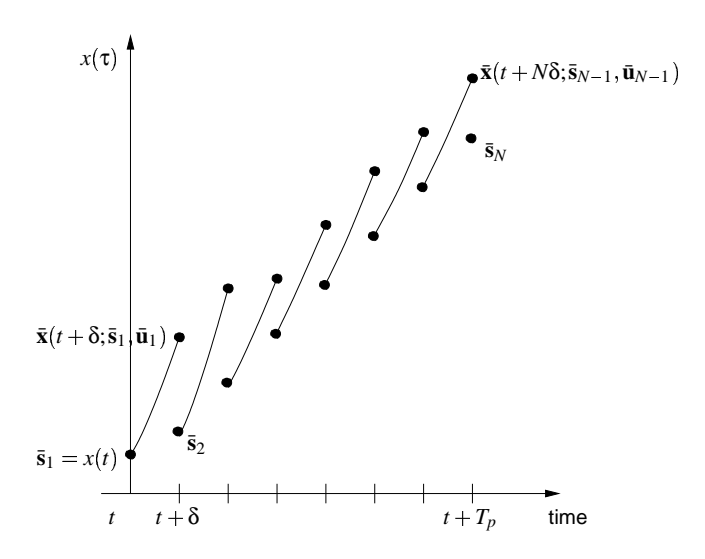


Figure 7: Simultaneous approach.

that the state trajectory pieces fit together. Thus additionally to the input vector $\{\bar{\mathbf{u}}_1, \dots \bar{\mathbf{u}}_N\}$ also the vector of the $\bar{\mathbf{s}}_i$ appears as optimization variables.

For both approaches the resulting optimization problem is often solved using sequential quadratic programming techniques (SQP). Both approaches have different advantages and disadvantages. For example the introduction of the "initial" states \bar{s}_i as optimization variables does lead to a special banded-sparse structure of the underlying QP-problem. This structure can be taken into account to lead to a fast solution strategy [8, 24, 74]. In comparison the matrices for the sequential approach are often dense and thus the solution is expensive to obtain. A drawback of the simultaneous approach is, that only at the end of the iteration a valid state trajectory for the system is available. Thus if the optimization cannot be finished in time, nothing can be said about the feasibility of the trajectory at all.

3.2.1 Remarks on State and Input Equality Constraints

In the description given above, the state and input constraints were not taken into account. The key problem is, that they should be satisfied for the whole state and input vector. While for a suitable parametrized input signal (e.g. parametrized as piecewise constant) it is not a problem to satisfy the constraints since only a finite number of points must be checked, the satisfaction of the state constraints must in general be enforced over the whole state trajectory. Different possibilities exist to consider them during the optimization:

• Satisfaction of the constraints at the sampling instances: An approximated satisfaction of the constraints can be achieved by requiring, that they are at least satisfied at the sampling instances, i.e. at the sampling times it is required:

$$\mathbf{l}(\bar{\mathbf{u}}(t_i), \bar{\mathbf{x}}(t_i)) \le \mathbf{0}. \tag{41}$$

Notice, that this does not guarantee that the constraints are satisfied for the predicted trajectories in between the sampling instances. However, since this approach is easy to implement it is often used in practice.

Adding a penalty in the cost function: An approach to enforce the constraint satisfaction exactly for the whole
input/state trajectory is to add an additional penalty term to the cost function. This term is zero as long as the
constraints are satisfied. Once the constraints are not satisfied the value of this term increases significantly, thus
enforcing the satisfaction of the constraints. The resulting cost function may look as following:

$$J(\mathbf{x}(t), \bar{\mathbf{u}}(\cdot); T_p) := \int_t^{t+T_p} \left(F(\bar{\mathbf{x}}(\tau), \bar{\mathbf{u}}(\tau)) + \mathbf{p}(\mathbf{l}(\bar{\mathbf{x}}(\tau)), \bar{\mathbf{u}}(\tau)) \right) d\tau + E(\bar{\mathbf{x}}(t+T_p))$$
(42)

where **p** in the case that only one nonlinear constraint is present might look like shown in Figure 8. A drawback

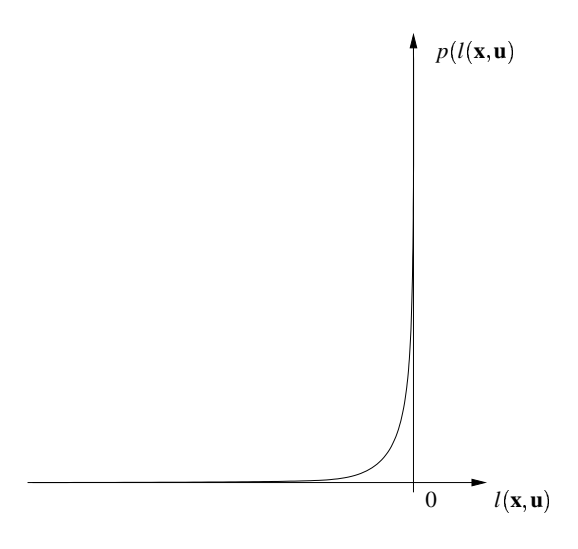


Figure 8: Constraint penalty function for one nonlinear constraint.

of this formulation is, that the resulting optimization problem is in general difficult to solve for example due to the resulting non-differentiability of the cost function outside the feasible region of attraction.

3.2.2 Efficient NMPC Formulations

One should notice, that besides an efficient solution strategy of the occurring open-loop optimal control problem the NMPC problem should be also formulated efficiently. Different possibilities for an efficient NMPC formulation exist:

- Use of short horizon length without loss of performance and stability [17, 34, 63]: As was outlined in Section 2 short horizons are desirable from a computational point of view, but long horizons are required for closed-loop stability and in order to achieve the desired performance in closed-loop. The general NMPC scheme outlined in Section 2.1.2 offers a way out of this dilemma. It uses a terminal region constraint in combination with a terminal penalty term. The terminal penalty term can be used to given a good approximation of the infinite horizon cost utilizing a local control law. Additionally the terminal region constraint is in general not very restrictive, i.e. does not complicate the dynamic optimization problem in an unnecessary manner, as for example in the zero terminal constraint approach. In some cases, e.g. stable systems, feedback linearizable systems or systems for which a globally valid control Lyapunov function is known it can even be removed. Thus such an approach offers the possibility to formulate a computationally efficient NMPC scheme with a short horizon while not sacrificing stability and performance.
- Use of suboptimal NMPC strategies, feasibility implies stability [17, 34, 56, 70]: In general no global minima of the open-loop optimization must be found. It is sufficient to achieve a decrease in the value function at every time to guarantee stability. Thus stability can be seen as being implied by feasibility. If one uses an optimization strategy that delivers feasible solutions at every sub-iteration and a decrease in the cost function, the optimization can be stopped if no more time is available and still stability can be guaranteed. The key

obstacle is that optimization strategies that guarantee a feasible and decreasing solution at every iteration are normally computationally expensive.

• Taking the system structure into account [2, 60, 61]: It is also noticeable, that the system structure should be taken into account. For example for systems for which a flat output is known the dynamic optimization problem can be directly reduced to a static optimization problem. This results from the fact that for flat systems the input and the system state can be given in terms of the output and its derivatives as well as the system initial conditions. The drawback however is, that the algebraic relation between the output and the derivatives to the states and inputs must be known, which is not always possible.

Combining the presented approaches for an efficient formulation of the NMPC problem and the efficient solution strategies of the optimal control problem, the application of NMPC to realistically sized applications is possible even with nowadays computational power. Besides the problem of stability of the closed-loop and the output-feedback problem, the efficient solution of the resulting open-loop optimal control problem is important for any application of NMPC to real processes. Summarizing, a real-time application of NMPC is possible [8, 29, 59] if: a) NMPC schemes that do not require a high computational load and do not sacrifice stability and performance, like QIH-NMPC, are used and b) the resulting structure of the open-loop optimization problem is taken into account during the numerical solution.

4 Application Example-Real-Time Feasibility of NMPC

To show that nonlinear predictive control can be applied to even rather large systems if efficient NMPC schemes and special tailored numerical solution methods are used, we give some results from a real-time feasibility study of NMPC for a high-purity distillation column as presented in [5, 24, 25, 59]. Figure 9 shows the in this study considered 40 tray high-purity distillation column for the separation of Methanol and n-Propanol. The binary mixture is fed in the

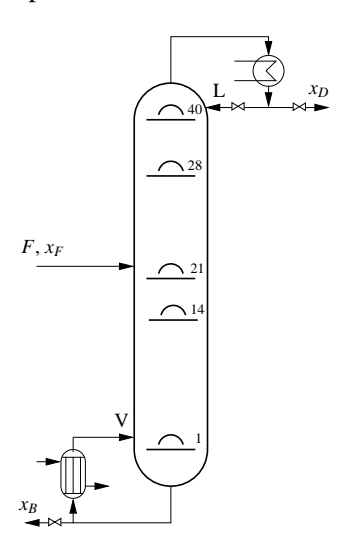


Figure 9: Scheme of the distillation column

column with flow rate F and molar feed composition x_F . Products are removed at the top and bottom of the column with concentrations x_B and x_D respectively. The column is considered in L/V configuration, i.e. the liquid flow rate L and the vapor flow rate V are the control inputs. The control problem is to maintain the specifications on the product concentrations x_B and x_D . For control purposes, models of the system of different complexity are available. As usual in distillation control, x_B and x_D are not controlled directly. Instead an inferential control scheme which controls the deviation of the concentrations on tray 14 and 28 from the setpoints is used, i.e. only the concentration deviations from the setpoint on trays 14 and 28 plus the inputs are penalized in the cost-function. The QIH-NMPC control scheme is used for control. The terminal region and terminal penalty term have been calculated as suggested in Sect. 2.1.3. In Table 1 the maximum and average CPU times necessary to solve one open-loop optimization problem for the QIH-NMPC scheme in case of a disturbance in x_F with respect to different model sizes are shown. Considering that the

Table 1: Comparison of the average and maximum CPU time in seconds necessary for the solution of one open-loop optimal control problem. The results are obtained using MUSCOD-II [12] and QIH-NMPC for models of different size. The prediction horizon of is 10 minutes and a controller sampling time $\delta = 30$ sec is used

model size	max	avrg
42	1.86s	0.89s
164	6.21s	2.48s

sampling time of the process control system connected to the distillation column is 30sec, the QIH-NMPC using the appropriate tool for optimization is even real-time feasible for the 164^{th} order model. Notice, that a straightforward solution of the optimal control problem for the 42^{nd} order model using the optimization-toolbox in Matlab needs in average 620sec to find the solution and is hence not real-time implementable. Also a numerical approximation of the infinite horizon problem by increasing the prediction horizon sufficiently enough is not real-time feasible as shown in [32]. More details and simulation results for the distillation column example can be found in [5, 24, 59]. First experimental results on a pilot scale distillation column are given in [25].

The presented case study underpins, that NMPC can be applied in practice already nowadays, if efficient numerical solution methods and efficient NMPC formulations (like QIH-NMPC) are used.

5 Conclusions

Model predictive control for linear constrained systems has been shown to provide an excellent control solution both theoretically and practically. The incorporation of nonlinear models poses a much more challenging problem mainly because of computational and control theoretical difficulties, but also holds much promise for practical applications. In this note an overview over the theoretical and computational aspects of NMPC is given. As outlined some of the challenges occurring in NMPC are already solvable. Nevertheless many unsolved questions remain. Here only a few are noticed as a guide for future research:

- Output feedback NMPC: While some first results in the area of output feedback NMPC exist, none of them
 seem to be applicable to real processes. Especially the incorporation of suitable state estimation strategies in the
 NMPC formulation must be further considered.
- **Robust NMPC Formulations:** By now a few robust NMPC formulations exist. While the existing schemes increase the general understanding they are computationally intractable to be applied in practice. Further research is required to develop implementable robust NMPC strategies.
- Industrial Applications of NMPC: The state of industrial application of NMPC is growing rapidly and seems to follow academically available results more closely than linear MPC. However, none of the NMPC algorithms provided by vendors include stability constraints as required by control theory for nominal stability; instead they rely implicitly upon setting the prediction horizon long enough to effectively approximate an infinite horizon. Future developments in NMPC control theory will hopefully contribute to making the gap between academic and industrial developments even smaller.

Acknowledgements

The authors gratefully acknowledge Lars Imsland and Bjarne Foss from the Department of Engineering Cybernetics, NTNU Trondheim, Norway for the ongoing cooperation in the area of output-feedback NMPC. Parts of Sect. 2.4 are based on this cooperation. Furthermore the authors would like to acknowledge the fruitful cooperation with Moritz Diehl, Hans Georg Bock and Johannes Schlöder from the Center for Scientific Computing (IWR) at the University of Heidelberg, Germany in the area of efficient solution of NMPC as outlined in Sect. 3 and Sect. 4.

- [1] M. Alamir. Optimization based nonlinear observers revisited. Int. J. Contr., 72(13):1204–1217, 1999.
- [2] M. Alamir and P. Bonard. Globally stabilising discontinuous feedback law for a class of nonlinear systems. *European J. of Control*, 1(2):44–50, 1996.
- [3] M. Alamir and G. Bornard. Stability of a truncated infinite constrained receding horizon scheme: The general discrete nonlinear case. *Automatica*, 31(9):1353–1356, 1995.
- [4] F. Allgöwer, T. A. Badgwell, J. S. Qin, J. B. Rawlings, and S. J. Wright. Nonlinear predictive control and moving horizon estimation An introductory overview. In P. M. Frank, editor, *Advances in Control, Highlights of ECC'99*, pages 391–449. Springer, 1999.
- [5] F. Allgöwer, R. Findeisen, Z. Nagy, M. Diehl, H.G. Bock, and J.P. Schlöder. Efficient nonlinear model predictive control for large scale constrained processes. In *Proceedings of the Sixth International Conference on Methods and Models in Automation and Robotics*, pages 43–54. Miedzyzdroje, Poland, 2000.
- [6] A.N. Atassi and H.K. Khalil. A separation principle for the stabilization of a class of nonlinear systems. *IEEE Trans. Automatic Control*, 44(9):1672–1687, 1999.
- [7] R. Bellman. Dynamic Programming. Princeton University Press, Princeton, New Jersey, 1957.
- [8] L. Biegler. Efficient solution of dynamic optimization and NMPC problems. In F. Allgöwer and A. Zheng, editors, *Nonlinear Predictive Control*, pages 219–244. Birkhäuser, 2000.
- [9] T. Binder, L. Blank, H.G. Bock, R. Burlisch, W. Dahmen, M. Diehl, T. Kronseder, W. Marquardt, J.P. Schlöder, and O. von Stryk. Introduction to model based optimization of chemical processes on moving horizons. In M. Groetschel, S.O. Krumke, and J. Rambau, editors, *Online Optimization of Large Scale Systems: State of the Art*, pages 295–339. Springer, 2001.
- [10] R. R. Bitmead, M. Gevers, and V. Wertz. *Adaptive Optimal Control The Thinking Man's GPC*. Prentice Hall, New York, 1990.
- [11] R. Blauwkamp and T. Basar. A receding-horizon approach to robust output feedback control for nonlinear systems. In *Proc. 38th IEEE Conf. Decision Contr.*, pages 4879–4884, San Diego, 1999.
- [12] H.G. Bock, M. Diehl, D. Leineweber, and J. Schlöder. A direct multiple shooting method for real-time optimization of nonlinear DAE processes. In F. Allgöwer and A. Zheng, editors, *Nonlinear Predictive Control*, pages 245–268. Birkhäuser, 2000.
- [13] H.G. Bock, M. Diehl, J.P. Schlöder, F. Allgöwer, R. Findeisen, and Z. Nagy. Real-time optimization and nonlinear model predictive control of processes governed by differential-algebraic equations. In *Proc. Int. Symp. Adv. Control of Chemical Processes*, *ADCHEM*, pages 695–703, Pisa, Italy, 2000.
- [14] H. Chen. Stability and Robustness Considerations in Nonlinear Model Predictive Control. Fortschr.-Ber. VDI Reihe 8 Nr. 674. VDI Verlag, Düsseldorf, 1997.
- [15] H. Chen and F. Allgöwer. A quasi-infinite horizon predictive control scheme for constrained nonlinear systems. In *Proc. 16th Chinese Control Conference*, pages 309–316, Qindao, 1996.
- [16] H. Chen and F. Allgöwer. Nonlinear model predictive control schemes with guaranteed stability. In R. Berber and C. Kravaris, editors, *Nonlinear Model Based Process Control*, pages 465–494. Kluwer Academic Publishers, Dodrecht, 1998.
- [17] H. Chen and F. Allgöwer. A quasi-infinite horizon nonlinear model predictive control scheme with guaranteed stability. *Automatica*, 34(10):1205–1218, 1998.
- [18] H. Chen, C.W. Scherer, and F. Allgöwer. A game theoretic approach to nonlinear robust receding horizon control of constrained systems. In *Proc. Amer. Contr. Conf.*, pages 3073–3077, Albuquerque, 1997.

- [19] H. Chen, C.W. Scherer, and F. Allgöwer. A robust model predictive control scheme for constrained linear systems. In 5th IFAC Symposium on Dynamics and Control of Process Systems, DYCOPS-5, pages 60–65, Korfu, 1998.
- [20] G. De Nicolao, L. Magni, and R. Scattolini. Stabilizing nonlinear receding horizon control via a nonquadratic terminal state penalty. In *Symposium on Control, Optimization and Supervision, CESA'96 IMACS Multiconference*, pages 185–187, Lille, 1996.
- [21] G. De Nicolao, L. Magni, and R. Scattolini. Stabilizing receding-horizon control of nonlinear time-varying systems. In *Proc. 4rd European Control Conference ECC'97*, Brussels, 1997.
- [22] G. De Nicolao, L. Magni, and R. Scattolini. Stability and robustness of nonlinear receding horizon control. In F. Allgöwer and A. Zheng, editors, *Nonlinear Predictive Control*, pages 3–23. Birkhäuser, 2000.
- [23] S. de Oliveira Kothare and M. Morari. Contractive model predictive control for constrained nonlinear systems. *IEEE Trans. Automat. Contr.*, 45(6):1053–1071, 2000.
- [24] M. Diehl, R. Findeisen, Z. Nagy, H.G. Bock, J.P. Schlöder, and F. Allgöwer. Real-time optimization and nonlinear model predictive control of processes governed by differential-algebraic equations. *J. Proc. Contr.*, 2002. In press.
- [25] M. Diehl, I. Uslu, R. Findeisen, S. Schwarzkopf, F. Allgöwer, H.G. Bock, T. Bürner, E.D. Gilles, A. Kienle, J.P. Schlöder, and E. Stein. Real-time optimization of large scale process models: Nonlinear model predictive control of a high purity distillation column. In M. Groetschel, S.O. Krumke, and J. Rambau, editors, *Online Optimization of Large Scale Systems: State of the Art*, pages 363–384. Springer, 2001.
- [26] F. Esfandiari and H.K. Khalil. Output feedback stabilization of fully linearizable systems. *Int. J. Control*, 56(5):1007–1037, 1992.
- [27] R. Findeisen and F. Allgöwer. Nonlinear model predictive control for index–one DAE systems. In F. Allgöwer and A. Zheng, editors, *Nonlinear Predictive Control*, pages 145–162. Birkhäuser, Basel, 1999.
- [28] R. Findeisen and F. Allgöwer. A nonlinear model predictive control scheme for the stabilization of setpoint families. *Journal A, Benelux Quarterly Journal on Automatic Control*, 41(1):37–45, 2000.
- [29] R. Findeisen, F. Allgöwer, M. Diehl, H.G. Bock, J.P. Schlöder, and Z. Nagy. Efficient nonlinear model predictive control. In 6th International Conference on Chemical Process Control CPC VI, pages 454–460, 2000.
- [30] R. Findeisen, H. Chen, and F. Allgöwer. Nonlinear predictive control for setpoint families. In *Proc. Amer. Contr. Conf.*, pages 260–4, Chicago, 2000. ACC.
- [31] R. Findeisen, L. Imsland, F. Allgöwer, and B.A. Foss. Output feedback nonlinear Predictive control -a separation principle approach. To appear in proceedings of 15th IFAC World Congress, 2001.
- [32] R. Findeisen, Z. Nagy, M. Diehl, F. Allgöwer, H.G. Bock, and J.P. Schlöder. Computational feasibility and performance of nonlinear model predictive control. In *Proc. 6st European Control Conference ECC'01*, pages 957–961, Porto, Portugal, 2001.
- [33] R. Findeisen and J.B. Rawlings. Suboptimal infinite horizon nonlinear model predictive control for discrete time systems. Technical Report # 97.13, Automatic Control Laboratory, Swiss Federal Institute of Technology (ETH), Zürich, Switzerland, 1997. *Presented at the NATO Advanced Study Institute on Nonlinear Model Based Process Control*.
- [34] F.A. Fontes. A general framework to design stabilizing nonlinear model predictive controllers. *Syst. Contr. Lett.*, 42(2):127–143, 2000.
- [35] E. Gurkovics. Receding horizon control via bolza-type optimization. Syst. Contr. Lett., 35(2):195–200, 1998.

- [36] L. Imsland, R. Findeisen, E. Bullinger, F. Allgöwer, and B.A. Foss. A note on stability, robustness and performance of output feedback nonlinear model predictive control. Accepted for publication in *J. Proc. Contr.*, 2001.
- [37] L. Imsland, R. Findeisen, E. Bullinger, F. Allgöwer, and B.A. Foss. On output feedback nonlinear model predictive control using high gain observers for a class of systems. In *6th IFAC Symposium on Dynamics and Control of Process Systems*, *DYCOPS-6*, pages 91–96, Jejudo, Korea, 2001.
- [38] A. Jadbabaie, J. Yu, and J. Hauser. Unconstrained receding horizon control of nonlinear systems. *IEEE Trans. Automat. Contr.*, 46(5):776 –783, 2001.
- [39] S.S. Keerthi and E.G. Gilbert. Optimal infinite-horizon feedback laws for a general class of constrained discrete-time systems: Stability and moving-horizon approximations. *J. Opt. Theory and Appl.*, 57(2):265–293, 1988.
- [40] D.L. Kleinman. An easy way to stabilize a linear constant system. *IEEE Trans. Automat. Contr.*, 15:692, 1970.
- [41] J.H. Lee and B. Cooley. Recent advances in model predictive control and other related areas. In J.C. Kantor, C.E. Garcia, and B. Carnahan, editors, *Fifth International Conference on Chemical Process Control CPC V*, pages 201–216. American Institute of Chemical Engineers, 1996.
- [42] L. Magni, D. De Nicolao, and R. Scattolini. Output feedback receding-horizon control of discrete-time nonlinear systems. In *Preprints of the 4th Nonlinear Control Systems Design Symposium 1998 - NOLCOS'98*, pages 422–427. IFAC, July 1998.
- [43] L. Magni, G. De Nicolao, and R Scattolini. Output feedback and tracking of nonlinear systems with model predictive control. *Automatica*, 37(10):1601–1607, 2001.
- [44] L. Magni, G. De Nicolao, and R Scattolini. A stabilizing model-based predicitve control algorithm for nonlinear systems. *auto*, 37(10):1351–1362, 2001.
- [45] L. Magni, G. De Nicolao, R. Scattolini, and F. Allgöwer. Robust receding horizon control for nonlinear discrete-time systems. To appear in Proceedings 15th IFAC World Congress, 2002, 2001.
- [46] L. Magni, H. Nijmeijer, and A.J. van der Schaft. A receding-horizon approach to the nonlinear h_{∞} control problem. *auto*, 37(5):429–435, 2001.
- [47] L. Magni and R. Sepulchre. Stability margins of nonlinear receeding–horizon control via inverse optimality. *Syst. Contr. Lett.*, 32(4):241–245, 1997.
- [48] D.Q. Mayne. Optimization in model based control. In *Proc. IFAC Symposium Dynamics and Control of Chemical Reactors, Distillation Columns and Batch Processes*, pages 229–242, Helsingor, 1995.
- [49] D.Q. Mayne. Nonlinear model predictive control: An assessment. In J.C. Kantor, C.E. Garcia, and B. Carnahan, editors, *Fifth International Conference on Chemical Process Control CPC V*, pages 217–231. American Institute of Chemical Engineers, 1996.
- [50] D.Q. Mayne. Nonlinear model predictive control. In F. Allgöwer and A. Zheng, editors, *Nonlinear Predictive Control*, pages 24–44. Birkhäuser, 2000.
- [51] D.Q. Mayne and H. Michalska. Receding horizon control of nonlinear systems. *IEEE Trans. Automat. Contr.*, 35(7):814–824, 1990.
- [52] D.Q. Mayne, J.B. Rawlings, C.V. Rao, and P.O.M. Scokaert. Constrained model predictive control: stability and optimality. *Automatica*, 26(6):789–814, 2000.
- [53] E.S. Meadows, M.A. Henson, J.W. Eaton, and J.B. Rawlings. Receding horizon control and discontinuous state feedback stabilization. *Int. J. Contr.*, 62(5):1217–1229, 1995.
- [54] E.S. Meadows and J.B. Rawlings. Receding horizon control with an infinite horizon. In *Proc. Amer. Contr. Conf.*, pages 2926–2930, San Francisco, 1993.

- [55] H. Michalska. A new formulation of receding horizon stabilizing control without terminal constraint on the state. *European J. of Control*, 3(1):1–14, 1997.
- [56] H. Michalska and D.Q. Mayne. Robust receding horizon control of constrained nonlinear systems. *IEEE Trans. Automat. Contr.*, AC-38(11):1623–1633, 1993.
- [57] H. Michalska and D.Q. Mayne. Moving horizon observers and observer-based control. *IEEE Trans. Automat. Contr.*, 40(6):995–1006, 1995.
- [58] M. Morari and J.H. Lee. Model predicitve control: Past, present and future. *Comp. and Chem. Eng.*, 23(4/5):667–682, 1999.
- [59] Z. Nagy, R. Findeisen, M. Diehl, F. Allgöwer, H.G. Bock, S. Agachi, J.P. Schlöder, and D. Leineweber. Real-time feasibility of nonlinear predictive control for large scale processes a case study. In *Proc. Amer. Contr. Conf.*, pages 4249–4254, Chicago, 2000. ACC.
- [60] V. Nevistić and M. Morari. Constrained control of feedback-linearizable systems. In *Proc. 3rd European Control Conference ECC*'95, pages 1726–1731, Rome, 1995.
- [61] N. Petit, M.B. Miliam, and R.M. Murray. Inversion based contrained trajectory optimization. In *Nonlinear Control Systems Design Symposium 2001 NOLCOS'01*. IFAC, July 2001.
- [62] E. Polak and T.H. Yang. Moving horizon control of linear systems with input saturation and plant uncertainty. Part 1. Robustness. *Int. J. Contr.*, 58(3):613–638, 1993.
- [63] J. Primbs, V Nevistić, and J. Doyle. Nonlinear optimal control: A control Lyapunov function and receding horizon perspective. *Asian Journal of Control*, 1(1):14–24, 1999.
- [64] S.J. Qin and T.A. Badgwell. An overview of industrial model predictive control technology. In J.C. Kantor, C.E. Garcia, and B. Carnahan, editors, *Fifth International Conference on Chemical Process Control CPC V*, pages 232–256. American Institute of Chemical Engineers, 1996.
- [65] S.J. Qin and T.A. Badgwell. An overview of nonlinear model predictive control applications. In F. Allgöwer and A. Zheng, editors, *Nonlinear Predictive Control*, pages 369–393. Birkhäuser, 2000.
- [66] C.V. Rao. *Moving Horizon Estimation of Constrained and Nonlinear Systems*. PhD thesis, University of Wisconsin–Madison, 1999.
- [67] C.V. Rao, J.B. Rawlings, and D.Q. Mayne. Constrained state estimation for nonlinear discrete-time systems: Stability and moving horizon approximations. Submitted for publication in *IEEE Transactions on Automatic Control*, 1999.
- [68] J. B. Rawlings. Tutorial overview of model predictive control. *IEEE Contr. Syst. Magazine*, 20(3):38–52, 2000.
- [69] D.G. Robertson and J.H. Lee. A least squares formulation for state estimation. *J. Proc. Contr.*, 5(4):291–299, 1995.
- [70] P.O.M. Scokaert, D.Q. Mayne, and J.B. Rawlings. Suboptimal model predictive control (feasibility implies stability). *IEEE Trans. Automat. Contr.*, 44(3):648–654, 1999.
- [71] P.O.M. Scokaert, J.B. Rawlings, and E.S. Meadows. Discrete-time stability with perturbations: Application to model predictive control. *Automatica*, 33(3):463–470, 1997.
- [72] A. Teel and L. Praly. Tools for semiglobal stabilization by partial state and output feedback. *SIAM J. Control and Optimization*, 33(5):1443–1488, 1995.
- [73] A. Tornambè. High-gain observers for non-linear systems. Int. J. of Systems Science, 23(9):1475–1489, 1992.
- [74] S. J. Wright. Applying new optimization algorithms to model predictive control. In J.C. Kantor, C.E. Garcia, and B. Carnahan, editors, *Fifth International Conference on Chemical Process Control CPC V*, pages 147–155. American Institute of Chemical Engineers, 1996.
- [75] G. Zimmer. State observation by on-line minimization. *Int. J. Contr.*, 60(4):595–606, 1994.

Adaptive λ -tracking for higher relative degree systems

Eric Bullinger

Frank Allgöwer

Institut für Systemtheorie technischer Prozesse, Universität Stuttgart, 70550 Stuttgart, Deutschland, {bullinger,allgower}@ist.uni-stuttgart.de

Keywords: lambda-tracking, adaptive control, high-gain, robust stability, universal stabilization.

Abstract

This paper proposes a relatively simple adaptive controller for systems with higher relative degree. Only little information on the system is needed: only the relative degree and a lower bound on the positive high-frequency gain. The zero-dynamics does not need to be asymptotically stable, boundedness is sufficient. The controller achieves λ -tracking for a large class of nonlinear systems and consists of a high-gain observer, a high-gain observer-state feedback and a common adaptation of both high-gain parameters. The adaptation increases the gains of the observer and the state-feedback whenever the control objective, namely that the tracking error is of magnitude not larger than λ , is not attained. The controller's adaptation converges and the control objective is achieved at least asymptotically.

1 Motivation

For many control applications, good models are not available or their parameters are not precisely known. A possibility to control these systems is to use an adaptive λ -tracking controller. For designing this controller, only the knowledge of the model structure, not of precise parameter values is needed. Therefore, the controller is robust for a large class of uncertainties. In particular, the relative degree of the system is needed and has to be strong. The controller order is equal to the relative degree, independently of the system dimension. The zero-dynamics of the system can be locally unstable, asymptotic stability is only required n the large. The last piece of information needed is a lower bound of the high-frequency gain. Together, this enables the stabilization of a relatively large class of systems.

Exact tracking is not required for many applications. Based on the necessary performance and on the measurement quality, the user can specify a tolerance for the tracking error which should be achieved. The objective of λ -tracking is that the tracking error asymptotically tends to $[-\lambda, \lambda]$ where λ is a tolerance specified by the user.

Most controllers achieving λ -tracking can only be used for systems having a relative degree of one. The adaptive λ -tracking controller proposed in this thesis extends the system class to systems with higher relative degree. This is achieved by having in the controller an observer which estimates the output of the system and its first r-1 derivatives. Another component of the controller is an observer-based state-feedback. Both the controller and the state-feedback include a high-gain parameter, the controller gain k. For a sufficiently large value of this parameter, the controller is guaranteed to achieve λ -tracking. Instead of fixing this parameter a priori, the following adaptation scheme is used. The parameter k is increased if the output is outside of the λ -strip and kept constant within. This allows to start with a relatively small value for k and, nevertheless, being robust for a large class of uncertainties.

A further advantage of the proposed adaptive λ -tracking controller is its relatively simple structure which is helpful for implementing it and for understanding how the controller works. The main drawbacks of the adaptive λ -tracking controller are that the performance is not directly addressed and that the parameter k might become large. On the one hand, this increases the sensitivity to measurement noise. Also peaking is then more likely. On the other hand, a small k usually means that the tracking error is for quite a long time relatively large.

1.1 λ -tracking

A classical control objective is to asymptotically regulate the output y of a system to a constant reference y_{ref} , i.e. for $y(t) \in \mathbb{R}$

$$y(t) \to y_{ref}$$
 for $t \to \infty$.

In many practical applications, such an objective is either not achievable or too restrictive. Instead, a certain output error is often a better choice. For example, if an upper and lower bound for a temperature during normal operation is specified, why should the controller keep the temperature constant up to the precision of the thermometer? Asymptotic λ -stabilization, usually just called λ -stabilization, is a suitable control objective for such applications. The output is not required to converge exactly to the steady-state y_{ref} , but to a ball of radius $\lambda > 0$ around it, i.e. for $y(t) \in \mathbb{R}$,

$$y(t) - y_{ref} \to [-\lambda, +\lambda] \text{ for } t \to \infty,$$

see also Figure 1.

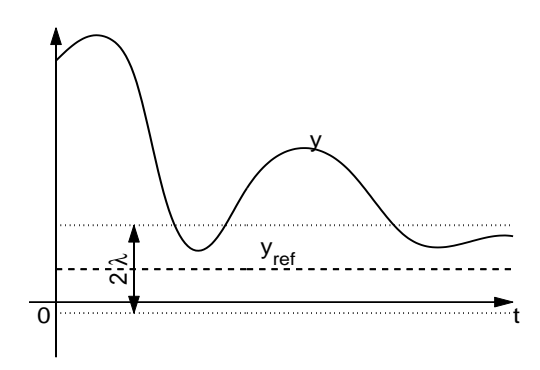


Figure 1: Sketch of λ -stabilization. Output y in solid, reference y_{ref} in dashed, λ -strip as dotted lines.

The concept of approximate tracking was introduced in the field of adaptive controllers in [17]. The term λ -tracking was coined in [13], (see also [12, 20]). If the reference is a steady-state, then this control objective is called λ -stabilization [20].

A classical example of approximate tracking is relay controllers that stabilize a system up to a limit cycle (see for example [11, 9]). If the limit cycle lies inside the λ -strip, this is a sort of λ -stabilization. Another well established result is the steady-state offset: Linear systems without an open-loop pole at the origin do not converge to a constant, non-zero reference under proportional control (see for example [24]). Closely related is also the concept of strong practical stability [16]. In contrary to λ -tracking, where the λ -strip is only attractive, strong practical stability also requires the λ -strip to be invariant, i.e. that the output does not leave the λ -strip and that the output error during the transient can be made arbitrarily small. Thus, it guarantees that there is no peaking (see [22])

Another method achieving asymptotic output tracking is to include a model of the reference signal in the controller (internal model principle, see [10]). For minimum phase, relative degree one systems, asymptotic tracking can also be achieved without an internal model by using a discontinuous controller of the following form [19]

$$u = -k((y - y_{ref}) + sign(y - y_{ref}))$$

for a sufficiently large k. This controller is similar to sliding mode controllers (see for example [15]), where $y - y_{ref}$ is equivalent to the height above the sliding surface $\{x|y(x) - y_{ref} = 0\}$. Such a controller requires arbitrary fast switching and will usually lead to chattering. Therefore, for many applications, a continuous controller is preferable. Such a controller is proposed in the following.

1.2 High-gain

The proposed controller achieves λ -tracking by increasing a gain as much as necessary. This gain increase leads to robustness against model uncertainties. An important condition in this context is high-gain stabilizability which is defined in Definition 1 below and illustrated by the following example.

A very simple feedback is the following proportional output feedback:

$$u = -ky. (1)$$

This controller has only one parameter, namely k. It can for example be used to stabilize linear systems of dimension one, i.e.

$$\dot{y} = \alpha y + \beta u \tag{2}$$

with positive high-frequency gain β . It is easy to see that if a specific system (2) can be stabilized by the controller (1) with $k = k^*$, then also any larger k stabilizes (2). A controller with this property is called high-gain controller, see Definition 1 below.

Definition 1 (High-gain controller, parameter, stabilization) A controller parameterized by a single parameter k stabilizing a given system for any $k \ge k^*$ is called high-gain controller, its parameter k high-gain parameter. A system stabilizable by a high-gain controller is called high-gain stabilizable.

Definition 1 is a generalization of the definition in [8, 12] where the controller is a static output feedback.

The main restriction of the controller (1) is that this high-gain controller can only be used for systems of relative degree one and some of relative degree two (see e.g. [8, 3]).

2 Setup

This section first presents the system class the proposed adaptive observer-based state-feedback controller can be applied to. Then the controller components, the observer, the state-feedback and the adaptation are presented separately.

2.1 System class

The proposed controller is applicable to single-input single-output systems that are affine in the input:

$$\dot{x} = f(x) + g(x) \cdot u, \quad x \in \mathbb{R}^n, \tag{3a}$$

$$y = h(x). (3b)$$

For the results to hold, the following assumptions on the system must be satisfied.

Assumption 1 (Known relative degree) The relative degree r is known and strong, i.e. for all $x \in \mathbb{R}^n$

$$L_g L_f^i h(x) \equiv 0, i = 0, \dots, r - 2,$$

 $g(x) = L_g L_f^{r-1} h(x) \neq 0.$ (4)

Assumption 2 (Positive high-frequency gain) The high-frequency gain g(x) is strictly positive and globally bounded away from zero by some known constant g > 0,

$$g(x) \ge g$$
 for all $x \in \mathbb{R}^n$.

The following definition is needed for describing the system class.

Definition 2 (Affine sector bound) A function $f: \mathbb{R}^n \to \mathbb{R}^n$ is in the set \mathcal{A} if for some m > 0 it can be decomposed as

$$f(x) = f_0(x) + F(x)x, f_0(\cdot) : \mathbb{R}^n \to \mathbb{R}^n, F(\cdot) : \mathbb{R}^n \to \mathbb{R}^{n \times n},$$

where for all $x \in \mathbb{R}^n$

$$||f_0(x)|| < m, ||F(x)|| < m.$$

Remark 1 Special cases of functions $f(.) \in A$ are functions satisfying for some constants m_1 , m_2

$$||f(x)|| < m_1 + m_2 ||x||,$$

or

$$\lim_{\|x\| \to \infty} \frac{\|f(x)\|}{\|x\|} = m_2.$$

Therefore, the class \mathcal{A} is a generalization of sector bounded nonlinearities. Figure 2 shows a sketch of a possible one-dimensional function.

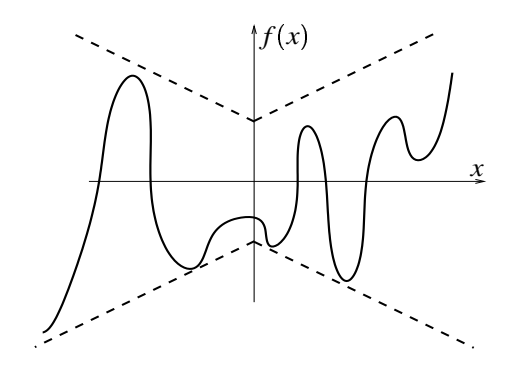


Figure 2: Example of a one-dimensional function $f \in \mathcal{A}$.

This enables to state the main assumption on the system class.

Assumption 3 (Bounded nonlinearities) There exists a coordinate transformation $[\xi^T, \eta^T]^T = T(x)$ transforming (3) into input-normalized Byrnes-Isidori normal form (5) (see [6, 7, 14])

$$y = \xi_1$$

$$\dot{\xi}_i = \xi_{i+1} \quad \text{for } i = 1, \dots, r-1$$

$$\dot{\xi}_r = \alpha(\xi, \eta) + g(\xi, \eta)u$$

$$\dot{\eta} = \tilde{\theta}(\xi, \eta)$$
(5)

with

$$\xi(t) = \left[\xi_1(t), \dots, \xi_r(t)\right]^T \in \mathbb{R}^r$$

$$\eta(t) \in \mathbb{R}^{n-r},$$

where the following conditions hold:

- 1. $\alpha(\cdot) \in \mathcal{A}$,
- 2. $g(\cdot)$ is bounded,
- 3. $\tilde{\theta}(\cdot, \xi_2, \dots, \xi_r, \eta) \in \mathcal{A} \text{ for all } (\xi_2, \dots, \xi_r, \eta) \in \mathbb{R}^{n-1}$,
- 4. $\tilde{\theta}(\xi_1,\cdot,\ldots,\cdot)$ is bounded for all $\xi_1 \in \mathbb{R}$

Assumption 4 (Zero dynamics) The zero-dynamics of (5) can be decomposed as

$$\dot{\eta} = \tilde{\theta}(0, \eta) = \theta(\eta) + \tilde{w}(\eta)$$

where $\tilde{w}(\cdot)$ is bounded and the dynamics $\dot{\eta} = \theta(\eta)$ are globally exponentially stable.

Under Assumption 3 and 4, (5) can be rewritten as

$$\dot{\xi} = J\xi + b(\mathbf{y}^T(\xi, \mathbf{\eta})\xi + \mathbf{\phi}^T(\xi, \mathbf{\eta})\mathbf{\eta} + g(\xi, \mathbf{\eta})u + v(\xi, \mathbf{\eta})))$$
(6a)

$$\dot{\eta} = \chi(\xi, \eta)y + \theta(\eta) + w(\xi, \eta) \tag{6b}$$

$$y = c^T \xi, \tag{6c}$$

with $\xi(t) \in \mathbb{R}^r$, $\eta(t) \in \mathbb{R}^{n-r}$ and

$$J = \begin{bmatrix} 0 & 1 & 0 \\ & & \ddots \\ & & & 1 \\ & & & 0 \end{bmatrix}, \ b = \begin{bmatrix} 0 \\ \vdots \\ 0 \\ 1 \end{bmatrix},$$

$$c^{T} = \begin{bmatrix} 1 & 0 & \dots & 0 \end{bmatrix}.$$

All functions are bounded:

$$g(\xi, \eta) \ge \underline{g}, v, \theta, w, \chi, \phi, \psi \in \mathcal{L}_{\infty}(\mathbb{R}^n).$$

Remark 2 In [21] it is shown that any linear system with relative degree r is transformable into

$$\dot{\xi} = J\xi + b(\psi^T \xi + \phi^T \eta + gu)$$
$$\dot{\eta} = \chi y + H\eta$$
$$y = c^T \xi.$$

The system (6) can be seen as a nonlinear generalization of this.

\Diamond

2.2 Objective

The control objective is to asymptotically track a reference signal $y_{ref}(\cdot)$ while tolerating a tracking error smaller than a user-defined λ (λ -tracking):

$$|y-y_{ref}| \to [0,\lambda].$$

All states should remain bounded, i.e. $x \in \mathcal{L}_{\infty}([0,\infty))$. The reference signal $y_{ref}(\cdot)$ is considered to be in $W^{r,\infty}$, the set of all bounded functions that are absolutely continuous on compact subintervals and whose first r derivatives are essentially bounded.

For the given system and objective, an adaptive output-feedback "state-space" controller is designed. It consists of an adaptive high-gain observer and an adaptive high-gain state-feedback controller, described in the following.

3 Controller structure

The adaptive λ -tracking controller can be decomposed into a high-gain observer (Section 3.1) and a high-gain state-feedback (Section 3.2). The adaptation of the gains is described in Section 3.3.

3.1 Full-order observer

The observer is an adaptive version of the high-gain observer introduced by [18] (see also [23]) as proposed in [5]. The observer is presented in observability normal form [26] and given by

$$\dot{\hat{x}} = \hat{A}_{\hat{\kappa}}\hat{x} + p_{\hat{\kappa}}e \tag{7a}$$

$$e = y - y_{ref} \tag{7b}$$

with $\hat{x}(t) \in \mathbb{R}^r$ and

$$\hat{A}_{\hat{\kappa}} = J - p_{\hat{\kappa}} c^T, \ p_{\hat{\kappa}} = \begin{bmatrix} p_{r-1} \cdot \hat{\kappa} & p_{r-2} \cdot \hat{\kappa}^2 & \dots & p_1 \cdot \hat{\kappa}^{r-1} & p_0 \cdot \hat{\kappa}^r \end{bmatrix}^T.$$

The parameters p_i are chosen such that $p(s) = s^r + \sum_{i=0}^{r-1} p_i s^i$ is Hurwitz. For any positive value of the observer gain $\hat{\kappa}$, the spectrum of $\hat{A}_{\hat{\kappa}}$ lies in the open left half plane and the observer dynamics are stable. No further knowledge of the system besides that of the relative degree is needed for the design of this observer. The observer gain $\hat{\kappa}$ is adapted according to the adaptation law described below.

3.2 Observer-state feedback controller

The controller is an observer-state feedback

$$u = -q_{\kappa}\hat{x},\tag{8}$$

where

$$q_{\kappa} = \begin{bmatrix} q_0 \cdot \kappa^r, & \cdots, & q_{r-1} \cdot \kappa \end{bmatrix}^T$$

The parameters q_i are chosen such that

$$q_g(s) = s^r + g \sum_{i=0}^{r-1} q_i s^i$$
 (9)

is Hurwitz for all $g \ge \underline{g}$ where \underline{g} is a lower bound of the high-frequency gain of the system. A root-locus argument in g shows that $q_g(s)$ is Hurwitz for all $g \ge g$ if and only if $\sum_{i=0}^{r-1} q_i s^i$ is Hurwitz and the q_i are sufficiently small.

The adaptation law for the controller gain κ is described below.

3.3 Gain adaptation

The adaptation for the observer gain $\hat{\kappa}$ and the controller gain κ is chosen such that the gains are increased as long as the amplitude of the tracking error e is larger than the user-defined bound λ (the control objective).

The observer and controller gains are given by

$$\hat{\kappa} = k^{\alpha} \tag{10a}$$

$$\kappa = k^{\beta} \tag{10b}$$

where the parameters α and β have to satisfy

$$\alpha > \beta > 0. \tag{11}$$

For given polynomials $p(\cdot)$ and $q_{\tilde{g}}(\cdot)$, there exist positive constants ε and μ such that for all $\tilde{g} \geq \underline{g}$, $p(\cdot)$ and $q_{\tilde{g}}(\cdot)$ are in $H(\varepsilon,\mu)$, see Appendix C. The parameters ε and μ can be interpreted as a measure of robustness with respect to time scaling for ε and the decay rate of the differential equation corresponding to the polynomial for μ .

With some $\lambda > 0$, $\gamma > 0$ and $k(0) = k_0 > 0$, the adaptation parameter k satisfies the differential equation:

$$\dot{k} = d_{\lambda}^2(e, k),\tag{12a}$$

$$d_{\lambda}(e,k) = \frac{\gamma}{k^{\tilde{\gamma}}} \begin{cases} |e| - \lambda & \text{for } |e| > \lambda, \\ 0 & \text{for } |e| \le \lambda, \end{cases}$$
 (12b)

where $\tilde{\gamma}$ has to satisfy

$$\tilde{\gamma} > 2\alpha\varepsilon + (\alpha - \beta)(2r - 3) - \frac{1}{2}$$
 for $r > 1$, (12c)

$$\tilde{\gamma} \ge 2\beta \varepsilon - \frac{1}{2}$$
 for $r = 1$. (12d)

Remark 3 The parameters α and β can be used to tune individually the "gains" of the observer and the controller, respectively. The adaptation law ensures a monotonic increase of the observer and controller gains. Also the observer gain $\hat{\kappa}$ grows faster than the controller gain κ for $k \geq 1$.

The parameter $\tilde{\gamma}$ slows down the adaptation, particularly when k is large. Its lower bound depends on the relative degree, the choice of the exponents α and β and on the polynomials $p(\cdot)$ and $q(\cdot)$. For systems with relative degree one, ε can be chosen to be zero, and $\tilde{\gamma}=0$ is a valid choice for the relative degree one case.

4 Result on λ -tracking and convergence of the adaptation

The main result is Theorem 1 stating that the combination of the adaptive observer (7) with the adaptive controller (8) and using the adaptation law (12) with (10) and (11) to close the loop for an arbitrary system satisfying Assumptions 1 to 4 yields asymptotic convergence of the tracking error to the λ -strip. Furthermore, the adaptation converges, no finite escape time can occur and all states remain bounded.

Theorem 1 (Full-order adaptive λ-tracking controller)

Define the constants $\varepsilon > 0$ and $\mu > 0$ so that the polynomials $p(\cdot)$ and $q_{\tilde{g}}(\cdot)$ are in $H(\varepsilon,\mu)$ for all $\tilde{g} \geq \underline{g}$. Then the application of the λ -tracking controller (7), (8), (12) with $\hat{\kappa} = k^{\alpha}$, $\kappa = k^{\beta}$ and $\alpha > \beta > 0$ to any system satisfying Assumptions 1 to 4 with any reference signal $y_{ref}(\cdot) \in W^{r,\infty}$ results in a closed-loop system which, independently of the initial values $x(0) \in \mathbb{R}^n$, $\hat{x}(0) \in \mathbb{R}^r$ and k(0) > 0 has a unique solution existing on the whole half axis $t \in [0,\infty)$ and, moreover,

- a) $(x(\cdot), \hat{x}(\cdot), k(\cdot)) \in \mathcal{L}_{\infty}([0, \omega)),$
- b) $\lim_{t\to\infty} |y(t) y_{ref}(t)| \le \lambda$.

The proof of Theorem 1 consists of five steps. The first part shows that k cannot go to infinity on the maximal domain of existence. Then, boundedness of the observer states \hat{x} and thus of the plant input u is proven. Part three shows boundedness of the plant states x. Step four yields that the solution of the differential equations exists for all times. A consequence of the first and fourth step is the convergence of the adaptation parameter k and by that of κ and κ . The proof concludes by showing that the tracking error converges to the λ -strip.

Proof (of Theorem 1)

1.a) Boundedness of the adaption parameters. Since this part of the proof is rather tedious, a short sketch of the proof is given. First, the closed loop is transformed into a coordinate system with states for the tracking and the observer error and their time-derivatives (\bar{x} -coordinates). Then a k-dependent time scaling is applied (\bar{x} -coordinates). In the resulting coordinates it is possible to define a Lyapunov-like function V such that it can be used to bound \dot{k} : $\dot{k} \leq \bar{M}V(\bar{x},k)$ for some $\bar{M}>0$. The boundedness of k is concluded by contradiction: It is assumed that k grows to infinity. Upper bounding the derivative of V along closed-loop trajectories yields that $\dot{V} \leq -2\tilde{\mu}V = \dot{V}_{\text{max}}$ for some $\tilde{\mu}>0$. An upper bound for V can be derived by the integration of \dot{V}_{max} . This bound is then used together with $\dot{k}\leq \bar{M}V(\bar{x},k)$ to show that k cannot grow to infinity. Therefore, the adaptation parameter k has to remain bounded.

The nonlinear closed-loop system is given by (6), (7),(8), (12), and takes the form

$$\dot{\xi} = \left(J + b\psi^T(\xi, \eta)\right)\xi + b\left(\phi^T(\xi, \eta)\eta + g(\xi, \eta)(-q_{\kappa}^T\hat{x}) + \nu(\xi, \eta)\right) \tag{13a}$$

$$\dot{\eta} = \chi(\xi, \eta)y + \theta(\eta) + w(\xi, \eta), \tag{13b}$$

$$\dot{\hat{x}} = \hat{A}_{\hat{\kappa}}\hat{x} + p_{\hat{\kappa}}e,\tag{13c}$$

$$\dot{k} = d_{\lambda}^2(e, k),\tag{13d}$$

$$e = c^T \xi - y_{ref} \tag{13e}$$

with

$$\xi(0) = \xi_0 \in \mathbb{R}^r, \eta(0) = \eta_0 \in \mathbb{R}^{n-r}$$
$$\hat{x}(0) = \hat{x}_0 \in \mathbb{R}^r, k(0) = k_0 > 0.$$

In the following, the arguments of $g(\cdot)$, $\phi(\cdot)$, $\chi(\cdot)$, $\theta(\cdot)$, $\nu(\cdot)$ and $w(\cdot)$ are dropped to increase readability. For the reference signal and its derivatives, the following notation is used:

$$\hat{y}_{ref} = \begin{bmatrix} y_{ref}, & \dot{y}_{ref}, & \dots, & y_{ref}^{(r-1)} \end{bmatrix}^T \in \mathbb{R}^r,$$

$$y_{ref} = \begin{bmatrix} y_{ref}, & \dot{y}_{ref}, & \dots, & y_{ref}^{(r)} \end{bmatrix}^T \in \mathbb{R}^{r+1}.$$

It clearly holds that

$$\dot{\hat{\mathbf{y}}}_{ref} = J\hat{\mathbf{y}}_{ref} + b\mathbf{y}_{ref}^{(r)}$$

Introduce the coordinates

$$\bar{x} = \begin{bmatrix} \bar{x}_1 \\ \bar{x}_2 \\ \bar{x}_3 \end{bmatrix} = \begin{bmatrix} \hat{\xi} \\ \eta \\ \hat{e} \end{bmatrix} = \begin{bmatrix} \xi - \hat{y}_{ref} \\ \eta \\ \hat{y}_{ref} - \hat{x} \end{bmatrix},$$

where $\hat{\xi} = \begin{bmatrix} e & \dot{e} & \dots & e^{(r-1)} \end{bmatrix}^T$ denotes the tracking error and its derivatives, and \hat{e} is the observer error, the closed-loop system is given by

$$\dot{\bar{x}} = \begin{bmatrix}
\left(J + b\bar{\psi}^{T}(\cdot)\right)(\bar{x}_{1} + \hat{y}_{ref}) + b\bar{\phi}^{T}(\cdot)\bar{x}_{2} - b\bar{g}(\cdot)q_{\kappa}^{T}(\bar{x}_{1} - \bar{x}_{3}) + b\bar{v}(\cdot) - J\hat{y}_{ref} - by_{ref}^{(r)} \\
\bar{\chi}(\cdot)(c^{T}\bar{x}_{1} + y_{ref}) + \bar{\theta}(\bar{x}_{2}) + \bar{w}(\cdot) \\
\left(J + b\bar{\psi}^{T}(\cdot))(\bar{x}_{1} + \hat{y}_{ref}) + b\bar{\phi}^{T}(\cdot)\bar{x}_{2} - b\bar{g}(\cdot)q_{\kappa}^{T}(\bar{x}_{1} - \bar{x}_{3}) + b\bar{v}(\cdot) - J\hat{y}_{ref} - by_{ref}^{(r)} \\
- (J - p_{\hat{\kappa}}c^{T})(\bar{x}_{1} - \bar{x}_{3}) - p_{\hat{\kappa}}c^{T}\bar{x}_{1}
\end{bmatrix}$$

$$= \begin{bmatrix}
\left(J + b\left(\bar{\psi}^{T}(\cdot) - \bar{g}(\cdot)q_{\kappa}^{T}\right)\bar{x}_{1} + b\bar{\phi}^{T}\bar{x}_{2} + b\bar{g}(\cdot)q_{\kappa}^{T}\bar{x}_{3} + b\bar{v}(\cdot) + \bar{B}y_{ref} \\
\bar{\chi}(\cdot)c^{T}\bar{x}_{1} + \theta(\cdot) + \bar{w}(\cdot) + \bar{\chi}(\cdot)y_{ref} \\
b\left(\bar{\psi}^{T}(\cdot) - \bar{g}(\cdot)q_{\kappa}^{T}\right)\bar{x}_{1} + b\bar{\phi}^{T}(\cdot)\bar{x}_{2} + \left(b\bar{g}(\cdot)q_{\kappa}^{T} + \hat{A}_{\hat{\kappa}}\right)\bar{x}_{3} + b\bar{v}(\cdot) + \bar{B}y_{ref}
\end{bmatrix}$$

$$e = c^{T}\bar{x}_{1}$$
(14a)

with

$$\bar{B} = b \left[|\psi^T(\cdot)| - 1 \right]$$

$$\bar{v}(\bar{x}_1, \bar{x}_2, \hat{y}_{ref}) = v(\xi, \eta),$$
similarly for $\bar{w}(\cdot), \bar{\chi}(\cdot), \bar{\theta}(\cdot), \bar{\phi}(\cdot), \bar{\psi}(\cdot)$ and $\bar{g}(\cdot)$.

Using that $\hat{\kappa} = k^{\alpha}$ and $\kappa = k^{\beta}$, the matrices $J - \bar{g}(\cdot)bq_{\kappa}^{T}$ and $\hat{A}_{\hat{\kappa}} = J - \hat{p}_{\hat{\kappa}}c^{T}$ can both be factored with the help of

$$K_r = \operatorname{diag}\{1, k, \dots, k^{r-1}\}\$$

as

$$J - \bar{g}(\cdot)bq_{\kappa}^{T} = k^{\beta}K_{r}^{\beta}\bar{\bar{A}}_{11}K_{r}^{-\beta}$$

$$\hat{A}_{\hat{\kappa}} = J - p_{\hat{\kappa}}c^{T} = k^{\alpha}K_{r}^{\alpha}\bar{\bar{A}}_{33}K_{r}^{-\alpha}$$
(15)

with

$$\bar{\bar{A}}_{11}(\bar{g}(\cdot)) = J - \bar{g}(\cdot)bq^T \text{ with } q = q_{\kappa}|_{\kappa=1},$$
$$\bar{\bar{A}}_{33} = J - pc^T \text{ with } p = \hat{b}_{\hat{\kappa}}|_{\hat{\kappa}=1}.$$

By assumption, the polynomials $p(\cdot)$ and $q_{\tilde{g}}(\cdot)$ are in $H(\varepsilon,\mu)$ for all $\tilde{g} \geq g$. Therefore, the matrices $\bar{A}_{11}(\bar{g}(\cdot))$ and $\bar{A}_{11}(\bar{g}(\cdot))$ are in the set $H(\varepsilon,\mu)$ for all $g \ge \underline{g}$, see Definition 4. A k-dependent time-scaling is now applied to (14) by defining new coordinates \bar{x} via a gain-dependent transfor-

$$\bar{\bar{x}} = \bar{\bar{C}}\bar{K}^{-1}\bar{x} \tag{16}$$

where

$$\begin{split} \bar{\bar{C}} &= \operatorname{diag}\{c_1I_r, c_2I_m, c_3I_r\}\\ c_i(k) &= k^{\tilde{c}_i}, \ \tilde{c}_i \in \mathbb{R}, \ i = 1, 2, 3,\\ \bar{\bar{K}} &= \operatorname{diag}\{K_r^{\beta}, I_m, K_r^{\alpha}\}. \end{split}$$

The matrix \bar{K}^{-1} can be seen as a k-dependent time scaling of (14).

The coefficients \tilde{c}_1 , \tilde{c}_2 and \tilde{c}_3 have to satisfy the following inequalities:

$$-(r-\frac{1}{2})\beta < \tilde{c}_2 - \tilde{c}_1 < \frac{1}{2}\beta,\tag{17a}$$

$$-(r - \frac{1}{2})(\alpha - \beta) < \tilde{c}_1 - \tilde{c}_3 < -(r - \frac{3}{2})(\alpha - \beta), \tag{17b}$$

$$-(r-\frac{1}{2})\alpha < \tilde{c}_2 - \tilde{c}_3, \tag{17c}$$

$$\tilde{c}_2 < \tilde{c}_1, \tag{17d}$$

$$\tilde{c}_3 - (r - 1)\alpha < \tilde{c}_1 + \frac{1}{2}\alpha,\tag{17e}$$

$$0 \ge \max\{\beta \varepsilon + \tilde{c}_1, \alpha \varepsilon + \tilde{c}_3\} - \frac{1}{2}\tilde{c}_1, \tag{17f}$$

$$\tilde{\gamma} + \tilde{c}_1 \ge -\frac{1}{2}.\tag{17g}$$

Remark 4 The inequalities (17a) to (17f) are needed to bound V. More precisely, the inequalities (17a), (17b) and (17c) are necessary for the compensation by quadratic expansion of the cross terms $\|\bar{x}_i\| \|\bar{x}_i\|$ with $i \neq j$ in (36). The inequalities (17d) and (17e) are coming from the linear terms in $\|\bar{x}_i\|$ in (36). Inequality (17f) ensures that the factor of $\frac{\dot{k}}{k}$ in $\frac{d}{dt}V$ is non-positive, see (32). Finally, inequality (17g) makes it possible to bound $\frac{\dot{k}}{k}$ by V, see (28).

Lemma 1, page 15 shows that the inequalities (17) are solvable for \tilde{c}_1 , \tilde{c}_2 and \tilde{c}_3 . The time derivative of the coordinate transformation matrices \bar{C} and \bar{K}^{-1} is

$$\frac{d}{dt}\bar{C} = \operatorname{diag}\left\{\frac{d}{dt}c_{1}I_{r}, \frac{d}{dt}c_{2}I_{m}, \frac{d}{dt}c_{3}I_{r}\right\}, \frac{d}{dt}c_{i} = \tilde{c}\frac{\dot{k}}{k}c_{i},$$

$$\frac{d}{dt}K_{r}^{-\alpha} = -\alpha\frac{\dot{k}}{k}\Delta K_{r}^{-\alpha}, \frac{d}{dt}K_{r}^{-\beta} = -\beta\frac{\dot{k}}{k}\Delta K_{r}^{-\beta}$$

with

$$\Delta = \operatorname{diag}\{0, 1, \dots, r-1\}.$$

In the \bar{x} -coordinates, the closed-loop differential equations are

$$\frac{d}{dt}\bar{\bar{x}} = \begin{bmatrix}
K_r^{-\beta} \left(\bar{\bar{A}}_{11} + b\bar{\bar{\psi}}^T(\cdot)\right) K_r^{\beta}\bar{\bar{x}}_1 + \frac{c_1}{c_2}K_r^{-\beta}b\phi^T\bar{\bar{x}}_2 + \frac{c_1}{c_3}K_r^{-\beta}b\bar{\bar{g}}(\cdot)q_\kappa^TK_r^{\alpha}\bar{\bar{x}}_3 + K_r^{-\beta}c_1b\bar{\bar{v}}(\cdot) \\
\frac{c_2}{c_1}\bar{\bar{\chi}}(\cdot)c^T\bar{\bar{x}}_1 + c_2\bar{\theta}(c_2^{-1}\bar{\bar{x}}_2) + c_2\bar{\bar{w}}(\cdot) \\
\frac{c_3}{c_1}K_r^{-\alpha}b\left(\bar{\bar{\psi}}^T(\cdot) - \bar{\bar{g}}(\cdot)q_\kappa^T\right)K_r^{\beta}\bar{x}_1 + \frac{c_3}{c_2}K_r^{-\alpha}b\phi^T\bar{\bar{x}}_2 + K_r^{-\alpha}\left(b\bar{\bar{g}}(\cdot)q_\kappa^T + \bar{\bar{A}}_{33}\right)K_r^{\alpha}\bar{x}_3 + c_3K_r^{-\alpha}b\bar{\bar{v}}(\cdot)\right] \\
+ \bar{\bar{C}} \underbrace{\begin{bmatrix}K_r^{-\beta}\bar{B} \\ \bar{\bar{\chi}}(\cdot)\bar{c} \\ K_r^{-\alpha}\bar{B}\end{bmatrix}}_{=:\bar{B}} y_{ref} - \frac{\dot{k}}{k} \underbrace{\begin{bmatrix}-\tilde{c}_1 + \beta\Delta \\ -\tilde{c}_2 \\ -\tilde{c}_3 + \alpha\Delta\end{bmatrix}}_{=:\Psi} \bar{\bar{x}} \\
= \begin{bmatrix}k^{\beta}\bar{A}_{11}\bar{x}_1 \\ \bar{\theta}(\bar{x}_2) \\ k^{\alpha}\bar{A}_{33}\bar{x}_3\end{bmatrix} + \begin{bmatrix}\bar{\bar{E}}_{11} & \bar{\bar{E}}_{12} & \bar{\bar{E}}_{13} \\ \bar{\bar{E}}_{21} & \bar{\bar{E}}_{22} & \bar{\bar{E}}_{23} \\ \bar{\bar{x}}_3\end{bmatrix} \begin{bmatrix}\bar{\bar{x}}_1 \\ \bar{\bar{x}}_2 \\ \bar{\bar{x}}_3\end{bmatrix} \begin{bmatrix}c_1K_r^{-\beta}b\bar{\bar{v}}(\cdot) \\ c_2\bar{w}(\cdot) \\ c_3K_r^{-\alpha}b\bar{\bar{v}}(\cdot)\end{bmatrix} + \bar{\bar{C}}\bar{\bar{B}}y_{ref} - \frac{\dot{k}}{k}\Psi\bar{\bar{x}} \tag{18a}$$

$$e = c_1^{-1}c^T\bar{\bar{x}}_1 \tag{18b}$$

with

$$\begin{split} \bar{\bar{E}}_{11} &= K_r^{-\beta} b \bar{\bar{\psi}}^T(\cdot) K_r^{\beta}, & \bar{\bar{E}}_{12} &= \frac{c_1}{c_2} K_r^{-\beta} b \phi^T, & \bar{\bar{E}}_{13} &= \frac{c_1}{c_3} K_r^{-\beta} b \bar{\bar{g}}(\cdot) q_{\kappa}^T K_r^{\alpha}, \\ \bar{\bar{E}}_{21} &= \frac{c_2}{c_1} \bar{\bar{\chi}}(\cdot) c^T, & \bar{\bar{E}}_{22} &= \bar{\bar{E}}_{23} &= 0, \\ \bar{\bar{E}}_{31} &= \frac{c_3}{c_1} K_r^{-\alpha} b \left(\bar{\bar{\psi}}^T(\cdot) - \bar{\bar{g}}(\cdot) q_{\kappa}^T \right) K_r^{\beta}, & \bar{\bar{E}}_{32} &= \frac{c_3}{c_2} K_r^{-\alpha} b \phi^T, & \bar{\bar{E}}_{33} &= K_r^{-\alpha} b \bar{\bar{g}}(\cdot) q_{\kappa}^T K_r^{\alpha}. \end{split}$$

To shorten the notation, the highest exponent of k in any matrix element will be denoted by $\operatorname{ord}_k(\cdot)$ (see Definition 5, page 18). Straightforward calculations give the following bounds:

$$\operatorname{ord}_{k} \bar{\bar{E}}_{11} = 0, \qquad \operatorname{ord}_{k} \bar{\bar{E}}_{12} = \left(\frac{\tilde{c}_{1}}{\tilde{c}_{2}}\right) - (r-1)\beta < \frac{\beta}{2}$$

$$\operatorname{ord}_{k} \bar{\bar{E}}_{13} = \left(\frac{\tilde{c}_{1}}{\tilde{c}_{3}}\right) + (r-1)(\alpha-\beta) + \beta < \frac{\alpha+\beta}{2}$$

$$\operatorname{ord}_{k} \bar{\bar{E}}_{21} = \left(\frac{\tilde{c}_{2}}{\tilde{c}_{1}}\right) < \frac{\beta}{2}, \quad \operatorname{ord}_{k} \bar{\bar{E}}_{22} = \operatorname{ord}_{k} \bar{\bar{E}}_{23} = 0$$

$$\operatorname{ord}_{k} \bar{\bar{E}}_{31} = \left(\frac{\tilde{c}_{3}}{\tilde{c}_{1}}\right) - (r-1)(\alpha-\beta) + \beta < \frac{\alpha+\beta}{2}$$

$$\operatorname{ord}_{k} \bar{\bar{E}}_{32} = \left(\frac{\tilde{c}_{3}}{\tilde{c}_{2}}\right) - (r-1)\alpha < \frac{\alpha}{2}, \quad \operatorname{ord}_{k} \bar{\bar{E}}_{33} = \beta.$$

where

$$\begin{split} \bar{B}_1 &= K_r^{-\beta} \bar{B} & \text{ord}_k \bar{B}_1 = -(r-1)\beta \\ \bar{B}_2 &= \bar{\chi}(\cdot) \tilde{c} & \text{ord}_k \bar{B}_2 = 0 \\ \bar{B}_3 &= K_r^{-\alpha} \bar{B} & \text{ord}_k \bar{B}_3 = -(r-1)\alpha \\ \bar{\theta}(\bar{x}, k) &= c_2 \bar{\theta}(c_2^{-1} \bar{x}_2) \\ \bar{g}(\bar{x}, k) &= g(x, \hat{x}, \hat{y}_{ref}), \text{ ibid. for } \bar{v}, \bar{w}, \bar{\chi}, \bar{\phi}, \bar{\psi}. \end{split}$$

As the matrices $\bar{A}_{11}(\bar{g}(\cdot))$ and \bar{A}_{33} are in the set $H(\varepsilon,\mu)$ for all $g \ge \underline{g}$, there exist symmetric, positive definite solutions P_1 and P_3 such that for any $g(\cdot) \ge g$ the following Lyapunov equations hold:

$$\bar{\bar{A}}_{ii}^T P_i + P_i \bar{\bar{A}}_{ii} < -\mu P_i,$$
 $i = 1, 2, 3,$ (19a)

$$P_i(\Delta + \varepsilon I) + (\Delta + \varepsilon I)P_i > 0 i = 1,3. (19b)$$

The functions $\bar{x}_1 \mapsto V_1(\bar{x}_1) = \bar{x}_1^T P_1 \bar{x}_1$ and $\bar{x}_3 \mapsto V_3(\bar{x}_3) = \bar{x}_3^T P_3 \bar{x}_3$ are used as a sort of Lyapunov function candidates for \bar{x}_1 and \bar{x}_3 , respectively. By Assumption 4, there exist positive constants m_1 , m_2 , m_3 and m_4 and a function $\eta \mapsto \tilde{V}_2(\eta)$ such that

$$m_1 \|\eta\|^2 \le \tilde{V}_2(\eta) \le m_2 \|\eta\|^2,$$
 (20a)

$$\frac{\partial}{\partial \eta} \tilde{V}_2(\eta) H_2(\eta) \le -m_3 \|\eta\|^2, \tag{20b}$$

$$\|\frac{\partial}{\partial \mathbf{n}}\tilde{V}_2(\mathbf{\eta})\| \le m_4 \|\mathbf{\eta}\|. \tag{20c}$$

This result can for example be found in [25]. In the \bar{x}_2 -coordinates,

$$V_2(\bar{\bar{x}}_2) = c_2^2 \tilde{V}_2(c_2^{-1}\bar{\bar{x}}_2)$$

can be chosen as a Lyapunov function candidate. It then follows from (20) that

$$|m_1||\bar{x}_2||^2 < V_2(\bar{x}_2) < m_2||\bar{x}_2||^2$$
 (21a)

$$\frac{\partial}{\partial \bar{\bar{x}}_2} V_2(\bar{\bar{x}}_2) \bar{\bar{\theta}}_2(\bar{\bar{x}}_2) \le -m_3 \|\bar{\bar{x}}_2\|^2 \tag{21b}$$

$$\|\frac{\partial}{\partial \bar{\bar{x}}_2} V_2(\bar{\bar{x}}_2)\| \le m_4 \|\bar{\bar{x}}_2\|.$$
 (21c)

Now, the Lyapunov function candidates $V_i(\cdot)$ are combined to a single function

$$V(\bar{x}, k) = \frac{1}{2}D^2(\bar{x}, k)$$
 (22a)

with

$$D(\bar{\bar{x}},k) = \begin{cases} \nu(\bar{\bar{x}}) - \rho(k), & \text{if } \nu(\bar{\bar{x}}) \ge \rho(k) \\ 0, & \text{if } \nu(\bar{\bar{x}}) < \rho(k). \end{cases}$$
 (22b)

This is a sort of Lyapunov function candidate for (18a) where

$$v(\bar{x}) = \sqrt{V_1(\bar{x}_1) + V_2(\bar{x}_2) + V_3(\bar{x}_3)}, \tag{22c}$$

$$\rho(k) = \frac{\lambda}{2} \frac{c_1(k)}{\sqrt{\|P_1^{-1}\|}}.$$
(22d)

The k-dependent parameter ρ has been chosen in such a way that

$$\nu(\bar{x}) \le 2\rho(k) \Rightarrow |e| \le \lambda \Rightarrow \dot{k} = 0. \tag{23}$$

To see this, combine (16), (18b) and (22) to

$$|e| \le \frac{\|\bar{x}_1\|}{c_1} \le \frac{\sqrt{\|P_1^{-1}\|}}{c_1(k)} \nu(\bar{x}) \le \frac{\sqrt{\|P_1^{-1}\|}}{c_1(k)} \sqrt{2V(\bar{x},k)} + \frac{\lambda}{2}. \tag{24}$$

Since

$$\nu(\bar{\bar{x}}) \le 2\rho(k) \Leftrightarrow V(\bar{\bar{x}}, k) \le \frac{1}{2}\rho^2(k),\tag{25}$$

(22d) and (24) yield

$$\nu(\bar{x}) < 2\rho(k) \Rightarrow |e| < \lambda$$

which is in the dead-zone of the gain adaptation, implying that

$$v(\bar{x}) < 2\rho(k) \Rightarrow \dot{k} = 0.$$

The function $V(\bar{x}, k)$ will be used to upper bound \dot{k} . From (12), the definition of the adaptation, it holds that

$$\dot{k} \le \frac{\gamma^2}{k^2 \tilde{\gamma}} (|e| - \lambda)^2. \tag{26}$$

From (24) follows that

$$(|e| - \lambda)^2 \le \frac{\|P_1^{-1}\|}{c_1^2(k)} 2V(\bar{x}, k). \tag{27}$$

Combining (26) and (27) yields

$$\dot{k} \le \frac{\gamma^2}{k^{2\bar{\gamma}}} \frac{\|P_1^{-1}\|}{c_1^2(k)} 2V(\bar{\bar{x}}, k). \tag{28}$$

Using (17g), it holds for some $\bar{M} > 0$ that

$$\frac{\dot{k}}{k} \le \bar{M}V(\bar{\bar{x}}, k). \tag{29}$$

(29) is the first key inequality of Step 1 of the Proof.

From now on the k-dependency of $V(\cdot)$, $D(\cdot)$ and $\rho(\cdot)$ will be dropped to increase the readability.

From the theory of ordinary differential equations it follows that the initial value problem (13) possesses an absolutely continuous solution $(\bar{x}(\cdot), k(\cdot))$: $[0, \omega) \to \mathbb{R}^{n+1}$, maximally extended over $[0, \omega)$ for some $\omega \in (0, \infty]$.

The derivative of V along the trajectory of the system (13) (denoted for ease of exposition by $\frac{d}{dt}$) is for all $t \in [0, \omega)$ and for all values of \bar{x}

$$\frac{d}{dt}V(\bar{x}) = D(\bar{x})\frac{d}{dt}D(\bar{x}) = D(\bar{x})\left(\frac{d}{dt}v(\bar{x}) - \frac{d}{dt}\rho(k)\right) = D(\bar{x})\left(\frac{\frac{d}{dt}(V_{1}(\bar{x}_{1}) + V_{2}(\bar{x}_{2}) + V_{3}(\bar{x}_{3}))}{2v(\bar{x})} - \frac{d\rho(k)}{dt}\right) \\
= \frac{1}{2}\frac{D(\bar{x})}{v(\bar{x})}\left(k^{\beta}\bar{x}_{1}^{T}2P_{1}\bar{A}_{11}\bar{x}_{1} + 2\frac{\partial V_{2}(\bar{x}_{2})}{\partial\bar{x}_{2}}H_{2}(\bar{x}_{2}) + k^{\alpha}\bar{x}_{3}^{T}2P_{3}\bar{A}_{33}\bar{x}_{3} + 2\sum_{j=1}^{3}\bar{x}_{1}^{T}P_{1}\bar{E}_{1j}\bar{x}_{j}\right) \\
+ 2\frac{\partial V_{2}(\bar{x}_{2})}{\partial\bar{x}_{2}}\bar{E}_{21}\bar{x}_{1} + 2\sum_{j=1}^{3}\bar{x}_{3}^{T}P_{3}\bar{E}_{3j}\bar{x}_{j} + 2\bar{x}_{1}^{T}P_{1}c_{1}K_{r}^{-\beta}bv(\cdot) + 2\frac{\partial V_{2}(\bar{x}_{2})}{\partial\bar{x}_{2}}c_{2}w(\cdot) \\
+ 2\bar{x}_{3}^{T}P_{3}c_{3}K_{r}^{-\alpha}bv(\cdot) + \left(2\bar{x}_{1}^{T}P_{1}c_{1}K_{r}^{-\beta}\bar{B} + 2\frac{\partial V_{2}(\bar{x}_{2})}{\partial\bar{x}_{2}}c_{2}\chi(\cdot)\tilde{c}^{T} + 2\bar{x}_{3}^{T}P_{3}c_{3}K_{r}^{-\alpha}\bar{B}\right)y_{ref} \\
- \frac{\dot{k}}{k}\bar{x}_{1}^{T}2P_{1}\Psi_{1}\bar{x}_{1} - 2\frac{\dot{k}}{k}\frac{\partial V_{2}(\bar{x}_{2})}{\partial\bar{x}_{2}}\Psi_{2}\bar{x}_{2} - \frac{\dot{k}}{k}\bar{x}_{3}^{T}2P_{3}\Psi_{3}\bar{x}_{3}\right) - \frac{\dot{k}}{k}\operatorname{ord}_{k}(\rho)\rho(k)D(\bar{x}). \tag{30}$$

The last four terms in (30) are analyzed first:

$$N(\bar{\bar{x}}) := -\frac{D(\bar{\bar{x}})}{2\nu(\bar{\bar{x}})} \left(\frac{\dot{k}}{k} \bar{\bar{x}}_1^T 2 P_1 \Delta_1 \bar{\bar{x}}_1 + 2 \frac{\dot{k}}{k} \frac{\partial V_2(\bar{\bar{x}}_2)}{\partial \bar{\bar{x}}_2} \Delta_2 \bar{\bar{x}}_2 + \frac{\dot{k}}{k} \bar{\bar{x}}_3^T 2 P_3 \Delta_3 \bar{\bar{x}}_3 + \frac{\dot{k}}{k} \operatorname{ord}_k(\rho) \rho(k) 2 \nu(\bar{\bar{x}}) \right)$$

$$= -\frac{D(\bar{\bar{x}})}{\nu(\bar{\bar{x}})} \frac{\dot{k}}{k} \left((-\beta \epsilon - \tilde{c}_1) \bar{\bar{x}}_1^T P_1 \bar{\bar{x}}_1 - \tilde{c}_2 \bar{\bar{x}}_2^T P_2 \bar{\bar{x}}_2 + (-\alpha \epsilon - \tilde{c}_3) \bar{\bar{x}}_3^T P_3 \bar{\bar{x}}_3 + \tilde{c}_1 \rho(k) \nu(\bar{\bar{x}}) \right), \tag{31}$$

where (19b) has been used. For $||\bar{x}|| > 2\rho$, (31) simplifies to

$$N(\bar{\bar{x}}) \le D(\bar{\bar{x}}) \frac{\dot{k}}{k} \left(\max\{\beta \varepsilon + \tilde{c}_1, \alpha \varepsilon + \tilde{c}_3\} - \frac{\tilde{c}_1}{2} \right) v^2(\bar{\bar{x}})$$
(32)

and using (17f) to

$$N(\bar{\bar{x}}) \le 0. \tag{33}$$

In the case of $||\bar{x}|| < 2\rho$, (23) yields

$$N(\bar{\bar{x}}) = 0. \tag{34}$$

Combining (33) and (34), it holds for all \bar{x} that

$$N(\bar{x}) \le 0. \tag{35}$$

Using (35), (30) simplifies to

$$\begin{split} \frac{d}{dt}V(\bar{\bar{x}}) &\leq -\frac{D(\bar{\bar{x}})}{v(\bar{\bar{x}})} \left(k^{\beta}V_{1}(\bar{\bar{x}}_{1}) + \frac{m_{3}}{m_{1}}V_{2}(\bar{\bar{x}}_{2}) + k^{\alpha}V_{3}(\bar{\bar{x}}_{3}) + \sum_{i=1,3} \sum_{j=1}^{3} \|P_{i}\| \|\bar{\bar{E}}_{ij}\| \|\bar{\bar{x}}_{i}\| \|\bar{\bar{x}}_{i}\| \|\bar{\bar{x}}_{j}\| \\ &+ \|\frac{\partial V_{2}(\bar{\bar{x}}_{2})}{\partial \bar{\bar{x}}_{2}} \| \|\bar{\bar{E}}_{21}\| \|\bar{\bar{x}}_{1}\| + \sum_{i=1,3} c_{i} \|P_{i}\| \|\bar{\bar{K}}_{i}^{-1}b\| \|\bar{\bar{x}}_{i}\| \|v(\cdot)\| + c_{2} \|\frac{\partial V_{2}(\bar{\bar{x}}_{2})}{\partial \bar{\bar{x}}_{2}} \| \|w(\cdot)\| \\ &+ \left(\sum_{i=1,3} c_{i} \|P_{i}\| \|\bar{\bar{K}}_{i}^{-1}\bar{B}\| \|\bar{\bar{x}}_{i}\| + c_{2} \|\frac{\partial V_{2}(\bar{\bar{x}}_{2})}{\partial \bar{\bar{x}}_{2}} \| \|\chi(\cdot)\| \|\tilde{c}\| \right) \|y_{ref}\| \right). \end{split}$$

Now assume that k tends to infinity as $t \to \omega$. This will lead to a contradiction. The assumption that $y_{ref} \in W^{r,\infty}$ implies that y_{ref} is bounded almost everywhere. Also almost everywhere bounded are $v(\cdot)$, $w(\cdot)$ and $\chi(\cdot)$. Therefore, there exists a constant M > 0 such that for almost all $t \in [0, \omega)$

$$\frac{d}{dt}V(\bar{\bar{x}}) \leq -\frac{D(\bar{\bar{x}})}{v(\bar{\bar{x}})} \left(\frac{\mu}{2} k^{\beta} V_{1}(\bar{\bar{x}}_{1}) + \frac{m_{3}}{m_{1}} V_{2}(\bar{\bar{x}}_{2}) + \frac{\mu}{2} k^{\alpha} V_{3}(\bar{\bar{x}}_{3}) - M \sum_{i=1}^{3} \sum_{j=1}^{3} ||\bar{\bar{E}}_{ij}|| ||\bar{\bar{x}}_{i}|| ||\bar{\bar{x}}_{j}|| - M \left(c_{1} k^{-(r-1)\beta} ||\bar{\bar{x}}_{1}|| + c_{2} ||\bar{\bar{x}}_{2}|| + c_{3} k^{-(r-1)\alpha} ||\bar{\bar{x}}_{3}|| \right) \right).$$
(36)

Using quadratic expansion, the bounds on $||E_{ij}||$, inequalities (17) and monotonicity of k, there exist positive constants $\tilde{\mu}$, M_1 and \tilde{M} and a time $t_1 \in [0, \infty)$ such that the gain k(t) is sufficiently large for almost all $t \in [t_1, \omega)$ to ensure

$$\frac{d}{dt}V(\bar{\bar{x}}) \leq -\tilde{\mu}\frac{D(\bar{\bar{x}})}{\nu(\bar{\bar{x}})} \left(V_1(\bar{\bar{x}}_1) + V_2(\bar{\bar{x}}_2) + V_3(\bar{\bar{x}}_3) - \tilde{M}c_1^2k^{-M_1}\right) - \tilde{\mu}D(\bar{\bar{x}}) \left(\nu(\bar{\bar{x}}) - \tilde{M}k^{-M_1}c_1\frac{c_1}{\nu(\bar{\bar{x}})}\right).$$

By (22d) and monotonicity of k, there exists $t_2 \in [t_1, \infty)$ such that for almost all $t \in [t_2, \omega)$

$$\frac{d}{dt}V(\bar{\bar{x}}) \le -\tilde{\mu}D(\bar{\bar{x}})\left(\nu(\bar{\bar{x}}) - \rho\frac{\rho}{\nu(\bar{\bar{x}})}\right). \tag{37}$$

For $v(\bar{x}) > \rho$, this reduces to

$$\frac{d}{dt}V(\bar{x}) \le -\tilde{\mu}D(\bar{x})\left(\nu(\bar{x}) - \rho\right). \tag{38}$$

In the case of $v(\bar{x}) \leq \rho$, (37) is simplified to

$$\frac{d}{dt}V(\bar{\bar{x}}) \le 0 \text{ as } D(\bar{\bar{x}}) = 0. \tag{39}$$

Thus, by combining (38) and (39) it holds for all \bar{x} and for almost all $t \in [t_2, \omega)$ that

$$\frac{d}{dt}V(\bar{x}) \leq -\tilde{\mu}D^2(\bar{x}) = -2\tilde{\mu}V^2(\bar{x}).$$

Therefore, for all $t \in [t_2, \omega)$,

$$V(\bar{\bar{x}}(t), k(t)) \le e^{-2\tilde{\mu}(t-t_2)} \cdot V(\bar{\bar{x}}(t_2), k(t_2)). \tag{40}$$

Inequality (40) is the second key inequality of this part of the Proof. If $\omega < \infty$, then (29) and (40) yield that $k(\cdot) \in \mathcal{L}_{\infty}([0,\omega))$. If $\omega = \infty$, then by (40), V enters in finite time the interval $[0,\rho^2/2]$ which by (23) and (25) implies that $|e| \le \lambda$. Whence, the dead-zone in the gain adaptation (12) yields that $k(\cdot) \in \mathcal{L}_{\infty}([0,\omega))$. In both cases, this contradicts the assumption on unboundedness of $k(\cdot)$, thus proving boundedness of $k(\cdot)$.

1.b) Boundedness of the observer states. As $k(\cdot)$ is bounded, $d_{\lambda}(\cdot) \in \mathcal{L}_{2}([0,\omega))$. From this, (12) and the Hölder inequality, it follows that

$$\gamma^{-1}k^{\tilde{\gamma}}(\cdot)d_{\lambda}(\cdot) \in \mathcal{L}_{2}([0,\omega)). \tag{41}$$

Using (12) again yields

$$\gamma^{-1}k^{\tilde{\gamma}}d_{\lambda}(e,k) = egin{cases} |e|-\lambda & ext{for } |e| \geq \lambda, \ 0 & ext{for } |e| \leq \lambda. \end{cases}$$

Therefore.

$$|e(\cdot)| - \gamma^{-1} k^{\tilde{\gamma}}(\cdot) d_{\lambda}(e(\cdot), k(\cdot)) \in \mathcal{L}_{\infty}([0, \omega)). \tag{42}$$

Combining (41) and (42) yields

$$|e(\cdot)| = \underbrace{|e(\cdot)| - \gamma^{-1} k^{\tilde{\gamma}}(\cdot) d_{\lambda}(\cdot)}_{\in \mathcal{L}_{\infty}([0,\omega))} + \underbrace{\gamma^{-1} k^{\tilde{\gamma}}(\cdot) d_{\lambda}(\cdot)}_{\in \mathcal{L}_{2}([0,\omega))} \in \mathcal{L}_{\infty}([0,\omega)). \tag{43}$$

Boundedness of $k(\cdot)$ ensures the existence of a k_{ω} such that

$$k_{\omega} = \limsup_{t \in [0, \omega)} k(t).$$

Defining $\hat{A} = \hat{A}_{\hat{K} = k_{\alpha}^{\alpha}}$, $\hat{A}_1 = \hat{A}_{\hat{K}} - \hat{A}$, (13c) is equivalent to

$$\dot{\hat{x}} = \hat{A}\hat{x} + \hat{A}_1\hat{x} + \hat{b}e,\tag{44}$$

where \hat{A} is Hurwitz, $||\hat{A}_1||$ decreases monotonically to zero and $||\hat{b}||$ is bounded. Therefore, it follows from Variation of Constants \hat{x} is bounded, i.e.

$$\hat{x}(\cdot) \in \mathcal{L}_{\infty}^{r}([0, \omega)). \tag{45}$$

As $u = -q_k \hat{x}$, this directly ensures that

$$u(\cdot) \in \mathcal{L}_{\infty}([0, \omega)).$$
 (46)

1.c) Boundedness of the system states. The previous part has shown that *e* and *y* are bounded almost everywhere. The internal dynamics of (6) are

$$\dot{\eta} = H(\eta) + \chi(\xi, \eta)y + w(\xi, \eta).$$

By Variation of Constants, it follows that

$$\eta(\cdot) \in \mathcal{L}_{\infty}^{n-r}([0,\omega)). \tag{47}$$

The remaining states*, i.e. ξ , satisfy

$$\dot{\xi} = J\xi + b\left(\psi^{T}(\cdot)\xi + \phi^{T}(\cdot)\eta + g(\cdot)u(\cdot) + v(\cdot)\right)
= (J + b\psi^{T}(\cdot))\xi + b\tilde{v},$$
(48)

where $\tilde{v} \in \mathcal{L}_{\infty}([0,\omega))$. It is trivial to see that the system (48) is observable from ξ_1 . Therefore, there exists a $l \in \mathbb{R}^{1 \times r}$ s.t.

$$\dot{\zeta} = (J + b\psi^{T}(\cdot)) \zeta + l(y - lc)$$
$$= (J - lc + b\psi^{T}(\cdot)) \zeta + ly$$

^{*}This part of the proof is due to G. Weiss, Imperial College, London.

is an observer for (48) in the case of $\tilde{v} \equiv 0$, if J - lc is Hurwitz and sufficiently robust to cope with the perturbation $b\psi^T(\cdot)$ (see e.g. Theorem 2 in [2]). Boundedness of y ensures boundedness of ζ . The observer error, $\xi - \zeta$ satisfies

$$\frac{d}{dt}(\xi - \zeta) = (J - lc + b\psi^{T}(\cdot))(\xi - \zeta) + b\tilde{v}.$$

Therefore, it is bounded and

$$\xi(\cdot) \in \mathcal{L}_{\infty}^{r}([0,\omega)). \tag{49}$$

1.d) Global existence of a unique solution. As k, x and \hat{x} are bounded on $[0, \omega)$, it follows by maximality of ω that $\omega = \infty$.

1.e) Convergence of the tracking error. It remains to show that the λ -strip is attractive. This is achieved by showing that $\lim_{t\to\infty} d_{\lambda}(e(t),k(t))=0$. Since $e(\cdot)$ and $k(\cdot)$ are bounded, it follows that $\dot{k}(\cdot)=d_{\lambda}^2(\cdot)\in \mathcal{L}_1([0,\omega))$. Using $\dot{e}=c[Ax-bq_k\hat{x}]-\dot{y}_{ref}$ and the boundedness of $x(\cdot)$ and $\hat{x}(\cdot)$, it can be concluded that $\dot{e}(\cdot)\in \mathcal{L}_{\infty}([0,\infty))$. As

$$\frac{d}{dt}d_{\lambda}^{2} = 2d_{\lambda}\left(\frac{\gamma}{k\tilde{\gamma}}\frac{e\dot{e}}{|e|} - \tilde{\gamma}\frac{\dot{k}}{k}d_{\lambda}\right) \in \mathcal{L}_{\infty}([0,\infty)),$$

 $d_{\lambda}^2(\cdot)$ is uniformly continuous. This, together with $d_{\lambda}^2(\cdot) \in \mathcal{L}_1([0,\infty))$ yields, by Barbălat's Lemma [1] that $\lim_{t\to\infty} d_{\lambda}^2(t)=0$.

This completes the proof of Theorem 1.

5 Extensions

Theorem 1 requires that $\alpha > \beta$. The limiting case $\alpha = \beta$ can also be handled if the following extra conditions are satisfied

- 1. The matrix $\tilde{A} = J pc^T gbq^T$ is Hurwitz for all possible g.
- 2. The matrix $\begin{bmatrix} A_{11} & bq^T \\ bq^T & \tilde{A} \end{bmatrix}$ is Hurwitz for all possible g.

These conditions are necessary as the state-feedback and the observer are adapted at the same speed. Thus, it is necessary that the observer is stable under the "perturbation" by the state-feedback (first condition) and that the cross-coupling between tracking and observation error is not too large (second condition).

Another possible extension is to allow time-variation of the system. As long as the variations are slow enough, the control objective is attained by the same controller.

6 Conclusions

This paper proposes an adaptive λ -tracking controller with full-order observer that guarantees to achieve λ -tracking for a large class of nonlinear systems and reference signal. If the system can be transformed Byrnes-Isidori normal form as in Assumption 3 and the relative degree and a lower bound of the high-frequency gain \underline{g} are known, then the adaptive λ -tracking controller proposed here is well suited for achieving that the tracking error $y-y_{ref}$ asymptotically converges to the λ -strip. The width of this strip, λ , is a parameter which can be chosen by the user and does usually depend on the specifications, on model uncertainties and on the quality of the measurement. In comparison with other approaches, the controller proposed here uses a full-order high-gain observer. This has the advantage that the output y does not enter the feedback part of the controller directly. As this observer estimates filtered derivatives of the output y and the feedback part is a linear combination of the observer states, the controller has a very simple structure. This makes it much easier to tune the parameters of the controllers as they have a clear meaning.

The practical applicability and performance of the proposed controller has been shown when applied to a control problem in anesthesia [4].

A Scaling coefficients

Lemma 1 (Scaling functions in the Proof of Theorem 1) For any $\tilde{\gamma}$ satisfying (12c), (12d) there exist k-dependent functions c_1 , c_2 and c_3 satisfying the inequalities (17).

Proof (of 1)

2.a) Solvability for \tilde{c}_2 . Combining (17a) and (17d) yields the inequality

$$-(r-\frac{1}{2})\beta < \tilde{c}_2 - \tilde{c}_1 < 0,$$

or, equivalently

$$\tilde{c}_2 - \tilde{c}_1 = \delta, \quad \delta \in I_{\delta} = (-(r - \frac{1}{2})\beta, 0).$$
 (50)

Inequality (17b) can be written in the following way:

$$\tilde{c}_1 - \tilde{c}_3 = -(r - \frac{1}{2})(\alpha - \beta) + \gamma, \quad \gamma \in I_\gamma = (0, \alpha - \beta)$$

$$(51)$$

Adding (50) and (51) results in

$$\tilde{c}_2 - \tilde{c}_3 = -(r - \frac{1}{2})(\alpha - \beta) + \delta + \gamma$$

> $-(r - \frac{1}{2})(\alpha - \beta) - (r - \frac{1}{2})\beta$.

Thus,

$$\tilde{c}_2 - \tilde{c}_3 > -(r - \frac{1}{2})\alpha,$$

which is the same as (17c). As I_{δ} is nonempty for positive β , the inequalities (17) are solvable for c_2 for any given c_1 and c_3 .

2.b) Solvability for \tilde{c}_1 and \tilde{c}_3 .

Case: $\tilde{c}_1 + \beta \varepsilon \ge \tilde{c}_3 + \alpha \varepsilon$:

As $\alpha \ge \beta$, it follows from (17b) that

$$0 \leq \tilde{c}_1 - \tilde{c}_3 < -(r - \frac{3}{2})(\alpha - \beta).$$

This inequality is solvable only if r = 1. Therefore, $\tilde{c}_1 + \beta \varepsilon \ge \tilde{c}_3 + \alpha \varepsilon$ implies that r = 1.

Using $\tilde{c}_1 + \beta \varepsilon \ge \tilde{c}_3 + \alpha \varepsilon$, (17f) is simplified to

$$0 \ge \beta \varepsilon + \frac{1}{2} \tilde{c}_1$$

which is equivalent to

$$\tilde{c}_1 \le -2\beta \varepsilon.$$
 (52)

Case: $\tilde{c}_1 + \beta \varepsilon < \tilde{c}_3 + \alpha \varepsilon$:

$$0 \ge \alpha \varepsilon + \tilde{c}_3 - \frac{1}{2}\tilde{c}_1.$$

Using (51) this inequality can be solved for c_1 :

$$0 \ge \alpha \varepsilon + \tilde{c}_1 + (r - \frac{1}{2})(\alpha - \beta) - \gamma - \frac{1}{2}\tilde{c}_1,$$

or, equivalently to

$$\tilde{c}_1 < -2\alpha\varepsilon - 2(r - \frac{1}{2})(\alpha - \beta). \tag{53}$$

Case: arbitrary \tilde{c}_3 :

Combining (52) and (53), the following inequality has to be satisfied by c_1 independently of c_3 :

$$\tilde{c}_1 \le -2\beta \varepsilon \quad \text{for } r = 1,$$

 $\tilde{c}_1 < -2\alpha \varepsilon - (\alpha - \beta)(2r - 1) \quad \text{for } r > 1.$ (54)

By (17g),

$$\tilde{c}_1 \ge -\tilde{\gamma} - \frac{1}{2}.\tag{55}$$

Combining (54) with (55) yields

$$-\tilde{\gamma} \le \tilde{c}_1 < -2\alpha\varepsilon - 2(\alpha - \beta)(r - \frac{1}{2}) \quad \text{for } r > 1, \tag{56a}$$

$$-\tilde{\gamma} \le \tilde{c}_1 \le -2\alpha \varepsilon \qquad \qquad \text{for } r = 1. \tag{56b}$$

By (12c), (12d), these inequalities are solvable for \tilde{c}_1 .

Rewriting inequality (17b) as

$$\tilde{c}_3 - \tilde{c}_1 < (r - \frac{1}{2})(\alpha - \beta) = (r - \frac{1}{2})\alpha - \underbrace{(r - \frac{1}{2})\beta}_{>0}$$

reveals that (17e) is contained in (17b). Thus, given a \tilde{c}_1 satisfying (56), any \tilde{c}_3 satisfying (17b) and any \tilde{c}_2 satisfying (17a) is a solution of the system of inequalities (17).

B Polynomials in $H(\varepsilon, \mu)$

The controller described in Section 4 performs a sort of adaptive time scaling. A Lyapunov function for such a system can be found if the system is stable and the adaptation is not too fast, see Remark 7 in Appendix C. To characterize the possible adaptation speed, it is necessary to introduce measures for the decay rate μ , and the robustness with respect to time-scaling ε , of a Hurwitz polynomial or matrix.

Definition 3 (Polynomial in $H(\varepsilon,\mu)$) A polynomial $p(\cdot) = s^r + \sum_{i=0}^{r-1} p_i s^i$ belongs to the class $H(\varepsilon,\mu)$ if there exists a symmetric, positive definite matrix P such that the companion matrix

$$A_c = \begin{bmatrix} 0 & 1 \\ \vdots & & \ddots \\ 0 & & 1 \\ -p_0 & \dots & -p_{r-1} \end{bmatrix}$$

satisfies for $\Psi_r = \text{diag}\{0, 1, ..., r-1\}$ the inequalities

$$A_c^T \cdot P + P \cdot A_c \le -2\mu P, \tag{57a}$$

$$\Psi_r \cdot P + P \cdot \Psi_r > -2\varepsilon P. \tag{57b}$$

Remark 5 By (57a), $H(\varepsilon,\mu)$ is a subset of the Hurwitz polynomials. It is shown in [3] that for any polynomial $p(\cdot)$ there exist scalars $\underline{\varepsilon}$ and $\bar{\mu}$ such that

$$p(\cdot) \in H(\varepsilon,\mu)$$
 for all $\varepsilon \ge \underline{\varepsilon}$ and for all $\mu \le \bar{\mu}$.

C Matrices in $H(\varepsilon,\mu)$

Definition 4 (Matrix in $H(\varepsilon, \mu)$) A matrix A_c belongs to the class $H(\varepsilon, \mu)$ if there exists a symmetric, positive definite matrix P such that for $\Psi_r = \text{diag}\{0, 1, \ldots, r-1\}$ the inequalities (57a) and (57b) are satisfied.

Remark 6 If
$$A_c \in H(\varepsilon, \mu)$$
 then any matrix $A_c - m\Psi_r$ is Hurwitz for $m < \frac{\mu}{\varepsilon}$.

Remark 7 Define the system

$$\dot{x} = kKAK^{-1}x$$

with $A \in \mathbb{R}^r$ a Hurwitz matrix and

$$K = \operatorname{diag}\{1, k, \dots, k^{r-1}\}\$$

where k is a positive function increasing monotonically over time. Define the coordinates

$$z = K^{-1}x.$$

Then

$$\dot{z} = kAz - \frac{\dot{k}}{k}\Psi_r z \tag{58}$$

with

$$\Psi_r = \text{diag}\{0, 1, \dots, r-1\}.$$

In the z-coordinates, a Lyapunov-function V can easily be defined:

$$V = k^{-2\gamma} z^T P z \tag{59}$$

for some γ and any positive definite matrix P satisfying

$$0 > A^T P + PA. (60)$$

Then, along any trajectory of (58), the time derivative of (59) is

$$\dot{V} = k^{-2\gamma} z^T \left(PA + A^T P - \frac{\dot{k}}{k} (P\Psi_r + \Psi_r P + 2\gamma P) \right) z. \tag{61}$$

As $k \ge 0$ and $\dot{k} \ge 0$, \dot{V} in (61) is negative definite for any k, \dot{k} only if

$$0 \ge P\Psi_r + \Psi_r P + 2\gamma P. \tag{62}$$

 \Diamond

 \Diamond

If $A \in H(\varepsilon,\mu)$, then there exists a positive definite matrix \bar{P} satisfying (60) such that

$$-2\bar{\gamma}\bar{P} > \bar{P}\Psi_r + \Psi_r\bar{P} > -2\varepsilon\bar{P}.$$

for any $\bar{\gamma} \geq \gamma$. Thus, for any $\gamma \leq \varepsilon$, $V = k^{-2\gamma} z^T Pz$ is a Lyapunov function.

Remark 8 Analyzing (62) reveals that $\tilde{\Psi}_r = \Psi_r + \gamma I$ satisfies

$$0 > \bar{P}\tilde{\Psi}_r + \tilde{\Psi}_r\bar{P}$$

The matrix $\tilde{\Psi}_r$ corresponds to the time-scaling matrix $\tilde{K} = k^{-\gamma}K$.

D Order of a matrix

The following definition helps writing the bounds on the matrices in a more compact way.

Definition 5 (Order of a polynomial) *The highest exponent of k in any element of a matrix M is denoted* $\operatorname{ord}_k(M)$, *i.e. for the matrix M defined by*

$$M_{i,j} = \sum_{l=l_{\min}^{(i,j)}}^{l_{\max}^{(i,j)}} k^l m_l^{(i,j)}, \quad \text{ord}_k(M) = \max_{i,j} \{l_{\max}^{(i,j)}\}.$$

For example, $\operatorname{ord}_k(\alpha k^2 + \beta + \gamma k^{-1}) = 2$.

References

- [1] I. Barbălat. Systemes d'équations différentielles d'oscillations non linéaires. *Rev. Math. Pur. Appl.*, 4:267–270, 1959. Acad. Republ. Popul. Roum.
- [2] R. Bellman. *Stability Theory of Differential Equations*. International Series in Pure and Applied Mathematics. McGraw-Hill, New York, 1953.
- [3] E. Bullinger. *Adaptive* λ-tracking for Systems with Higher Relative Degree. PhD thesis, Swiss Federal Institute of Technology (ETH), 2000.
- [4] E. Bullinger, C. W. Frei, T. J. Sieber, A. H. Glattfelder, F. Allgöwer, and A. M. Zbinden. Adaptive λ-tracking in anesthesia. In E. Carson and E. Salzsieder, editors, *Preprints of the 4th IFAC Symposium Modelling and Control in Biomedical Systems*, pages 217–222, Oxford, UK, 2000. Pergamon.
- [5] E. Bullinger, A. Ilchmann, and F. Allgöwer. A simple adaptive observer for nonlinear systems. In *Proc. of the IFAC Nonlinear Control Systems Design*, *NOLCOS98*, *Enschede*, *The Netherlands*, volume 3, pages 806–811, 1998. Preprints.
- [6] C. I. Byrnes and A. Isidori. A frequency domain philosophy for nonlinear systems with applications to stabilization and to adaptive control. In *Proc. of the 23rd IEEE Conf. on Decision and Control*, volume 3, pages 1569–1573, 1984.
- [7] C. I. Byrnes and A. Isidori. Global feedback stabilization of nonlinear systems. In *Proc. of the 24th IEEE Conf. on Decision and Control*, volume 2, pages 1031–1037, 1985.
- [8] M. Corless. Simple adaptive controllers for systems which are stabilizable via high gain feedback. *IMA J. of Mathematical Control & Information*, 8(4):379–387, 1991.
- [9] O. Föllinger. Nichtlineare Regelungen I. Oldenbourg, München, 1969.
- [10] B. A. Francis and W. M. Wonham. The internal model principle for linear multivariable regulators. *J. Appl. Maths. Optimization*, 2(2):170–194, 1975.
- [11] J. E. Gibson. Nonlinear Automatic Control. McGraw-Hill, New York, 1963.
- [12] A. Ilchmann. *Non-Identifier-Based High-Gain Adaptive Control*. Number 189 in Lecture notes in control and information sciences. Springer-Verlag, Berlin, 1993.
- [13] A. Ilchmann and E. P. Ryan. Universal λ -tracking for nonlinearly-perturbed systems in the presence of noise. *Automatica*, 30(2):337–346, 1994.
- [14] A. Isidori. Nonlinear Control Systems. Springer, London, third edition, 1995.
- [15] H. K. Khalil. Nonlinear Systems. Prentice Hall, Upper Saddle River, NJ, second edition, 1996.
- [16] J. La Salle and S. Lefschetz. *Stability by Liapunov's Direct Method*, volume 4 of *Mathematics in Science and Engineering*. Academic Press, New York, 1961.
- [17] I. M. Y. Mareels. A simple selftuning controller for stably invertible systems. *Syst. Control Lett.*, 4(1):5–16, 1984.

- [18] S. Nicosia and A. Tornambè. High-gain observers in the state and parameter estimation of robots having elastic joints. *Syst. Control Lett.*, 13(4):331–337, 1989.
- [19] E. P. Ryan. Universal $w^{1,\infty}$ -tracking for a class of nonlinear systems. Syst. Control Lett., 18(3):201–210, 1992.
- [20] E. P. Ryan. A nonlinear universal servomechanism. *IEEE Trans. Automatic Control*, 39(4):753–761, 1994.
- [21] P. Sannuti. Direct singular perturbation analysis of high-gain and cheap control problems. *Automatica*, 19(1):41–51, 1983.
- [22] H. J. Sussmann and P. V. Kokotović. The peaking phenomenon and the global stabilization of nonlinear systems. *IEEE Trans. Aut. Control*, 36(4):424–440, 1991.
- [23] A. Tornambè. High-gain observers for non-linear systems. Int. J. of Systems Science, 23(9):1475–1489, 1992.
- [24] H. Unbehauen. Regelungstechnik I. Friedr. Vieweg & Sohn, Braunschweig, 6th edition, 1989.
- [25] M. Vidyasagar. Nonlinear Systems Analysis. Prentice Hall, Englewood Cliffs, NJ, second edition, 1993.
- [26] M. Zeitz. Canonical forms for nonlinear systems. In A. Isidori, editor, *Nonlinear Control System Design*. *Selected papers from the IFAC-Symposium, Capri, Italy*, pages 33–38. Pergamon Press, Oxford, 1989.

21st Benelux Meeting on Systems and Control Veldhoven, The Netherlands, March 19-21, 2002

USING MODEL-BASED OPTIMIZATION TO IMPROVE BIOTECHNOLOGICAL PROCESSES



Julio R. Banga

Process Engineering Group, IIM (CSIC), Vigo (Spain)

http://www.iim.csic.es/~julio/ http://www.iim.csic.es/~gingproc/

COLLABORATORS







Eva Balsa-Canto

Carmen G. Moles

Antonio A. Alonso

Process Engineering Group, IIM (CSIC), Vigo (Spain)

http://www.iim.csic.es/~gingproc/

Work supported by grants from the EU (4th and 5th FP) and the Spanish Government (MCyT)

Structure of talks



USING MODEL-BASED OPTIMIZATION TO IMPROVE

BIOTECHNOLOGICAL PROCESSES

WEDNESDAY, MARCH 20, 8:30 -9:30:

>PART (i): LOCAL OPTIMIZATION METHODS

- >THURSDAY, MARCH 21, 10:00 11:00:
 - >PART (ii): GLOBAL OPTIMIZATION METHODS

PART (i): Summary



PART (i): LOCAL OPTIMIZATION METHODS

- > Introduction
- > Mathematical Models of Bio-Processes
- > Optimization of Dynamic Models
- > Dynamic Optimization: statement and solution methods
- > Sensitivity Analysis: first and second order
- > TNHp: a new second order code
- > Case Studies (bioreactors)
- > Extension to distributed systems
- > Conclusions and Future Work

Bio-process Model Wathematical Optimization Design Design Operation Control

Mathematical Models of Bio-Processes



Main characteristics:

- Non-linear, dynamic models (i.e. batch or semi-batch processes)
- Nonlinear constraints coming from safety and/or quality demands
- Distributed systems (temperature, concentration, etc.), usually with coupled transport phenomena
- >Thus, mathematical models consist of sets of DAEs, PDAEs, or even IPDAEs, with possible logic conditions (transitions, I.e. hybrid systems)
- >> PDAEs models are usually transformed into DAEs (I.e. discretization methods)

Optimization of Dynamic Models: Some Problem Types



> Dynamic optimization (open loop optimal control)

To find the optimal operating policies (controls) of a nonlinear dynamic system in order to optimize a performance index (functional)

>Integrated process design and control optimization

Find simultaneously the static design variables, the operating conditions and the controllers which minimize capital and operation costs while maximizing controllability

> Parameter estimation (inverse problem, model calibration)

Find the parameters of a nonlinear dynamic model which give the best fit to a set of experimental data

Statement of (dynamic) optimization problems



Find u(t), v and t, to minimize:

$$J(\mathbf{z}, \mathbf{u}) = \psi(\mathbf{z}(t_f)) + \int_{t_0}^{t_f} \phi(\mathbf{z}(t), \mathbf{u}(t), t) dt$$

System dynamics (DAEs):

$$f(\dot{z},z,u,v)=0$$

Path constraints:

$$\mathbf{h}(\mathbf{z}(t),\mathbf{u}(t),\mathbf{v},t) = \mathbf{0}$$

$$\mathbf{g}(\mathbf{z}(t),\mathbf{u}(t),\mathbf{v},t) \leq \mathbf{0}$$

Bounds:

s.t.

$$\mathbf{u}^{\mathrm{L}}(t) \leq \mathbf{u}(t) \leq \mathbf{u}^{\mathrm{U}}(t)$$
$$\mathbf{v}^{\mathrm{L}} \leq \mathbf{v} \leq \mathbf{v}^{\mathrm{U}}$$

 $\mathbf{z} \in \Re^{n}$: state variables

 $\mathbf{u} \in \Re^{\sigma}$: control variables

 $v \in \Re^{\eta}$: time invariant parameters

This problem is usually converted to an NLP-DAEs

(e.g. via CVP in the case of DO)

Dynamic optimization: solution methods



- Indirect methods: numerical solution of the necessary conditions for optimality (MPP) → two or multipoint BVP, difficult to solve
- **② Dynamic programming** techniques (e. g. IDP) → very costly, hard to tune
- Oirect methods transform the original problem into a nonlinear programming (NLP) problem. Two strategies:
 - > Simultaneous, or complete parameterization (collocation)
 - > <u>Sequential</u>, or control vector parameterization (CVP)

Control Vector Parameterization (CVP)



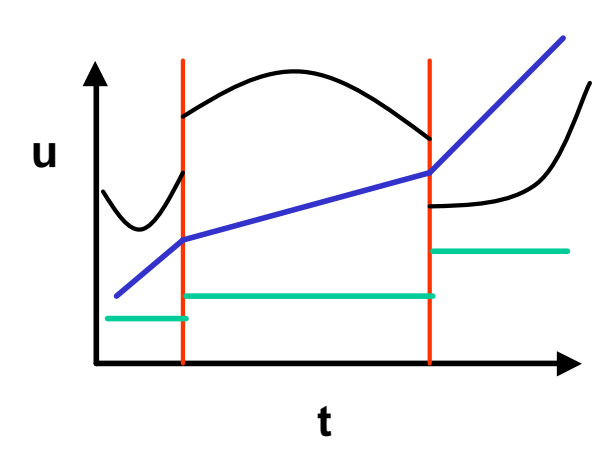
- Time horizon is divided into *r* elements
- Controls are approximated using some basis functions (e.g. piecewise-constant or linear)
- → Outer NLP which requires the solution of an inner IVP for each function evaluation, with gradients computed through first order sensitivities (solution of extended IVP)

Nonlinear dynamic optimization problem



NONLINEAR
PROGRAMMING PROBLEM
(NLP)

Find the parameters v to minimize the objective J



Resulting NLP-DAEs problem



>> Find v to minimize:

$$C = c(v, z, p)$$

- > subject to constraints
 - → System dynamics (DAEs):

$$f(\dot{z}, z, \mathbf{v}, \mathbf{p}) = 0$$
$$z(t_0) = \mathbf{x}_0$$

→ Path constraints:

$$h(z, p, v) = 0$$
$$g(z, p, v) \le 0$$

→ Upper & lower bounds:

$$v^L < v < v^U$$

v: decision variables

z : state variablesp : parameters

Solving the NLP-DAEs problem



- Direct methods transform the original problem into a constrained NLP
- If this NLP is convex, it can be solved efficiently by local (gradient-based methods)
 - New second order local method (with V. S. Vassiliadis)



- ♦ If the NLP is non-convex, global optimization (GO) techniques must be used
 - Stochastic & deterministic GO methods (part II)

Sensitivity analysis: first order

Sensitivity analysis within CVP methods allows the calculation of the **gradient** of the objective w.r.t. **v** using **first order sensitivities**:

$$\frac{\partial \mathbf{f}}{\partial \mathbf{z}} \frac{\partial \mathbf{z}}{\partial \mathbf{v}} + \frac{\partial \mathbf{f}}{\partial \mathbf{z}} \frac{\partial \mathbf{z}}{\partial \mathbf{v}} + \frac{\partial \mathbf{f}}{\partial \mathbf{u}} \frac{\partial \mathbf{u}}{\partial \mathbf{v}} + \frac{\partial \mathbf{f}}{\partial \mathbf{v}} = \mathbf{0}_{n \times p} \qquad \qquad \frac{\partial \mathbf{z}}{\partial \mathbf{v}}(\mathbf{t}_0) = \frac{\partial \mathbf{z}_0}{\partial \mathbf{v}}(\mathbf{v})$$

$$p = \sigma p + \eta$$

Gradient
$$\frac{\partial J}{\partial \mathbf{v}}$$

- ★Original DAEs and first order sensitivities share the same Jacobian: $\begin{bmatrix} \frac{\partial f}{\partial z}, \frac{\partial f}{\partial z} \end{bmatrix}$
- → Direct decoupled integration schemes are possible
- © Could we use second order sensitivities to compute exact Hessian?

Sensitivity analysis: second order

$$\begin{split} &\left\{\left[\frac{\partial \mathbf{f}}{\partial \mathbf{z}}\otimes\mathbf{I}_{p}\right]\frac{\partial^{2}\mathbf{z}}{\partial\mathbf{v}^{2}}+\left[\frac{\partial \mathbf{f}}{\partial \mathbf{z}}\otimes\mathbf{I}_{p}\right]\frac{\partial^{2}\mathbf{z}}{\partial\mathbf{v}^{2}}\right\}+\left[\mathbf{I}_{n}\otimes\left(\frac{\partial\mathbf{z}}{\partial\mathbf{v}}\right)^{T}\right]\left[\frac{\partial^{2}\mathbf{f}}{\partial\mathbf{z}^{2}}\frac{\partial\mathbf{z}}{\partial\mathbf{v}}+\frac{\partial^{2}\mathbf{f}}{\partial\mathbf{z}\partial\mathbf{z}}\frac{\partial\mathbf{u}}{\partial\mathbf{v}}+\frac{\partial^{2}\mathbf{f}}{\partial\mathbf{v}\partial\mathbf{z}}\right]+\\ &\left[\mathbf{I}_{n}\otimes\left(\frac{\partial\mathbf{z}}{\partial\mathbf{v}}\right)^{T}\right]\left[\frac{\partial^{2}\mathbf{f}}{\partial\mathbf{z}\partial\mathbf{z}}\frac{\partial\mathbf{z}}{\partial\mathbf{v}}+\frac{\partial^{2}\mathbf{f}}{\partial\mathbf{z}^{2}}\frac{\partial\mathbf{z}}{\partial\mathbf{v}}+\frac{\partial^{2}\mathbf{f}}{\partial\mathbf{u}\partial\mathbf{z}}\frac{\partial\mathbf{u}}{\partial\mathbf{v}}+\frac{\partial^{2}\mathbf{f}}{\partial\mathbf{v}\partial\mathbf{z}}\right]+\left[\frac{\partial\mathbf{f}}{\partial\mathbf{u}}\otimes\mathbf{I}_{p}\right]\frac{\partial^{2}\mathbf{u}}{\partial\mathbf{v}^{2}}+\left[\mathbf{I}_{n}\otimes\left(\frac{\partial\mathbf{u}}{\partial\mathbf{v}}\right)^{T}\right]\\ &\left[\frac{\partial^{2}\mathbf{f}}{\partial\mathbf{z}\partial\mathbf{u}}\frac{\partial\mathbf{z}}{\partial\mathbf{v}}+\frac{\partial^{2}\mathbf{f}}{\partial\mathbf{z}\partial\mathbf{u}}\frac{\partial\mathbf{z}}{\partial\mathbf{v}}+\frac{\partial^{2}\mathbf{f}}{\partial\mathbf{u}^{2}}\frac{\partial\mathbf{u}}{\partial\mathbf{v}}+\frac{\partial^{2}\mathbf{f}}{\partial\mathbf{v}\partial\mathbf{u}}\right]+\left[\frac{\partial^{2}\mathbf{f}}{\partial\mathbf{z}\partial\mathbf{v}}\frac{\partial\mathbf{z}}{\partial\mathbf{v}}+\frac{\partial^{2}\mathbf{f}}{\partial\mathbf{z}\partial\mathbf{v}}\frac{\partial\mathbf{u}}{\partial\mathbf{v}}+\frac{\partial^{2}\mathbf{f}}{\partial\mathbf{v}^{2}}\right]=\mathbf{0}_{n\cdot\mathbf{p}\times\mathbf{p}}\\ &\frac{\partial^{2}\mathbf{z}}{\partial\mathbf{v}^{2}}(\mathbf{t}_{0})=\frac{\partial^{2}\mathbf{z}_{0}}{\partial\mathbf{v}^{2}}(\mathbf{v})\\ &\overset{\beta}{\partial\mathbf{v}^{2}}(\mathbf{t}_{f})&\overset{\beta}{\mathbf{v}^{2}}&\overset{\beta}{\partial\mathbf{v}^{2}}(\mathbf{t}_{f})&\overset{\beta}{\partial\mathbf{v}^{2}}&\overset{\beta}{\partial\mathbf{v}^{2}}(\mathbf{v})\\ &\overset{\beta}{\partial\mathbf{v}^{2}}(\mathbf{v}_{f})&\overset{\beta}{\partial\mathbf{v}^{2}}&\overset{\beta}{\partial\mathbf{v}^{2}}(\mathbf{v}_{f})&\overset{\beta}{\partial\mathbf{v}^{2}}&\overset{\beta}{\partial\mathbf{v}^{2}}(\mathbf{v}_{f})&\overset{\beta}{\partial\mathbf{v}^{2}}&\overset{\beta}{\partial\mathbf{v}^{2}}&\overset{\beta}{\partial\mathbf{v}^{2}}(\mathbf{v}_{f})&\overset{\beta}{\partial\mathbf{v}^{2}}&\overset{\beta}{\partial\mathbf{v}^{2}}&\overset{\beta}{\partial\mathbf{v}^{2}}(\mathbf{v}_{f})&\overset{\beta}{\partial\mathbf{v}^{2}}&\overset{\beta}{\partial\mathbf{v}^{2}}(\mathbf{v}_{f})&\overset{\beta}{\partial\mathbf{v}^{2}}&\overset$$

- **★**Original DAEs, first and second order sensitivities still share the same Jacobian!
- → Direct decoupled integration scheme possible for gradient & Hessian
- → BUT, full evaluation of state variables Hessian very costly!

Full augmented system

Original system (DAEs)

$$f(z,z,u,v)=0_{\cap}$$
 $z(t_0)=z_0(v)$

First order sensitivities

$$\frac{\partial \mathbf{f}}{\partial \dot{\mathbf{z}}} \frac{\partial \dot{\mathbf{z}}}{\partial \mathbf{v}} + \frac{\partial \mathbf{f}}{\partial \mathbf{z}} \frac{\partial \mathbf{z}}{\partial \mathbf{v}} + \frac{\partial \mathbf{f}}{\partial \mathbf{u}} \frac{\partial \mathbf{u}}{\partial \mathbf{v}} + \frac{\partial \mathbf{f}}{\partial \mathbf{v}} = \mathbf{0}_{\mathsf{nx}\tilde{p}} \qquad \frac{\partial \mathbf{z}}{\partial \mathbf{v}} (\mathbf{t}_0) = \frac{\partial \mathbf{z}_0}{\partial \mathbf{v}} (\mathbf{v})$$

Second order sensitivities

$$\begin{split} \left\{ &\frac{\partial}{\partial \dot{z}} \circ I_{\widetilde{D}} \right\} \frac{\partial^2 \dot{z}}{\partial v^2} + \left[\frac{\partial}{\partial z} \circ I_{\widetilde{D}} \right] \frac{\partial^2 z}{\partial v^2} \right\} + \left[I_n \otimes \left(\frac{\partial \dot{z}}{\partial v} \right)^T \right] \left[\frac{\partial^2 f}{\partial \dot{z}^2} \frac{\partial \dot{z}}{\partial v} + \frac{\partial^2 f}{\partial z \partial \dot{z}} \frac{\partial u}{\partial v} + \frac{\partial^2 f}{\partial v \partial \dot{z}} \right] + \\ &\left[I_n \otimes \left(\frac{\partial z}{\partial v} \right)^T \right] \left[\frac{\partial^2 f}{\partial z \partial \dot{z}} \frac{\partial \dot{z}}{\partial v} + \frac{\partial^2 f}{\partial z^2} \frac{\partial z}{\partial v} + \frac{\partial^2 f}{\partial u \partial z \partial v} + \frac{\partial^2 f}{\partial v \partial z} \right] + \left[\frac{\partial}{\partial u} \circ I_{\widetilde{D}} \right] \frac{\partial^2 u}{\partial v^2} + \left[I_n \otimes \left(\frac{\partial u}{\partial v} \right)^T \right] \\ &\left[\frac{\partial^2 f}{\partial z \partial u} \frac{\partial \dot{z}}{\partial v} + \frac{\partial^2 f}{\partial z \partial v} \frac{\partial z}{\partial v} + \frac{\partial^2 f}{\partial u \partial v} \frac{\partial u}{\partial v} + \frac{\partial^2 f}{\partial v \partial v} \right] + \left[\frac{\partial^2 f}{\partial z \partial v} \frac{\partial \dot{z}}{\partial v} + \frac{\partial^2 f}{\partial v \partial v} \frac{\partial u}{\partial v} + \frac{\partial^2 f}{\partial v^2} \right] = 0_n \cdot \tilde{p} \times \tilde{p} \\ &\frac{\partial z^2}{\partial v^2} \left(t_0 \right) = \frac{\partial z_0^2}{\partial v^2} \left(v \right) \end{split}$$

Restricted second order information



Use product form of Hessian times a search direction, H.p., as used in Truncated Newton (TN) algorithms (e.g. Nash, 1984):

Post-multiplying by a vector $\mathbf{p} \in \mathbb{R}^{p}$

$$\frac{\partial \mathbf{f}}{\partial \mathbf{z}} \mathbf{S}^{\mathrm{T}} + \frac{\partial \mathbf{f}}{\partial \mathbf{z}} \mathbf{S}^{\mathrm{T}} + \mathbf{A}(\mathbf{z}, \mathbf{z}, \mathbf{u}, \mathbf{v}) = \mathbf{0}_{\mathbf{n} \cdot \mathbf{p} \times 1} \qquad \mathbf{S}(\mathbf{t}_0) = \left(\mathbf{p}^{\mathrm{T}} \left[\frac{\partial^2 \mathbf{z}_{01}}{\partial \mathbf{v}^2} (\mathbf{v}) \right] \dots \mathbf{p}^{\mathrm{T}} \left[\frac{\partial^2 \mathbf{z}_{0n}}{\partial \mathbf{v}^2} (\mathbf{v}) \right] \right)$$

$$s_i = \frac{\partial^2 z_i}{\partial v^2} p$$

$$s_i = \frac{\partial^2 z_i}{\partial v^2} p$$
 $\dot{s}_i = \frac{\partial^2 z_i}{\partial v^2} p$ $\dot{p} = \sigma \rho + \eta$

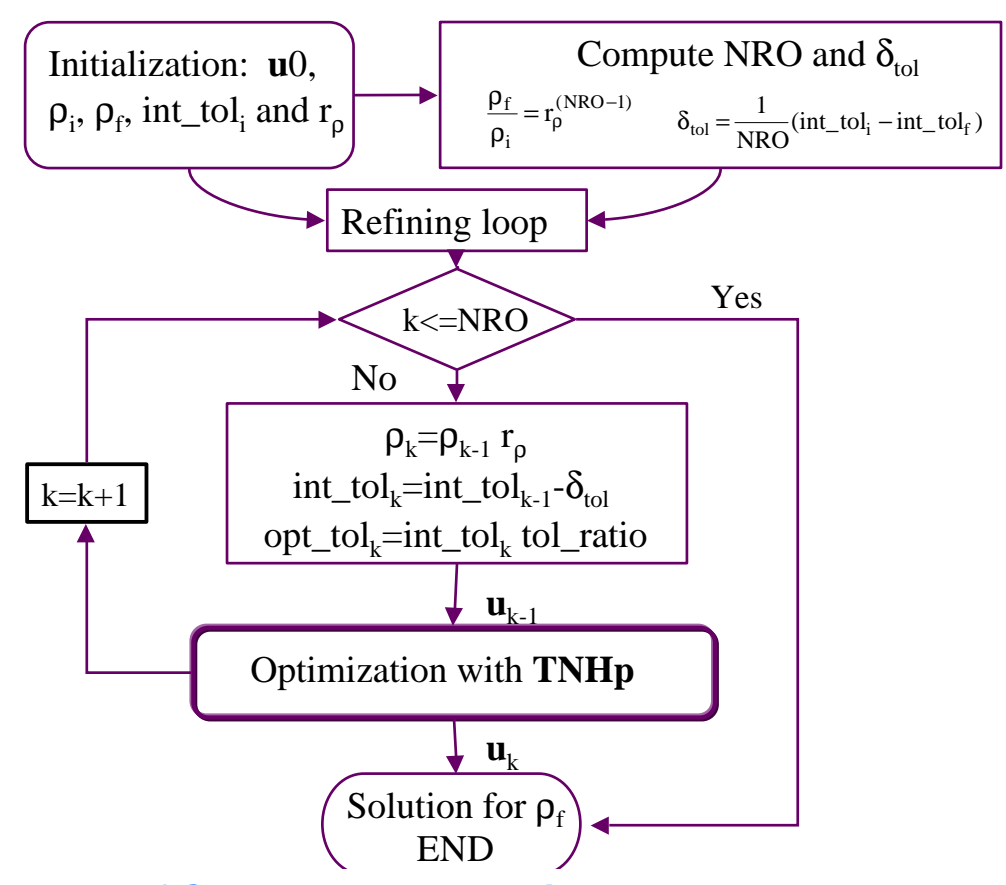
$$\tilde{\rho} = \sigma \rho + \eta$$

Size of extended IVP using H.p
$$n+2\times(n\times\tilde{\rho})$$

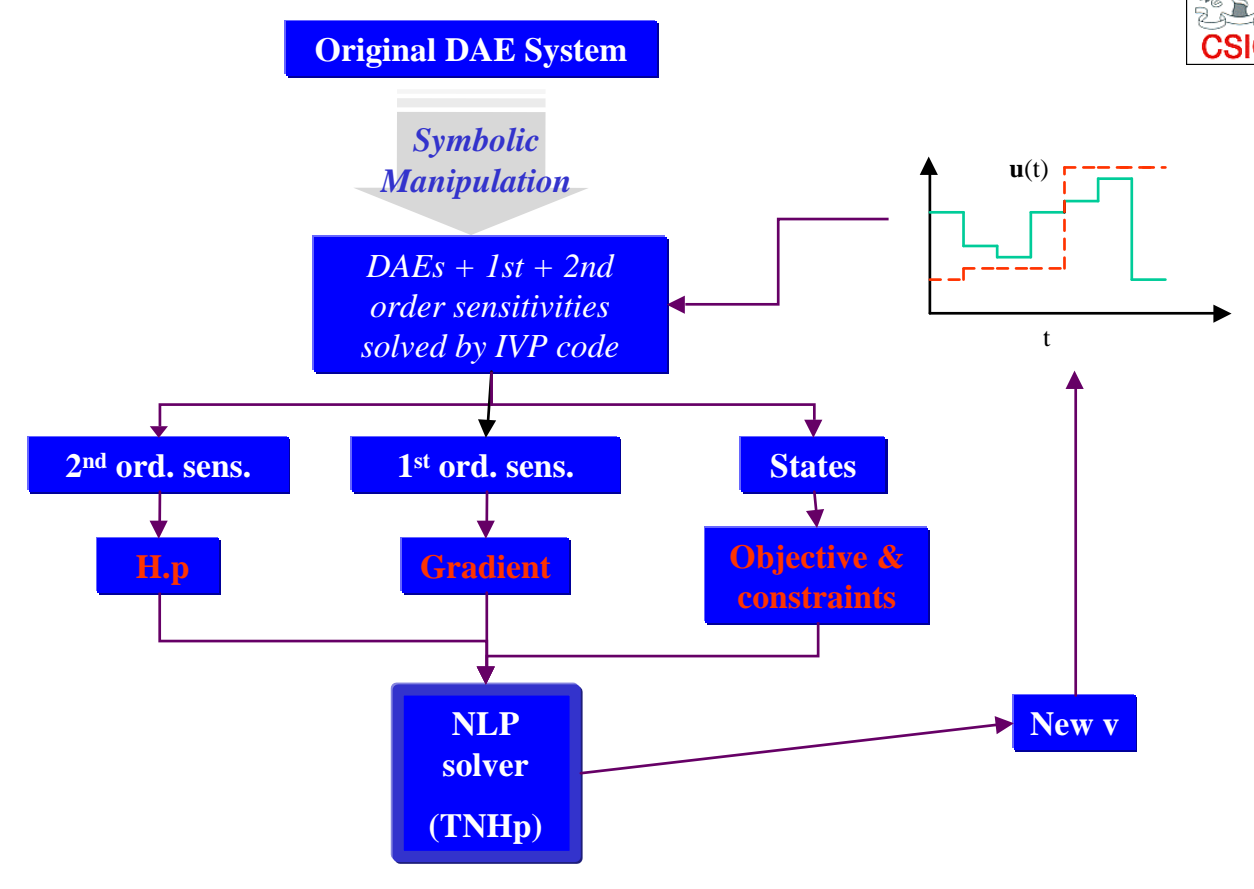
- ★ The original TN code of Nash uses finite differences to generate H.p., which is then used for the iterative solution of Newton equations
- **→ TNHp code: the** exact H.p is used by a modified TN code, resulting in enhanced and fast convergence, even for large-scale problems
- → The computational cost of exact H.p is roughly twice that of a first order sensitivity evaluation, and can be done efficiently
- ightharpoonup To achieve **high discretization levels** (r) with moderate computation times: mesh refining approach (successive re-optimizations of increasing r values)

CSIC

Mesh refining approach



Basic scheme of CVP approach used in TNHp





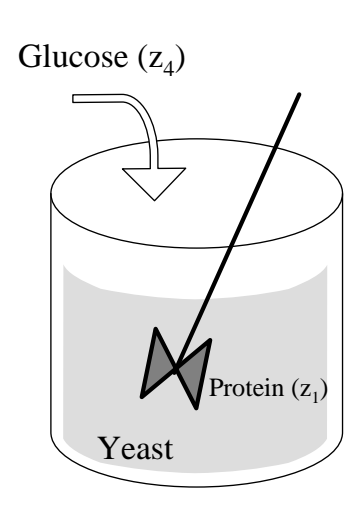
Case I: Park-Ramirez (PR) fed-batch bioreactor:

- The objective is to maximize the secreted heterologous protein by a yeast strain in a fed-batch culture.
- The dynamic model accounts for host-cell growth, gene expression, and the secretion of expressed polypeptides.
- One control variable (glucose input feedrate) and five state variables.

TNHp: optimization of fed-batch bioreactors



Case I: Park-Ramirez (PR) fed-batch bioreactor:



Maximize:
$$J = z_1(t_f)z_5(t_f)$$

s. t.:
$$z_1 = g_1(z_2 - z_1) - (u/z_5)z_1$$

$$z_2 = g_2z_3 - (u/z_5)z_2$$

$$z_3 = g_3z_3 - (u/z_5)z_3$$

$$z_4 = -7.3g_3z_3 + (u/z_5)(20 - z_4)$$

$$z_5 = u$$

$$z(0) = \begin{bmatrix} 0 & 0 & 1 & 5 & 1 \end{bmatrix}^T$$

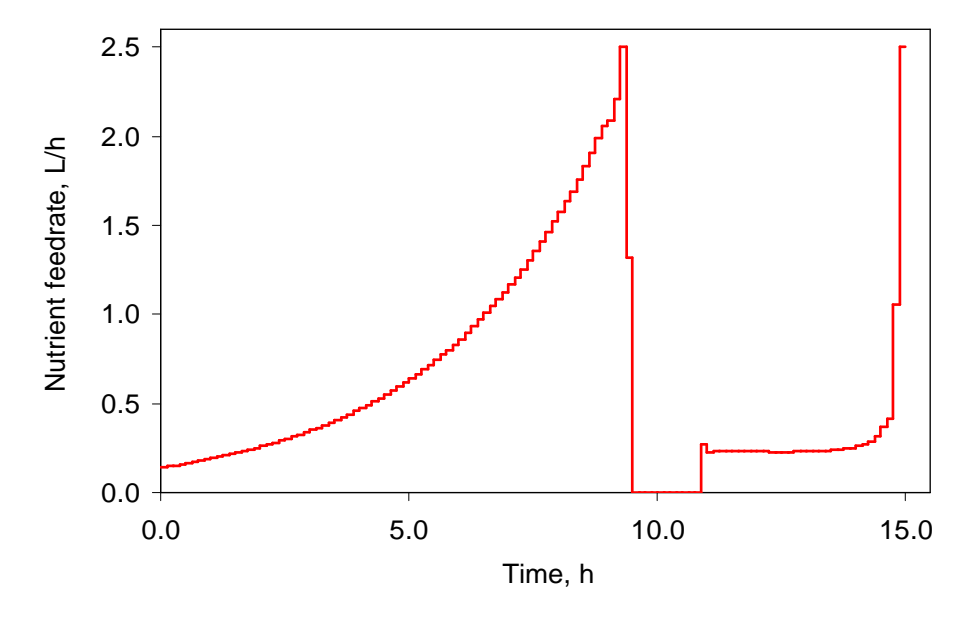
with:

$$g_1 = \frac{4.75g_3}{0.12 + g_3} \qquad g_2 = \frac{z_4}{0.1 + z_4} \exp(-5.0z_4)$$
$$g_3 = \frac{21.87z_4}{(z_4 + 0.4)(z_4 + 62.5)}$$

TNHp: optimization of fed-batch bioreactors



Example of results: optimal control profile for PR



- > TNHp computed better performance indexes than those previously reported
- ➤ Very modest CPU times (9 300 s of PC/Pentium III), i.e. from 20 up to 400 times faster than previous results, even for very refined profiles (300 s for the case of 320 time elements).

TNHp: optimization of fed-batch bioreactors



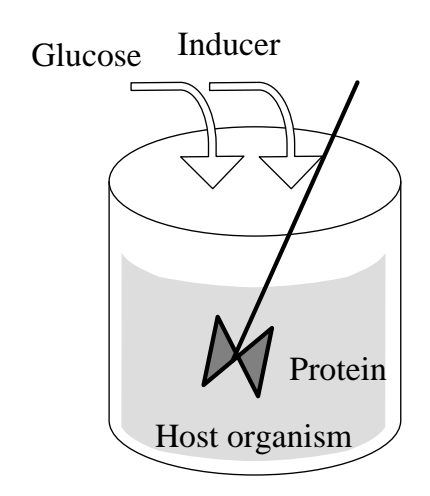
Case II: Lee-Ramirez (LR) fed-batch bioreactor:

- The objective is to maximize the profitability of a process of induced foreign protein production by recombinant bacteria in a fed-batch bioreactor, using the nutrient and the inducer feeding rates as the control variables.
- Different values (Q) for the ratio of the cost of inducer to the value of the protein production were considered.
- Two control variables and seven state variables.

TNHp: optimization of fed-batch bioreactors

CSIC

Case II: Lee-Ramirez (LR) fed-batch bioreactor:



Maximize:
$$J = z_4(t_f)z_1(t_f) - Q \int_{t_0}^{t_f} u_2(t) dt$$

s. t.: $\dot{z}_1 = u_1 + u_2$
 $\dot{z}_2 = \mu z_2 - (u_1 + u_2)z_2/z_1$
 $\dot{z}_3 = u_1 C_n^f/z_1 - (u_1 + u_2)z_3/z_1 - Y^{-1}\mu z_2$
 $\dot{z}_4 = R_{fp}z_2 - (u_1 + u_2)z_4/z_4$
 $\dot{z}_5 = u_2 C_i^f/z_1 - (u_1 + u_2)z_5/z_1$
 $\dot{z}_6 = -k_1 z_6$
 $\dot{z}_7 = k_2(1 - z_7)$
 $z(0) = \begin{bmatrix} 1 & 0.1 & 40 & 0 & 0 & 1 & 0 \end{bmatrix}^T$
 $\mu = \mu(z_3, z_5, z_6, z_7)$

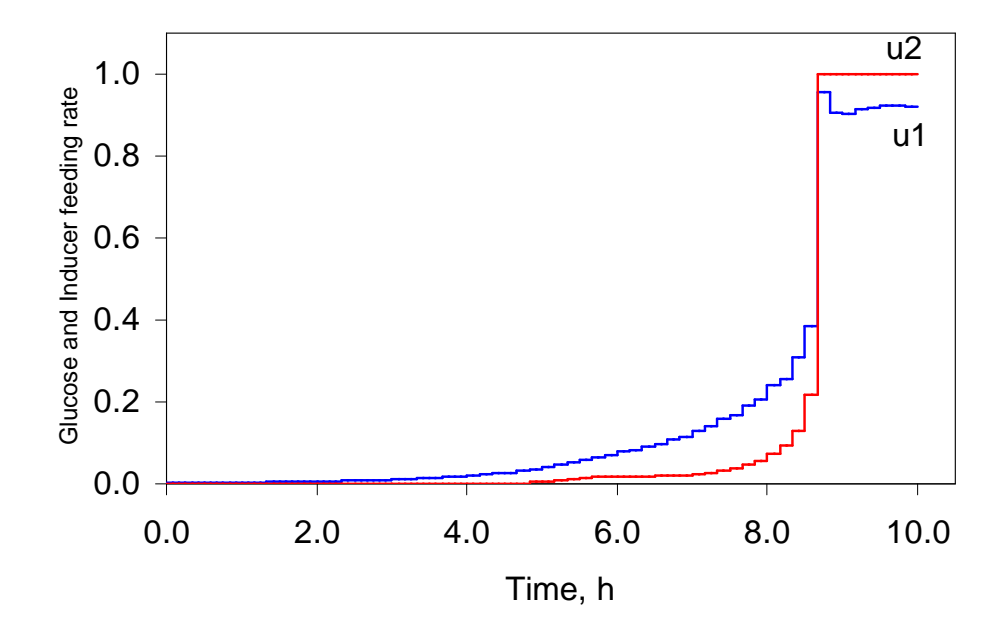
Bounds:

$$0 \le u_1 \le 1$$
 $0 \le u_2 \le 1$

TNHp: optimization of fed-batch bioreactors



Example of results for LR bioreactor: optimal controls for Q = 0

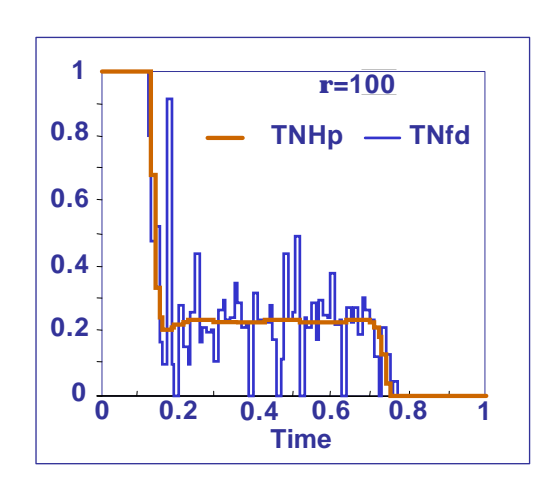


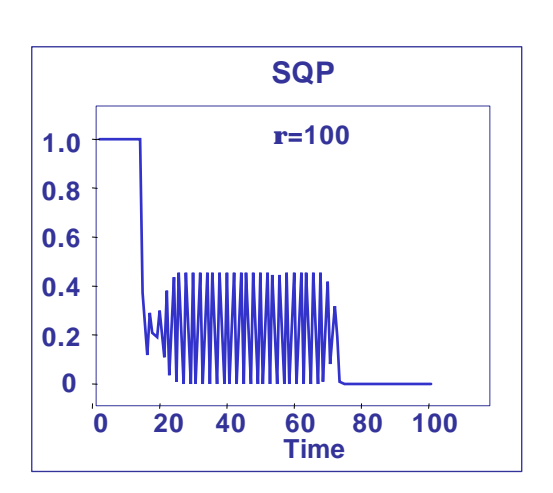
- **★ TNHp** computed **similar performance indexes** to those previously reported
- ★ Very fast: 3-5 s of CPU time (PC/Pentium III)

TNHp: additional advantages



Very good convergence, low noise, even for singular arcs

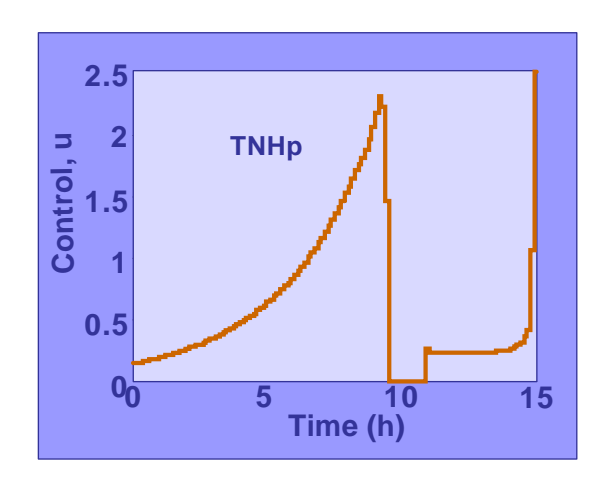


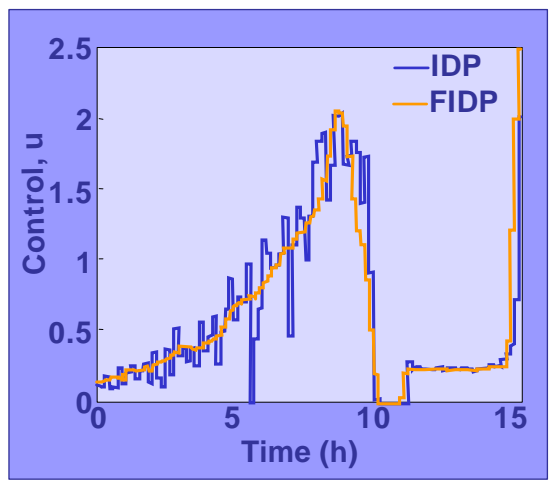


TNHp: additional advantages



Faster and with better convergence properties than latest dynamic programming methods (e.g. IDP)





Conclusions



The use of **exact first and second order information**, implemented in **TNHp**, resulted in **two major advantages**:

- a significant reduction in function and gradient evaluations was observed due to the use of second order information, which although requires the more expensive second order information evaluation, results in overall computational savings
- **2** the ability to consider **very fine discretization levels** for the underlying **controls** has been enhanced both by the high precision and speed of convergence but also by the use of the **mesh-refining technique**

In terms of performance and quality of solutions for many case studies, results achieved are comparable or better than the ones found in literature, with much reduced computation times

On-going work:

- A version for **dynamic optimization of distributed process systems** using sparse IVP solvers is already operative, and cases of up to 5000 states have been solved.
- **2** A closed-loop (receeding horizon dynamic optimization) version in the near future.

Structure of talks



USING MODEL-BASED OPTIMIZATION TO IMPROVE

BIOTECHNOLOGICAL PROCESSES

- **>WEDNESDAY, MARCH 20, 8:30 -9:30:**
 - >PART (i): LOCAL OPTIMIZATION METHODS
- >THURSDAY, MARCH 21, 10:00 11:00:
 - >PART (ii): GLOBAL OPTIMIZATION METHODS

PART (ii): Summary



PART (ii): GLOBAL OPTIMIZATION METHODS

- > Introduction
- > Optimization of Dynamic Models
- > Multimodality: Need of Global Optimization (GO)
- > How to Solve It? Global Optimization Methods
- > Complexity Issues
- >> Stochastic methods of GO
- ➤ Case Studies
- > Scaling up: Cluster Computing
- > Conclusions and Future Work

Optimization of Dynamic Models: Some Problem Types



> Dynamic optimization (open loop optimal control)

To find the optimal operating policies (controls) of a nonlinear dynamic system in order to optimize a performance index (functional)

>Integrated process design and control optimization

Find simultaneously the static design variables, the operating conditions and the controllers which minimize capital and operation costs while maximizing controllability

> Parameter estimation (inverse problem, model calibration)

Find the parameters of a nonlinear dynamic model which give the best fit to a set of experimental data

Resulting NLP-DAEs problem



>> Find v to minimize:

$$C = c(v, z, p)$$

- > subject to constraints
 - → System dynamics (DAEs):

$$f(\dot{z}, z, \mathbf{v}, \mathbf{p}) = 0$$
$$z(t_0) = \mathbf{x}_0$$

→ Path constraints:

$$h(z, p, v) = 0$$
$$g(z, p, v) \le 0$$

→ Upper & lower bounds:

$$v^L \le v \le v^U$$

v: decision variables

z: state variables

p: parameters

Solving the NLP-DAEs problem



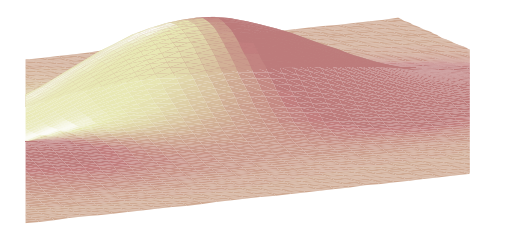
- Direct methods transform the original problem into a constrained NLP
- If this NLP is convex, it can be solved efficiently by local (gradient-based methods)
- ♦ If the NLP is non-convex, global optimization (GO) techniques must be used
 - Stochastic & deterministic GO methods

Multimodal (non-convex) optimization problems

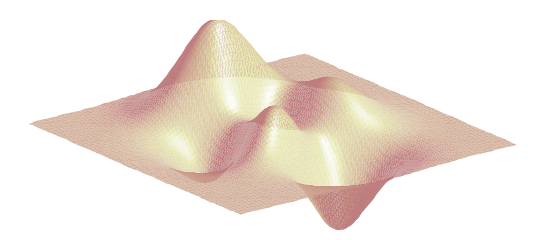


Unconstrained, 2D simple visual example:

Unimodal



Multimodal (non-convex)



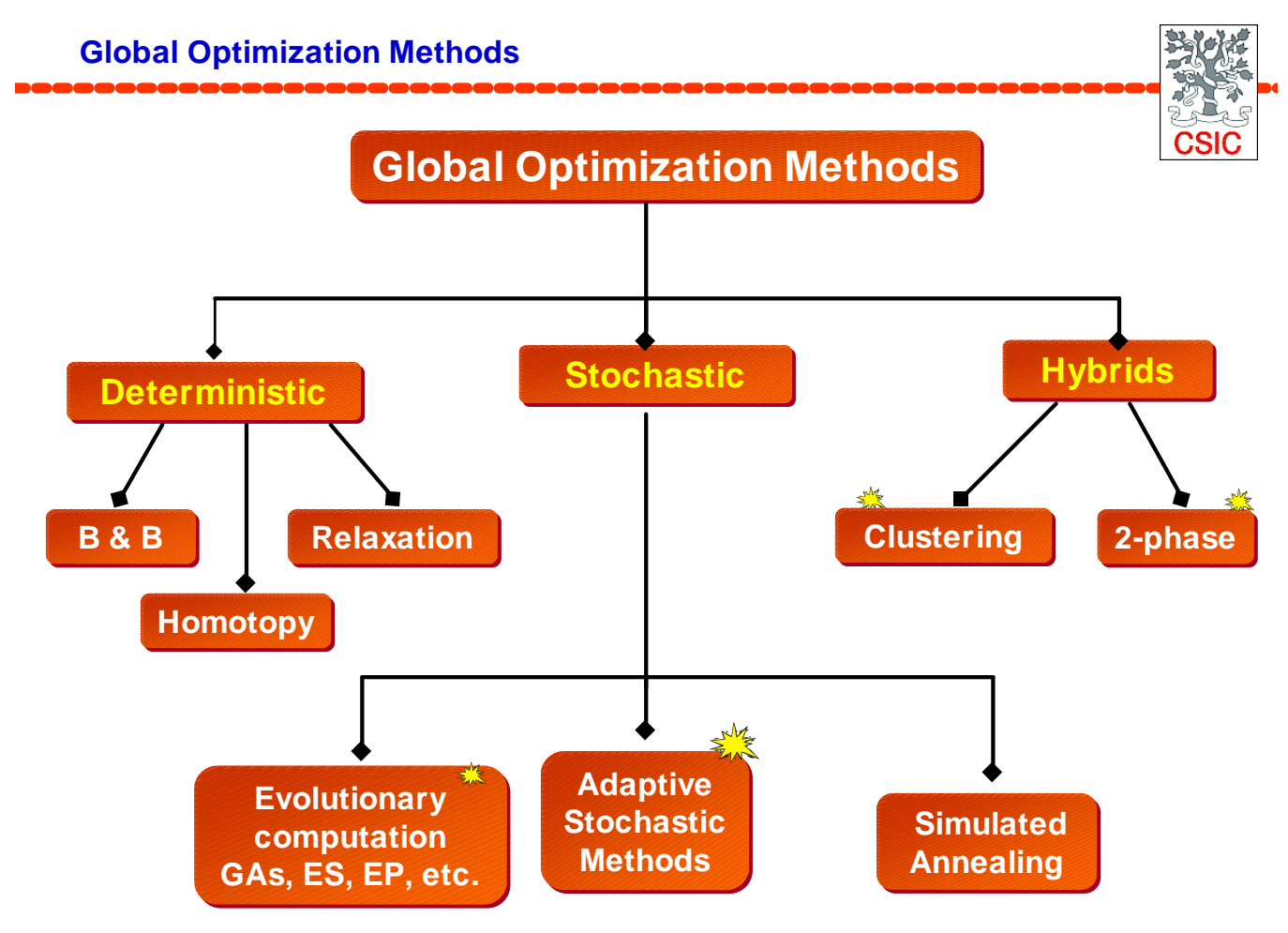
- >Standard methods (e.g. SQP, or even ms-SQP) fail!
 - > Need of Global Optimization (GO) methods

Global Optimization of Nonlinear Dynamic Systems



Main difficulties:

- The objective function and constraints are usually not smooth
- Each simulation is expensive (large CPU time)
- Gradients must be computed numerically
 - Increased number of simulations needed
 - Tolerances cause more non-smoothness
- There is a need for gradient-free, robust and efficient methods capable of working with black-box models



Global Optimization of Nonlinear Dynamic Systems

- > Deterministic methods: recent work of the group of Floudas, based on B&B.
 - → Elegant approach, solving to global optimality
 - → Drawbacks:
 - •significant computational effort even for small problems
 - several differentiability conditions
- > Stochastic methods: several approaches (Luus et al, Banga et al, etc. 1990-2001)
 - → Approximate solutions found in reasonable CPU times
 - → Arbitrary black-box DAEs can be considered (incl. discontinuities etc.)
 - → Main drawback:
 - •Global optimality can not be guaranteed

✓ Our objectives:

- → Methods:
 - → To select the best stochastic methods (efficient, robust // constraints)
 - → To design hybrid methods
- → Problems:
 - → To solve NLP-DAEs with IVP of "black-box" type
 - → To solve large-scale NLP-DAEs (> 100 decision vars, > 10000 states)

"I would rather be certain of a good result than hopeful of a great one..."

(Warren Buffett)

Stochastic Methods: a critical review of promising methods



Simulated Annealing (Kirkpatrick et al, '80s) Genetic Algorithms (Holland, '70s) Adaptive Stochastic Methods (Rastrigin,'50s)

Evolution
Strategies
(ES)
(Rechenberg & Schwefel, '60s)

- > GA, SA and other metaheuristics (TS, ACO, etc.): very popular but ...
- >ES and several adaptive stochastic methods have nice properties:
 - pretty good efficiency and robustness
 - good scaling properties (almost linear...)
 - inherent parallel nature

Complexity Issues



- NFL theorem (Wolpert and McReady, 1997)
 - Basics: impossibility theorem?

"Without any structural assumptions on an optimization problem, no algorithm can perform better on average than blind search"

("needle in a haystack")

- Real implications (ANFL theorem)
- Convergent approaches
 - Ordinal optimization (Y. C. Ho)
 - Soft computing
 - Evolutionary methods
 - Adaptive stochastic methods

Examples of Applications of GO in Bioprocess Engineering



- Integrated process design:
 - Aseptic processing
 - Wastewater treatment plants
- Parameter estimation:
 - Distributed diffusion-reaction systems
 - Nonlinear biochemical pathways
 - Optimal experimental design (dynamic exp.)
- Dynamic optimization:
 - Batch and semi-batch liquid fermentation
 - Distributed diffusion-reaction systems
 - Thermal processing (sterilization, pasteurization)
 - Air drying
 - Solid-state fermentation

Integrated process design

CSIC

Traditional approach
Sequential design
(ignores the interaction
of design and control)



Optimal steady state w.r.t. economic measure



Process control issues

Simultaneous approach



It considers operability together with economic issues (challenging problems)

Integrated process design: statement



>> Find v to minimize:

$$C = f_1 + f_2 + f_3$$

- > subject to constraints
 - → System dynamics (DAEs):

$$f(\dot{x}, x, v, p) = 0$$

$$\boldsymbol{x}(t_0) = \boldsymbol{x}_0$$

→ Path constraints:

$$\boldsymbol{h}(\boldsymbol{x},\boldsymbol{p},\boldsymbol{v}) = 0$$

$$g(x, p, v) \leq 0$$

→ Upper & lower bounds:

$$v^L \le v \le v^U$$

 \mathbf{f}_{l} : capital cost

 \mathbf{f}_2 : operation cost

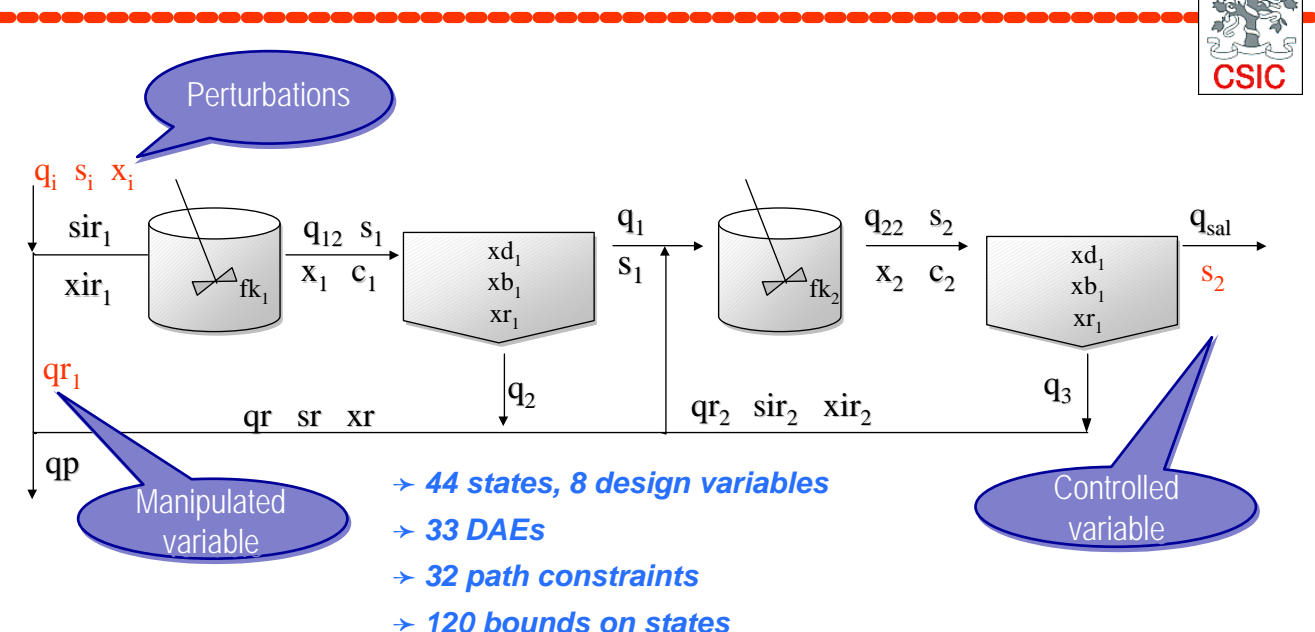
 f_3 : controllability cost

v: decision variables

x: state variables

p: parameters

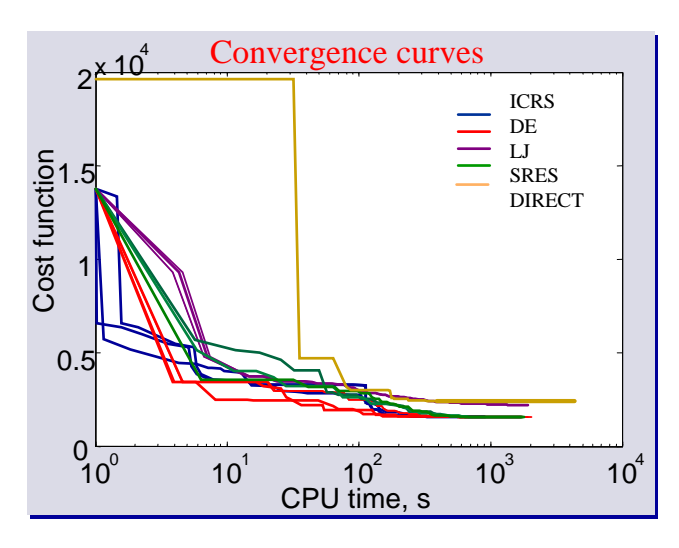
Integrated process design: waste-water plant example



Objetive: to find the design of the units, the operating conditions and the parameters of the controller which minimize a weighted sum (C) of economic terms (f_{econ}) and a controllability measure (ISE)

Integrated process design: selected results



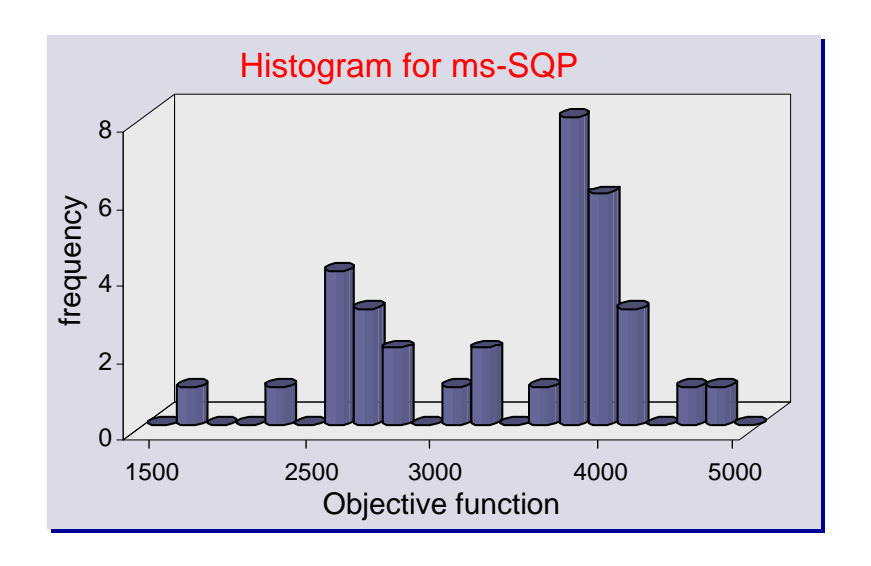


	GLOBAL	ICRS	DE	SQP
С	<u>1544.54</u>	1551.02	1545.47	3495.7
$oldsymbol{f}_{econ}$	1145.87	1165.14	1138.16	3002.94
ISE	0.3986	0.3858	0.4073	0.4927
CPU,s	251.84	916.35	983.89	35.18
Neval	8307	19229	10530	330

- Csendes' **GLOBAL** clustering method, simple adaptive stochastic methods (e.g. **ICRS**) and **DE** presented the best convergence rates, with reasonable CPU times (minutes in a PC-PIII)
- ES methods: similar performance but with longer CPU times
- SQP local method failed (as expected)

Integrated process design: failure of multi-start



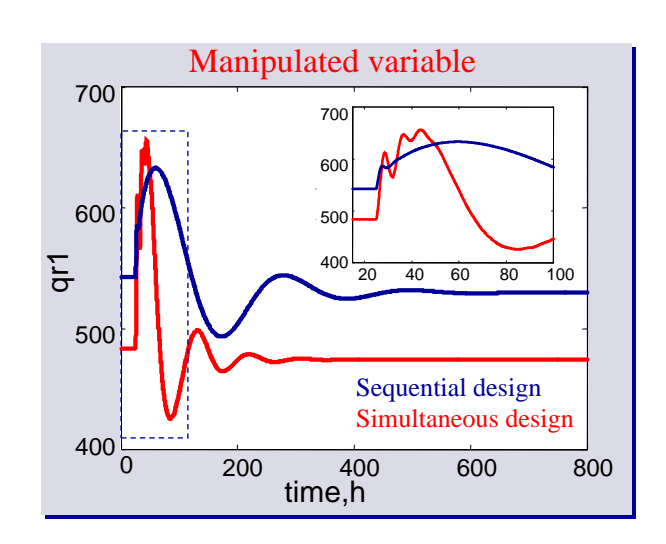


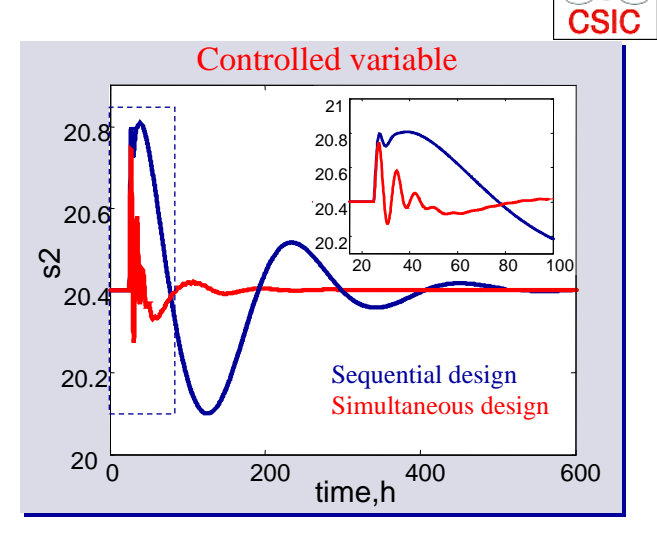
Large number of local solutions. The best ms-SQP result (after 500 runs) was:

C=1644.65

SQP always converged to local solutions (even with multi-start N=500)

Traditional vs. integrated process design





Sequential design method (traditional two-steps): plant design cheaper than the one found by the simultaneous approach, but its controllability is very poor (very large ISE value, 25 times larger)

Parameter estimation for DAEs models



> Highly non-linear, large dynamic models

- → Usually > 20 DAEs
- → Usually > 50 decision variables (parameters to estimate)

© Objetive: minimize time-weighted sum

$$f = \sum_{i=1}^{n} \sum_{j=1}^{m} w_{ij} ((y_{teor}(i) - y_{exp}(i))_{j})^{b}$$

> subject to DAEs constraints

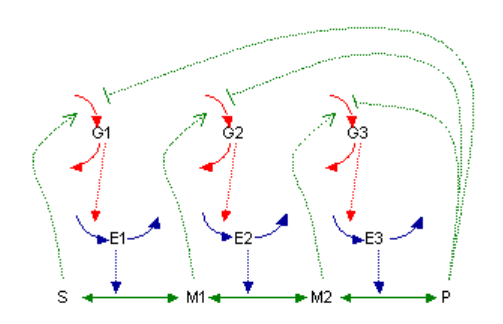
 y_{exp} : experimental data y_{teor} : predicted values

Parameter estimation for nonlinear biochemical pathways









> Collaboration with P. Mendes (Virginia Bioinformatics Institute)

- → Small metabolic pathway (3-step, 36 parameters) seems tractable (several hours of PIII using uES, with record results)
- → Cases with 100 parameters still not solved succesfully...

© On-going work.....

Optimal Experimental Design (OED)



- \Rightarrow Performing experiments to obtain a rich enough set of $y_m(t)$ is a costly and time-consuming activity
- The purpose of **optimal experimental design (OED)** is to devise the necessary dynamic experiments in such a way that the parameters are estimated from the resulting experimental data with the best possible statistical quality
- ♦ Statistical quality: usually a measure of the accuracy and/or decorrelation of the estimated parameters
- ♦ OED applied to linear steady state models is a well known subject
- **© OED of non-linear dynamic models (DAEs)**: more challenging

Collaboration with Jan Van Impe & K. Versyck (K. U. Leuven) LEUVEN



Statement of OED problem (dynamic systems)



- ♦ The OED problem can be formulated as a <u>dynamic optimization</u> (optimal control) problem:
 - To **find** a set of **time-varying input variables** (controls) for the dynamic experiments optimizing the quality of the estimated parameters in some statistical sense.
- ♦ Criteria based on the Fisher information matrix:

$$\boldsymbol{F} = \int_{0}^{t_f} \left(\frac{\mathbf{N}y}{\mathbf{N}p}(t) \right)^{\mathrm{T}} \boldsymbol{Q}(t) \left(\frac{\mathbf{N}y}{\mathbf{N}p}(t) \right) dt$$

where *Q* is inverse of the measurement error covariance matrix.

- > Scalar functions f of F evaluated in p_o are used as OED criteria for increasing the practical identifiability of the model parameters from experimental data.
- \Leftrightarrow **Remark**: for linear systems, F^{-1} evaluated in p^* is the error covariance matrix of the BLUE. For non-linear models, we assume the output can be approximated as a 1st order Taylor series expansion in the vicinity of p*. During experimental design for parameter estimation a so-called nominal parameter set p_o is to be used instead of the unknown true process parameters p*

S.t.

Statement of OED as a Dynamic Optimization Problem



Find $\mathbf{u}(t)$ and $\mathbf{t_f}$ to minimize:

$$J = \phi(\mathbf{F})$$
, with $\mathbf{F} = \int_{0}^{t_f} \left(\frac{\mathbf{g} \mathbf{y}}{\mathbf{g} \mathbf{p}}(t) \right)^{\mathsf{T}} \mathbf{Q}(t) \left(\frac{\mathbf{g} \mathbf{y}}{\mathbf{g} \mathbf{p}}(t) \right) dt$ @ p=p₀

System dynamics (DAEs) and algebraic constraints:

$$f[\dot{x}, x, p, u, t] = 0$$
$$h[x, y, p, u, t] = 0$$
$$g[x, y, p, u, t] \le 0$$

Bounds for the controls:

$$\mathbf{u}^{\!\scriptscriptstyle L}(t)\!\leq\!\mathbf{u}\,(t)\!\leq\!\mathbf{u}^{\!\scriptscriptstyle U}(t)$$

 $\mathbf{x} \in \mathbb{R}^n$: state variables $\mathbf{y} \in \mathbb{R}^n$: output variables

 $\mathbf{u} \in \mathbb{R}^{\sigma}$: control variables

Scalar functions of F as OED criteria



- ♦ Examples of common scalar functions of *F* (to min.) are:
- \diamond **D-criterion** (determinant of F), which measures the global accuracy of the estimated parameters J=-|F|
- $ightharpoonup \phi$ **Modified E-criterion** (condition number of F), which measures the parameter decorrelation

$$J = \Lambda(F) = I_{max}(F) / I_{min}(F)$$

 \diamond **A-criterion** (trace of inverse of **F**), which measures the arithmetic mean of estimation error

$$J = \operatorname{trace}(F^{-1})$$

- ♦ Which one? It depends on the requirements of the application
- ♦ <u>Remark</u>: the minimum of the modified E-cost is known exactly (1.0)

OED: case study





Model: dynamics of a **fed-batch bioreactor** where one biomass is growing on one limiting substrate, assuming **non-monotonic Haldane growth kinetics**.

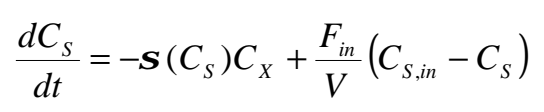
Objective: to **estimate the Haldane parameters** K_p and K_i based on **measurements of two model outputs**, i.e. the substrate concentration C_S and the biomass concentration C_X . The **volumetric feed rate** u(t) into the fed-batch bioreactor is considered as the control input for the dynamic experiments.

OED (DO) problem: to find u(t) so as maximum global accuracy and/or decorrelation of the estimates for Kp and Ki is obtained, s.t.:

- the differential equality constraints (model dynamics),
- bounds for the control and the states,
- \triangleright path inequality constraints on C_S to guarantee model validity (balanced growth).

<u>Remarks</u>: information matrix \mathbf{F} computed from the sensitivities obtained by solving an extended IVP. For \mathbf{Q} : additive, uncorrelated, zero-mean white Gaussian noise is assumed on the measurements of the substrate concentration C_s and the biomass concentration C_s

OED case study: dynamic model



$$\frac{dC_X}{dt} = \mathbf{m}(C_S)C_X - \frac{F_{in}}{V}C_X$$

$$\frac{dV}{dt} = F_{in}$$

$$\mathbf{S}(C_S) = \frac{1}{Y_{X/S}} \mathbf{m}(C_S) + m$$

$$\mathbf{m}(C_S) = \mathbf{m}_m \frac{C_S}{K_p + C_S + C_S^2 / K_i}$$

 K_p [g/L] indicates how fast the optimum for μ is reached K_i [g/L] is the inhibition parameter



 C_X [g DW/L] biomass concentration V [L] volume of the liquid phase

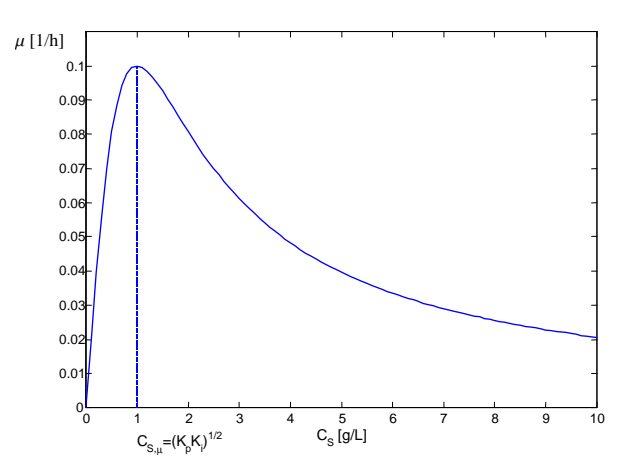
 $C_{S,in}$ [g/L] substrate concentration in the influent

 F_{in} [L/h] flow rate of influent

σ [g/g DW h] specific substrate consumption rate

 μ [1/h] specific growth rate

 $Y_{X/S}$ [g DW/g] biomass on substrate yield coefficient m [g/g DW h] (overall) specific maintenance demand



OED subproblems



The following two sub-problems were considered:

① Optimal control for parameter decorrelation: the cost function is the modified E-cost (ratio of the maximum and minimum eigenvalues of matrix F).

Min.
$$J = \Lambda(\mathbf{F}) = \mathbf{I}_{max}(\mathbf{F}) / \mathbf{I}_{min}(\mathbf{F})$$

2 Optimal control for parameter accuracy: the cost function is the D-cost (determinant of matrix F).

$$Min.$$
 $J = -|F|$

For these problems, Versyck et al (1997) followed an ad hoc heuristic procedure, based on theoretical analysis of the optimal process performance feed rate profile, to design optimal control inputs. Their results are used for comparison.

OED: numerical solutions using CVP methods



→ Control parameterizations based on piecewise constant and piecewise linear polynomials were tested, taking 10-20 time elements (fixed & varying length)

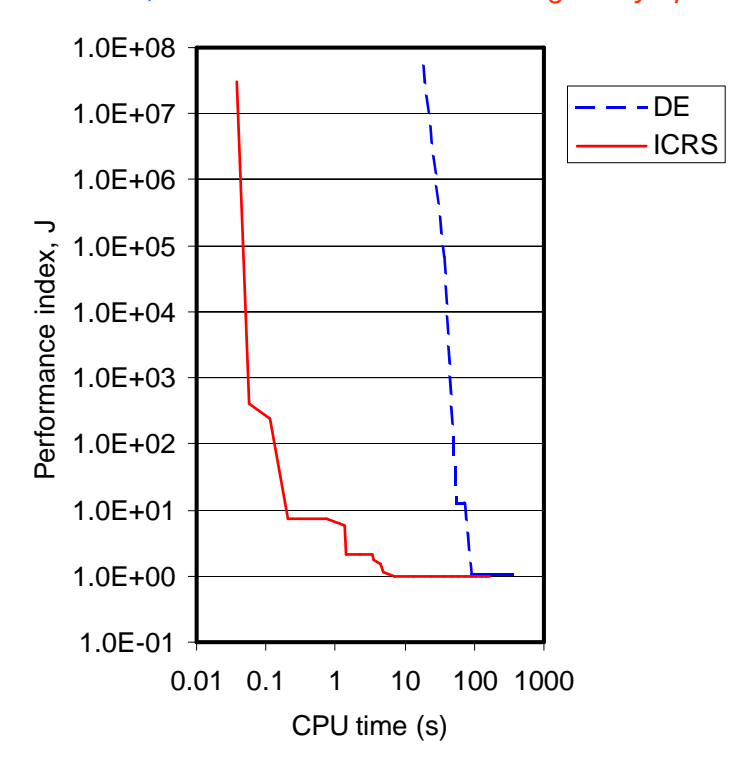
Solution of the main NLP:

- ★ Several deterministic (SQP-based) local solvers were tested, but many difficulties were encountered: convergence failures, or convergence to local solutions after excessive computation times were found (alternative reformulation?)
- ★ In contrast, the **stochastic ICRS and DE solvers** arrived to very **good solutions** in very **reasonable computation times**

OED sub-problem [1] (modified E-cost)

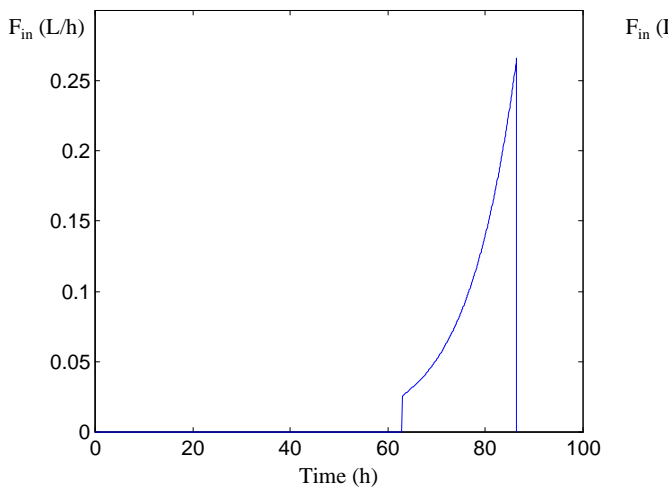
CSIC

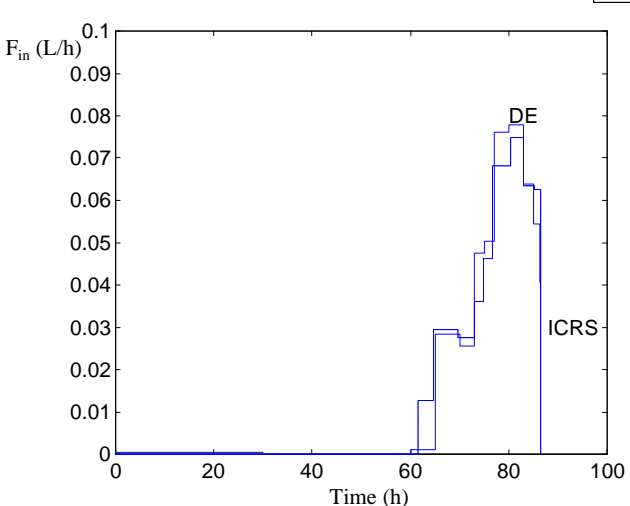
The stochastic solvers arrived to cost functions very close to 1.0 (within a tolerance of 10⁻⁵) in very modest computation times (order of minutes in a PC Pentium-II). In this case, we know these solutions are globally optimal.



OED: comparison of results (modified E-cost)







Optimal feed rate by Versyck et al (1997), J = 1.0

Optimal feed rates obtained with ICRS and DE, J = 1.0

Banga, J. R., K. J. Versyck and J. F. Van impe (2000) Numerical strategies for optimal experimental design for parameter identification of non-linear dynamic (bio-)chemical processes. Presented at ESCAPE-10, May 7-10, Firenze, Italy.

Other examples



- ♦ Several challenging problems have been solved in other collaborations kept with:
- ♦ Optimization of hybrid dynamic systems (Prof. P. Barton) MIT
- ♦ Non-linear model predictive control (Prof. W. D. Seider)
- ♦ Dynamic optimization of thermal processing (Prof. Paul Singh)



→ Dynamic optimization of microwave processing (EU project coordinated by Prof. B. Nicolaï)



♦ Dynamic optimization of large dynamic systems (Prof. Y. Kevrekidis) Princeton University

Check papers at http://www.iim.csic.es/~julio/

Stochastic methods are easy to parallelize (e.g. "islands approach") > scheme "master-worker", using PARALIZE > able to run on heterogeneous networks > easy to implement (no need of PVM or MPI) by means of: Chalmers PARALIZE Matlab

1

0

0

Virtual Network

Computing

Speedup for ICRS in a LAN of NT PCs

Number of processors

4

5

6

7

3

1

Conclusions



- Global optimization of dynamic models: a means of ensuring optimality in decision support tools for:
 - >> Process design
 - > Operating procedures synthesis
 - > Model calibration
- > For many bioprocesses, optimal operating procedures provide significant improvements over nominal processes
- > Local strategies (e.g. SQP), even with multi-start, are of little help
- GO methods: simple adaptive stochastic methods, clustering methods and Evolution Strategies (ES) presented the best performance
- > Parallel versions of these methods can be created very easily using standard environments
- >> Be careful with over-hyped "popular" techniques!
- > On-going work on deterministic and hybrid GO methods...

Current and future work



- On-going work:
 - Scaling up to larger and more complex problems
 - → Integrated design and control of large plants and distributed systems with > 10⁴ states using the parallel solvers
 - → Extension to process and control superstructures (different design alternatives) problems (MIOCPs)
 - → Parameter estimation problems with >100 parameters
 - → Optimal control of large (e.g. distributed) systems with > 10⁴ states (ROM via POD)

Minicourse

Benelux Meeting on Systems and Control 2002

Financial Engineering and Control

Hans Schumacher

Department of
Econometrics and Operations Research
Tilburg University

Purpose of the minicourse

Topics to be treated:

- how to model financial markets
- how to construct protection against unpredictable changes
- applications including: pension funds, energy markets

Topic not to be treated:

 how to make a million dollars by trading in the stock market.

2

Main concern: risk management

Some truisms about risk:

- risk cannot be avoided
- risk can be diminished
- reduction of risk comes at a price.

Also: there is economic value in reducing risk.

The minicourse will concentrate on financial risk and the use of financial instruments.

Financial risk arises due to fluctuations in markets (exchange rates, interest rates, energy prices, stock prices, ...) as well as from general economic factors such as inflation, and from other sources.

Two main methods of reducing risk

General ways of reducing risk:

- diversificationMarkowitz, Sharpe, . . .
- hedging
 Black, Scholes, Merton, . . .

Diversification concentrates on the joint characteristics of assets; hedging concentrates on the risk factors behind asset prices. (No sharp distinction.)

Both methods may be developed in a Static as well as in a dynamic setting.

Examples . . .

A simple example of diversification

How to divide investment between two assets such that total risk is minimized?

Assume:

the values of the two assets (say, X_1 and X_2) are jointly normally distributed, with expectations μ_1 and μ_2 , variances σ_1^2 and σ_2^2 , and correlation coefficient ρ .

Problem:

find α_1 and α_2 , with $\alpha_1 \geq 0$, $\alpha_2 \geq 0$, $\alpha_1 + \alpha_2 = 1$, such that the variance of $\alpha_1 X_1 + \alpha_2 X_2$ is minimized.

Is the best policy to invest everything in the asset that has the lowest variance?

Variants

The story becomes different when

- not only variance, but also expected value is taken into account (mean-variance optimization)
- negative ("short") positions are allowed.

Further extensions:

- multiple periods, or continuous time (leading to stochastic optimal control)
- non-normal distributions (various risk measures)
- include liabilities
- robustness.

Solution

Solve a quadratic optimization problem.

Invest everything in the safest asset if

$$\rho \geq \sigma_1/\sigma_2$$

(assuming X_1 is the safest asset). If the above inequality is not satisfied, then the minimum is reached for a nontrivial combination of the two assets.

Numerical example: assume $\sigma_1=1$, $\sigma_2=2$, and $\rho=0$. Then the optimal solution is to invest 80% in the safe asset and 20% in the risky asset. Variance obtained with this allocation:

$$0.8^2 * 1 + 0.2^2 * 4 = 0.64 + 0.16 = 0.8$$
.

If everything would have been invested in the safest asset, the variance would have been 1.

A simple example of hedging

Consider a pension fund that holds a bond portfolio to cover its future liabilities.

Let r be the annual interest rate (assumed to be the same for all maturities.)

Current value of expected payments to be made:

$$P = \sum_{k=1}^{K} (1+r)^{-k} P_k.$$

Current value of bond portfolio:

$$B = \sum_{k=1}^{K} (1+r)^{-k} B_k.$$

We would like to have at least B=P. But there is more.

Duration matching

Both current values are sensitive to changes in the interest rate. Define the duration of a series of cash flows C_1, \ldots, C_k by:

$$D(C_1, \dots, C_k) = \frac{\sum_{k=1}^K k(1+r)^{-k} C_k}{\sum_{k=1}^K (1+r)^{-k} C_k}.$$

The relative change of the current values of the cash flows C_k due to a change Δr in the interest rate r is approximately equal to

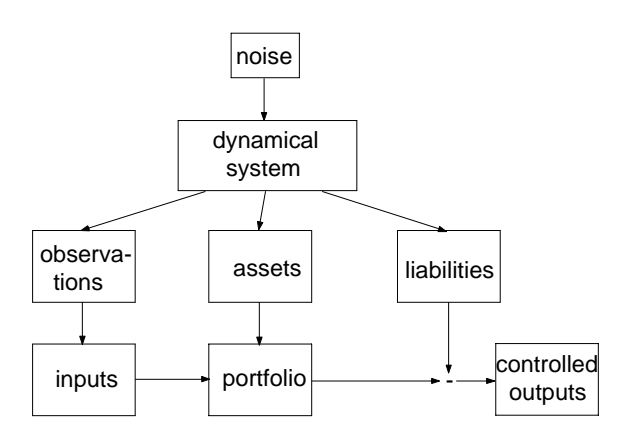
$$-\frac{\Delta r}{1+r}D(C_1,\ldots,C_k).$$

Consequently, the position of the pension fund is made insensitive to interest rate changes, at least to first order, if the payments (P_1,\ldots,P_k) and the bonds (B_1,\ldots,B_k) are duration matched, that is,

$$D(B_1, \ldots, B_k) = D(P_1, \ldots, P_k).$$

9

General picture



Observations typically include current asset prices.

Inputs usually are portfolio weights. The controlled output is often a net value.

11

Extensions

Hedging aims at obtaining insensitivity to certain risk factors by finding suitable combinations of assets that are all influenced by the same risk factors.

This is a model-based activity because the dependence of asset values on risk factors needs to be modeled.

For instance, it was assumed above that the interest rate is the same for all maturities. This is a model assumption. Like all model assumptions, it is not entirely true. More advanced hedging schemes use models for the entire term structure of interest rates.

The Black-Scholes revolution in finance is based on the introduction of dynamic hedging strategies.

10

Peculiarities of financial models

Financial models have a number of peculiar properties, which distinguish them from general dynamical models.

• The value of the sum of two portfolios is the sum of their values.

This is a linearity property which relates to the effects of inputs (portfolio weights) on controlled outputs.

 No control strategy can produce a noise-free positive net value from a zero initial investment.

This is an economic principle known as absence of arbitrage. It leads to a constraint on the way that asset prices depend on state variables; this will be discussed in more detail below.

194

Another peculiarity

There is also a certain constraint on input functions that needs to be imposed.

This is most easily explained in discrete time. Let S_t denote a vector of asset prices and let u_t denote a vector of corresponding portfolio weights. The control $\{u_t\}$ is said to be self-financing if for all t:

$$u_{t+1} \cdot S_{t+1} = u_t \cdot S_{t+1}$$

This entails a single linear constraint on the vector of control inputs at each time t.

Rewrite the above using the forward difference operator:

$$\Delta(u_t \cdot S_t) = u_t \cdot (\Delta S_t).$$

This suggests the continuous-time version

$$d(u_t \cdot S_t) = u_t \cdot dS_t$$

where d is an "infinitesimal forward difference."

13

The chain rule

We think of the vector of asset prices S_t as dependent upon state variables and time, say $S_t = \pi(t, X_t)$; moreover, a differential equation for X_t would be given. To write controlled output $V_t = \int_0^t u_{\mathcal{T}} \cdot dS_{\mathcal{T}}$ as a function of inputs and states, it would then be natural to use the chain rule

$$dS_t = \frac{\partial \pi}{\partial t} dt + \frac{\partial \pi}{\partial x} dX_t.$$

Consider in general the relation

$$y(t) = \phi(x(t)).$$

According to the usual chain rule, we can compute y(t) approximately by

$$y(t) \approx y(0) + \sum \phi'(x(t_i))(x(t_{i+1}) - x(t_i))$$

but it turns out that this may not be a good approximation if $x(\cdot)$ is a highly irregular function of time.

15

Result of a portfolio strategy

Let S_t denote a vector of asset prices, and let u_t be a vector of corresponding portfolio weights. The portfolio value is given by

$$V_t := u_t \cdot S_t$$
.

In discrete time, the change in portfolio value between time t and time t+1 is given by

$$V_{t+1} - V_t = u_t \cdot (S_{t+1} - S_t)$$

or in Δ notation

$$\Delta V_t = u_t \cdot \Delta S_t$$

So portfolio value at time T is given by

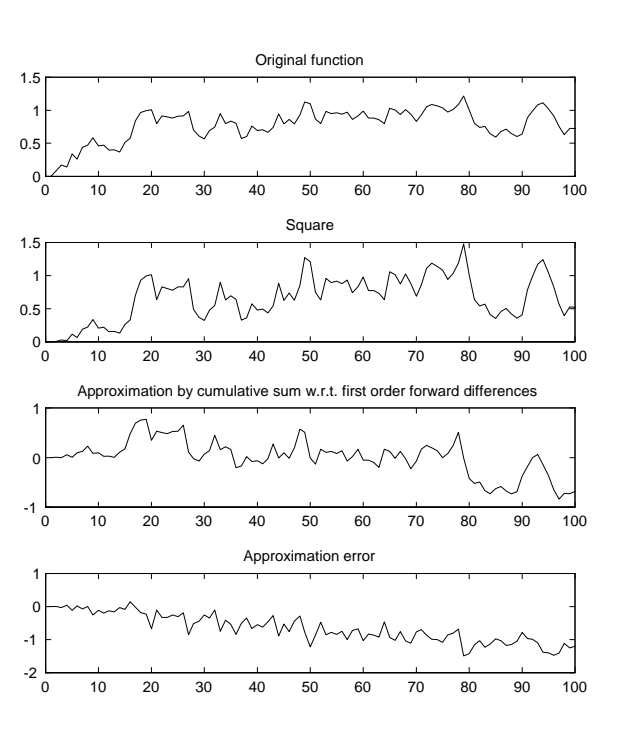
$$V_T = V_0 + \sum_{t=0}^{T-1} u_t \cdot \Delta S_t$$

The analogous formula in continuous time is

$$V_T = V_0 + \int_0^T u_t \cdot dS_t$$

14

The need for a second-order term



A modified chain rule (Itô)

A better approximation is obtained if we also include the second-order term. So our new chain rule becomes: if $y(t) = \phi(x(t))$, then

$$dy = \phi'(x) dx + \frac{1}{2} \phi''(x) d[x, x]$$

where the term "d[x,x]" is the infinitesimal version of

$$\Delta[x, x](t) = (x(t + \Delta t) - x(t))^{2}.$$

We will also need a vector version:

$$dy = \frac{\partial \phi}{\partial x}(x) dx + \frac{1}{2} \operatorname{tr} \left(\frac{\partial^2 \phi}{\partial x^2}(x) d[x, x] \right)$$

where now d[x,x] is a matrix with entries of the form $d[x_i,x_j]$, and ${\rm tr}$ denotes "trace".

17

Example 1: Black-Scholes (Samuelson)

State equation:

$$dX_t = \mu X_t dX_t + \sigma X_t dW_t$$

where μ and σ are constants and W_t is Brownian motion.

Assets:

$$S_t = X_t$$
$$B_t = e^{rt}$$

where r is a constant.

This is a model for a stock price (S_t) and a fixed-interest account (B_t) .

An alternative formulation of the same model:

$$dZ_t = (\mu - \frac{1}{2}\sigma^2)dt + \sigma dW_t$$

$$S_t = \exp(Z_t)$$

$$B_t = e^{rt}$$

19

This is obtained from the transformation $Z_t = \log X_t$.

A general financial model

A state-space model:

$$dX_t = \mu_X(t, X_t)dt + \sigma_X(t, X_t)dW_t$$

$$S_t = \pi_S(t, X_t)$$

$$dV_t = u_t \cdot dS_t$$

where

- we follow (largely) the convention of denoting stochastic variables by capital letters
- we also follow the convention of using μ for "drift" and σ for "volatility"
- W_t denotes Brownian motion, so dW_t/dt is "white noise"
- π is a mnemonic for "price".

18

Example 2: Vasicek

State equations: (drop subscript t)

$$dX_1 = a(b - X_1)dt + \sigma dW$$

$$dX_2 = X_1X_2dt$$

where a and b are constants.

Assets:

$$M = X_2$$
$$B_T = \pi_T(X_1)$$

This is a simple model for bond prices. The asset M denotes a "money market account" (a checking account that brings a variable interest rate X_1). The asset B_T is a bond that pays one euro at time T.

The pricing function π_T is not specified in the model above, but it has to satisfy certain constraints. . .

Absence-of-arbitrage requirement

Consider again the state-space model

$$dX_t = \mu_X(t, X_t)dt + \sigma_X(t, X_t)dW_t$$

$$S_t = \pi_S(t, X_t).$$

By making use of the chain rule we can write

$$dS_t = \mu_S(t,X_t)dt + \sigma_S(t,X_t)dW_t$$
 for certain functions $\mu_S = \mu_S(t,x)$ and $\sigma_S = \sigma_S(t,x).$

Recall: "arbitrage" means that a riskless profit can be made from a zero investment.

Thm. The above model allows no arbitrage if and only if there exist functions $\rho(t,x)$ and $\lambda(t,x)$ such that

$$\mu_S - \rho \pi_S = \sigma_S \lambda.$$

21

Market completeness

The Black-Scholes equation may be written in the form

$$\mu_S = \begin{bmatrix} \pi_S & \sigma_S \end{bmatrix} \begin{bmatrix}
ho \\ \lambda \end{bmatrix}$$

Note: all variables are functions of t and x. Sizes:

 μ_S , π_S : m-vectors (m= number of assets) σ_S : $m \times k$ matrix (k= number of noise inputs)

 ρ : scalar (short-term interest rate)

 λ : k-vector (risk premia).

When the matrix $[\pi_S(t,x) \ \sigma_S(t,x)]$ of size $m \times (k+1)$ has full column rank for all (t,x), our model is said to be a Complete market.

23

Obviously this requires $m \ge k + 1$.

The Black-Scholes equation

Condition for absence of arbitrage:

$$\mu_S - \rho \pi_S = \sigma_S \lambda.$$

Interpretation of the left hand side: net return (ρ is the short-term interest rate). Interpretation of the right hand side: sensitivity coefficients times risk premia.

By expanding the functions μ_S and σ_S using the chain rule, we obtain the following more explicit form:

$$\frac{\partial \pi_S}{\partial t} + \frac{\partial \pi_S}{\partial x} \mu_X + \frac{1}{2} \operatorname{tr} \frac{\partial^2 \pi_S}{\partial x^2} \sigma_X \sigma_X^T - \rho \pi_S$$
$$= \frac{\partial \pi_S}{\partial x} \sigma_X \lambda.$$

This is the Black-Scholes equation. It is a linear partial differential equation that specifies a relation between the state space parameters μ_X and σ_X and the pricing function π_S .

22

Finding the risk premia

In a complete market, the functions ρ and λ may be inferred from the model data.

Example: the standard Black-Scholes model.

$$\mu_S = \begin{bmatrix} \mu x \\ re^{rt} \end{bmatrix}, \quad \pi_S = \begin{bmatrix} x \\ e^{rt} \end{bmatrix}, \quad \sigma_S = \begin{bmatrix} \sigma x \\ 0 \end{bmatrix}$$

It follows that

$$\rho = r, \qquad \lambda = \frac{\mu - r}{\sigma}.$$

Pricing functions for other assets that depend on the state variables of the model can now be determined from the BS equation. Moreover, a hedging strategy can be developed...

Noise cancellation (a.k.a. replication)

Let a state space model be given, and assume it is a complete market. Introduce a liability L (say a contract to pay at a given time T an amount $\nu(X_T)$) and let $\pi_L(t,x)$ be its price function, which must satisfy the BS equation.

We want to find a replication strategy: $u_t = \phi(t, X_t)$ such that $V_T = \nu(X_T)$.

Determine $\phi = \phi(t, x)$ such that

$$\begin{bmatrix} \pi_L & \sigma_L \end{bmatrix} = \phi^T \begin{bmatrix} \pi_S & \sigma_S \end{bmatrix}$$

i.e. $\pi_L = \phi^T \pi_S$ and $\sigma_L = \phi^T \sigma_S$. Because $\mu_L - \rho \pi_L = \sigma_L \lambda$ (BS eqn.) it follows that also $\mu_L = \phi^T \mu_S$.

From $\phi^T\pi_S=\pi_L$ it follows that ϕ is replicating. To show that ϕ is self-financing, note:

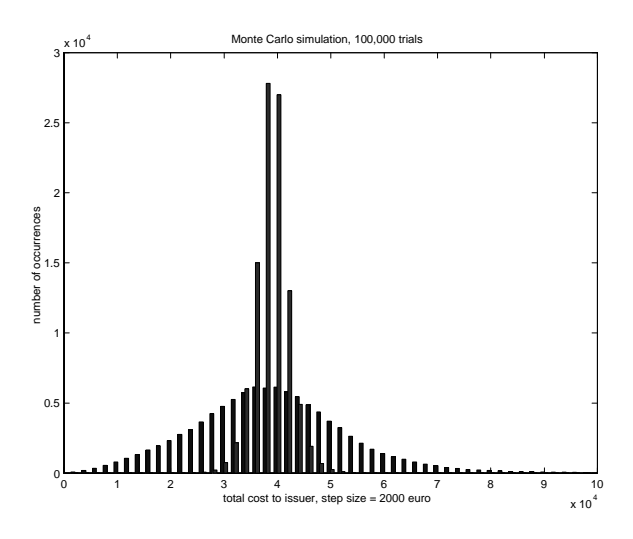
$$dV = dL = \mu_L dt + \sigma_L dW$$

= $\phi^T (\mu_S dt + \sigma_S dW) = \phi^T dS$.

25

Effect of rebalancing frequency

Monthly rebalancings (left bars) vs. daily rebalancings (right bars).



It is still assumed in this simulation that volatility is constant.

27

Remarks on replication

It has been shown that, in a complete market, every liability can be hedged in such a way that no risk remains — i.e. total noise cancellation. This seems to good to be true.

- It has been assumed that trading can take place continuously, without transactions costs
- The model may neglect a number of risk factors, so that the market is not really complete
- The hedge will not be fully effective if the true dynamics is not as supposed in the model

The standard BS model supposes that the parameter σ ("volatility") is constant. This is often seen as the main source of error in hedging. A typical remedy is to "re-calibrate" the model frequently (i.e. choose new volatility on the basis of observed prices).

26

Hedging against inflation

A model for bond prices that also takes inflation into account:

$$dX_1 = X_2 dt$$

$$dX_2 = \alpha (\bar{X}_2 - X_2) dt + \sigma_2 dW$$

$$dX_3 = \beta (\bar{X}_3 - X_3) dt + \sigma_3 dW$$

where the noise input W has dimension 2. Bond prices are fixed by assuming specifications for the short-term interest rate ρ and the risk premium λ :

$$\rho(t,x) = x_2 + x_3, \quad \lambda(t,x) = \lambda \text{ (constant)}.$$

The interpretation is as follows: X_1 is log-inflation; X_2 is the rate of inflation; X_3 is the short-term interest rate after correction for inflation.

One may now ask for instance whether it is possible to construct a strategy based on (nominal) bonds that will produce an indexed bond (payment of $\exp((X_1)_T)$ at time T).

A general Gaussian bond market

More generally than above:

$$dX = (FX + f)dt + GdW$$

(F, G constant matrices, f a constant vector), and

$$\rho(t,x) = h'x, \quad \lambda(t,x) = \lambda$$

(h and λ constant vectors).

Bond prices can be determined from the BS equation. After some computation:

$$\pi_T(t,x) = \exp(a(T-t) + b(T-t)x)$$

where the scalar function a(t) and the vector function b(t) can be determined explicitly; in particular

$$b(t) = -h' \int_0^t e^{Fs} ds.$$

29

Completeness in the inflation model

Alternative formulation of sufficient condition for completeness:

for all k-tuples of unequal times t_1,\ldots,t_k , the $k\times k$ matrix

$$M(t_1, \dots, t_k) := \begin{bmatrix} h'e^{Ft_1} \\ \vdots \\ h'e^{Ft_k} \end{bmatrix} G$$

is invertible.

In our original inflation model, this comes down to checking invertibility of

$$M(t_1, t_2) = \begin{bmatrix} e^{-\alpha t_1} & e^{-\beta t_1} \\ e^{-\alpha t_2} & e^{-\beta t_2} \end{bmatrix} \begin{bmatrix} \sigma_2 \\ \sigma_3 \end{bmatrix}.$$

We find that, assuming the row vectors σ_2 and σ_3 are independent, the model is complete with three bonds if $\alpha \neq \beta$. And so the indexed bond can be formed (in the model...).

31

Checking for completeness

The indexed bond can be manufactured from nominal bonds if the model defines a complete market, where assets are bonds of various maturities.

From the pricing function π_T , the volatility σ_T can be determined via the chain rule:

$$\sigma_T(t,x) = -\pi_T(t,x) h' \left(\int_0^{T-t} e^{Fs} ds \right) G.$$

Sufficient condition for market completeness: the matrix

$$\begin{bmatrix} 1 & -h' \left(\int_0^{T_1 - t} e^{Fs} ds \right) G \\ \vdots & \vdots \\ 1 & -h' \left(\int_0^{T_{k+1} - t} e^{Fs} ds \right) G \end{bmatrix}$$

is invertible for each $t \in [0, T]$.

30

Equivalent martingale measures

We have used the Black-Scholes equation to describe absence of arbitrage. There is an alternative (stochastic) formulation:

"Main theorem of mathematical finance"

Arbitrage is excluded if and only if there exists a probability distribution on the set of paths in the model such that the relative price of any asset at a given time t is equal to the expected relative price of the asset at any given later time, the expectation being taken based on the information available at time t.

"Relative price": price with respect to a fixed asset ("numéraire").

A probability distribution as above is called a "martingale measure."

199

Intuition behind the theorem

Existence of an arbitrage opportunity means that there is SOMe strategy that produces a positive result along all trajectories.

Existence of a martingale measure implies that, for any strategy, the average result over all trajectories (w.r.t. that measure) is zero.

Therefore the existence of a martingale measure implies that there can be no arbitrage opportunity.

The main theorem of mathematical finance states that the reverse conclusion is true as well.

33

Optimization in a complete market

Consider a problem of the form

$$\label{eq:energy_equation} \text{maximize} \quad E[\,U(V_T)\,]$$
 subject to $\ dV_t = u_t dS_t, \quad V_0 = v_0$

where S_t may be given as an output of a state space model driven by one or more Brownian motions, and $U(\cdot)$ denotes a utility function.

Standard approach: apply method of dynamic programming. This leads to a nonlinear partial differential equation.

Assume now that we have a complete market and that our variables are already taken with respect to a numéraire. Then there is a unique equivalent martingale measure that makes $\{S_t\}$ a martingale, and we have the replication theorem. Note: $\{V_t\}$ becomes a martingale too.

35

An alternative pricing formula

Prices can be computed on the basis of the Black-Scholes equation. An alternative formula can be given on the basis of equivalent martingale measures:

$$\frac{S_t}{N_t} = E_{\mathsf{Q}} \left[\left. \frac{S_T}{N_T} \right| \mathcal{F}_t \right]$$

where ${\bf Q}$ denotes the martingale measure, and N is a chosen numéraire.

In continuous-time models, change of measure comes down to change of drift (Girsanov's theorem). Therefore the above formula is often convenient.

Thm.: An arbitrage-free market is complete if and only if there is exactly one equivalent measure (for a given numéraire) such that all relative price processes are martingales.

34

The martingale method

Break up the optimization problem in two steps:

- 1. maximize E[V] subject to the single constraint $E_{\mathbb{Q}}[V] \leq v_0$ (Q denotes the equivalent martingale measure)
- 2. use the replication theorem to determine the strategy that will produce V.

Note: first step is a static optimization problem with a single side constraint. Second step requires the solution of a linear partial differential requation. (In some applications, the second step need not be carried out.)

This is the "martingale method." It may be generalized to the case of incomplete markets, but the application is more complicated (requires minimization over the set of all equivalent martingale measures).

200

The story of Metallgesellschaft

Metallgesellschaft AG (Frankfurt) is a large corporation doing business in metal, mining, and engineering. It owned a US-based oil business MGRM (MG Refining and Marketing). In 1992, MGRM set up a scheme in which it granted long-term contracts for delivery of oil to customers for a fixed price, covering periods up to ten years. The exposure to oil price risk was hedged by the purchase of short-term contracts ("futures") for which a liquid market exists.

Under market conditions of 1993, the strategy required an enormous amount of cash input with no substantial income yet from oil deliveries. MG decided to stop the hedging scheme and wrote off about \$ 1.5 billion.

A case of financial engineering failure?

37

The price of a futures contract

A futures contract with maturity T is a contract to deliver a given commodity, say one barrel of oil, at time T for a price F_T to be paid when delivery is made. So the market value at time t of a contract to deliver a barrel of oil at time t is $e^{-r(T-t)}F_T$. This value should satisfy the BS equation. The BS equation for the t-futures price t-futures futures futures price t-futures price t-futures futures futures futures futures futures futures futures futures futures fu

$$\mu_T(t,x) = \sigma_T(t,x)\lambda(x)$$

where

$$\mu_T = \frac{\partial \pi_T}{\partial t} + \frac{\partial \pi_T}{\partial x} \mu_X + \frac{1}{2} \frac{\partial^2 \pi_T}{\partial x^2} \sigma_X^2$$

$$\sigma_T = \frac{\partial \pi_T}{\partial x} \sigma_X$$

39

with the final condition $\pi_T(T, x) = x$.

This may be solved numerically.

A model for the oil price

Assume a model with one state and one noise input; take the oil price X_t as state variable.

$$dX_t = \mu_X(X_t) dt + \sigma_X(X_t) dW_t$$

Let $\mu_X(x)$ be positive when x is low, and negative when x is high.

Oil may be used for consumption as well as for investment. The BS equation is therefore written as follows (r is interest rate, K is storage cost):

$$\mu_X(x) - r\pi_X(x) - K \le \sigma_X(x)\lambda(x)$$

 $\lambda(x) \ge 0$

where for each x at least one of the inequalities is satisfied with equality. Solve to find the market price of oil price risk:

$$\lambda(x) = \max\left(\frac{\mu_X(x) - r\pi_X(x) - K}{\sigma_X(x)}, 0\right)$$

38

Special cases

Case 1: oil price high — oil is consumption good.

In this case the price of oil risk is zero. The futures price is then the expected price of a barrel of oil at time T according to the given model. ("Expectation-based" pricing.)

Case 2: oil price low — oil is investment good.

In this case the futures price is equal to the cost of buying a barrel of oil now and storing it until maturity. ("Arbitrage-based" pricing.)

The formula of the previous transparency interpolates between the two ("two-regime pricing", Bühler et al., 2001).

Some concrete results: see Fig. 1.

Different models: different feedback rules

Idea of hedging: since both (say) the 6-month futures contract and the contract for delivery in 10 years are sensitive to the current oil price in a well-defined way (given a model), take a position in 6-month futures so that the loss or gain in value of this position due to oil price change will offset the corresponding loss or gain in the 10-year contract.

However, different models lead to rather different policies (see Fig. 2).

MGRM used the arbitrage-based rule.

Note: a mis-hedge does not necessarily lead to a loss; it may actually produce a gain. Risk reduction is not achieved, however.

41

Conclusions (1)

- A new branch of engineering is emerging: financial engineering
- Model-based thinking has gained acceptance in the finance industry during 80s and 90s — process still continuing; keyword: liquidity
- Main focus not so much stock markets, but rather loans (fixed/floating swaps, credit ratings,...), and commodities incl. energy
- Dynamic hedging: taking decisions on the basis of incoming observations — familar to control theory
- Peculiarities of financial markets: absence of arbitrage, martingale measures

Stability?

It is a common assumption in financial modeling that individual traders cannot influence market dynamics.

However, the joint behavior of all traders does affect market dynamics.

Fig. 3 shows electricity prices at the Amsterdam Power Exchange (APX) during 2001. Electricity has been traded at APX since 1999. The exchange now covers about 10% of the Dutch electricity market.

Investigations are being carried out concerning the cause of the peaks in June and December 2001. Similar price peaks caused interruptions of power delivery to Californian homes in the winter of 2000/2001.

42

Conclusions (2)

- Basic point of view: model asset prices as dependent on basic risk factors
- Strong laws as a result of absence of arbitrage (especially in continuous time)
- Models focused on particular markets; no attempt to model "the economy"
- Martingale method: new optimization technique
- Developments just beginning: robustness, noisy observations,...

202

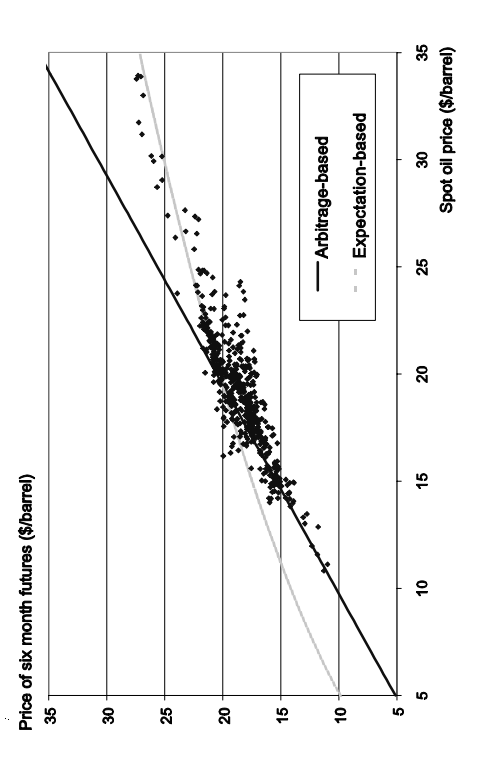


Figure 1: Adapted from: W. Bühler, O. Korn, R. Schöbel, Pricing and Hedging of Oil Futures. A Unifying Approach, working paper, 2001.



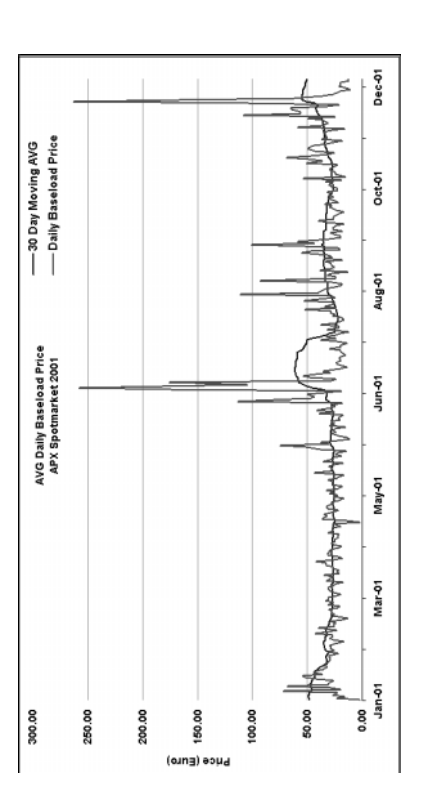


Figure 3: Taken from www. apx. nl .
47

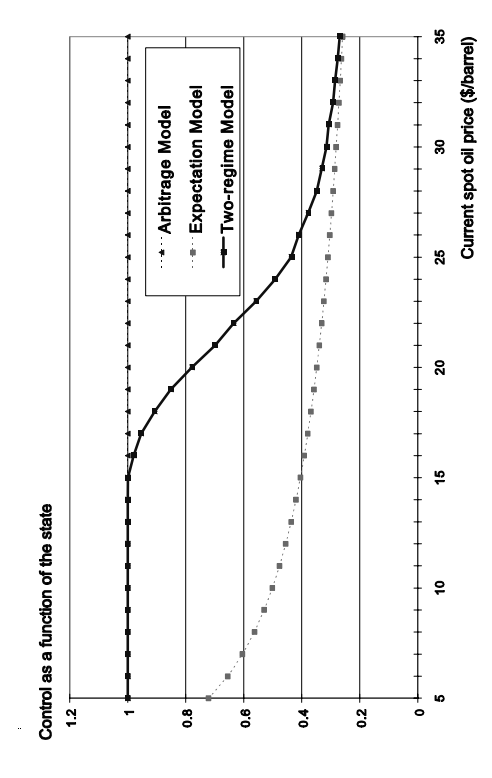


Figure 2: Adapted from Bühler et al., 2001.

Part 3 List of Participants

1 dr.ir. R.G.K.M. Aarts

CTW / WA

University of Twente

P.O. Box 217

7500 AE Enschede

The Netherlands

+31 53 489 25 57

R.G.K.M.Aarts@utwente.nl

2 P.-A. Absil

Institut Montefiore

Universite de Liege

Grande Traverse 10

4000 Liege

Belgium

+32-4-3662697

absil@montefiore.ulg.ac.be

3 Prof. Dr Dipl-Ing F. Allgöwer

Institute for Systems Theory in Engineering

University of Stuttgart

-

D-70550 Stuttgart

Germany

+49-711-685 6300

allgower@ist.uni-stuttgart.de

4 Prof.dr.ir. J. van Amerongen

Drebbel Institute for Mechatronics

University of Twente

P.O. Box 217

7500 AE Enschede

Netherlands

+31 53 4892791

J.vanAmerongen@el.utwente.nl

5 Ir. N.P.I. Aneke

Mechanical Engineering

TU Eindhoven

P.O.Box 513

5600 MB Eindhoven

The Netherlands

040.247.2611

n.p.i.aneke@tue.nl

6 Msc. Astrid

Electrical Engineering

Eindhoven University of Technology

PO Box 513

5600 MB Eindhoven

The Netherlands

31-40-247 3284

p.astrid@tue.nl

7 Mr. El Bahir

Service d'Automatique et d'Analyse des Systèmes

ULB

50, Av. F.D. Roosevelt, CP 165/55

1050 Brussels

Belgium

+32.2.650.37.44

elbahir@labauto.ulb.ac.be

8 Dr J. R. Banga

Process Engineering Group

Instituto de Investigaciones Marinas (C.S.I.C)

Eduardo Cabello 6

36208 Vigo

Spain

+34 986 214 473

julio@iim.csic.es

9 Tom A. L. Bellemans

ESAT - SCD K.U.Leuven

Kasteelpark Arenberg 10

B-3001 Leuven

Belgium

+ 32 16 32 11 59

tom.bellemans@esat.kuleuven.ac.be

10 M.N. Belur

Institute voor Wiskunde,

University of Groningen,

Inst. Wiskunde, PO Box 800

9700 AV Groningen

The Netherlands

+31-50-3636496

M.N.Belur@math.rug.nl

11 ir. H.H.J. Bloemen

Applied Sciences, Kluyver Lab for Biotechnology

Delft University of Technology

Julianalaan 67

2628 BC Delft

The Netherlands

015-2782998

H.Bloemen@tnw.tudelft.nl

12 Prof. Rene Boel

EESA, Univ. Gent

SYSTeMS Research Group

Technologiepark-Zwijnaarde 9

B9052 Gent

Belgium

+32-(0)9-2645658

rene.boel@rug.ac.be

13 Pr. Dr. Ir. Ph. Bogaerts

Control Engineering and System Analysis

Université Libre de Bruxelles

Av. F.-D. Roosevelt, 50 C.P.165/55

B-1050 Brussels

Belgium

32-2-650.26.76 (or 26.75)

Philippe.Bogaerts@ulb.ac.be

14 Dr.ir. X.J.A. Bombois

Department of Applied Physics

Delft University of Technology

Lorentzweg 1

2628 CJ Delft

The Netherlands

015 27 85150

x.j.a.bombois@tnw.tudelft.nl

15 Ir. R. Bos

Department of Applied Physics

Delft University of Technology

Lorentzweg 1

2628 CJ Delft

The Netherlands

015 27 85331

r.bos@tn.tudelft.nl

16 dr.ir. P.C. Breedveld

Drebbel Institute for Mechatronics

University of Twente

P.O. Box 217

7500 AE Enschede

Netherlands

+31 53 4892792

P.C.Breedveld@el.utwente.nl

17 PhD Student Brüls

LTAS - Aérospatiale, Mécanique et Matériaux

Université de Liège

Institut de Mécanique et de Génie Civil, chemin des

Chevreuils 1, Bât B52

4000 Liège

Belgium

+32.4.366.48.54

o.bruls@ulg.ac.be

18 M. CADIC

Department of Mathematical Sciences

University of Twente

P.O. Box 217

7500 AE Enschede

The Netherlands

053-489 3453

m.cadic@math.utwente.nl

19 ir. M.I. Parra Calvache

Systems and Control Group

Delft University of Technology

Mekelweg 2

2628CD Delft

The Netherlands

miparra@hotmail.com

20 Dr. Chen

Intelligent Mechanics

Kinki University

931 Nishimitani, Uchita

649-6493 Naga-gun

Japan

+81-736-77-3888

chen@mec.waka.kindai.ac.jp

21 K. De Cock

Electrical Engineering (ESAT-SCD)

K.U.Leuven

Kasteelpark Arenberg 10

B-3001 Leuven

Belgium

+32-(0)16 32 18 42

decock@esat.kuleuven.ac.be

22 Dr. J. Cortes

Systems, Signals and Control

University of Twente

P.O. Box 217

7500 AE Enschede

The Netherlands

(53) 4893456

j.cortesmonforte@math.utwente.nl

23 ir. P.J.L. Cuijpers

EESI

TU/e

Den Dolech 2

5600 MB Eindhoven

Netherlands

+31 (0) 40 2478216

P.J.L.Cuipers@tue.nl

24 Researcher Defays

Systems

Institut Montefiore

Grande Traverse, 10, Bât B28

4000 Liège

Belgium

+3243663749

defays@montefiore.ulg.ac.be

25 Dr.ir. A.J. Den Dekker

Department of Applied Physics Delft University of Technology

Lorentzweg 1 2628 CJ Delft The Netherlands

a.j.dendekker@tnw.tudelft.nl

26 B. Demeulenaere

015 27 81823

KULeuven - PMA Celestijnenlaan 300B 3001 Heverlee Belgium

bram.demeulenaere@mech.kuleuven.ac.be

27 Drs. J.W. van Dijk

Instituut voor Wiskunde & Informatica

Rijks Universiteit Groningen

P.O. Box 800

9700 AV Groningen Groningen

Nederland

+31 050 3636496

J.W.van.Dijk@math.rug.nl

28 Dr. ir. J. van Dijk

Mechanical Eng

University Twente

p.o. box 217

7500 AE Enschede

Netherlands

053-4892601

j.vandijk@wb.utwente.nl

29 Ir. B.G. Dijkstra

Systeem en Regeltechniek Technische Universiteit Delft

Mekelweg 2 2528 CD Delft Netherlands 015-2785617

B.G.Dijkstra@wbmt.tudelft.nl

30 Ir. S.G. Douma

Department of Applied Physics Delft University of Technology

Lorentzweg 1 2628 CJ Delft The Netherlands 015 27 85189

s.g. doum a@tnw.tudelft.nl

31 ir. V. Duindam

Drebbel Institute for Mechatronics

University of Twente

P.O. Box 217

7500 AE Enschede

Netherlands

+31 53 4892817

V.Duindam@el.utwente.nl

32 J.C. Engwerda

Dept. of Econometrics and Operations Research

Tilburg University P.O. Box 90135 5000 LE Tilburg The Netherlands 013-4662174

Engwerda@kub.nl

33 Phd Student D. Ernst

Electrical Engineering

University of Liege

Institut Montefiore B28, Sart-Tilman

4020 Liege BELGIUM +32 4 366 96 37

ernst@montefiore.ulg.ac.be

34 dr. ir. H.A. van Essen

Mechanical Engineering

Technische Universiteit Eindhoven

P.O. Box 513

5600 MB Eindhoven

The Netherlands

040 - 2472998

h.a.v.essen@tue.nl

35 ir. P.J. Feenstra

Drebbel Institute for Mechatronics

University of Twente

P.O. Box 217

7500 AE Enschede

Netherlands

+31 53 4892704

P.J.Feenstra@el.utwente.nl

36 I. Goethals

ESAT/SCD

KULeuven/ESAT/SCD Kasteelpark Arenberg 10 B3001 Heverlee - Leuven

Belgium

+32 495 677785

igoethal@esat.kuleuven.ac.be

37 Mr. J.T. Gravdahl

Dept. of Engineering Cybernetics

Norwegian University of Science and Technology

O.S. Bragstads plass 2D N-7491 TRONDHEIM

NORWAY

+47 73 59 43 93

tommy.gravdahl@itk.ntnu.no

38 Ir V Grosfils

Control Engineering and System Analysis

Université Libre de Bruxelles (ULB)

50, Av. F.D. Roosevelt, CP 165/55

1050 Brussels

Belgium

32-2-650.26.13

vgrosfil@labauto.ulb.ac.be

39 Dipl.-Ing. J. E. Haag

Laboratoire d'Automatique

Faculté Polytechnique de Mons

Boulevard Dolez 31

B-7000 Mons

Belgium

+32 65 37 4131

haag@fpms.ac.be

40 dr. ir. M.F. Heertjes

Mechatronics Research

Philips CFT

PO Box 218

5600 MD Eindhoven

The Netherlands

+31 40 2733424

marcel.heertjes@philips.com

41 ir. Hegyi

Control Systems Engineering

Delft University of Technology

P.O. Box 5031

2600 GA Delft

Netherlands

015-2782087

A.Hegyi@its.tudelft.nl

42 Dr.ir. E. J. Van Henten

IMAG BV

P.O.Box 43

6700 AA Wageningen

The Netherlands

0317 411933

e.j.vanhenten@imag.wag-ur.nl

43 m.sc. hesseling

mechanical engineering

TUE

po box 513

5600 MB eindhoven

the netherlands

+31 40 247 2811

R.J.Hesseling@tue.nl

44 Dennis H. van Hessem

Mechanical Engineering

TU DELFT

Mekelweg 2

2628 CD DELFT

The Netherlands

0152781720

d.h.vanhessem@wbmt.tudelft.nl

45 Dr. P.S.C. Heuberger

Department of Applied Physics

Delft University of Technology

Lorentzweg 1

2628 CJ Delft

The Netherlands

015 27 85331

p.s.c.heuberger@tnw.tudelft.nl

46 Prof.dr.ir. P.M.J. Van den Hof

Department of Applied Physics

Delft University of Technology

Lorentzweg 1

2628 CJ Delft

The Netherlands

015 27 84509

p.m.j.vandenho@tnw.tudelft.nl

47 Ir C.W.J. Hol

Mechanical Engineering

Delft University of Technology

Mekelweg 2

2628 CD Delft

The Netherlands

015-2788573

c.w.j.hol@wbmt.tudelft.nl

48 ir. J. Holterman

Drebbel Institute for Mechatronics

University of Twente

P.O. Box 217

7500 AE Enschede

Netherlands

+31 53 4892707

J.Holterman@el.utwente.nl

49 ir. L. Huisman

Chemical Engineering

Eindhoven University of Technology

P.O. Box 513

5600 MB Eindhoven

Netherlands

+31 40 2473284

1.huisman@tue.nl

50 O.V. Iftime

Faculty of Applied Mathematics

University of Twente

P.O. 217

7500 AE Enschede

The Netherlands

053 489 3469

o.v.iftime@math.utwente.nl

51 Prof. J. Van Impe

Department of Chemical Engineering

Katholieke Universiteit Leuven

Kasteelpark Arenberg 22

3001 Leuven

Belgium

+32-16/32.19.47

jan.vanimpe@agr.kuleuven.ac.be

52 ir. L. Jabben

Advanced Mechatronics

Tu-Delft

Mekelweg 2

2628 CD Delft

NL.

015-2783142

l.jabben@wbmt.tudelft.nl

53 Bram de Jager

Dept. of Mechanical Engineering

Technische Universiteit Eindhoven

P.O Box 513

5600 MB Eindhoven

The Netherlands

+31 40 2472784

A.G.de.Jager@wfw.wtb.tue.nl

54 MSc, D Jeltsema

Electrical Engineering

Delft University of Technology

P.O. Box 5031

2600 GA Delft

The Netherlands

+31-(0)15-278-5489

d.jeltsema@its.tudelft.nl

55 D. Jibetean

PNA

CWI Amsterdam

POBox 94079

1090 GB Amsterdam

The Netherlands

020 592 4167

d.jibetean@cwi.nl

56 Dr. I. Jikuya

Faculty of Applied Physics

University of Twente

P.O. Box 217

7500 AE ENSCHEDE

The Netherlands

+31 53 489 1089

I.Jikuya@tn.utwente.nl

57 Ir. G. Jiroveanu

SYSTeMS Research Group

University of Ghent

Zwijnaarde 9

9052 Ghent

Belgium

0032.09.221.90.03

jirog@systems.rug.ac.be

58 Prof.dr.ir. J.B. Jonker

Engineering Technology

University of Twente

P.O. box 217

7500 AE Enschede

the Netherlands

+31 53 4892591

j.b.jonker@ctw.utwente.nl

59 ir. D.S. Jovanovic

Drebbel Institute for Mechatronics

University of Twente

P.O. Box 217

7500 AE Enschede

Netherlands

+31 53 4892788

D.S.Jovanovic@el.utwente.nl

60 S. Juliana

Control and Simulation division, Fac of Aerospace

Engineering

TU Delft

Kluyverweg 1

2629 HS Delft

The Netherlands

(015)2785867

s. juliana@lr.tudelft.nl

61 A. A. Julius

Mathematical Sciences

Twente University

P.O. Box 217

7500 AE Enschede

The Netherlands

+31-53-4893459

julius@math.utwente.nl

62 A. Juloski

MBS

TU/e

5600

MB Eindhoven

Netherlands

+31 62 485 56 56

a.juloski@tue.nl

63 S. K. Kanev

Applied Physics

University of Twente

P.O.Box 217

7500 AE Enschede

The Netherlands

+31-53-489-1089

S.K.Kanev@TN.UTwente.NL

64 Dr. K.J. KEESMAN

Systems and Control Group

Wageningen University

Postbus 43

6700 AA Wageningen

The Netherlands

0317 483780

karel.keesman@user.aenf.wau.nl

65 Prof. M. Kinnaert

Control Engineering and System Analysis

Université Libre de Bruxelles

CP 165/55, 50 Av. F.D. Roosevelt

1050 Brussels

Belgium

322 650 22 87

kinnaert@labauto.ulb.ac.be

66 Ir. M.W.T. Koot

TU/e Mechanical Engineering

Control Engineering

P.O. Box 513

5600 MB Eindhoven

The Netherlands

040-2472072

michielk@dse.nl

67 D Kostic

Department of Mechanical Engineering

Eindhoven University of Technology

PO Box 513

5600 MB Eindhoven

The Netherlands

040 2475730

d.kostic@tue.nl

68 M.Sc. T. Krilavicius

Computer Science, Formal Methods and Tools

University of Twente

P.O. Box 217

7500 AE Enschede

The Netherlands

+31648355899

krilavic@cs.utwente.nl

69 ir. B.J. de Kruif

Drebbel institute of Mechatronics

University of Twente

P.O. Box 217

7500 AE Enschede

053-4892707

b.j.dekruif@utwente.nl

70 dr.ir. R. Langerak

Computer Science

University of Twente

P.O. Box 217

7500 AE Enschede

The Netherlands

+31-53-4893714

langerak@cs.utwente.nl

71 Ph.D. student Lapierre

Dept of Montefiore, Signal Processing Group

Université de Liège

Bâtiment B28

B-4000 Liège

Belgium

+32 4 366 37 41

f.lapierre@ulg.ac.be

72 C Lauwerys

Mechanical Engeneering

K.U.Leuven

Celestijnenlaan 300B

3001 Heverlee

Belgium

+3216322534

christophe.lauwerys@mech.kuleuven.ac.be

73 dr.ir. A.A.J. Lefeber

Mechanical Engineering

Eindhoven University of Technology

PO Box 513

5600 MB Eindhoven

The Netherlands

+31 40 2475821

A.A.J.Lefeber@tue.nl

74 PhD student Lefebvre

Dept. of mechanical engineering

K.U.Leuven

Celestijnenlaan 300B

3001 Heverlee (Leuven)

Belgium

+32 16 32 27 73

Tine.Lefebvre@mech.kuleuven.ac.be

75 Ir R. Lepore

Laboratoire d'Automatique

Faculté Polytechnique de Mons

Boulevard Dolez, 31

B-7000 Mons

Belgium

+32 (0)65 374140

lepore@fpms.ac.be

76 Ir. M. Leskens

Applied Physics

Delft University of Technology

Lorentzweg 1

2628 CJ Delft

The Netherlands

015-2784263

M.Leskens@mep.tno.nl

77 Ir C. Levrie

Laboratoire d'Automatique

Faculté Polytechnique de Mons

31 Boulevard Dolez

7000 Mons

Belgium

+32 (0)65 374140

levriec@mail.fpms.ac.be

78 Prof. M. J. M. Loccufier

Electrical Energy, Systems and Automation

Ghent University

Technologiepark-Zwijnaarde 9

B-9052 Zwijnaarde-Gent

Belgium

+ 32 (0) 9 264 55 87

Mia.Loccufier@rug.ac.be

79 MSc Lopezlena

Control Systems Engineering

Delft University of Technology

P.O. Box 5031

2600 GA Delft

Netherlands

015-2785489

R.Lopezlena@its.tudelft.nl

80 Ph D. Student Manuel

Systems

Institut Montefiore

Grande Traverse 10, Bât. B28

4000 Liège

Belgium

+3243663739

gerard@montefiore.ulg.ac.be

81 Ivan Markovsky

ESAT

K.U.Leuven

Kasteelpark Arenberg 10

B-3001 Leuven-Heverlee

Belgium

+32-16-321897

ivan.markovsky@esat.kuleuven.ac.be

82 ir. Stork Martijn

Mechanical Engineering Systems and Control Group

Delft Technical University

Mekelweg 2

2628 CD Delft

The Netherlands

m.stork@wbmt.tudelft.nl

83 Ph. Student, S Martínez

Mathematics

IMAFF (CSIC)

C/ Serrano, 123

28006 Madrid

Spain

91 5616800 ext. 1114

s.martinez@imaff.cfmac.csic.es

84 E.G. van der Meche

Mechanical Engineering

Delft University of Techology

Mekelweg 2

2628 CD Delft

015 2782725

e.g.vandermeche@wbmt.tudelft.nl

85 A. A. Moelja

Systems, Signals, and Control Dept, Fac of Math

Sciences

University of Twente

P.O. Box 217

7500 AE Enschede

The Netherlands

+31-53-4894162

moelja@math.utwente.nl

86 Dr.ir. M.J.G. van de Molengraft

W

TU/e

P.O. Box 513

5600 MB Eindhoven

Netherlands

+31 40 2472998

M.J.G.v.d.Molengraft@tue.nl

87 Prof. Dr. Ir. Bart De Moor

Elektrotechniek, ESAT-SCD (SISTA)

K.U.Leuven

Kasteelpark Arenberg 10

3001 Leuven

Belgium

32/16/32.17.15

bart.demoor@esat.kuleuven.ac.be

88 Dr. Ir. D.A. Lizarraga N

Mechanical Engineering

TU/e

Den Dolech 2, Postbus 513

5600MB Eindhoven

Nederland

040-2472611

D.Lizarraga@tue.nl

89 Prof.Dr. Nijmeijer

DCT

TUE

Postbus 513

5600 MB Eindhoven

The Netherlands

040-2473203

H.Nijmeijer@tue.nl

90 Prof. E.J.L. Noldus

Electrical Energy, Systems and Automation

Ghent University

Technologiepark-Zwijnaarde 9

B-9052 Zwijnaarde-Gent

Belgium

+ 32 (0) 9 264 55 78

Noldus@autoctrl.rug.ac.be

91 M.R. Opmeer

Wiskunde en Informatica

Rijksuniversiteit Groningen

P.O. Box 800

9700 AV Groningen Groningen

Nederland

31 050 3633999

opmeer@math.rug.nl

92 ir. B. Orlic

Drebbel Institute for Mechatronics

University of Twente

P.O. Box 217

7500 AE Enschede

Netherlands

+31 53 4892817

B.Orlic@el.utwente.nl

93 MSc A. Pavlov

Mechanical Engineering

Eindhoven University of Technology

POBox 513

5600 MB Eindhoven

The Netherlands

040-2474227

A.Pavlov@tue.nl

94 AAP Pelckmans

ESAT-SCD/SISTA

K.U.Leuven

Kasteelpark Arenberg 10

3001 Heverlee/Leuven

Belgium

-

kristiaan.pelckmans@esat.kuleuven.ac.be

95 Dr. A. Yu. Pogromsky

Mechanical Engineering

Eindhoven University of Technology

POB 513

5600 MB Eindhoven

The Netherlands

040 247 28 49

A.Pogromsky@tue.nl

96 dr j.w. polderman

mathematical sciences

university of twente

p.o. box 217

7500 ae enschede

the netherlands

053-4893438

j.w.polderman@math.utwente.nl

97 Ir. S Postma

University Twente/ Lab. Mechanical Automation the Netherlands Institute for Metals Research

PO Box 217

7500 AE Enschede the Netherlands +31 (0)53 4894846

s.postma@ctw.utwente.nl

98 Prof Dr Preisig

Systems & Control Group

TU Eindhoven

PO 513

5600 MB Eindhoven The Netherlands +31 40 247 2578 H.Preisig@tue.nl

99 MSc. D. Putra

Mechanical Engineering

Technical University of Eindhoven

P.O. Box 513

5600 MB Eindhoven

Netherlands (040)2474850 d.putra@tue.nl

100 Ir F. Renard

Automatic Control Laboratory Faculté Polytechnique de Mons

Boulevard Dolez 31

7000 MONS Belgium

+32 65 37 41 32 renard@fpms.ac.be

101 Dr Ch. Renotte

Laboratoire d'Automatique Faculté Polytechnique de Mons

Boulevard Dolez, 31 B-7000 Mons Belgium

+32 (0)65 374139 renotte@fpms.ac.be

102 Dr. Ir. N.A.W. van Riel

Electrical Engineering

Eindhoven University of Technology

P.O. box 513

5600 MB Eindhoven The Netherlands 040 247 5506

N.A.W.v.Riel@tue.nl

103 dr. J.J.M. Rijpkema

Mechanical Engineering

Eindhoven University of Technology

P.O.Box 513

5600 MB Eindhoven

the Netherlands

040-2473170

j.j.m.rijpkema@tue.nl

104 ir. J Rogge

SYSTeMS Research Group, EESA

Universiteit Gent

Technologiepark Zwijnaarde 9

9052 Gent Belgium +3292645657

jonathan.rogge@rug.ac.be

105 prof.dr.A.J. van der Schaft

Mathematical Sciences University of Twente

P.O.Box 217

7500AE Enschede Netherlands 053-4893449

a.j.vanderschaft@math.utwente.nl

106 Dr. ir. J.M.A. Scherpen

ITS

Delft University of Technology

P.O. Box 5031 2600 GA Delft Netherlands 015-2786152

j.m.a.scherpen@its.tudelft.nl

107 Ir. M.G.E. Schneiders

Mechanical Engineering Control Systems Technology

WH -1.138

PO Box 513 Eindhoven

m.g.e.schneiders@tue.nl

108 J.M. Schumacher

Dept. of Econometrics and OR

Tilburg University PO Box 90153 5000 LE Tilburg The Netherlands +31-(0)13-4662050

jms@kub.nl

109 Dr. Ir. SEHAB

Service d'Automatique

Faculté Polytechnique de Mons

Boulevard Dolez N°31

 $7000 \; Mons$

BELGIUM

+3265374131

sehab@autom.fpms.ac.be

110 Prof. R. SEPULCHRE

Electrical Engineering and Computer Science

University of Liège Insitut Montefiore, B28

4000 Liege Belgium 043662987

r.sepulchre@ulg.ac.be

111 H. B. Siahaan

Electrical Engineering

TU Eindhoven

PO Box 513

5600 MB Eindhoven

The Netherlands

(040) 2473307

h.siahaan@tue.nl

112 ir. Ilse Y.M. Smets

Chemical Engineering Department

BioTeC - KULeuven Kasteelpark Arenberg 22

3001 Leuven

Belgium

+32 - 16 - 32.19.19

ilse.smets@agr.kuleuven.ac.be

113 ir. I. Soute

Mechatronics Equipment

Philips CFT PO Box 218

5600 MD Eindhoven

The Netherlands

iris.soute@philips.com

114 ir. F.B. Sperling

Mechatronics Research

Philips CFT PO Box 218

5600 MB Eindhoven

The Netherlands +31 40 27 32580

frank.sperling@philips.com

115 Ph. D. Student, G. STAN

System and Control

University of Liège

Institut Montefiore, B28, Sart-Tilman

B-4020 Liege

Belgium

+32 4 366 2696

gb.stan@ulg.ac.be

116 Prof.Dr.Ir. M. Steinbuch

DCT

TUE

Postbus 513

5600 MB Eindhoven

The Netherlands

040-2475444

M.Steinbuch@tue.nl

117 Dr J.D. Stigter

Food and Agrotechnology

Wageningen UR

Mansholtlaan 10-12

6708 PA Wageningen

The Netherlands

hans.stigter@user.aenf.wau.nl

118 Ir. B. Stouten

Electrical Engineering

Technische Universiteit Eindhoven

513

5600 MB Eindhoven

The Netherlands

+31.40.247.3588

b.stouten@tue.nl

119 prof. dr. ir. G. van Straten

Dept. Agrotechnology and Food Sci

Wageningen University

Mansholtlaan 10

6708 PA Wageningen

The Netherlands

+31.317.483331/482124/482980

gerrit.vanstraten@user.aenf.wau.nl

120 Ir. S.N. Strubbe

Applied Mathematics

University of Twente

PO Box 217

7500 AE Enschede

Holland

053-4893459

strubbe@math.utwente.nl

121 ir. H. Super

Faculty of Engineering, Laboratory of Mechanical

Automation

University of Twente

P.O. Box 217

7500AE Enschede

the Netherlands

053-4894846

h.super@ctw.utwente.nl

122 Ir. A. A. Tiagounov

Department of Electrical Engineering

Technische Universiteit Eindhoven

P.O. Box 513

5600 MB Eindhoven

The Netherlands

+31 40 2473307

a.tiagounov@tue.nl

123 Dr. H.L. Trentelman

Dept. of Mathematics

University of Groningen

P.O. Box 800

9700 AV Groningen

The Netherlands

050 3633998

h.l.trentelman@math.rug.nl

124 Ir. M. C. M. Troffaes

EESA (SYSTeMS)

Universiteit Gent

Technologiepark 9

B-9052 Zwijnaarde

Belgie

3292645655

Matthias. Troffaes@rug.ac.be

125 Ir. D. Vaes

Dep. of Mechanical Engineering

KULeuven

Celestijnenlaan 300B

B-3001 Heverlee

Belgium

david.vaes@mech.kuleuven.ac.be

126 Patrick Vansevenant

Dept.of Computer Science

K.U. Leuven

Celestiinenlaan 200 A

3001 Heverlee (Leuven)

Belgium

patrick.vansevenant@cs.kuleuven.ac.be

127 Ir. L.B. Verdickt

Chemical Engineering

BioTeC

Kasteelpark Arenberg 22

B-3001 Leuven

Belgium

+32 16 32 19 19

liesbeth.verdickt@agr.kuleuven.ac.be

128 ir. V. Verdult

Information Technology and Systems

Delft University of Technology

P.O. Box 5031

2600 GA Delft

The Netherlands

+ 31 (0) 15 27 85768

v.verdult@its.tudelft.nl

129 ir. M.H.A. Verwoerd

Drebbel Institute for Mechatronics

University of Twente

P.O. Box 217

7500 AE Enschede

Netherlands

+31 53 4892704

M.H.A. Verwoerd@el.utwente.nl

130 dr.ir. T.J.A. de Vries

Drebbel Institute for Mechatronics

University of Twente

P.O. Box 217

7500 AE Enschede

Netherlands

+31 53 4892817

T.J.A.deVries@el.utwente.nl

131 Ir. S. De Waele

Department of Applied Physics

Delft University of Technology

Lorentzweg 1

2628 CJ Delft

The Netherlands

015 27 85331

waele@tnw.tudelft.nl

132 Ir. R. R. Waiboer

Laboratory of Mechanical Automation

Netherlands Institute for Metals Research / Univer-

sity of Twente

P.O. Box 217

7500 AE Enschede

Netherlands

+31 53 489 5442

r.r. waiboer @utwente.nl

133 dr. ir. M.M.J. Van de Wal

Mechatronics Research

Philips CFT

PO Box 218

5600 MD Eindhoven

The Netherlands

+31 40 27 39211

M.M.J.van.de.Wal@philips.com

134 Ir. J. WANG

Mechanical Engineering

Katholieke Universiteit Leuven

Celestijnenlaan 300B

3001 Heverlee

Belgium

+32-16-322833

jian.wang@mech.kuleuven.ac.be

135 M.B. Groot Wassink

Mechatronics Equipment

Philips CFT

PO Box 218

5600 MD Eindhoven

The Netherlands

+31 40 27 39211

matthijs.groot.wassink@philips.com

136 Dr. S. Weiland

Department of Electrical Engineering

Eindhoven University of Technology

P.O. Box 513

5600 MB Eindhoven

The Netherlands

+31.40.2473577

s.weiland@tue.nl

137 Ir. M.R. Westerweele

MBS-CS

TUE

513

5600 MB Eindhoven

The Netherlands

040-2472507

m.r.westerweele@tue.nl

138 Dr. R.L. Westra

Dep. Mathematics

Universiteit Maastricht

OP-box 616

6200 MD Maastricht

Netherlands

043-3883722

westra@math.unimaas.nl

139 Dr. J. J. WINKIN

Mathematics

University of Namur

8 Rempart de la Vierge

5000 NAMUR

Belgium

+32 - 81 - 72 49 10

Joseph.Winkin@fundp.ac.be

140 Ir. M.E. Van Wissen

Chemical Technology

Delft University of Technology

Julianalaan 136

2628 BL Delft

The Netherlands

+31 15 2784466

m.e.vanwissen@tnw.tudelft.nl

141 Dr. A. Vande Wouwer

Service d'Automatique

Faculté Polytechnique de Mons

31 Boulevard Dolez

7000 Mons

Belgium

+32-(0)65374141

Alain.VandeWouwer@fpms.ac.be

142 Yucai Zhu

Electrical Engineering

Eindhoven University of Technology

P.O. Box 513

5600 MB Eindhoven

The Netherlands

y.zhu@tue.nl

143 Dr. H.J. Zwart

Faculty of Mathematical Sciences

University of Twente

P.O. Box 217

7500 AE Enschede

The Netherlands

053-4893464

h.j.zwart@math.utwente.nl